THE REGULATION OF THE CYTOSKELETON IN PROMOTING AXON GROWTH

KRISTY LYNN WILLIAMS

The regulation of the cytoskeleton in promoting axon growth

By

© Kristy Lynn Williams

A thesis submitted to the School of Graduate Studies in partial fulfillment of the requirements for the degree of Doctor of Philosophy

Division of BioMedical Sciences

Faculty of Medicine

Memorial University of Newfoundland

September 2009

Abstract

The overall objective of this study was to investigate the role that the small heat shock protein Hsp27 plays in neurite initiation and growth, through its regulation of the neuronal cytoskeleton. The present investigation was carried out using adult rat dorsal root ganglion (DRG) neurons to study the behavior of neurite initiation and extension.

The extracellular environment triggers the production and extension of a neurite via extracellular cues. To trigger morphological changes in the neuron these cues must be transformed into signals that converge on the cytoskeleton. The cytoskeletal components, such as actin, tubulin and neurofilament light chain (NF-L), can be modified though interaction with other cellular proteins, including Hsp27. Hsp27 is regulated through intracellular signaling cascades, and has been demonstrated to interact with cytoskeletal components. This positioning of Hsp27 as a possible transducer of extracellular signals to the cytoskeleton formed the basis for my hypothesis that Hsp27 plays a role in neurite growth.

In Chapter 2 I showed that Hsp27 was present and colocalized with actin and tubulin in lamellipodia, filopodia, focal contacts, neurite shafts, branch points and growth cones during the stages of neurite formation and growth. The use of upstream p38 MAPK pharmacological inhibitors attenuated Hsp27 phosphorylation resulting in aberrant neurite growth. Further study of the effects of the p38 MAPK inhibitors in Chapter 5 indicated they increased F-actin levels in the neuron, suggesting a link between Hsp27 phosphorylation and actin dynamics in neurite growth.

Chapter 3 confirmed the importance of the presence, and protein level of Hsp27 in neurite growth. Small interfering RNA (siRNA) was used to knock down endogenous Hsp27 protein levels in the DRG neurons, resulting in decreased neurite growth and altered actin localization. Alternatively, overexpression of Hsp27, resulted in increased neurite growth.

An attempt was made to clarify the role of Hsp27 phosphorylation in Chapter 4; this was done using rodent hamster Hsp27 constructs with mutations in their serine 15, and serine 90 phosphorylation sites to mimic either constitutively nonphosphorylated or constitutively phosphorylated Hsp27. Results suggested that the phosphorylation state of Hsp27 plays a role in neurite growth; specifically, constitutive phosphorylation of either site was inhibitory to neurite growth.

These results support my hypothesis that Hsp27 is involved in neurite growth via regulation of the actin cytoskeleton, although the underlying mechanisms have not been fully elucidated in neurons.

Acknowledgements

I wish to thank Dr. Karen Mearow for all of her encouragement, support and guidance throughout this process, both academic and otherwise. Thank you for your help in opening doors to so many amazing opportunities for me, for allowing me the opportunity to move to Newfoundland and carry out your research visions, as well as the ability to attend conferences, and publish my findings. I truly appreciate all that you have done.

I would also like to thank Dr's Terry Lynn Young and Daniel MacPhee who served as members of my supervisory committee for their comments, suggestions and support.

Thanks to Dr. Jules Dore for the much appreciated technical advice.

Special thanks are due to Masuma Rahimtula and Firoozeh Nafar for their assistance in various aspects of this project, and their continuing support.

I would like to thank my lab mates for their support. Thanks Elaine and Budd for helping me get settled and showing me the ins and outs of the lab. Thank you Sherri for your friendship, and always being there to bounce ideas off of. Thanks to Mike for your friendship and enthuasism.

I wish to acknowledge the support of the Natural Sciences and Engineering Research Council for funding my experiments.

Table of Contents

List of Figures

List of Abbreviations

+TIPS	plus end tracking proteins
ADP	adenosine diphosphate
Ala(A)	alanine
ANOVA	analysis of variance
APC	adenomatous polyposis coli
Akt/PKB	protein kinase B
AraC	cytosine arabinoside
Arg /A	arginine
Arp2/3	complex of actin related proteins 2 and 3
ATP	adenosine-5'-triphosphate
BAD	Bcl-2 associated death promoter
Bcl-2	B-cell lymphoma 2
BDNF	brain derived neurotrophic factor
cdc42	cell division cycle 42
cAMP	cyclic adenosine monophosphate
cGMP	cyclic guanosine monophosphate
CHO	chinese hamster ovary cell line
CLIPs	cytoplasmic linker proteins
CLASP	CLIP-associated protein
CMT	Charcot-Marie Tooth disease
CNS	central nervous system
CP	capping protein
CytD	cytochalasin D
DNA	deoxyribonucleic acid
dHMN	distal hereditary motor neuropathy
DRG	dorsal root ganglion
EB	end binding protein
Ena	'enabled' protein
ECL	enhanced chemiluminesence
ECM	extracellular matrix
EGFP	enhanced green fluorescent protein
F-actin	filamentous actin
FAK	focal adhesion kinase
G-actin	globular actin
GDNF	glial cell line derived neurotrophic factor
GDP	guanosine diphosphate
GFAP	glial fibrillary acidic protein
Glu (E)	glutamic acid
GTP	guanosine triphosphate
HeLa	HeLa cell line

HRP	horseradish peroxidase
HSF	heat shock transcription factor
HSP	heat shock proteins
Hsp27/ HspB1	heat shock protein 27
Hsp20	heat shock protein 20
Hsp70	heat shock protein 70
IB4+ve	*griffonia simplicifolia* isolectin B4 binding DRG neurons
ICC	immunocytochemistry
KIFs	kinesin superfamily of proteins
KIF1A	kinesin family member 1A
KPS	Lysine-Proline-Serine
LN	laminin
MAG	myelin associated glycoprotein
MAPs	Microtubule associated proteins
MAP1	Microtubule associated protein family 1
MAP2	Microtubule associated protein family 1
MAP2c	Microtubule associated protein 2c
MAP1A	Microtubule associated protein 1A
MAP1B	Microtubule associated protein 1B
MAPK	mitogen activated protein kinase
MK3	MAP kinase-activated protein kinase 3
MK5	MAP kinase-activated protein kinase 5
MKK2	mitogen activated protein kinase activated protein kinase-2
NB	neurobasal
NEFL	neurofilament light chain gene
NF	neurofilament
NF-H/ NF-200	neurofilament heavy chain
NF-L	neurofilament light chain
NF-M	neurofilament medium chain
NGF	nerve growth factor
NT-3	neurotrophin 3
OD	optical density
P38 MAPK	p38-mediated mitogen activated protein kinase
PBS	phosphate buffered saline
PC12	pheochromocytoma cell line
PDZ	post synaptic density protein domain
PH	plextrin homology
pHsp27	phosphorylated Hsp27
PI45P2	Phosphatidylinositol (4,5) biphosphate
PKC	protein kinase C
PKD	protein kinase D
PL	polylysine
PNS	peripheral nervous system
Rac1	ras-related C3 botulinum toxin substrate 1

RET	transmembrane tyrosine receptor kinase
RhoA	Rho associated coiled-coil kinase
RNA	ribonucleic acid
RNAi	interfering RNA
ROCK	RhoA kinase
SB	p38 MAPK inhibitor - SB203580 and SB202190
SDS PAGE	sodium dodecyl sulfate polyacrylamide gel electrophoresis
Ser (S)	serine
SEM	standard error of the mean
sHSP	small heat shock protein family
siRNA	small interfering RNA
TBS	tris-buffered saline
TBS-T	tris-buffered saline plus tween-20
TGF- β	transforming growth factor beta
Thr	threonine
TIFF	tagged image file format
Trk	tropomyosin-related kinase
TrkA	tropomyosin-related kinase A
TrkB	tropomyosin-related kinase B
TrkC	tropomyosin-related kinase C
TTL –	tubulin tyrosine ligase
VASP	vasodilator-stimulated phosphoprotein
WDPF	tryptophan - aspartic acid - proline - phenylalanine

CHAPTER 1 INTRODUCTION

1.1 Hsp27 in neurite regeneration

The main hypothesis for this thesis is that Hsp27 directly and indirectly interacts with the neuronal cytoskeleton to influence neurite initiation and growth patterning required for neurite regeneration. The introduction will focus on areas of relevance to this thesis, namely, axonal regeneration and *in vitro* models of eliciting neurite growth, regulation of the cytoskeleton in stages of neurite initiation and growth patterning, Heat Shock Proteins (HSPs), the role of Hsp27 in survival, and interactions between Hsp27 and the actin, microtubule and neurofilament cytoskeleton that may be involved in neurite growth.

1.1.1 Regeneration

In order to regain function following axon injury, regeneration of an operational connection is necessary. Three steps are required in this process: the injured neuron must survive, the damaged axon must be able to extend to innervate its original target, and the axon must be remyelinated and form functional synapses on the target. Both the survival of the injured neuron and its ability to form functional synapses depend on its ability to extend and grow precisely to reinnervate its target. The extension and regrowth of the damaged axon requires the formation of a growth cone at the tip of the transected axon. Growth cones are the active structures that regulate neurite extension and guidance during development and regeneration (reviewed in Huber et al., 2003). Growth cones are able to elicit a specific growth response by using surface receptors to recognize guidance

cues and transduce these cues into physical rearrangement of cellular components via signaling cascades. Activation of a surface receptor triggers a specific intracellular signaling pathway, the stimulation of different receptors engage different signaling intermediates to obtain receptor specific effects. For example, pathways that signal to promote growth and regeneration are triggered by the presence of growth factors (neurotrophins – NGF, BDNF, and GDNF) and extracellular matrix proteins such as laminin, collagen and fibronectin (Teng and Tang, 2006; Tucker and Mearow, 2008). Compounds that signal to inhibit growth are triggered by components of myelin (myelin-associated glycoprotein (MAG) (McKerracher et al., 1994), Nogo (Chen et al., 2000; GrandPre et al., 2000), and the oligodendrocyte-myelin glycoprotein (OMgp)(Liu et al., 2006)) and the component of the ECM, chondroitin sulfate proteoglycans (Cafferty et al., 2007; Galtrey and Fawcett, 2007). Whether a particular environment is permissive or non-permissive for growth will depend upon the sum of the intracellular signaling cascades that are activated within the cell. In the central nervous system (CNS), axons do not regenerate to any great extent after injury, this is thought to be primarily due to the non-permissive growth environment, as well as an absence of appropriate growth promoting factors, resulting in a retraction bulb instead of a growth cone at the tip of the proximal axon stump (Erturk et al., 2007). In the peripheral nervous system (PNS), axons generally regenerate quite well, relative to CNS axons (Fenrich and Gordon, 2004; Fu and Gordon, 1997; Stoll et al., 2002).

The PNS is composed of all nerves lying peripheral to the pial covering of the CNS and include the craniospinal and autonomic nerves. Besides being a permissive

environment for the axonal growth of PNS axons, the PNS is also a permissive environment for CNS axonal growth, likely due to its growth stimulating extracellular matrix components such as laminin, collagen and fibronectin (Fu and Gordon, 1997; Grimpe and Silver, 2002; McKerracher et al., 1996; Vogelezang et al., 2001; Vogelezang et al., 1999).

1.1.1.1 *In vitro* models of axonal growth or regeneration

The finding that both CNS and PNS neurons will regenerate their neurites in a permissive environment has led to *in vitro* models being widely used to study the growth behavior of neurite initiation and extension in both CNS and peripheral neurons. In many models, neurotrophin stimulation is required for survival as well as to elicit neurite growth. Another widely used paradigm involves eliciting neurite growth by stimulating neurons with soluble laminin (Kohno et al., 2005). This approach is particularly useful in mature dorsal root ganglion (DRG) neurons where not all cells respond to a given neurotrophin (Tucker et al., 2006), and where neurotrophins are not required for survival of the mature neurons in culture.

1.1.1.2 Dorsal Root Ganglion neurons

DRG neurons are sensory neurons that carry information from the periphery to the CNS via a single extensive axon. The cell body, located in the dorsal root ganglion, puts out a single axon that bifurcates and sends one process centrally through the dorsal root of the spinal cord to synapse in the dorsal aspect of the spinal cord, and the other process

is sent peripherally to innervate either the skin, muscle or visceral organs (Devor, 1999) (Figure 1.1). Due to the pseudounipolar morphology of the DRG neuron it is difficult to determine which neuronal process is the axon and which is the dendrite when using *in vitro* cultures, and for this reason the process is usually called a neurite and will be referred to as such. *In vivo* the peripheral branch of the DRG neurite is able to regenerate while the central branch is generally considered to be unable to regenerate (Cai et al., 2001; Cao et al., 2006; Erturk et al., 2007).

The mature mammalian DRG is composed of a heterogeneous population of cells characterized by their neurochemistry, morphology, trophic requirements, and sensory modalities (Averill et al., 1995; Gavazzi et al., 1999; Ishikawa et al., 2005; Petruska et al., 2000; Priestley et al., 2002). In practice neurons of the DRG are classified into three primary categories: (1) Large and medium diameter neurons, that typically have large myelinated axons. These neurons are identified by their expression of neurofilament heavy chain (Averill et al., 1995; Ishikawa et al., 2005; Priestley et al., 2002; Tucker et al., 2006), and also express the p75 neurotrophin receptor and TrkC, although the presence of TrkA and TrkB receptors are also reported (Averill et al., 1995; Ishikawa et al., 2005; Priestley et al., 2002). These neurons are therefore able to respond to NT-3, NGF and BDNF which correspondingly bind to TrkC, TrkA, and Trk B. (2) Peptidergic neurons, consisting of both unmyelinated neurons with a small cell diameter, and cells with a medium cell diameter and small myelinated axons. Cells in this population express high levels of both the p75 neurotrophin receptor and TrkA, and therefore respond preferentially to NGF (Averill et al., 1995; Ishikawa et al., 2005; Priestley et al., 2002). (3) Non-peptidergic neurons

Figure 1.1: Location of the DRG neuron

The Dorsal Root Ganglion, located peripheral to the spinal cord, contains the cell bodies of the dorsal root ganglion neurons. Dorsal root ganglion neurons put out a single axon that bifurcates and sends one process centrally through the dorsal root of the spinal cord to send signals to the brain, and the other process is sent peripherally to innervate either the skin, muscle or visceral organs. (Erturk et al., 2007).

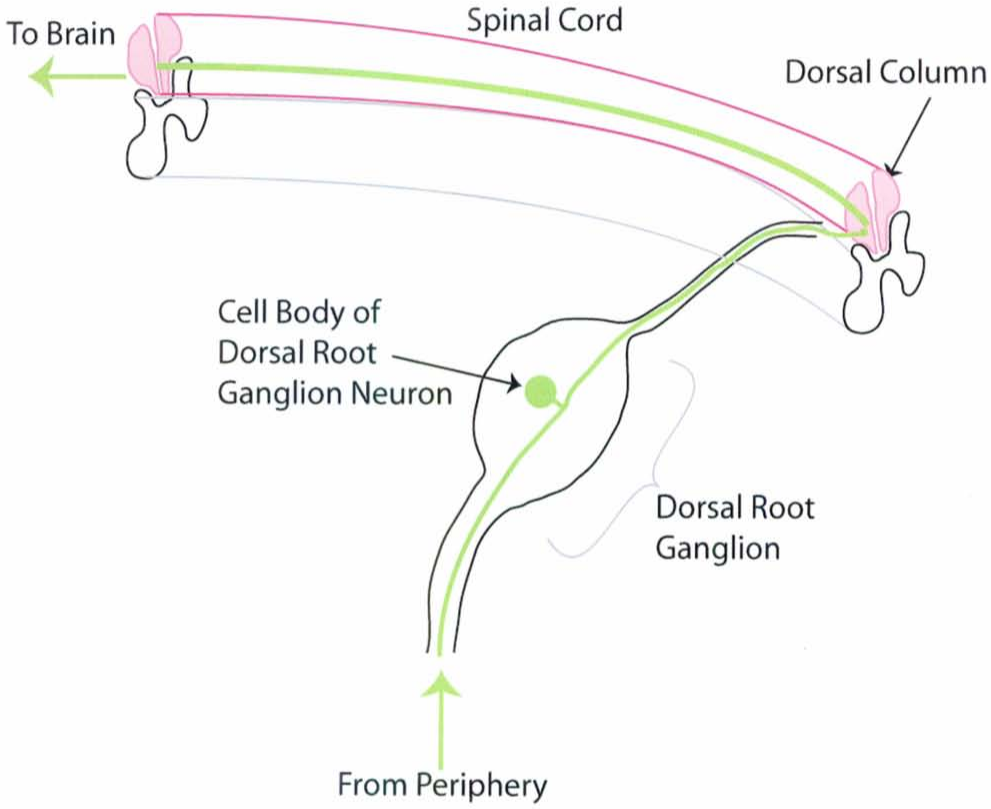
To Brain
Spinal Cord
Dorsal Column
Cell Body of
Dorsal Root
Ganglion Neuron
Dorsal Root
Ganglion
From Periphery

characterized by their ability to bind the lectin *Griffonia Simplicifolia* IB4, have primarily cell bodies with a small diameter and unmyelinated axons (Averill et al., 1995; Ishikawa et al., 2005; Priestley et al., 2002). These neurons are reported not to express the p75 or Trk receptors and are therefore unresponsive to NGF, NT3 and BDNF, however they do express the RET receptor and do respond to GDNF (Bennett et al., 1998; Kashiba et al., 2001; Molliver et al., 1997). The different expression of neurotrophin receptors within the three populations permits the regeneration of subpopulations of DRG neurons to be studied individually with differing neurotrophins. Additionally, because adult DRG neurons are not dependant on neurotrophins for survival, ECM components, such as laminin, may be used to stimulate neurite growth from the DRG neurons as an entire group, thus obviating complications of neurotrophin signaling or non-responsive populations.

1.1.2 The role of the cytoskeleton in neurite growth

Since Ramon y Cajal first observed the growth cone in sections of embryonic spinal cord stained with silver chromate (Cajal, 1890), scientists have been intrigued by the shape of neurons and the actions of their growth cones. In the early 20th century it was confirmed that a filamentous structure described by Cajal as a neurofibril network arose in the cell body and extended into the neurite (Cajal, 1928). It has since been discovered that Cajal's neurofibrillar network, now referred to as the neuronal cytoskeleton, consists of actin filaments, microtubules, and intermediate filaments, and that these components are essential in maintaining neurite structure. Additionally neurite initiation and growth patterning including extension, branching, and growth cone turning,

occur via extracellular regulation of actin filaments and microtubules. Compounds in the extracellular environment are recognized by cell surface receptors on the neuron and transformed into intracellular signals that converge on the cytoskeleton and result in morphological changes. In addition to cytoskeletal rearrangement these processes require synthesis and transport of cytoskeletal and membrane components to the site of growth for incorporation into the growing structure.

1.1.2.1 Neurite structure

The neurite can be structurally divided into two distinct regions; the neurite shaft, and the distal tip of the growing neurite referred to as the growth cone (Figure 1.2). The neurite shaft comprises the majority of the length of the neurite and is primarily used for transport. All three cytoskeletal components are present in the neurite shaft. Microtubules are bundled into a dense parallel array and give structure to the neurite as well as tracks for molecular motors to transport cargo. Neurofilaments are also bundled in the shaft and influence the diameter and conduction velocity of the neurite. Actin filaments are present directly under the cell membrane that surrounds the microtubules and neurofilaments. Observing the physical location of cytoskeletal elements in the neurite highlights how they are positioned to be involved in forming and regulating the structure of the neurite.

The growth cone consists of three domains: the peripheral domain, the transition domain and the central domain (Figure 1.2). The peripheral domain is an actin rich domain comprised primarily of the higher order actin structures lamellipodium and

Figure 1.2: Structure of the neurite

The neurite consists of two structural domains, the neurite shaft and the growth cone. Within the neurite shaft microtubules are bundled and give structure to the neurite, these bundles splay as they enter the central domain of the neurite. Neurofilaments are also found in the shaft and influence the diameter and conduction velocity of the neurite. Actin filaments are present directly under the cell membrane that surrounds the microtubules and neurofilaments. The growth cone consists of three domains: the peripheral domain, the transition domain and the central domain. The peripheral domain is actin rich and contains actin filaments in lamellipodium and filopodia. The transition domain is the interface between the peripheral and central domains, the actin filaments in this region limit how far microtubules from the central domain penetrate into the peripheral domain.

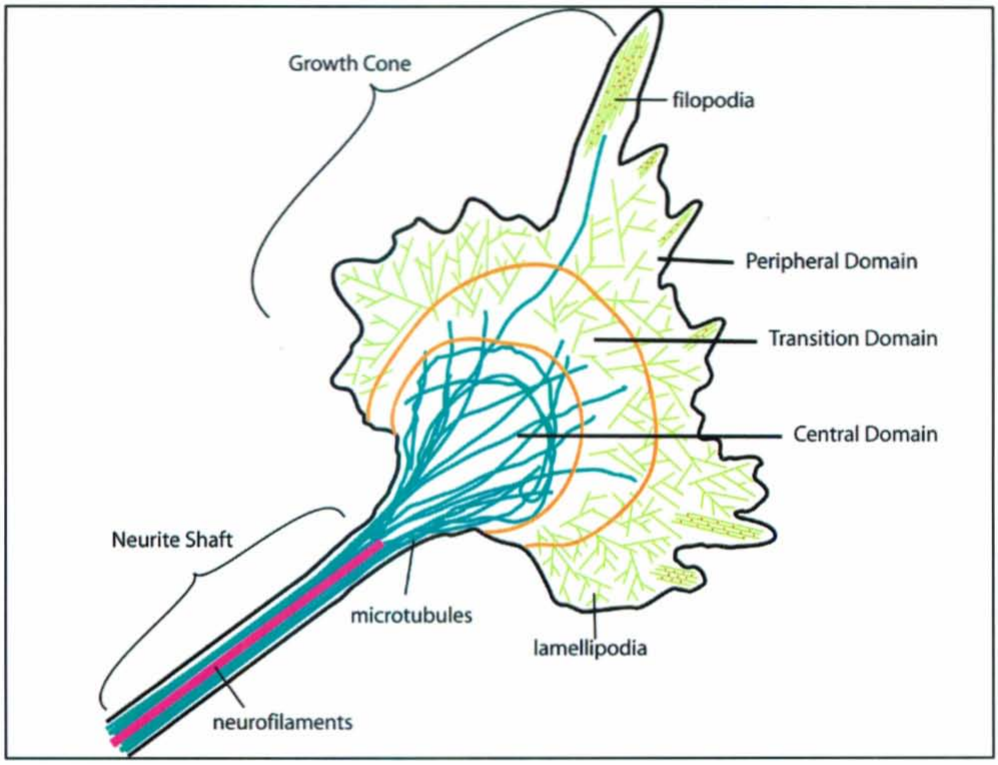
Growth Cone
filopodia
Peripheral Domain
Transition Domain
Central Domain
Neurite Shaft
microtubules
lamellipodia
neurofilaments

filopodia undergoing constant elongation and retraction as they are reorganized in response to the surrounding environment they are probing. The transition domain is the interface between the peripheral and central domains. Proteins in this region induce the formation of an actin rich arc that contacts microtubules from the central domain and limits how far the microtubules penetrate into the peripheral domain. The central domain contains microtubules, organelles, vesicles and neurofilaments. Microtubules in the central domain are no longer bound into dense bundled arrays as in the neurite shaft, instead they are splayed apart and even form loops during periods of growth cone pausing (Dent and Gertler, 2003; Dent and Kalil, 2001; Pak et al., 2008).

1.1.2.1.1 Actin in the neurite

The protein actin comprises many of the structures that determine the shape of the neuron and because it forms dynamic structures it imparts flexibility to the cell allowing it to change shape to respond to varying conditions. As mentioned previously, the active structure of the growing neurite is the growth cone. The growth cone is a highly motile structure whose growth can be specifically regulated in order to find its way to a particular location in the body. Within the cell, actin exists in two states: actin monomers, also known as globular actin (G-actin) and actin filaments, also known as microfilaments and filamentous actin (F-actin), and these filaments associate to form higher order actin structures lamellipodium and filopodia. The fine and precise directional movements of the growth cone are due to the regulation of actin via actin binding proteins. Actin binding proteins can regulate actin filament assembly, bundle or

crosslink actin into higher order structures, attach actin filaments to membranes and the ECM, or act as actin motor proteins.

Actin filaments are bi-helical polymers of actin monomers that assemble (polymerize) and disassemble (depolymerize) by the addition and removal of actin monomers at the ends of the polymer. Actin monomers are asymmetric and associate in a specific orientation leading to the filaments being a polar structure (Choo and Bray, 1978). The polarity of the actin filament results in the ends of an actin filament polymerizing at different rates; the rapidly growing end is the barbed end and the slower growing end, and the end with the greatest depolymerization, is the pointed end. *In vitro* actin monomers interact with adenine nucleotides, ATP or ADP, to promote the addition of monomers at the barbed end and their removal at the pointed end (Figure 1.3) (Korn et al., 1987). A variety of actin binding proteins regulate actin filament assembly by catalyzing ATP/ADP exchange, sequestering G-actin, promoting formation of new actin filaments (nucleation see Figure 1.4) and to stabilize or destabilize actin filaments in order to promote or inhibit reorganization of the actin cytoskeleton (Figure 1.5). Additionally plants, fungi and sponges have created a series of toxins as self defence mechanisms that bind to actin in similar ways as actin binding proteins, when purified these toxins are useful in the study of actin filament dynamics (Table 1.1).

Even when under steady state conditions actin filaments are dynamic and undergo a phenomenon known as treadmilling. During treadmilling the rate of polymerization at the barbed end is equal to the rate of depolymerization at the pointed end, resulting in the filament maintaining a constant length even though there is a net flux of subunits moving

Figure 1.3: Actin filament structure and treadmilling

In vitro actin monomers interact with adenine nucleotides, ATP or ADP, in a manner that promotes the addition of monomers at the barbed end and their removal at the pointed end. ATP bound actin (yellow) is preferentially added to the barbed end of actin filaments and after its incorporation into the filament the ATP is hydrolyzed to ADP (orange) and inorganic phosphate (Pi)(blue). After hydrolysis the phosphate initially remains bound to the ADP and is slowly released, after release the ADP bound actin has a reduced binding affinity for its neighboring subunits and is easily dissociated from the pointed end (Korn et al., 1987).

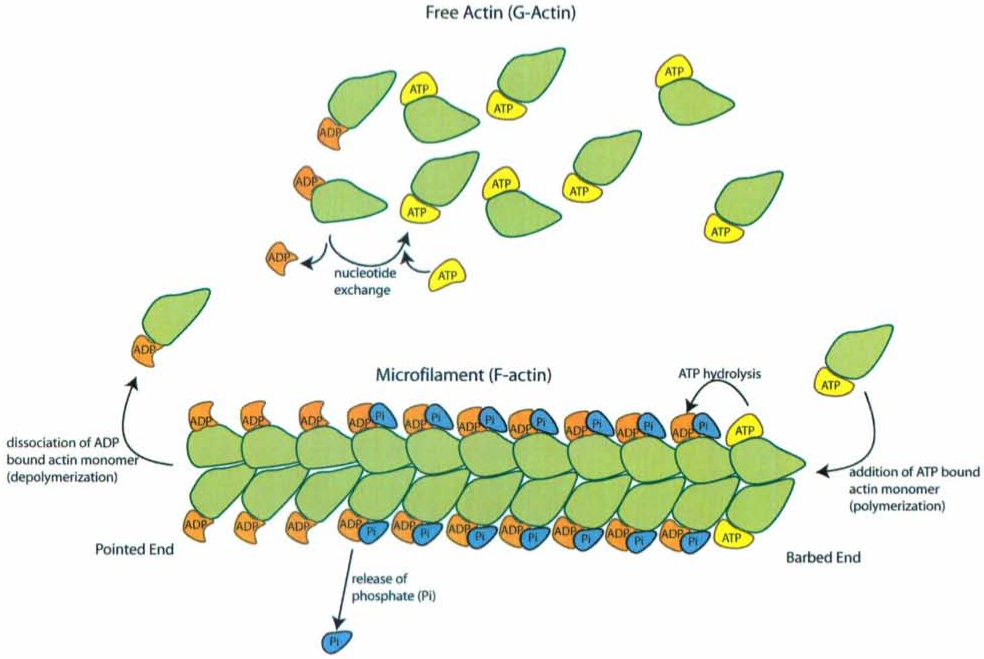
Free Actin (G-Actin)
ATP
ADP
nucleotide exchange
Microfilament (F-actin)
ATP hydrolysis
dissociation of ADP bound actin monomer (depolymerization)
addition of ATP bound actin monomer (polymerization)
Pointed End
Barbed End
release of phosphate (Pi)
Pi

Figure 1.4: Nucleation

Nucleation by an actin binding protein is required to catalyze actin filament formation because two actin monomers alone have a weak attraction for each other and rarely associate long enough for the addition of more monomers, however a trimer of actin monomers bind tightly and facilitates elongation of the filaments (Cooper et al., 1983; Frieden, 1983; Tobacman and Korn, 1983). Actin binding proteins act as actin nucleators and facilitate the formation of a trimer of actin subunits, and therefore assist in overcoming the rate-limiting step in actin filament growth. Formin induces the formation of unbranched actin filaments by barbed end nucleation and elongation (Goode and Eck, 2007), whereas the Arp2/3 complex is thought to require a pre-existing filament from which a new branch can be initiated, and therefore creates highly branched actin networks (Mullins et al., 1998).

Nucleation

Formin

nucleate assembly and remains associated with barbed end

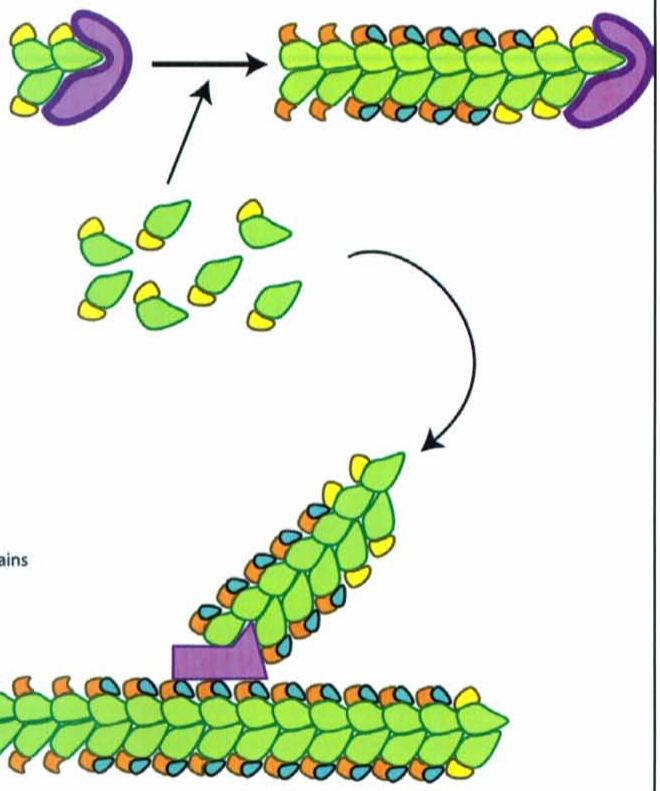

Arp2/3 complex

nucleates assembly of branches and remains associated with minus end branch point

Figure 1.5: Regulation of actin filament levels

Decreases in the levels of filamentous actin can be achieved by actin binding proteins in numerous ways such as by promoting disassembly, preventing assembly and severing existing filaments. The protein cofilin is involved in the disassembly process in two ways; it can sever actin filaments and additionally can bind to ADP-actin to catalyze depolymerization (Bamburg et al., 1999). Gelsolin also severs actin filaments, and additionally caps the filaments barbed ends to prevent them from elongating (Huang et al., 2006; Ono, 2007). Thymosin binds actin monomers and prevents their addition to the actin filament (Dedova et al., 2006). Capping protein (CP) binds to the barbed end of actin filaments to prevent assembly and disassembly at this end, however CP has no effect on the pointed end where continued disassembly will result in a shorter filament (Cooper and Sept, 2008).

Actin binding proteins can also act to increase the levels of filamentous actin in the cell by stabilizing the actin filament, promoting polymerization, and nucleating new filaments. Actin filaments may be stabilized by actin binding proteins that preventing the interaction of other "harmful" actin binding proteins with the actin filament. Tropomyosin stabilizes actin filaments by binding and affecting the filament shape in a manner that promotes further binding of tropomyosin and prevent cofilin from binding (Ono and Ono, 2002). Polymerization of the actin filament can be promoted by proteins such as profilin that bind to actin monomers and facilitate their addition to the barbed end of the actin filament by catalyzing actin nucleotide exchange. Additionally ENA/VASP has been recognized as an actin anti-capping protein, that binds to the barbed end of actin filaments preventing the addition of capping proteins and facilitating the addition of actin monomers (Bear et al., 2002).

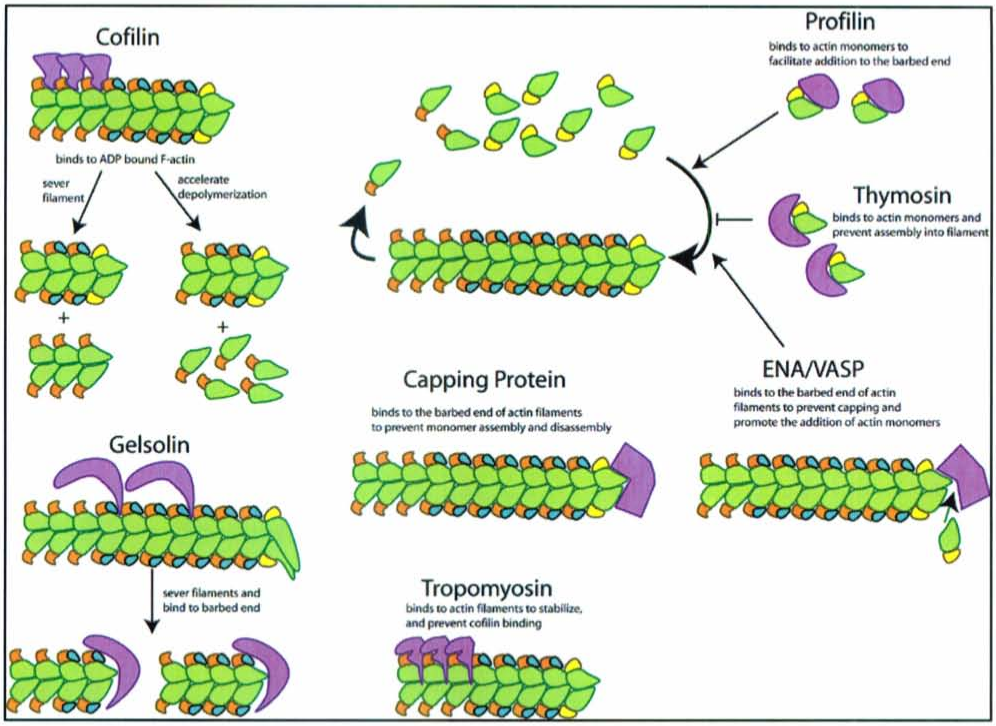
Cofilin
binds to ADP bound F-actin
sever filament
accelerate depolymerization
+
+
Profilin
binds to actin monomers to facilitate addition to the barbed end
Thymosin
binds to actin monomers and prevent assembly into filament
ENA/VASP
binds to the barbed end of actin filaments to prevent capping and promote the addition of actin monomers
Capping Protein
binds to the barbed end of actin filaments to prevent monomer assembly and disassembly
Gelsolin
sever filaments and bind to barbed end
Tropomyosin
binds to actin filaments to stabilize, and prevent cofilin binding

Table 1.1: Drugs that can alter actin filament polymerization

Drug	Binding Action	Result
Phalloidin	Binds and stabilizes actin filaments	Net increase in actin filaments (Dancker et al., 1975)
Cytochalasin	Binds barbed end of actin filaments, promotes the depolymerization of actin filaments	Loss of actin filament dynamics (Cooper, 1987)
Jasplakinolide	Binds and stabilizes actin filaments (is membrane permeable – unlike Phalloidin)	Net increase in actin filaments (Xie and Forer, 2008)
Latrunculin A	Binds monomeric G-actin to inhibit actin polymerization	Net decrease in actin filaments and filament dynamics (Wakatsuki et al., 2001)

filament maintaining a constant length even though there is a net flux of subunits moving through the filament (Theriot, 1997; Wegner, 1976). In migrating cells and growth cones the cells harness actin filament treadmilling to obtain forward protrusion of actin structures. The prevailing hypothesis for this protrusion is the molecular clutch model illustrating that physical coupling between the ECM and actin filaments allows traction forces to be transmitted to the substrate, resulting in local stopping of treadmilling and continued polymerization resulting in forward progression of the actin filament (Figure 1.6) (Bard et al., 2008). Actin binding proteins, such as ankyrins, vinculin, talin, α-actinin and catenin, that are able to link actin filaments to the plasma membrane by binding to integral membrane proteins, play an important role in the formation of the molecular clutch in response to extracellular cues (Bennett and Baines, 2001; Clark and Brugge, 1995).

In vitro actin filaments are able to form higher order structures such as the mesh like gel in lamellipodium, and the linear bundles in filopodia. These higher order structures are dependent on actin binding proteins to facilitate the attachment of separate actin filaments to one another (Figure 1.7) and to facilitate attachments to the ECM in order to assist in protrusion as described by the molecular clutch model.

Lamellipodium are found in the motile structures of migrating cells and in growth cones and consist of a branched network of actin filaments, undergoing treadmilling, with their barbed ends facing the plasma membrane and the pointed ends directed towards the interior of the cell or neurite (Figure 1.8). The branched network is achieved by actin binding proteins clamping filaments together at right angles, and by new

Figure 1.6: The molecular clutch model of actin based protrusion

A. Actin filaments undergo treadmilling *in vitro*, during treadmilling the rate of subunit addition at the barbed end is equal to the rate of depolymerization at the pointed end, resulting in the filament maintaining a constant length, even though there is a net flux of subunits moving through the filament. Retrograde flow of the actin filament result in the actin filament remaining stationary within the cell. **B**. Actin binding proteins that crosslink the actin filament to the membrane and extracellular matrix act as a molecular clutch by physically coupling the ECM to the actin filament allowing traction forced to be transmitted to the substrate and continued actin filament polymerization result in forward protrusion of the actin filament and membrane (**C**).

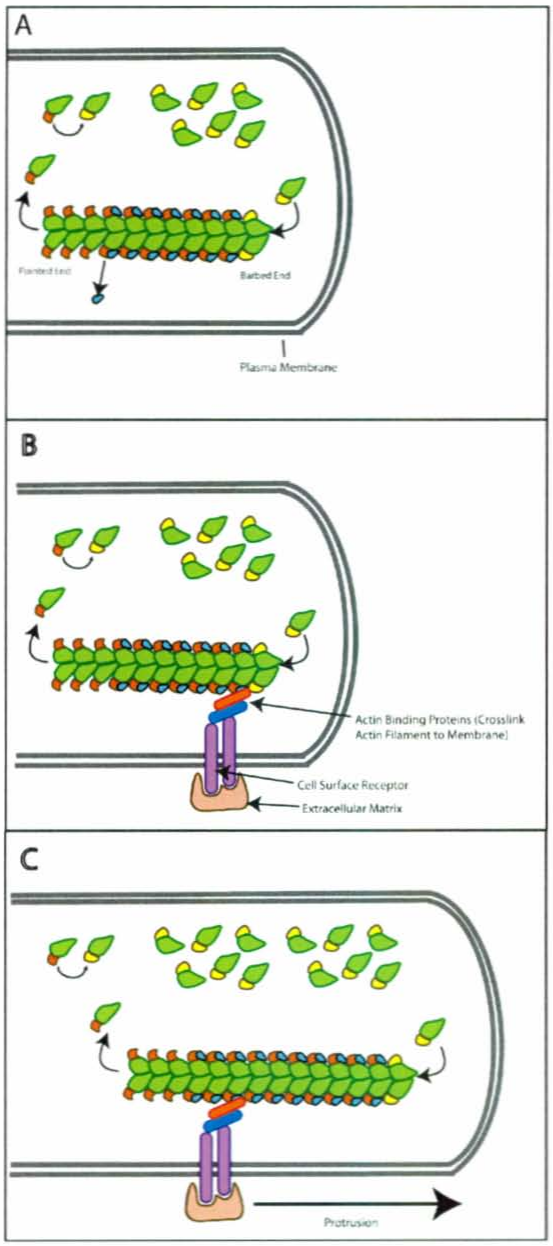
A
Pointed End
Barbed End
Plasma Membrane
B
Actin Binding Proteins (Crosslink
Actin Filament to Membrane)
Cell Surface Receptor
Extracellular Matrix
C
Protrusion

Figure 1.7 : Proteins that bundle and crosslink actin filaments

Actin binding proteins that bundle actin filaments, such as fascin, have two actin binding sites close together resulting in actin filaments being bound together into stiff parallel bundles (Jawhari et al., 2003). These parallel bundles that can strengthen the cell as actin ribs, and form protrusions into the extracellular space as filopodia which are structures found in growth cones.

Actin binding proteins that result in the formation of an actin filament gel, such as filamin, have two actin binding domain that are connected by a bent linkage resulting in formation of a loose gel by sticking filaments together at roughly right angles (Tseng et al., 2004). Crosslinking of actin filaments into non parallel branched arrays is important in the formation of lamellipodium, a sheet like protrusion filled with a branched network of actin present at the leading edge of motile cells and in growth cones.

Fascin

contain 2 actin binding sites to bundle actin filaments

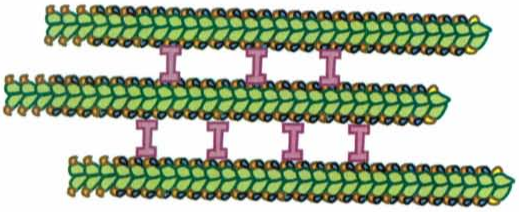

Filamin

contains 2 actin bnding sites connected by a bent arm to link actin filaments into a meshwork

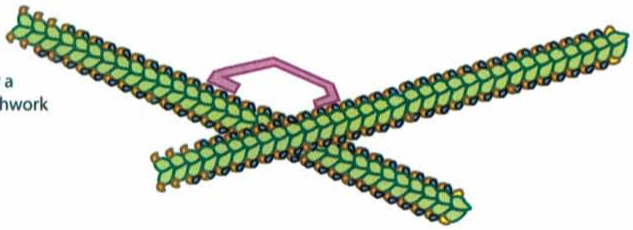

Figure 1.8: Structure of Lamellipodium and Filopodia

Lamellipodium are protrusive veil like structures, composed of a branched network of actin filaments that undergo subunit polymerization at their barbed ends and depolymerization at their pointed ends. In order to achieve and maintain the branched network new filaments are constantly being nucleated as branches off existing actin filaments by the Arp2/3 complex. The depth of the actin filament network is strictly regulated by I capping protein to cap new filaments, limiting their length, and by cofilin aiding in depolymerization at the filament pointed end.

Filopodia are thin finger like protractions filled with actin filaments cross linked by fascin into linear bundles. The actin filaments within filopodia elongate with the assistance of Ena/VASP, to protrude into the ECM. (Figure adapted from Figure 3 Mattila and Lappalainen, 2008).

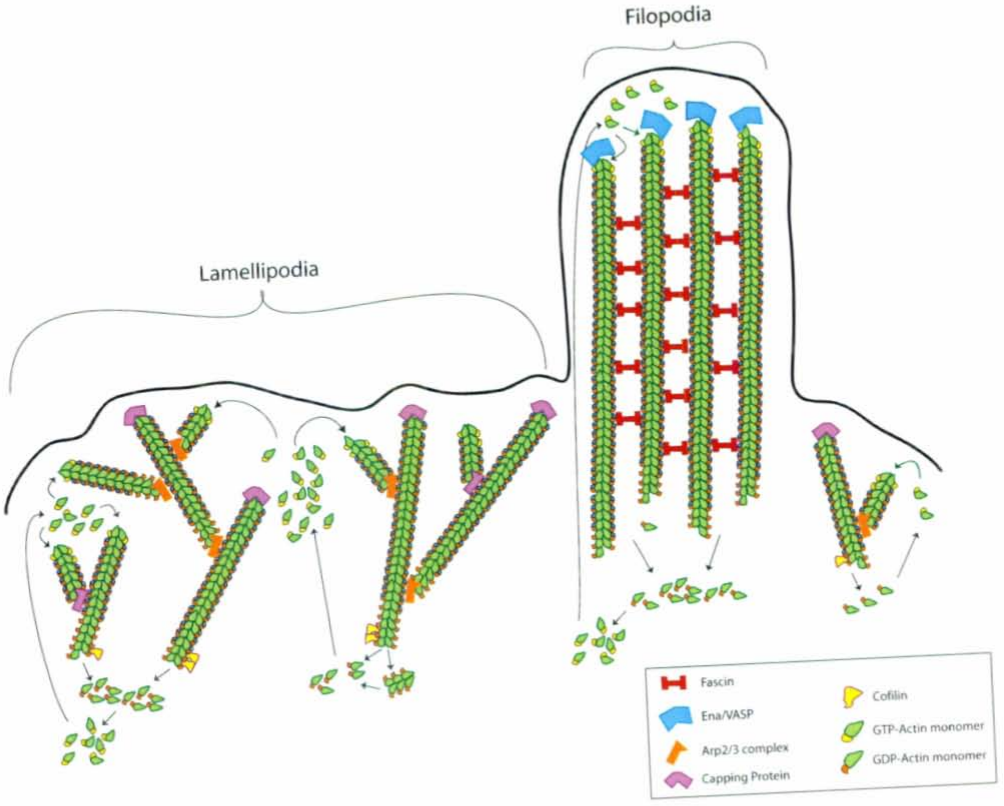
Filopodia
Lamellipodia
Fascin
Ena/VASP
Arp2/3 complex
Capping Protein
Cofilin
GTP-Actin monomer
GDP-Actin monomer

filaments being nucleated by the Arp2/3 complex as branches off existing actin filaments. In order to maintain the length of the actin network individual actin filament length is regulated by capping protein to cap new filaments, additionally cofilin aids in depolymerization at the filament pointed end.

Filopodia are thin finger like protrusions that probe the extracellular environment. The protrusions are filled with tight linear bundles of actin filaments, with their barbed ends pointing towards the plasma membrane (Figure 1.8). Exploratory behavior is promoted by a dynamic balance between actin polymerization at the barbed ends of a filament, and retrograde flow, and depolymerization of the actin filament bundle (Mallavarapu and Mitchison, 1999). Filopodial formation is thought to be initiated by recruitment of either a set of uncapped actin filaments of the Arp2/3 nucleated actin network or formin nucleated actin filaments (Mattila and Lappalainen, 2008). The barbed ends of these filaments are converged together by the activity of the molecular motor myosin-X (see Figure 1.9 for more on actin molecular motors) (Bohil et al., 2006; Tokuo et al., 2007). The force for membrane deformation during filopodial elongation is hypothesized to either come from the elongation of the barbed ends of the bundled actin filaments or by I-bar proteins that bind to the membrane to favor its deformation. The actin filaments elongate with the assistance of Ena/VASP, and are cross linked by fascin to form a stiff filopodial actin bundle (Mattila and Lappalainen, 2008) (Figure 1.8).

Signaling pathways will result in favoring the formation of one actin structure over another by differing in the activation of actin binding proteins in a particular location. The action of actin binding proteins is tightly connected to signal transduction

Figure 1.9: Actin molecular motor myosin

Myosins are a large family of motor proteins that walk along an actin filament in a directed fashion, besides their involvement in muscle contraction they are involved in vesicle and organelle transport in non-muscle cells. The myosin protein (purple) consists of one or two motor heat domains that bind to the actin filament and move along it in an ATP dependant manner (Richards and Cavalier-Smith, 2005). The tail of the myosin is implicated in binding to cargo or other structures in the cell.

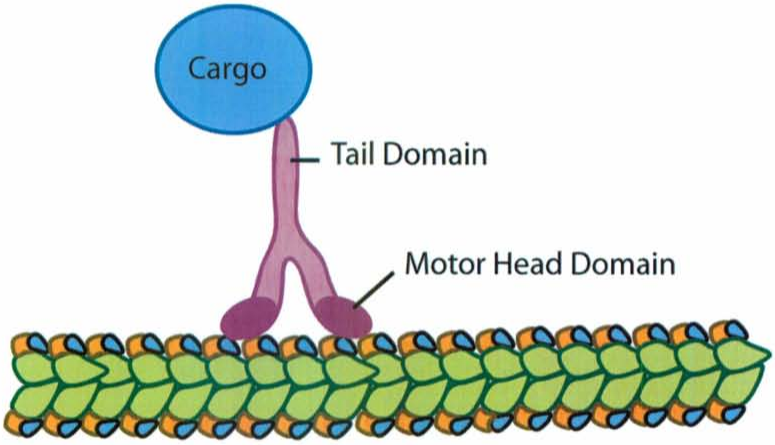
Cargo
Tail Domain
Motor Head Domain

pathways, as they are regulated by second messengers, phospholipids, protein kinases, and other signaling compounds specific for particular extracellular signals. For example, lamellipodium formation requires branching and capping of actin filaments, as well as other proteins to disassemble the pointed end of the structure. Proteins that are involved in the processes of creating and regulating lamellipodium (such as Arp2/3, capping protein, cofilin, and gelsolin) are activated and recruited to regions of lamellipodium formation and maintenance, while proteins that act to inhibit lamellipodium formation are excluded (Bamburg et al., 1999; Korobova and Svitkina, 2008; Mejillano et al., 2004). In contrast, the formation of filopodia requires recruitment of proteins that prevent capping and branching and facilitate of actin filament elongation and bundling, and thus Ena/VASP and fascin are recruited and activated in sites of filopodial formation (Figure 1.8) (Cohan et al., 2001; Korobova and Svitkina, 2008). Therefore by regulating proteins involved in capping, bundling, and filament elongation signaling will regulate the actin filament architecture of the cell.

Activation of small Rho-GTPases by growth factor and integrin receptors are possible mechanisms by which a cell can signal to induce lamellipodium and filopodia formation as both can mediate Rac1 and cdc42 activation (Etienne-Manneville and Hall, 2002; Hall, 1998; Price et al., 1998), and Rac1 activation signals formation of lamellipodium while cdc42 activation results in the formation of filopodia (Nobes and Hall, 1995; Steffen et al., 2004).

1.1.2.1.2 Tubulin in the neurite

Microtubules are an essential part of the neuronal cytoskeleton that gives the axons structure and their phenomenon of dynamic instability plays an important role in axon elongation and retraction. Additionally they comprise the structural tracks on which motor proteins transport cargo from the cell body required for neurite growth maintenance, and signaling to the neurite tip and back.

Microtubules are polarized structures composed of stable tubulin dimers assembled into long hollow cylinders with a diameter of 25nm, and a perimeter of thirteen dimers (Figure 1.10) (Amos, 2000; Luduena, 1998). The microtubule is stiff and difficult to bend due to all of the bonds that are found between the subunits that comprise it. Due to the arrangement of α/β subunits the resulting structure is polarized resulting in the end of the microtubule where β subunits are exposed being referred to as the plus end, and the other end with the α subunits referred to as the minus end. The polymerization and depolymerization activities differ depending on the end of the microtubule, such that the plus end is dynamic and increases and decreases n length, while the minus end is unstable and decreases in length unless it is stabilized (Desai and Mitchison, 1997). Each α or β monomer has one binding site for GTP, although only the GTP binding site on the β-monomer is in a position where nucleotides may be exchanged and therefore may be found with GTP or GDP bound (figure 1.10) (reviewed in Wade, 2007).

Free GTP bound α/β tubulin can be incorporated into the microtubule and its bound GTP is hydrolyzed into a GDP molecule shortly after incorporation. This delay in GTP hydrolysis results in a GTP cap existing on the distal tip of a growing microtubule.

Figure 1.10: Microtubule Structure

A. Tubulin dimers are assembled from one α-tubulin subunit (blue) and one β- tubulin subunit (grey), each α or β subunit has one binding site for GTP. The GTP bound to the α-tubulin monomer is bound in the interface between the α and β monomers and is an integral part of the α/β tubulin heterodimers (orange) whereas GTP binding site on the β-monomer is in a position where nucleotides may be exchanged and therefore may be found with GTP or GDP bound (reviewed in (Wade, 2007)). **B.** The α/β-tubulin heterodimers are arranged lengthwise in a linear array of alternating α and β subunits to form a protofilament. Hydrolysis of the β-tubulin bound GTP to GDP results in a conformational change in the α/β tubulin leading to a slight curvature outwards of the protofilament. **C.** Microtubules are polarized structures composed of tubulin dimers assembled into long hollow cylinders with a diameter of 25nm. Due to the arrangement of α/β subunits the resulting structure is polarized resulting in the end of the microtubule where β subunits are exposed being referred to as the plus end, and the other end with the α subunits referred to as the minus end. **D.** In mammals thirteen protofilaments constitute the circumference of a microtubule. **E.** Free GTP bound α/β tubulin can be incorporated into the microtubule and its bound GTP is converted into a GDP molecule shortly after incorporation, the delay in GTP hydrolysis results in a stable GTP cap existing on the tip of the growing microtubule. **F.** When addition of tubulin dimers occurs faster than GTP hydrolysis the GTP cap is maintained and slow growth of the microtubule occurs. **G.** When GTP hydrolysis occurs faster than α/β tubulin subunit addition the result is the loss of the microtubules GTP cap. The loss of the GTP cap means that the slight curvature from the GDP bound β-tubulin occurs at the tip of the microtubule weakening the bonds between the α/β tubulin protofilament, as a result the microtubule depolymerizes one hundred times faster than when the GTP cap is present.

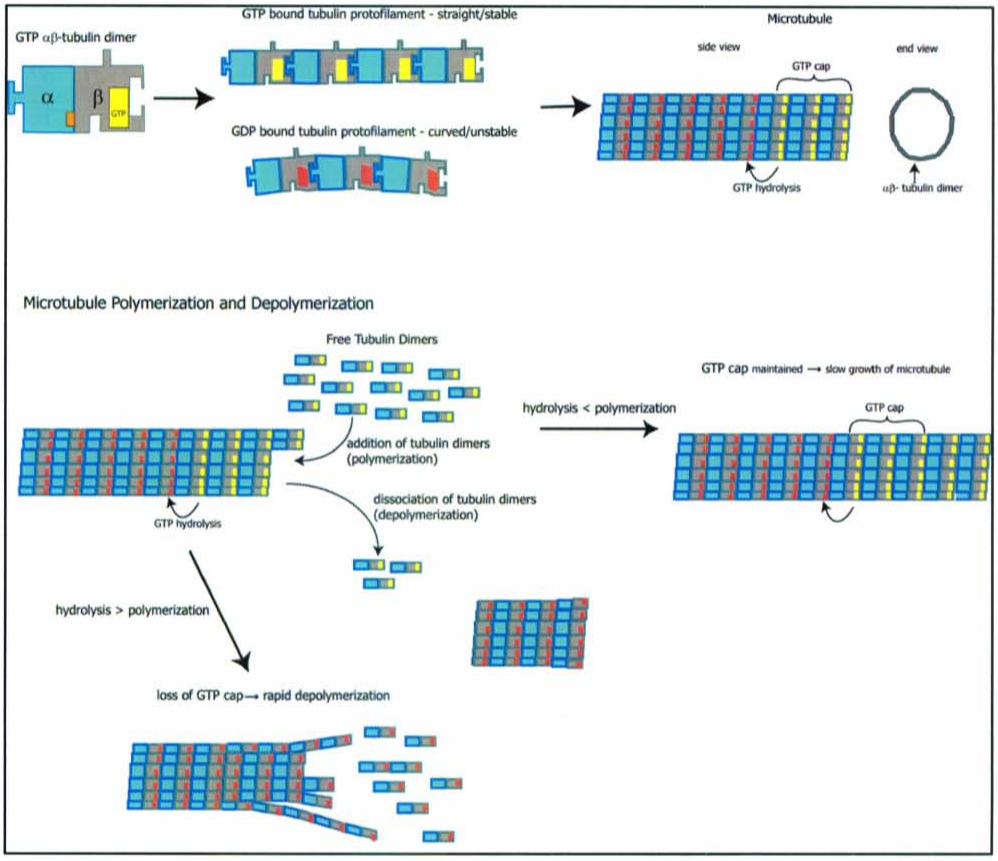
GTP αβ-tubulin dimer
α
β
GTP
GTP bound tubulin protofilament - straight/stable
GDP bound tubulin protofilament - curved/unstable
Microtubule
side view
end view
GTP cap
GTP hydrolysis
αβ- tubulin dimer
Microtubule Polymerization and Depolymerization
Free Tubulin Dimers
addition of tubulin dimers
(polymerization)
GTP hydrolysis
dissociation of tubulin dimers
(depolymerization)
hydrolysis > polymerization
loss of GTP cap → rapid depolymerization
hydrolysis < polymerization
GTP cap maintained → slow growth of microtubule
GTP cap

The GTP cap favors growth by promoting a stabilized microtubule structure (reviewed in Wade, 2007). When GTP hydrolysis occurs faster than α/β tubulin subunit addition the GTP cap is lost and the stabilization of the protofilament is lost with it. GDP bound β-tubulin protofilaments are slightly curved outward and when this occurs at the tip of the microtubule the bonds between the α/β tubulin protofilaments are weakened and as a result the microtubule depolymerizes one hundred times faster than when the GTP cap is present, this rapid depolymerization is referred to as catastrophe. The difference in depolymerization rates between GTP and GDP capped tubulin results in microtubules exhibiting dynamic instability where microtubules alternate between periods of slow growth, where there is a GTP cap in place, and periods of rapid disassembly. During neurite growth this dynamic instability allows for regulated extension and retraction.

Microtubules are nucleated *in vitro*, at a single microtubule-organizing center called the centrosome. Microtubules are nucleated at their minus end, and require the formation of a γ-tubulin ring complex, upon which plus end growth with α/β tubulin heterodimers can occur. In non neuronal cells microtubules primarily remain attached to the centrosome, however this is not the case in neuronal cells as no one microtubule stretches the entire length of the axon, instead the microtubule structure is composed of short overlapping segments of microtubules. In axons microtubules are arranged in the same direction with the plus end pointing towards the axon terminus, however in dendrites the microtubules are arranged in a mixed polarity arrangement.

The functions of α and β tubulin may be regulated by numerous covalent post-translational modifications. Although many of the specific functions of tubulin post-

translational modification have to still be elucidated, it appears that they play a role in distinguishing the age of the microtubule and altering the ability of microtubule binding proteins to bind to the filament, particularly the binding of the kinesin family of motor proteins which transport cargo from the cell body to the neurite tip.

Acetylation and subsequent deacetylation occurs on lysine 40 of α-tubulin after it has been incorporated into the microtubule resulting in high levels of acetylation at minus end of the microtubule and very low levels at the plus end (Brown et al., 1993), and is therefore an indicator of older filaments. Acetylation plays a positive role in motor-based trafficking as the kinesin family of motor proteins binds with higher affinity to acetylated microtubules, and as kinesin transports cargo from the cell body to neurite tip this promotes binding to older microtubules in the proximal neurite shaft and facilitates dissociation at the distal end (Bulinski, 2007; Dompierre et al., 2007; Reed et al., 2006).

Detyrosination and tyrosination affect the ability of two types of microtubule binding proteins to bind to microtubules and plays a role in neuronal organization and neurite extension (Erck et al., 2005). Detyrosinated tubulin results in the C-terminal tyrosine being removed from α-tubulin by an unidentified carboxypeptidase, and results in the recruitment of the family of kinesin molecular motors which bind preferentially to detyrosinated microtubules. Tyrosination results in the addition of a tyrosine to the C-terminal glutamate residue of detyrosinated α-tubulin. This reaction is catalyzed by tubulin tyrosine ligase (TTL) (Verhey and Gaertig, 2007; Westermann and Weber, 2003). The microtubule associated proteins +TIPS binds preferentially to tyrosinated microtubules. Microtubules are highly tyrosinated at their plus end and sparsely

tyrosinated at their minus end (Brown et al., 1993), and this may play a role in the preferential attachment and dissociation of molecular motors. Tyrosinated microtubules tend to be new labile microtubules.

Both α and β tubulin C-terminal tails can undergo polyglutamylation, the addition of glutamate onto existing glutamate residues in the protein. This modification is prevalent in neuronal cells and is involved with the binding of kinesin family protein binding (Ikegami et al., 2007). Additionally neuronal specific β tubulin can be phosphorylated (Hammond et al., 2008) though the functional significance of this modification remains to be elucidated.

Microtubule associated proteins (MAPs) control the actions of microtubules by regulating microtubule dynamics as well as by bundling microtubules and acting as molecular motors to traffic cargo along microtubules. Many of the MAPs are regulated through protein kinases, activated in response to cellular signaling pathways, and result in a close connection between changes in the extracellular environment, and control of the microtubule cytoskeleton. This coupling assists the neurite in probing and exploring the extracellular environment during neurite growth and retraction.

Microtubule dynamics can be regulated by microtubule associated proteins primarily through three mechanisms; (1) by binding to soluble tubulin subunits, (2) through binding to the plus end of microtubules (3) via binding to the side walls of microtubules.

The protein stathmin acts in a phosphorylation-dependant manner to promote disassembly of microtubules by binding to α/β tubulin dimers to prevent their assembly

into microtubules (Belmont et al., 1996; Jourdain et al., 1997; Sobel, 1991; Wittmann et al., 2004). By sequestering a large amount of the free α/β tubulin dimers, stathmin lowers the availability of free α/β tubulin dimers for incorporation, resulting in a decrease in the addition of subunits into the microtubule increasing the likelihood that GTP hydrolysis will occur faster than subunit addition and that the GTP cap will be lost and depolymerization and catastrophe will be favored (Manna et al., 2006).

Plus-end tracking proteins (+TIPs) are multidomain or multisubunit proteins that associate with the plus end of microtubules and have a wide range of functions. Their activities are regulated through phosphorylation, auto regulation and α-tubulin tyrosination/detyrosination. Many +TIPS modulate microtubule dynamics, and have different and sometimes opposing effects on these dynamics. For example the end binding (EB) family of proteins suppress catastrophe (Lansbergen and Akhmanova, 2006), while kinesin 13 family members promote catastrophe (Moores and Milligan, 2006). Cytoplasmic linker proteins (CLIPs) act as microtubule rescue factor and convert shrinking microtubules into growing microtubules (Komarova et al., 2002), while both CLIP-associated protein (CLASP) and adenomatous polyposis coli (APC) act to prevent microtubule catastrophe by coating the plus end to promote rescue and pausing of the microtubule (Galjart, 2005; Lansbergen and Akhmanova, 2006). Many +TIPS contain at least 2 tubulin dimer binding sites and therefore may promote polymerization of short oligomers (Slep and Vale, 2007). Additionally an important function of +TIPS is to link the microtubule to structures within the cell, some +TIPS such as APC and CLASPS are able to link the microtubule directly to the cells actin cortex, or to cortically bound factors

and can achieve targeted delivery of cargoes being transported on the microtubule (Etienne-Manneville et al., 2005; Moseley et al., 2007; Tsvetkov et al., 2007).

Microtubule associated proteins that bind along the side walls of microtubules may act to stabilize, bundle or sever the microtubule in response to signals from kinases to perform various functions. Katanin and Spastin bind to microtubules to sever them; the resulting severed proteins may either degrade because of their unprotected ends, or the shorter microtubules may be stabilized and may be used to probe the extracellular environment during branching, as short microtubules are more mobile (Yu et al., 2008). Microtubule associated proteins that promote the assembly of microtubules by binding to their sides to stabilize them were the first identified microtubule associated proteins and were named MAPs. The function of MAPs can be regulated by phosphorylation and dephosphorylation by protein kinases and phosphatases. Within the MAPs, two major protein families exist: the MAP1 and the MAP2/tau protein families. MAP1A and MAP1B are primarily expressed in neurons where they bind to microtubules to stabilize them. Additionally they have an actin binding domain and are believed to be a link between regulation of the actin filament and microtubule cytoskeleton (Goold and Gordon-Weeks, 2005). The MAP2/tau family of proteins bind to microtubules to stabilize them and also play an additional function in the organization of microtubule bundles. MAP2/tau proteins have two microtubule binding sites connected by a linker that projects away from the microtubule (Dehmelt and Halpain, 2005). This allows for two microtubules to be bound together with the length of the linker determining how closely the MAPS are packed together (Chen et al., 1992).

Microtubule motor proteins bind to the polarized microtubule and use energy from ATP hydrolysis to move along it and transport cargo from one end of the cell to the other. Two types of microtubule motor proteins exist: the kinesin superfamily of proteins (KIFs) and dyneins, both of which are primarily used for long distance transport within the neurite (Hirokawa and Takemura, 2004). Long distance transport in neurons is of importance as *in vivo* axons can reach great lengths, and unlike electrical signals that can be transported very fast in the form of an action potential the cell still needs the physical transport of molecules. For example many compounds that are synthesized in the cell body need to be transported to the axon tips, and correspondingly proteins and activated cellular signaling complexes need to be transported from sites of cellular interactions and stress signaling back to the cell body. The importance of microtubule motor proteins and transport can be observed by the fact that some mutations in motor proteins lead to disease (Zhao et al., 2001).

Two speeds of axonal transport have been observed within the neuron, fast axonal transport is associated with the transport of vesicular cargo necessary for synaptic activity and slow axonal transport is associated with the transport of the axonal cytoskeleton and cytosolic proteins. Initially it was believed that different motors were responsible for the different speeds of transport, however more recent findings (Roy et al., 2000; Wang and Brown, 2001; Wang et al., 2000) suggest that the same proteins are involved in both fast and slow transport and that the rates are the same when moving along the microtubules, but that slow transport is a result of intermittent pausing and bidirectional movement of transported elements.

KIFs transport cargo anterogradely (towards the axon tip) in axons by moving along microtubules towards their plus end (Amaratunga et al., 1993). The majority of KIFs are dimeric, and due to the fact that they have two microtubule binding domains they are able to walk along the microtubule in a hand over hand fashion. Cargo is bound to KIFs either directly or indirectly through adaptors or scaffolding proteins. KIF1A has a PH domain that permits it to bind directly to liposomes via PI45P2 phospholipids (reviewed in (Guzik and Goldstein, 2004)). The domain of kinesin to which the cargo binds appears to be important in directing the cargos transport, as cargo bound to conventional kinesin light chain is transported to axons, where cargo bound to conventional kinesin heavy chain is transported to the dendrites (reviewed in Hirokawa and Takemura, 2004)).

Cytoplasmic dyneins are microtubule motors that transport cargo retrogradely towards the cell body by moving along the microtubules towards their minus end (reviewed in Hirokawa and Takemura, 2004)). Dyneins are comprised of a multisubunit complex of heavy chains, light chains and motor domains. Binding sites within these domains permit the transport of specific cargo; for example the light chain is able to bind to neurotrophin receptors Trk A, B and C and is reported to be involved in the retrograde transport of NGF and Trk to the cell body (Yano et al., 2001). Cytoplasmic dynein associates with the large protein complex dynactin, which mediates the attachment of cargoes to dynein and enhances the processivity of transport (Hirokawa and Takemura, 2004).

1.1.2.1.3 Intermediate filaments in the neurite

Intermediate filaments are classified into five major families based on the cell type they are expressed in and when during development they are expressed (reviewed in (Godsel et al., 2008)). Intermediate filaments are flexible, ropelike fibers of around 10 nm in diameter, a diameter that is "intermediate" between that of actin filaments (6 nm) and microtubules (25 nm) (Herrmann et al., 2000). Intermediate filaments provide dynamic scaffolding to protect cells and tissues from mechanical and nonmechanical forms of stress and their protective roles are enhanced by regulation of intermediate filament associated proteins, intermediate filament mediated signaling events, and the positioning of organelles within the cell (Toivola et al., 2005). In neurons type III intermediate filaments peripherin and vimentin are present throughout the early stages of neurite outgrowth (Cochard and Paulin, 1984; Troy et al., 1990).I n PC12 cells peripherin expression is increased when neurite outgrowth is induced by NGF, and injured peripheral neurons show increased peripherin during axonal regeneration, suggesting a role for peripherin in neuronal differentiation and neurite outgrowth (Aletta et al., 1988; Aletta et al., 1989; Leonard et al., 1988; Oblinger et al., 1989). Type IV intermediate filaments, neurofilaments, are expressed as axons reach maturity and appear to be a major determinant of axon caliber and conduction velocity (Helfand et al., 2003).

Neurofilaments are the most predominant type of intermediate filament found in the neuron and function to support the axonal structure and are regulated by signaling pathways resulting in an increase in the diameter of the axon for large myelinated neurons. Additionally they appear to have a protective effect within the cell and may act

as scavengers for oxidative stress, protecting other critical factors from oxidative attack (Couillard-Despres et al., 1998).

Three different neurofilament proteins are expressed in neurons and are classified based on their molecular weight; the 68 kDa neurofilament light chain (NF-L), the 160 kDa neurofilament medium chain (NF-M) and the 205 kDa neurofilament heavy chain (NF-H). Not all three neurofilament proteins are required to be expressed in the cell at the same time. NF-H is not expressed in neurons that continually undergo dynamic structural changes, such as hippocampal neurons, but is expressed at high levels in large caliber myelinated neurons indicating that NF-H expression imparts stability on the neuron (Liu et al., 2004).

The neurofilament proteins all share the same three domain structure with the rest of the intermediate filaments consisting of a variable N-terminal head domain, a conserved central rod domain, and a variable C-terminal tail. The C-terminal tail for NF-L is much shorter than that of NF-M and NF-H and does not contain any phosphorylation sites. Historically, neurofilaments were thought to be composed only of the three neurofilament proteins. It was hypothesized that a core filament assembled from NF-L, with NF-M and NF-H co-assembling onto the core NF-L backbone with the NF-M and NF-H C-terminal tail domains extending away from the filament surface (Hirokawa et al., 1984; Hisanaga and Hirokawa, 1988). However recent developments suggest that the intermediate filament protein α-internexin is colocalized and incorporated into the neurofilament (Yuan et al., 2003). This is not surprising as α-internexin was previously

known to be expressed in neurons and is also a type IV intermediate filament protein like the neurofilament proteins.

The neurofilaments and α-internexin have a conserved central α-helical rod domain, containing a hydrophobic heptad repeat essential for assembly into the coiled coil dimer (Wong and Cleveland, 1990). Two coiled-coil dimers associate in an anti-parallel manner to form a tetramer, eight tetramers are packed laterally and longitudinally together forming the 10nm rope like filament (Heins and Aebi, 1994; Herrmann et al., 2000). Post-translational modification of the neurofilament protein affects their association into the filament as well as the packing of neurofilaments together.

Phosphorylation of the neurofilament proteins head domain influences neurofilament assembly (Dong et al., 1993; Sihag and Nixon, 1991) and plays a critical role of preventing neurofilaments from assembling in the cell body (Lee et al., 1988; Sternberger and Sternberger, 1983). Phosphorylation of ser44 of the NF-M head domain and phosphorylation of Ser55 in the NF-L head domain, blocks filament assembly, and results in filament disassembly (Fiumelli et al., 2008; Hisanaga and Hirokawa, 1990; Nakamura et al., 2000).

The packing of neurofilament proteins into the neurofilament is regulated by the phosphorylation of NF-M and NF-H at multiple KSP sequences in their C-terminal tail. C-terminal tail phosphorylation occurs within the axon and is triggered by Schwann cell signaling in myelinated axons (de Waegh et al., 1992). Neurofilaments are transported in the axon by 'slow transport' as the neurofilament tail becomes more phosphorylated, the speed of its transport slows further and eventually it is integrated with the neurofilament

as a stable structure (Ackerley et al., 2003; Shea et al., 2003; Yabe et al., 2000). One possible mechanism for this gradual decrease in transport speed is that phosphorylation of the neurofilament results in weakening its association with the molecular motor protein kinesin resulting in it no longer being transported (Jung et al., 2005; Yabe et al., 2000). Phosphorylation of neurofilament proteins is required for proper accumulation of neurofilaments during radial growth of myelinated axons (Sanchez et al., 1996; Sanchez et al., 2000). This is supported by the observation that loss of myelination results in decreased regional accumulation of NF's (Sanchez et al., 2000). It is hypothesized that the large amount of negative changes resulting from phosphorylation increases the electrostatic repulsion between filaments and is thus able to regulate axonal diameter and thereby regulate axon caliber (Garcia et al., 2003).

The packing of neurofilament proteins is also regulation by glycosylation of serine or threonine residues. Glycosylation of residues in NF-M and NF-H C-terminal tails prevents phosphorylation and thereby switch the neurofilaments from repulsive to associative, leading to the close packing of neurofilaments observed in the Nodes of Ranvier (Dong et al., 1993; Nixon, 1993).

1.1.2.2 Neurite Initiation and Growth Patterning

1.1.2.2.1 Neurite Initiation

During the development of a neuron, events must occur that result in disruption of the round cell symmetry and transformation of the non-polar sphere to a polar cell capable of initiating a neuritic process. Similar processes must occur in dissociated cell

cultures of primary neurons used as *in vitro* models of axon growth, since the isolation and dissociation process results in removal of neuritic processes resulting in the cell once again being faced with spherical symmetry. The predominant theory is that microdomains are formed in the non-polar cell from which extracellular ligands mediate neurite initiation (reviewed in da Silva and Dotti, 2002). Two hypotheses exist on how the microdomains form: the theory of ligand mediated microdomain **formation** supposes that neurons are symmetrical and the presence of a ligand induces the formation of a membrane microdomain from which neurites sprout, while the theory of ligand mediated microdomain **activation** supposes that neurons have a degree of membrane bound asymmetry and that the presence of a ligand activates neurite formation from this area (da Silva and Dotti, 2002). The microdomain activation theory is supported by evidence that membrane bound asymmetry occurs in other cell types, one example of such is during the development of *Drosophilia melanogaster,* proteins with PDZ domains are responsible for recruiting other proteins to the apical pole (Wodarz et al., 1999). Proteins with PDZ domains are responsible for membrane protein clustering and play a role in cell signaling and linkage of the actin cytoskeleton to the cell membrane indicating that one possible mechanism of neurite initiation may be via activation of ligand receptors contained in microdomains (da Silva and Dotti, 2002).

Both theories of neurite initiation depend on ligand-mediated interactions that result in the sprouting of neurites. Potential ligands are suggested to include extracellular matrix molecules such as tenascins, heparin-binding growth associated molecules, collagen, laminin, and the slit family of proteins or diffusible molecules such as fibroblast

growth factor, transforming growth factor-β (TGF-β) and the neurotrophins (Brose and Tessier-Lavigne, 2000; da Silva and Dotti, 2002; Joester and Faissner, 2001; Labelle and Leclerc, 2000; Rauvala and Peng, 1997; Tucker et al., 2001). Among possible receptors could be the integrins, as they can cluster into focal adhesions and signal cytoskeletal rearrangement through the use of secondary messengers. Additionally studies in *Xenopus*, and *C. elegans* indicate that mutating or knocking out integrin receptors have negative effects on neurite initiation (Baum and Garriga, 1997; Lilienbaum et al., 1995). Due to the enormous variations in the environment in which cells are grown and the variety of differing neurite morphologies that result, it is likely that neurite initiation is mediated through many different environmental cues and varying intracellular cascades. However, the signals that will converge on the cytoskeleton through regulation of actin binding proteins and microtubule associated proteins are likely to be similar. Growth favoring signals may affect the actin filament cytoskeleton by regulating actin binding proteins to tilt the balance to actin filament instability and favor breakage of round cell symmetry, while signals that discourage growth will modulate actin binding proteins to enhance actin filament stability and inhibit breaching of the membrane (reviewed by da Silva and Dotti, 2002)).

Many studies suggest an important role for regulation of the actin cytoskeleton in neurite initiation, and have hypothesized that the classic steps witnessed in neurite initiation, where first lamellipodium surround the cell followed by the lamellipodium segmenting to form a neurite, as essential for neurite initiation (da Silva and Dotti, 2002; Dehmelt and Halpain, 2004). However, while recent studies still implicate the actin

cytoskeleton in playing an important role in neurite initiation, recent evidence supports the existence of filopodia rather than the lamellipodium as requirements for neurite initiation (Dent et al., 2007). In addition to filopodia formation, the presence of dynamic microtubules is also an essential ingredient for neurite initiation (Dent et al., 2007). Microtubules are suspected to contact, and align along the actin bundles in filopodia that act as a scaffold increasing the possibility of several microtubules polymerizing along one actin bundle and crosslinking into a stable microtubule bundle. The actin-microtubule interactions are possibly a structural intermediate in the formation of a neurite shaft. The need for a link between actin and microtubules in neurite initiation is supported by studies showing that overexpression of MAP2c (which is able to bundle microtubules as well as to bind to actin) is able to induce process formation in neuroblastoma cells, while tau (which is able to bundle microtubules but cannot interact with actin) cannot induce process formation (Gordon-Weeks, 2004). Besides their interactions with actin, microtubules play roles in transporting materials to the site of neurite initiation, providing structure for the new neurites, and by associating with important signaling proteins to localize and regulate their activity.

1.1.2.2.2 Neurite Elongation

Neurites elongate over a surface through a conserved three step process (Figure 1.11) that has been shown in numerous neuron types including: California sea slug (*Aplysia californica)* (Goldberg and Burmeister, 1986), chicken (*Gallus gallus*) DRG neurons (Bray and Chapman, 1985), rodent sympathetic neurons

Figure 1.11: Three Steps in Neurite Elongation

A. Protrusion: a net increase in actin filament forming lamellipodium and filopodia in the growth cone, resulting in an enlarged peripheral domain. **B.** Engorgement: microtubules elongate and invade the central domain, and transitional domain. Pioneering microtubules enter the peripheral domain and interacting with filopodia in the direction of neurite growth. **C.** Consolidation: some actin filaments in the growth cone that are not in the direction of growth depolymerize, additionally the majority of actin filaments at the proximal part of the growth cone depolymerize to allow the membrane to shrink around the bundle of microtubules to form the neurite shaft. (Dent and Gertler, 2003).

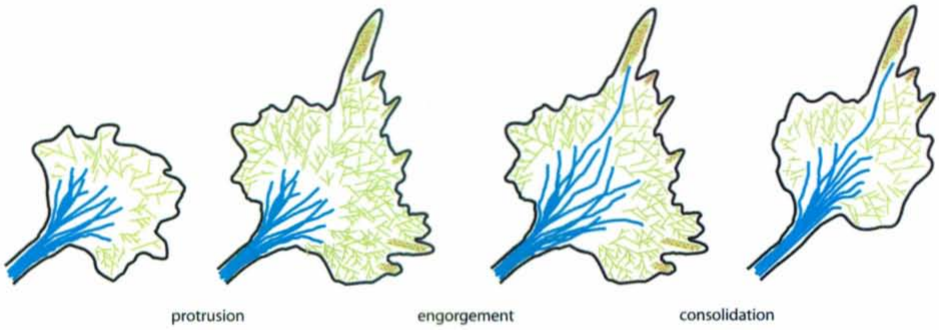
protrusion
engorgement
consolidation

(Aletta and Greene, 1988) and Rat (*Ratus norrvegicus)* cortical neurons (Kalil, 1996). The first step is the protrusion step where the peripheral domain of the growth cone enlarges in a particular direction through polymerization of actin filaments in lamellipodium and/or filopodia. During the engorgement step (Step 2) the microtubules elongate and invade the lamellipodium and filopodia closest to the central domain, converting what was once peripheral domain into transitional and central domain, during this phase the veils also become invested with vesicles though Brownian motion as well as directed microtubule based transport. The final step of the elongation is the consolidation of the proximal part of the growth cone to assume a cylindrical shape where transport of organelles is bidirectional. During the consolidation step the majority of actin filaments in the proximal part of the growth cone depolymerize allowing the membrane to shrink around the bundle of microtubules to form a cylindrical neurite shaft.

The three steps of neurite elongation all require regulated adjustment and modification of the microtubule and actin filament cytoskeletons. During protrusion actin polymerization and formation of lamellipodium and filopodia higher order actin structures is essential. Additionally as outlined previously the prevailing hypothesis for protrusion of actin structures is the molecular clutch model (Bard et al., 2008). This model holds that the ability of a neuron to extend its neurite over a substrate requires there to be a direct interaction with the substrate. *In vivo* this would be the ECM, the composition of which depends on the location in the body, PNS versus CNS. ECM molecules exert their effects by binding to a class of cell surface adhesion receptors called integrins (Giancotti and Ruoslahti, 1999; Guo and Giancotti, 2004). Integrins

receptors are found in the growth cone and on filopodia tips in an unligated (unbound to ECM) but activated state and are therefore primed to probe the matrix, creating sticky fingers along the leading edge promoting cell adhesion and migration (Galbraith et al., 2007). Upon binding to the ECM the integrin receptor undergoes a conformational change resulting in recruitment of a complex of signaling and adaptor proteins to its cytoplasmic tails (Giancotti, 2003). These proteins link the integrins to the actin cytoskeleton and stimulate internal signaling cascades to signal for cytoskeletal remodeling and neurite growth (Giancotti and Ruoslahti, 1999).

The consolidation step in neurite elongation requires targeted depolymerization of actin filaments and their higher order structures in the proximal area of the growth cone and due to the specific location involved may be achieved throught regulation or recruitment of actin binding proteins involved in depolymerization to that site. This step highlights the importance of disassembly and recycling of actin monomers in neurite elongation and supports that finding that more than just actin assembly is required for growth (Gallo et al., 2002).

The microtubule extension that is necessary for the engorgement stage and elongation of the neurite may actually drive elongation of the neurite without any actin structures present (Letourneau et al., 1987; Marsh and Letourneau, 1984). However the growth that results is uncoordinated and not directionally regulated, therefore the actin network might slow down growth cone elongation as barriers to rapid microtubule extension in order to regulate the direction of growth.

1.1.2.2.3 Growth cone turning

Growth cone turning *in vivo* is a requirement for an axon to follow a precise path leading to its target. Growth cones turn in response to the asymmetric presence of attractive and repulsive cues across their growth cone. These cues may be contact mediated, such as laminin or MAG, or soluble factors such as NGF or semaphorin. These cues are recognized by receptors on the surface of the growth cone and result in intracellular signaling pathways that regulate the actin and microtubule cytoskeletons in response to the varying concentrations of cues resulting in changes in local density or alignment of actin filaments to turn the growth cone (Figure 1.12) (Gallo and Letourneau, 2004; Luo, 2002; Turney and Bridgman, 2005). The requirement for regulation of the actin cytoskeleton for turning is supported by the findings that depletion of actin filaments in the growth cones inhibits turning (Letourneau et al., 1987; Marsh and Letourneau, 1984), and that the regulation of a single actin binding protein is sufficient to support either an attractive or a repulsive turn (Song and Poo, 1999). Cues that induce attraction and turning towards them increase actin filaments and bundles on the side of the growth cone the turning is occurring towards. The increase in actin bundles promotes interactions with microtubules and their +TIP proteins leading to turning behavior. Alternatively repulsive cues result in dissolution of actin filament bundles and loss of dynamic microtubules leading to growth cone collapse and repulsive turning (Zhou et al., 2004). The regulation of neurite turning *in vivo* where multiple guidance cues are present likely relies on the regulation of multiple actin binding proteins through multiple signaling gradients the affect both actin binding proteins as well as the interactions between actin filaments and microtubules.

Figure 1.12: Growth cone turning:

Growth cones respond to the asymmetric presence of attractive or repulsive cues across their growth cone by regulating their actin and microtubule cytoskeletons though location specific activation of actin binding proteins and microtubule associated proteins. **A.** Where there is no gradient of cues across the growth cone microtubule, and actin filament structures are present in similar amounts on each side of the growth cone. **B.** A gradient of attractive cues facilitates growth cone turning toward the increased areas of attractive cues (green). The attractive gradient results in increased polymerization and formation of higher order actin structures, as well as microtubule polymerization (both shown with yellow arrows) in areas of high attractive cues, while the portion of the growth cone with lower levels of attractive cues result in depolymerization and destabilizations of actin filaments and microtubules (black arrowhead). **C.** A gradient of repulsive cues results in growth cone turning away from high levels of the repulsive cues (red). The repulsive gradient acts in the opposite manner of the attractive gradient resulting in depolymerization and destabilization of actin filaments and microtubules (black arrowhead) at areas with high repulsive cues, and polymerization and stabilization of the cytoskeleton in areas of low repulsive cues (yellow arrow). (Adapted from Figure 1 - Kalil and Dent, 2005)

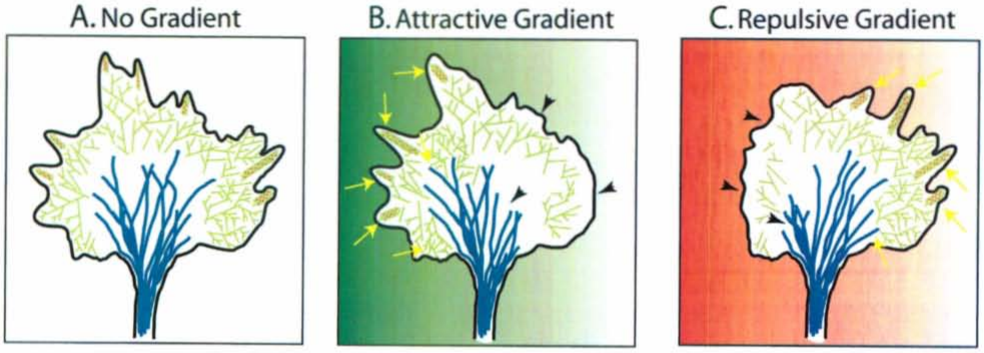
A. No Gradient
B. Attractive Gradient
C. Repulsive Gradient

1.1.2.2.4 Neurite Branching

Neurite branching occurs at two different locations within the neurite: the growth cone may split to form two branches (Figure 1.13) or a new branch can emerge from the middle of a neurite shaft in a process referred to as interstitial branching (Figure 1.14) (Dent and Gertler, 2003). *In vitro* branching occurs in many different situations, including following nervous system injury leading to functional recovery as well as neuropathic pain, at axon terminals in the presence of target derived chemoattractant (Kornack and Giger, 2005). In many CNS pathways, interstitial axon branches rather than primary axonal growth innervate target neurons (Dent and Gertler, 2003). Both interstitial branching and growth cone splitting require the accumulation of actin filaments (Dent and Kalil, 2001), and the formation of a filopodia(Luo, 2002). Additionally microtubules must be unbundled, and fragmented into short microtubules lengths that can probe both actin filament accumulations and filopodia (O'Connor and Bentley, 1993). The importance of the presence of multiple short fragmented microtubules is demonstrated by studies showing that over expression of the microtubule severing protein spastin, results in an increase in neurite branching (Yu et al., 2008).

In both growth cone splitting and interstitial branching from the axon shaft, elongation of the new branch occurs in the same method by which neurites elongate, and microtubules invade and remain in branches favored for further growth but withdraw from branches that regress. This suggests that cytoskeletal mechanisms underlying axon branching involve the reorganization of the microtubule array into a more labile form whereby microtubules can become debundled and fragmented, permitting microtubules to

Figure 1.13. Neurite Branching by Growth Cone Splitting

The growth cone contains dynamic actin filaments and higher order actin structures (green) and formation of actin filament accumulations and filopodia required for branching readily occurs. Microtubules (blue) are found tightly bundled in the neurite shaft and splay apart as they enter the central region of the growth cone. In paused growth cones microtubules form loops in the central region (**A**). During the transition from pausing to growth states reorganizing microtubules splay from their loops, fragment (**B**) and these new fragments contact with actin filaments to explore new directions of growth (**B,C**) (Dent and Gertler, 2003). Microtubule fragments engage with actin filament bundles in filopodia, creating a scaffold for other microtubules to align along (**D, E**). The aligned microtubules are bundled and the actin filaments proximate to the growth cone depolymerize resulting in the membrane shrinking around the microtubule bundles resulting in consolidation of the branched neurite (**F**).

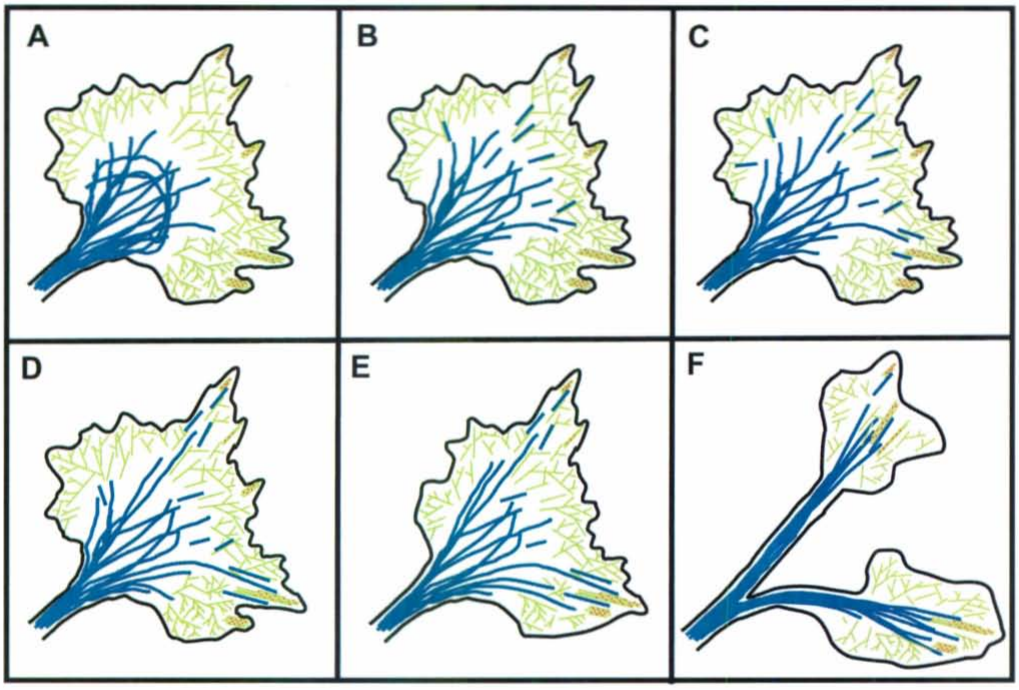
A
B
C
D
E
F

Figure 1.14: Interstitial Branching of Neurites

Under normal conditions actin filaments (green) and microtubules (blue) in the neurite shaft exist in a stable state (**A**). Cues that trigger branching result in unbundling of microtubules (B), and their fragmentation, as well as the reorganization of the actin cytoskeleton (B,C) (Dent and Gertler, 2003). The short fragmented microtubules colocalized with actin filament accumulations to explore new directions of growth(**D,E**) (Kornack and Giger, 2005). Exploring microtubules align along the actin filament bundles of filopodia creating a scaffold for other microtubules to align along **(F, G)**. The aligned microtubules are bundled and the actin filaments proximate to the neurite shaft depolymerize so that the membrane can shrink around the microtubule bundles resulting in consolidation of the new neurite branch **(H)**. (Dent et al.,2003).

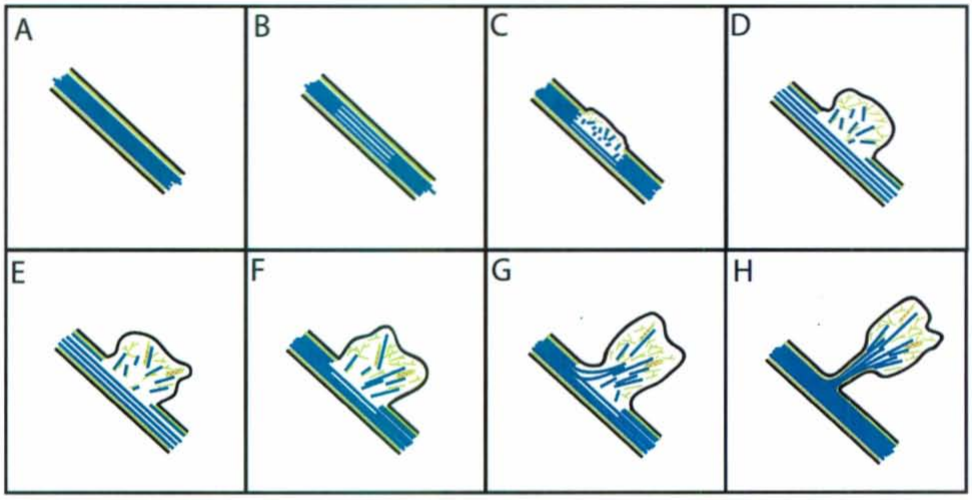
A
B
C
D
E
F
G
H

explore the growth cone and newly formed branches. Although branching in the growth cone and the axon shaft involve different initial cytoskeletal architecture, on a molecular level branching is achieved at both locations through parallel and direct targeting of both actin filaments and a subset of highly dynamic microtubules. Due to the differences in the original cytoskeleton between the location of branching a cue may have a different effect on a neurite depending on where it is applied to the neurite.

1.1.3 Hsp27

1.1.3.1 Heat Shock/ Stress Response

Cells respond to extracellular stresses by a variety of mechanisms; one common response is the heat shock or stress response and involves the induction of molecular chaperones and other cytoprotective proteins, including a set of proteins known as heat shock proteins (HSPs) (Hightower, 1991). This response may be elicited in reaction to a variety of stresses including radiation, oxidants, hypoxia, heat, or chemicals such as alcohols, transition metal ions, and peroxide (Hightower, 1991). Heat shock results in the alteration of metabolic processes and cellular structures including the cytoskeleton, where intermediate filaments are destabilized and form aggregates, microtubules disintegrate, and the actin cytoskeleton is reorganized (Glass et al., 1985; Iida et al., 1986; Welch and Suhan, 1985). A mild (non-lethal) stress is often sufficient to induce a stress response and provide cells with protection to subsequent potentially lethal insults; this is generally referred to as tolerance (Hightower, 1991; Mailhos et al., 1993; Quigney et al., 2003).

1.1.3.1.1 Induction of Stress Response

During a stress response the induction of molecular chaperones and cytoprotective proteins is primarily regulated at the level of transcription although there is some regulation of mRNA stability (reviewed in Shamovsky and Nudler, 2008). In higher eukaryotes the stress response is primarily mediated by heat shock transcription factors (HSFs). Genes that are translated in response to a stress response contain a heat shock element within their promoter region. Mammals express three distinct HSF proteins that are post-translationally modified upon stress, becoming active resulting in the formation of a trimer (Dai et al., 2007; Sarge et al., 1993; Westwood and Wu, 1993). The trimer has a high affinity for its conjugate DNA sequence, the heat shock element, and upon its translocation to the nucleus it binds to the heat shock element portion of the heat shock promoter and activates gene transcription (Taylor and Benjamin, 2005; Tonkiss and Calderwood, 2005).

Hsp27 has been shown to play a role at the level of translation in facilitating the stress response, and recovery afterwards. In heat shocked cells, Hsp27 plays a role in the inhibition of translation of mRNAs that are not part of the stress response. Hsp27 is suspected to inhibit translation by binding to eIF4G initiation factor and to facilitate dislocation of cap-initiation complexes (Cuesta et al., 2000). Following the heat shock response Hsp27 stimulates the recovery of RNA splicing as well as RNA and protein synthesis (Carper et al., 1997; Marin-Vinader et al., 2006).

1.1.3.1.2 Heat Shock Proteins

The family of proteins known as heat shock proteins (HSPs) contains five conserved classes of HSP's Hsp100, Hsp90, Hsp70, Hsp60, and the small heat shock proteins (sHSP) (Kim et al., 1998). The name 'heat shock protein' is a bit of a misnomer, as many proteins in the small heat shock protein family are not upregulated by temperature, and as mentioned previously those that are induced by heat can also be upregulated by a variety of chemical and physical stressors. However the name 'heat shock protein' has its roots in the discovery of the heat shock response over 45 years ago when Ferruccio Ritossa at the genetics institute in Pavia was looking at nucleic acid synthesis in the salivary gland puff of Drosophilia. When one of Ritossa' co-workers increased the temperature of the incubator in which Ritossa kept his tissue Ritossa observed a unique puffing pattern that required RNA but not protein synthesis (Ritossa, 1962; Ritossa, 1996). It was not known at the time of Ritossa's discovery that the puffs corresponded to active sites of increased transcription and translation, though it was later found that heat shock resulted in the production of a specific set of RNA's transcribed from the genes in the chromosomes where the heat shock puffs were formed and correspondingly the synthesis of a set of proteins (Tissieres et al., 1974). The proteins were identified on the basis of their sizes when run on a poly acrylamide gel electrophoresis (PAGE) and were named accordingly; for example the protein with a molecular weight of 27 kDa was named heat shock protein 27 (Hsp27), although Hsp27 is also referred to as Hsp25 (Ingolia and Craig, 1982). New guidelines have been proposed for HSP nomenclature, (Kampinga et al., 2009) under which Hsp27 is referred

to as HspB1; however this thesis will retain the useage of Hsp27. The stress resistance conferring properties of the HSPs is dependent on the ability of the Hsps to act as molecular chaperones and prevent protein aggregation. Cell survival is also increased by the presence of HSPs as some (Hsp70 and Hsp27) are able to act as inhibitors of cell death pathways, while others play roles as regulators of cell metabolism (Calderwood and Ciocca, 2008).

1.1.3.1.2.1 Small Heat Shock Proteins

The family of small heat shock proteins (sHSPs) in mammals contains ten members that have been identified based on the presence of common structural domains and not their chaperone activity or ability to exhibit stress inducible expression (Taylor and Benjamin, 2005). Many members of the sHSPs have been shown to act as ATP independent molecular chaperones to counteract the formation of aberrantly folded proteins playing protective roles in the intracellular transport of proteins, cytoskeletal architecture, translation regulations, intracellular redox homeostasis, and protection against spontaneous or stimulated cell death (Arrigo, 2007). Several members are induced by HSF1 activation in response to stress, while others like HspB2 are not (Suzuki et al., 1998).

Due to the presence of common structural domains within sHSPs researchers have been able to transfer and apply knowledge about the structures and interactions of some of the small heat shock proteins to other members of the class. The structure of sHSPs will be discussed further in section 1.1.3.2 in the context of the structure of Hsp27. The

sHSPs assemble into dimers and the dimers associate to form large complexes *in vitro*, consisting of 12 to 24 sHSP subunits (Haslbeck et al., 2005; Shi et al., 2006; White et al., 2006). The large sHSP complexes have been implicated in playing diverse roles in passively stabilizing stress-denatured proteins for subsequent handover to ATP dependant chaperones for refolding or degradation by the ubiquitin proteasome system (Ehrnsperger et al., 1997; Haslbeck et al., 2005).

1.1.3.2 Hsp27 Structure

Much of what is known about the structure of Hsp27 has been obtained, and confirmed through comparison of its sequence to that of other sHSPs. sHSPs have been notoriously difficult to obtain a crystal structure for, most likely due to their tendency to form large dynamic oligomers, which affects their ability to crystallize (Bova et al., 2000). The crystal structure of three sHSPs have been determined to date and has revealed that oligomers of sHSPs form as a result of multiple interactions in the α-crystallin domain, stabilized in some cases, by interaction with the hydrophobic sequences of the NH2 terminal (Kim et al., 1998; Koteiche and McHaourab, 2002; van Montfort et al., 2001b).

Under normal conditions Hsp27 forms large dynamic oligomers, consisting of approximately 24 monomers and having a molecular mass of 700 kDa (Lambert et al., 1999). Deletion studies and mutation of phosphorylation sites have shown that molecular interactions at the NH_2 terminus, as well as the phosphorylation state of the protein, are involved in the stability of the oligomeric structure (Kim et al., 1998; Lambert et al.,

1999; Rogalla et al., 1999; van Montfort et al., 2001b). The phosphorylation state, as well as oligomeric structure, of Hsp27 have been implicated in regulating its protein interactions as well as its activities in survival, as a chaperone, in cell signaling pathways, and through stabilization of the actin filament cytoskeleton.

1.1.3.2.1 Hsp27 Domains

The domain makeup of Hsp27 is common to all sHsps and contains three domains; a WD/EPF motif in the N-terminal region, a common C-terminal α-crystallin domain with a β-sheet sandwich fold, and a non-conserved flexible C-terminal domain (Figure 1.15A) (Arrigo, 2007; Chavez Zobel et al., 2005; Haslbeck et al., 2005; Theriault et al., 2004).

The amino (NH2-) terminus of Hsp27 contains a small proline, phenylalanine rich region containing a WD/EPF domain (Theriault et al., 2004). In Hsp27 the N-terminal phosphorylation site Ser15, directly precedes the WDPF domain. It has been found that Hsp27 requires its N-terminal region surrounding the WD/EPF motif in order to form oligomers larger than dimers (Lambert et al., 1999; Theriault et al., 2004). A model based on the structure of wheat Hsp16.5 suggests that the WD/EPF motif mediates intramolecular interactions along with a hydrophobic surface that is left exposed in the folded α-crystallin domain. This model proposes that phosphorylation of the Ser86 (Ser86 in rat, Ser90 in hamster, Ser82 in mouse) site affects intramolecular interactions, explaining how phosphorylation of Hsp27 causes deoligomerization of Hsp27 into dimers (Lambert et al., 1999; Lavoie et al., 1995; Theriault et al., 2004).

Figure 1.15: The structure and phosphorylation of Hsp27

A. Hsp27 is comprised of 3 domains, a WD/EPF domain, a conserved α-crystallin domain and a non conserved flexible C-terminal domain. **B.** Rat Hsp27 is phosphorylated at two serines (Ser15 and Ser86) by MKK2. **C.** Pharmacological inhibition of P38 MAPK activity upstream of Hsp27 result in inhibition of MKK2 activation and thereby inhibition of Hsp27 phosphorylation. **D.** Large oligomers form from non-phosphorylated Hsp27, phosphorylation of Ser86 of Hsp27 results in dissociation of the oligomers into dimers **(E)** and phosphorylation of Ser15 results of dissociation of the dimers into monomers **(F).**

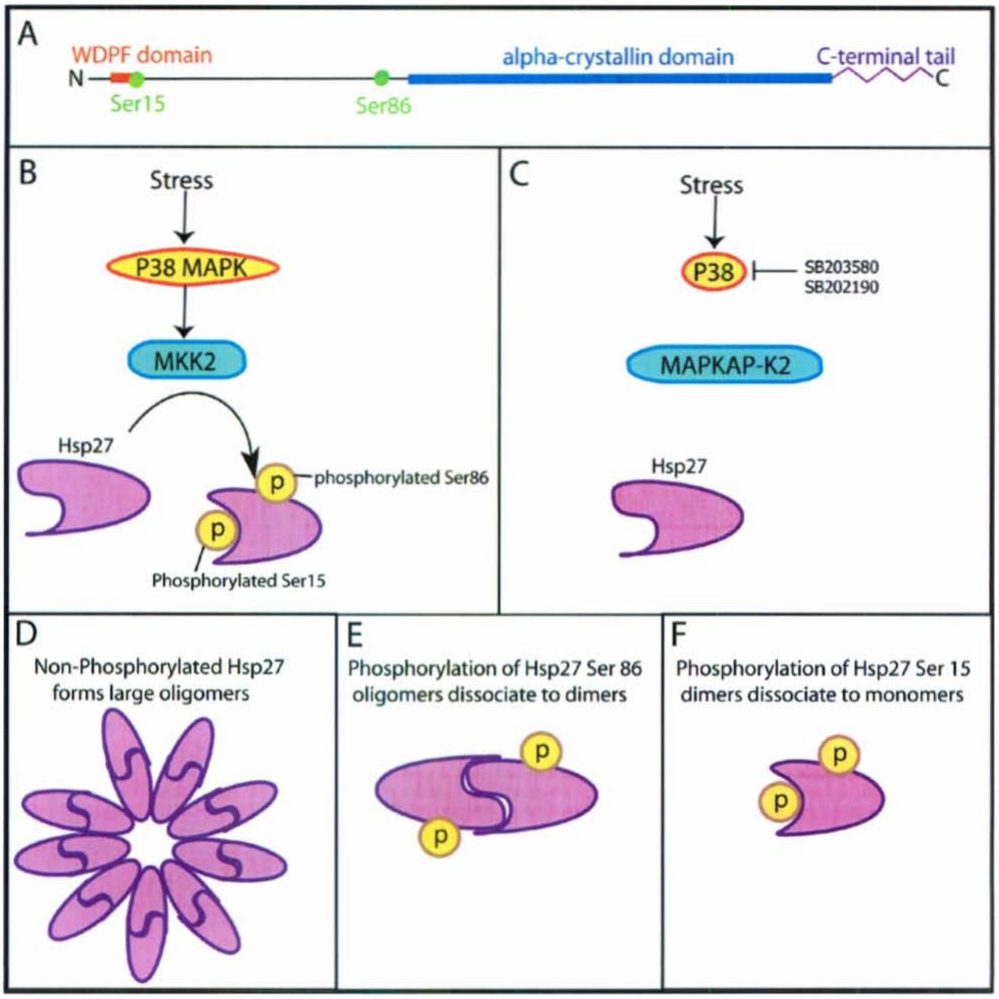
A
WDPF domain
N
Ser15
Ser86
alpha-crystallin domain
C-terminal tail
C
B
Stress
P38 MAPK
MKK2
Hsp27
p
phosphorylated Ser86
p
Phosphorylated Ser15
C
Stress
P38
SB203580
SB202190
MAPKAP-K2
Hsp27
D
Non-Phosphorylated Hsp27
forms large oligomers
E
Phosphorylation of Hsp27 Ser 86
oligomers dissociate to dimers
p
p
F
Phosphorylation of Hsp27 Ser 15
dimers dissociate to monomers
p
p

Even though the amino acid sequence for the α-crystallin domain varies between the sHsps, with the exception of a few conserved positions, the structure it folds into, a compact β-sheet sandwich fold, is conserved throughout the sHsp class (Kim et al., 1998; Van Montfort et al., 2001a; van Montfort et al., 2001b). The β-sheet sandwich consists of 2 layers, one of 3 and the other of 5 anti-parallel β-strands, that are connected by a short interdomain loop. α-crystallin domains can dimerize though their β-sheets to form a intersubunit composite β-sheet (Van Montfort et al., 2001a; van Montfort et al., 2001b). The interactions between the highly conserved α-crystallin domains indicate why sHsps dimerize with themselves but also why many of the sHSPs are able to form at least weak hetero dimers with other members of the sHsp class. The α-crystallin domain of sHSPs contains a conserved arginine, that appears to be involved in the structural integrity of the protein, and has recently been implicated in a variety of inherited diseases in humans. Mutation of the conserved arginine in αA-crystallin resulted in dominant congenital cataract disease (Litt et al., 1998), and a similar mutation in αB-crystallin was found in autosomal dominant desmin related myopathy (Vicart et al., 1998). Both mutations in αA crystallin and αB crystallin showed alterations in the supramolecular organization of the proteins, as well as the formation of large oligomers over 1000 kDa that collapsed into inclusion bodies resembling aggresomes (Bova et al., 1999; Chavez Zobel et al., 2003; Kumar et al., 1999; Perng et al., 1999b). A similar mutation in Chinese hamster Hsp27 was shown to destabilize the protein into dimers, as well as to partially aggregate in the cells indicating the importance of the conserved arginine and the α-crystallin

domain in association of Hsp27 and other sHsp dimers into oligomers, and of the structural integrity of the resulting oligomer (Chavez Zobel et al., 2005).

The C-terminal domain of Hsp27 is not conserved within the sHsp family and additionally displays considerable variability within homologues of Hsp27 found within eukaryotic organisms and in bacteria. While the function of the C-terminal tail remains to be elucidated, the crystal structures of two of the sHsps indicate that it is involved in stabilization of the oligomers (Kim et al., 1998; Van Montfort et al., 2001a; van Montfort et al., 2001b).

1.1.3.2.2 Hsp27 Phosphorylation

Hsp27 is phosphorylated on 3 serines in the human Hsp27 (Ser15, Ser78, Ser82) and 2 serines in the rodent Hsp27 (Ser15, and Ser86 in rat, Ser90 in hamster, Ser82 in mouse) by MAPKAP kinase-2 (MKK2) at both sites in many cell types; MKK2 is generally thought to be activated by p38MAPK (Huot et al., 1995; Landry et al., 1992; Mehlen and Arrigo, 1994). In smooth muscle and other cell types, other kinases such as MAP kinase-activated protein kinase 3 (MK3) (McLaughlin et al., 1996), MAP kinase-activated protein kinase 5 (MK5) (New et al., 1998), protein kinase C delta (PKCδ) (Maizels et al., 1998), protein kinase D (PKD) (Doppler et al., 2005), have been implicated in the phosphorylation of Hsp27, although the specific sites phosphorylated have not been determined. Hsp27 has also been shown to be phosphorylated on threonine 143 by cyclic guanosine monophosphate (cGMP)-dependant protein kinase in platelets. Phosphorylation of Thr143 in combination with phosphorylation of the serine

phosphorylation sites was shown to decrease the serine phosphorylation-dependant stimulation of actin polymerization necessary for platelet aggregation (Butt et al., 2001).

Phosphorylation of Hsp27 affects its activity in a manner that depends on the cell type and environmental conditions. Numerous studies show that oligomers of Hsp27 form from unphosphorylated Hsp27, and that phosphorylation of Hsp27 results in dissociation of the oligomers into dimers and monomers (Kato et al., 1994). Specifically, phosphorylation of Ser86 of rat Hsp27 resulted in dissociation of Hsp27 into dimers, and phosphorylation of Ser15 results in dissociation of dimers into monomers (Benndorf et al., 1994; Lambert et al., 1999). Besides being involved in oligomerization, the phosphorylation state of Hsp27 has also been implicated in the chaperone activity of Hsp27 as well being involved in the inhibition of apoptosis, and inhibition of actin polymerization (Bruey et al., 2000a; Bruey et al., 2000b; Landry and Huot, 1999; Rogalla et al., 1999).

The phosphorylation of Hsp27 can be studied *in vitro* using upstream pharmacological inhibitors of Hsp27 phosphorylation, as well as recombinant Hsp27 proteins. Commercially available p38 MAPK inhibitors (e.g., SB203580 and SB202190) act upstream of Hsp27 to inhibit the activity of p38 MAPK, resulting in inhibition of MKK2 activation and thereby decreasing Hsp27 phosphorylation (de Graauw et al., 2005; During et al., 2007). Many studies have taken advantage of recombinant DNA techniques to create and express Hsp27 with mutated phosphorylation sites. Mutation of the serine sites to alanine creates a nonphosphorylatable Hsp27 (for example, rodent Hsp27AA) while mutation of the serine sites to aspartic acid or glutamic acid results in a

protein that acts as a constitutively phosphorylated Hsp27 (rodent Hsp27EE or Hsp27DD) (Bruey et al., 2000a; Kubisch et al., 2004; Lambert et al., 1999; Theriault et al., 2004).

1.1.3.3 Role in survival

Hsp27 functions in numerous ways to promote survival in the face of environmental stress. In the face of stress the protective actions of Hsp27 have been attributed to its chaperone activity, ability to protect against oxidative stress, anti-apoptotic signaling abilities and its ability to stabilize the actin filament cytoskeleton.

Molecular chaperones interact with and stabilize non-native forms of proteins, and are not part of the final assembly of the protein (Ellis, 1987), but are involved in protein folding and assembly, transport, disaggregation of protein aggregates, and the unfolding of proteins (Saibil, 2008). In the early 1990's, Hsp27 was defined as a molecular chaperone for its ability to refold urea -denatured citrate synthase and α-glucosidase in an ATP-independent manner *in vitro* (Jakob et al., 1993). The mechanism of Hsp27 chaperone activity has been further defined, and large unphosphorylated oligomers of Hsp27 are thought to bind to and sequester misfolded proteins until they are either processed for refolding by ATP-dependant chaperones or degraded by the ubiquitin proteasome pathway (Ehrnsperger et al., 1997; Huot et al., 1997; Perng et al., 1999a; Theriault et al., 2004). These chaperone actions have been shown to be independent of the role of Hsp27 in thermoprotection and prevention of apoptosis, highlighting the fact

that Hsp27 functions to promote survival by a variety of independent methods (Mounier and Arrigo, 2002; Sun and MacRae, 2005).

Oxidative stress is caused as a result of high levels of reactive oxygen species, which are produced as a side product of the electron transport chain during the oxidative phosphorylation phase of respiratory energy production within the cell (Arrigo, 2007). Hsp27 acts to prevent cell death resulting from oxidative stress by decreasing the levels of reactive oxygen species; the amount of this decrease corresponds directly with the level of Hsp27 expression (Firdaus et al., 2006; Mehlen et al., 1996a; Preville et al., 1999; Rogalla et al., 1999). Hsp27 increases the resistance of cells against oxidative stress (caused by increasing the antioxidant defences of the cell) through mediating an increase in the level of, and by upholding the level of, the reduced form of glutathione in the cell (Mehlen et al., 1996a). Hsp27-mediated increase and maintenance of glutathione levels are directly responsible for protection of cell morphology, cytoskeletal architecture, and mitochondrial membrane potential by reducing lipid peroxidation, protein oxidation, and actin filament disruption (Paul and Arrigo, 2000; Preville et al., 1998; Preville et al., 1999). The phosphorylation state of Hsp27 has been suggested to play a role in glutathione increase as phosphorylated monomers were unable to decrease reactive oxygen species, indicating that the large oligomeric structure formed by unphosphorylated Hsp27 may be important for this activity (Rogalla et al., 1999).

Hsp27 has also been implicated in protecting the cell from oxidative stress by methods independent of its glutathione promoting activity. Hsp27 may act to inhibit the occurrence of oxidative stress by down-regulating intracellular iron levels that catalyze

the formation of hydroxyl radicals that oxidize proteins (Arrigo et al., 2005). Additionally Hsp27 may play a role in restoring the F-actin cytoskeleton after an oxidative stress, and is activated by the presence of reactive oxygen species which activate p38MAPK, leading to Hsp27 phosphorylation, which in turn promotes actin reorganization and resistance to cell death (Huot et al., 1997; Huot et al., 1996; Vigilanza et al., 2008).

Apoptosis is a form of programmed cell death by which unwanted cells are eliminated from the body. Within the developing nervous system nerve cells are produced in excess and apoptosis occurs to adjust the number of neurons to equal the number of targets. The survival of only neurons that have innervated targets occurs via target cells secreting survival signals or neurotrophins that promote survival; cells that do not receive these signals, or that do not receive sufficient amount of these signals, undergo apoptosis. Hsp27 functions to inhibit apoptosis through a variety of mechanisms including inhibiting caspases, mitochondrial cytochrome c release and by promoting the activity of pro-survival enzymes like Akt (Dodge et al., 2006; Mearow et al., 2002) Increase in Hsp27 levels increase the reisitance of the cells to several pro-apoptotic agents (Concannon et al., 2003; Mehlen et al., 1996b), and correspondingly decreasing Hsp27 expression sensitizes cells to apoptosis (Bausero et al., 2006; Kamada et al., 2007; Paul et al., 2002; Rocchi et al., 2006).

1.1.3.3.1 Hsp27 and survival in neurons

Hsp27 plays a protective role in neurons and its protective effects appear to be distinct from the protective effects of Hsp70 and other heat shock proteins (reviewed in (Franklin et al., 2005; Latchman, 2005)). Hsp27 is constitutively expressed in subpopulations of motor and sensory neurons in the adult rat nervous system (Plumier et al., 1997). However in DRG sensory neurons, constitutive expression of Hsp27 is minimal in neonatal neurons and levels are higher in adults in both cultures and intact DRGs (Dodge et al., 2006). Neonatal DRG neurons are dependent on nerve growth factor (NGF) for their survival, and undergo apoptosis without sufficient NGF (Dodge et al., 2006; Lewis et al., 1999). Overexpression of exogenous Hsp27, as well as upregulation of Hsp27 by a mild heat shock, protects both neonatal DRG neurons and PC12 cells against NGF withdrawal-induced cell death by increasing Akt activation and inhibiting caspase activation (Dodge et al., 2006; Mearow et al., 2002). In response to growth factor activation, Akt generates a survival signal by acting on the BAD/ Bcl-2 signaling pathway. Akt phosphorylates BAD resulting in its inactivation and dissociation from Bcl-2, rendering Bcl-2 active. Bcl-2 is an anti-apoptotic family member and when active (dissociated from BAD) can bind to and inhibit pro-apoptotic proteins and indirectly regulate the activity of caspases (Khor et al., 2004). Hsp27 modulates Akt activity, with the interaction between Hsp27 and Akt necessary for the anti-apoptotic activity of Akt (Konishi et al., 1997; Rane et al., 2003). Active Akt also inhibits cell death by phosphorylating and inactivating procaspase9 and by preventing the release of cytochrome c from mitochondria (Garrido et al., 1999; Paul et al., 2002).

1.1.3.4 Hsp27 and Neurite Growth

In order for a neurite to undergo successful growth patterning, the actin and microtubule cytoskeletons must be specifically regulated to initiate neurites as well as to facilitate their extension, branching, and turning. Additionally transport of cellular cargo from the cell body to the neurite tip and back again, is required to supply the building blocks necessary for extension to the growth cone, as well as to transport signals from the growth cone back to the cell body. Hsp27 is a likely candidate to be involved in neurite growth because of (1) its interactions with various cytoskeletal elements and signaling intermediates involved in regulating the cytoskeleton, and (2) its involvement in non-neuronal cell migration, which occurs via a similar process to neurite growth, and (3) its involvement in neurofilament assembly and role in transport within the cell have been highlighted by recent studies that mutations in Hsp27 are associated with peripheral neuropathies, in particular the axonal form of Charcot-Marie-Tooth disease (CMT) and distal hereditary motor neuropathy (dHMN) (Ackerley et al., 2006; Evgrafov et al., 2004; Irobi et al., 2004b).

Hsp27 interacts with several species of intermediate filaments, including glial fibrillary acidic protein (GFAP), vimentin, nestin and NF-L, and directly and indirectly regulate actin and microtubule dynamics, through its interactions with tau, 14-3-3 protein, the Arp2/3 complex and RhoA (Ackerley et al., 2006; Benndorf and Welsh, 2004; Evgrafov et al., 2004; Hargis et al., 2004; Hino et al., 2000; Jia et al., 2009; Kindas-Mugge et al., 2002; Lee et al., 2005; Liang and MacRae, 1997; Perng et al., 1999a; Tezel et al., 1999). The ability of Hsp27 to modulate the actin cytoskeleton, as well as to bind

to microtubules, places Hsp27 in a position to link regulation of the actin and microtubule cytoskeletons in a manner to direct neurite growth.

1.1.3.4.1 Possible roles for Hsp27 and the actin cytoskeleton in neurite growth

Hsp27 plays a role in regulating the actin filament cytoskeleton though direct interactions with actin, as well as by modulating the activities of actin binding proteins though signaling pathways. The interactions of Hsp27 and actin are important for many cell functions, including smooth muscle contraction, neutrophil chemotaxis and exocytosis, cell division, cell survival, cell migration and motility, neuronal differentiation, cell adhesion and attachment via focal adhesions and in neurite outgrowth (Brophy et al., 1998; Doshi et al., 2009; Hong et al., 2009; Jia et al., 2009; Jog et al., 2007; Lee et al., 2007; Lee et al., 2008; Piotrowicz et al., 1998; Schneider et al., 1998). Additionally Hsp27 colocalizes with actin filaments in cardiac (Lutsch et al., 1997), skeletal (Benndorf et al., 1994), and smooth muscle (Bitar et al., 1991; Ibitayo et al., 1999). As mentioned previously cell migration occurs via a process that shares many common mechanisms with neurite extension and supports a role for Hsp27 in neurite growth. The involvement of Hsp27 in neurite growth is also supported by the participation of Hsp27 in exocytosis which is required for cell membrane to be added to the growing neurite during neurite extension.

Hsp27 interacts directly with actin to prevent the polymerization and assembly of actin filaments in a manner that depends upon the phosphorylation state and oligomerization of Hsp27 (Figure 1.16). A critical region in Hsp27 for its interaction.

Figure 1.16: Direct interactions of Hsp27 and actin

Hsp27 and actin interact based on the oligomeric size and phosphorylation state of Hsp27. Numerous studies support the finding that non-phosphorylated monomeric Hsp27 binds to actin. However there is disagreement within the literature as to whether Hsp27 (purple) binds to actin monomers (green) (**A**), or binds to the barbed end of actin filaments to cap them (**B**). Independent of the manner in which Hsp27 binds actin its binding results in an inhibition of actin polymerization, either by sequestering actin monomers and preventing their addition (**A**) or by capping the actin filament and thereby preventing monomer addition(**B**). Phosphorylation of Hsp27 by MKK2 results in its dissociation from actin, resulting in actin polymerization(**C, D**). Control of the binding of Hsp27 to actin by phosphorylation may regulate actin filament dynamics by facilitating the transfer of monomers from pointed end depolymerization to sites of barbed end polymerization (**A, C**) or by binding to the barbed end to prevent capping proteins from binding and dissociating upon phosphorylation to permit elongation of the actin filament (**B, D**)

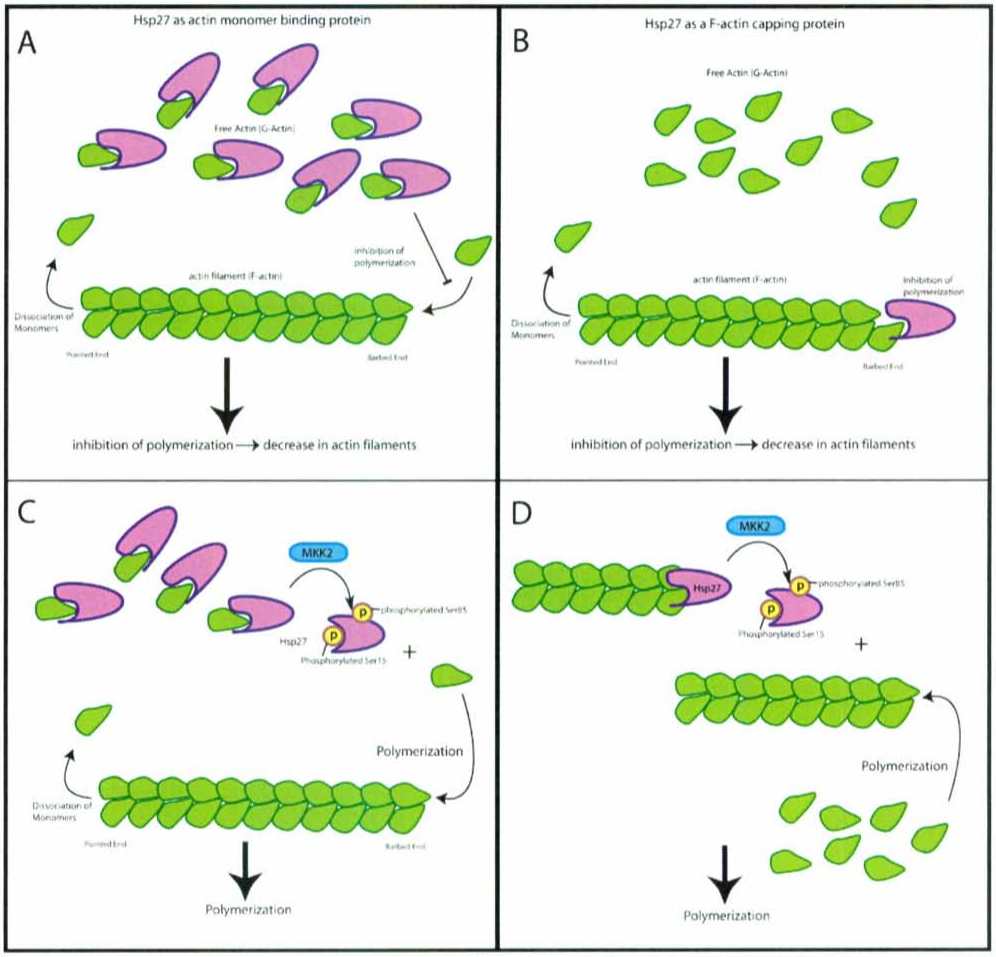
A
Hsp27 as actin monomer binding protein
Free Actin (G-Actin)
inhibition of polymerization
actin filament (F-actin)
Dissociation of Monomers
Pointed End
Barbed End
inhibition of polymerization → decrease in actin filaments
B
Hsp27 as a F-actin capping protein
Free Actin (G-Actin)
actin filament (F-actin)
inhibition of polymerization
Dissociation of Monomers
Pointed End
Barbed End
inhibition of polymerization → decrease in actin filaments
C
MKK2
P
phosphorylated Ser85
Hsp27
P
Phosphorylated Ser15
+
Polymerization
Dissociation of Monomers
Pointed End
Barbed End
Polymerization
D
MKK2
Hsp27
P
phosphorylated Ser85
P
Phosphorylated Ser15
+
Polymerization
Polymerization

with actin was identified as the peptide sequence I92-N106, this site was found to be responsible for the inhibition of actin polymerization, when added to solutions of G-actin in the presence of an actin nucleating factor (Wieske et al., 2001)

Reports differ on the method of action of Hsp27. Hsp27 was originally characterized as a barbed end capping protein (Figure 1.16 C), although recent reports suggest that Hsp27 impairs actin filament assembly by sequestering actin monomers (Figure 1.16 A), rather than by capping actin filaments (During et al., 2007; Miron et al., 1991; Pichon et al., 2004). Both of these models for Hsp27-based inhibition of actin filament assembly support the finding that only monomeric nonphosphorylated Hsp27 is able to inhibit actin filament polymerization (Benndorf et al., 1994; During et al., 2007). In the actin-capping model, Hsp27 was thought to cap actin filaments as a nonphosphorylated monomer and its phosphorylation resulted in dissociation from the actin filament and subsequent filament elongation (Benndorf et al., 1994; Guay et al., 1997; Landry and Huot, 1999; Lavoie et al., 1995; Miron et al., 1991). The actin sequestering model suggests that nonphosphorylated Hsp27 binds actin monomers resulting in an increase in the G-actin pool and a subsequent decrease in actin filament levels. Upon phosphorylation Hsp27 has been shown to dissociate from the actin monomers (During et al., 2007). The sequestering of G-actin by Hsp27 may also control actin nucleation by acting similarly to thymosin to prevent trimers of actin from spontaneously associating and nucleating new filaments. Although the roles of thymosin and F-actin capping proteins such as CP have yet to be elucidated in neurons they have been shown to be involved in higher order actin structure formation in other cell types,

and are good candidates, along with Hsp27, for being involved in the formation of these structures in neurite initiation and growth (reviewed in Cooper and Sept, 2008; Le Clainche and Carlier, 2008; Pak et al., 2008) (Mejillano et al., 2004).

Part of Hsp27's protective role in stressed cells has been attributed to its direct interactions with actin, resulting in increased actin filament stability. During stresses caused by heat, ATP depletion, cisplatin, hydrogen peroxide, cholecystokinin, and oxidative stress, Hsp27 increases the stability of the actin filament cytoskeleton, to protect the cell (Lavoie et al., 1993b; Lee et al., 2007; Schafer et al., 1999; Van Why et al., 2003; Vigilanza et al., 2008). Protection of the actin filament cytoskeleton by Hsp27 is dependent on the ability of Hsp27 to bind to denatured actin filaments, preventing their aggregation and facilitating reformation (Pivovarova et al., 2005). As with other roles that Hsp27 plays in the cell, it is possible that Hsp27 employs different methods of protecting the cytoskeleton during different types and intensities of stresses.

Hsp27 also regulates the actin filament cytoskeleton in a manner independent of its ability to bind directly to actin, by regulating actin binding proteins through its involvement in cell signaling pathways, possibly through its interactions with 14-3-3 protein, the Arp2/3 complex or RhoA, whose activities have been implicated in the activity of higher order actin structures in growth cones required for neurite growth (Figure 1.17) (Gehler et al., 2004; Jia et al., 2009; Loudon et al., 2006). An indirect role for Hsp27 in regulating actin filament dynamics is supported by the finding that the Hsp27 phosphorylation mutant, Hsp27EE, inhibits actin polymerization in HeLa cells but not in brain extracts (During et al., 2007). The different effects of Hsp27 on actin

Figure 1.17: The indirect effects of Hsp27 on the actin cytoskeleton

Hsp27 regulates the actin filament cytoskeleton independent of its ability to bind directly to actin, by regulating actin binding proteins through cell signaling pathways. Hsp27 has been implicated in the formation of focal adhesions, responsible for crosslinking actin filaments to the ECM for cell attachment and actin based protrusion. Additionally Hsp27 has been implicated in interacting with RhoA and facilitating the interactions of RhoA and ROCK required for signaling, phosphorylated Hsp27 has been found to bind to 14-3-3 protein, and its binding is suspected to inhibit 14-3-3 cofilin interactions, leading to dephosphorylation of cofilin and depolymerization of the actin cytoskeleton.

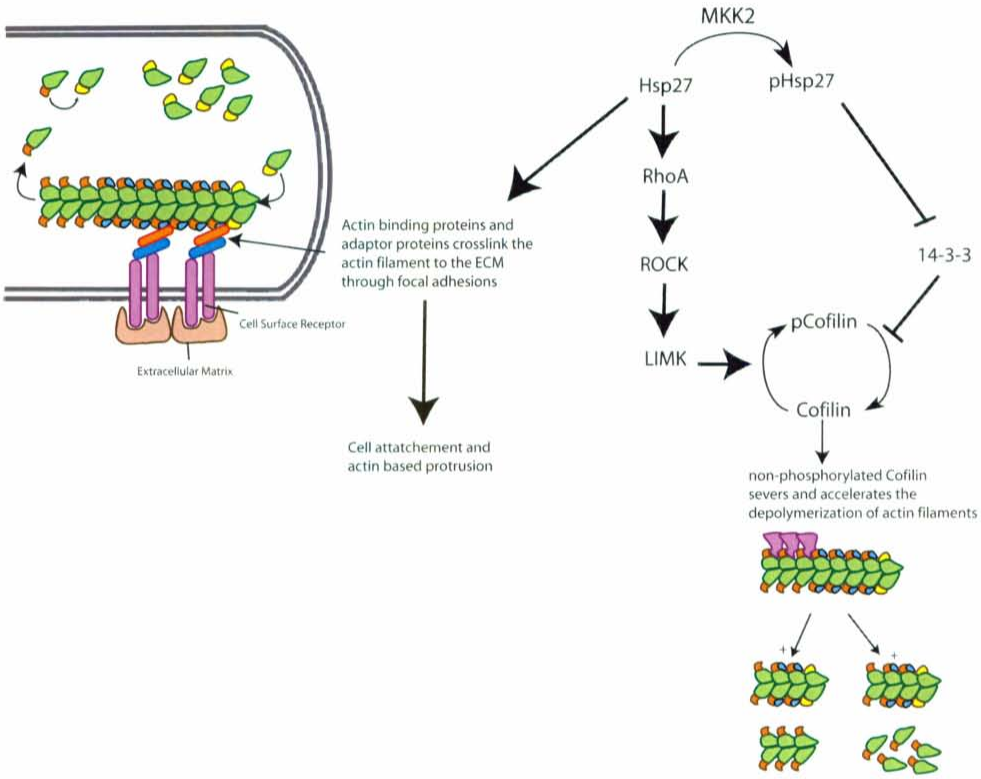
MKK2
Hsp27
pHsp27
RhoA
ROCK
LIMK
14-3-3
pCofilin
Cofilin
Actin binding proteins and adaptor proteins crosslink the actin filament to the ECM through focal adhesions
Cell Surface Receptor
Extracellular Matrix
Cell attatchement and actin based protrusion
non-phosphorylated Cofilin severs and accelerates the depolymerization of actin filaments

polymerization depending on the cell type indicates that the presence of cell type specific actin binding proteins and signaling intermediates determine the resulting change in actin filament polymerization.

Phosphorylated Hsp27 binds 14-3-3 protein in fibroblasts (Vertii et al., 2006). A similar interaction has been seen in another small heat shock protein, where following its phosphorylation by PKA, Hsp20 binds to 14-3-3. Hsp20 binding to 14-3-3 prevents the association of phosphorylated cofilin and 14-3-3, resulting in the dephosphorylation of cofilin to activate its catalysis of actin filament depolymerization. It has been hypothesized that Hsp27 interacts with 14-3-3, in a manner similar to Hsp20, and that binding of pHsp27 to 14-3-3 results in the activation of cofilin and actin filament depolymerization (Gaestel, 2006).

RhoA is a small GTPase known to regulate the actin cytoskeleton through signaling pathways and its effector ROCK (RhoA kinase) (Amano et al., 1997; Hall, 1998). Hsp27 interacts with RhoA (in smooth muscle), and is key in the formation of a complex between RhoA and ROCK, and signaling proteins downstream of ROCK activation, and is essential in the regulation of RhoA activation as well as downstream signaling (Patil and Bitar, 2006; Patil et al., 2004a; Patil et al., 2004b).

The Arp2/3 complex nucleates branches off of existing actin filaments, and aiding in the creation of a lamellipodium: a highly branched actin meshwork. Lamellipodium are found in the motile structures of migrating cells and in growth cones. A recent study has implicated Hsp27 as a direct binding partner for ArpC1a (Jia et al., 2009), a

component of the Arp2/3 complex, suggesting another possible role for Hsp27 in neurite growth.

Cell migration is a highly coordinated multistep process, and is similar to neurite initiation and extension and involves the regulation of the actin filament cytoskeleton by many of the same actin binding proteins (reviewed in Le Clainche and Carlier, 2008)). Hsp27 is required for cellular migration in a variety of cell types: leukocytes, smooth muscle, SW480 cells (human colon cancer cell line), neutrophils and fibroblasts (Doshi et al., 2009; Jog et al., 2007; Landry and Huot, 1999; Nomura et al., 2007; Pichon et al., 2004).

Nonphosphorylated Hsp27 is found at the leading edge of the lamellipodium in migrating cells and is displaced from this location by cytochalasin D treatment, suggesting that under normal conditions nonphosphorylated Hsp27 caps the barbed ends of actin filaments at the leading edge (Pichon et al., 2004). This role for Hsp27 is supported by the fact that motility is higher in cells that over express Hsp27 or capping proteins from the gelsolin family (Cunningham et al., 1991; Piotrowicz et al., 1998). It is hypothesized that the actin capping activity of Hsp27 is regulated at the leading edge by upstream intermediates in cell signaling pathways, specifically p38 MAPK, which is found transiently phosphorylated at the leading edge. This suggests that at the leading edge MKK2 must phosphorylate Hsp27 resulting in the dissociation of large oligomers, followed by rapid dephosphorylation resulting in Hsp27 interacting with actin barbed ends (Pichon et al., 2004).

Focal adhesions are sites of attachment of the cell to the extracellular matrix required for actin based protrusion in neurite growth (Robles and Gomez, 2006). Hsp27 has been implicated in numerous studies for playing a role in the organization of focal adhesions in non-neuronal cells (de Graauw et al., 2005; Gerthoffer and Gunst, 2001; Lee et al., 2008; Schneider et al., 1998) (Figure 1.17). The formation of focal adhesions involves integrin receptors. Upon binding to the ECM the integrin receptor undergoes a conformational change resulting in recruitment of a complex of signaling and adaptor proteins, including FAK (Focal adhesion kinase) to its cytoplasmic tails. These signaling and adaptor proteins link the integrin receptor to the actin cytoskeleton and stimulate internal signaling cascades that initiate cytoskeletal remodeling and neurite growth (Figure 1.17) (Giancotti, 2003; Giancotti and Ruoslahti, 1999). In addition to attachment and signaling to the cytoskeleton, binding of the ECM to the integrin receptor also results in ligand-induced integrin clustering, which stimulates the formation of large signaling and attachment sites at the cell surface called focal adhesions.

Hsp27 has been suggested to play a role in linking the actin cytoskeleton to the focal adhesion in non-neuronal cells, and can alter focal adhesions via the perturbation of the actin cytoskeleton (Schneider et al., 1998). Additionally overexpression of Hsp27 in fibroblasts results in enhanced adhesions by increasing FAK activation, suggesting that Hsp27 links integrins with the actin cytoskeleton (Lee et al., 2008). The involvement of Hsp27 in focal adhesion formation is further supported by the finding that fibroblasts overexpressing Hsp27 attach more efficiently to culture dishes, where as cells with low levels of Hsp27 do not form as strong attachments (Hirano et al., 2004).

As outlined above, Hsp27 may play roles in neurite growth via its various direct and indirect mechanisms of modulating the actin cytoskeleton. These findings suggest that through regulating the polymerization and depolymerization of actin filaments in specific locations within the neuron Hsp27 may be rearranging the cellular architecture for neurite growth. The involvement of Hsp27 in the formation of focal adhesions, and increased attachment also supports a role for Hsp27 in neurite growth. In addition to its role in modulating the actin cytoskeleton Hsp27 has also been implicated in binding to and stabilizing the microtubule cytoskeleton, by binding to microtubules as well as tau (Hino et al., 2000; Mehlen et al., 1996b; Shimura et al., 2004). Stabilization of microtubules promotes their extension necessary for neurite growth, additionally engagement of microtubules along actin filament bundles results in their stabilization and bundling and is thought to be a structural intermediate in the formation of a neurite, as well as in neurite extension (Dent et al., 2007). These findings implicate Hsp27 as possibly playing many roles in neurite initiation and growth patterning by regulating the microtubule and microfilament cytoskeleton.

1.1.3.4.2 Hsp27 and Peripheral Neuropathies

Recent studies have shown that missense mutations in small heat shock proteins including Hsp27 and Hsp22 are associated with peripheral neuropathies. Five mutations in Hsp27 have been found that lead to axonal form of CMT (CMT2) or dHMN (Table 1.2) (Evgrafov et al., 2004; Irobi et al., 2004b). Interestingly mutations in the NF-L gene

Table 1.2: Mutations in Hsp27 implicated in Peripheral Neuropathies

Nucleotide Change	Resulting Amino Acid Mutation	Domain of Mutation	Diagnosis	*in vitro* Phenotype
379C→T	R127W	α-crystallin domain	dHMN	
404C→T	S135F	α-crystallin domain	dHMN & CMT2	altered NF-L assembly, decrease in cell survival
406C→T	R136W	α-crystallin domain	CMT2	
452C→T	T151I	α-crystallin domain	dHMN	
545C→T	P182L	C- terminal tail	dHMN	insoluble aggregates in body, disrupted axonal transport, no mutant Hsp27 in neurites, and altered cellular localization of p150Glued

(NEFL) results in CMT2 and show similar phenotypes as Hsp27 mutants when expressed in cell cultures. Expression of the mutant NEFL gene results in alterations in the neurofilament network and disturbances in axonal transport (Perez-Olle et al., 2004; Perez-Olle et al., 2005), whereas expression of S135F Hsp27 mutant results in altered NF-L assembly, and the P182L Hsp27 mutant results in disrupted transport within the neurite and large insoluble aggregates in the cell body (Ackerley et al., 2006). The location of the mutations may provide insight into their alterations of the structure and function of Hsp27. The three mutations that result in alteration of amino acids 127, 135, and 136, are located close to the conserved arginine, (arg140), involved in maintaining the structural integrity of the protein. Mutation of Arg140 in Hsp27 results in the dissociation of Hsp27 oligomers to dimers, and in the formation of insoluble aggregates (Chavez Zobel et al., 2005). Mutation of the conserved arginine in other small heat shock proteins have been implicated in a variety of inherited diseases in humans resulting from structural instability and aggregation of the affected small heat shock protein (Litt et al., 1998; Vicart et al., 1998).

The missense mutation of Hsp27 resulting in peripheral neuropathies further implicate a role for Hsp27 in neurite regeneration, through involvement of neurofilament assembly as well as transport within the neurite (Ackerley et al., 2006).

Hypothesis and Objectives

The main question that I wished to investigate was whether Hsp27 plays a role in neurite regeneration of the sensory DRG neurons? Specifically, I was interested in whether Hsp27 influences neurite initiation and extension via its effects on cytoskeletal elements, and whether the phosphorylation of Hsp27 modifies its effects on the cytoskeleton and thereby influences neurite initiation and extension.

When I began my experiments there was very little information available on the role of Hsp27 in neurons apart from its role in survival, and although interactions between Hsp27 and different cytoskeletal elements had been documented in non-neuronal cells, they had not been investigated in neurons.

During the span of my research, a study was published in Nature Genetics (Evgrafov et al., 2004) reporting that mutations in human Hsp27 caused Charcot-Marie-Tooth disease (CMT2F) or distal hereditary motor neuropathies (dHMN). CMT2 forms of the disease are a result of axonal neuropathies, that appear to be a result of defects in axonal transport resulting from mutations in genes that are involved in maintaining or regulating the cytoskeleton. As well this study found that mutant Hsp27 had an effect on neurofilament light (NF-L) assembly. These findings added support to my original hypothesis that Hsp27 interacts with cytoskeletal elements in neurons, and provided impetus for my work.

To study this hypothesis, four specific objectives were developed

Objective 1: To determine if there is a temporal correlation between Hsp27 expression and DRG neurite growth, whether Hsp27 colocalizes with cytoskeletal elements, and the effect of Hsp27 phosphorylation on neurite growth. In initial experiments dissociated adult DRG neurons were cultured on laminin and using immunocytochemistry and confocal microscopy the location of Hsp27, pHsp27 and actin and tubulin was assessed. In order to determine the role of Hsp27 phosphorylation in neurite growth, cells were plated on polylysine with a pharmacological p38 MAPK inhibitor to inhibit the upstream pathway that leads to the phosphorylation of Hsp27; in subsequent experiments cells were stimulated with soluble laminin to induce neurite growth. Efficacy of the pharmacological p38 MAPK inhibitor on inhibiting Hsp27 phosphorylation was assessed by western blotting, and neurite growth was assessed using immunocytochemistry and confocal microscopy (Chapter 2).

Objective 2: To investigate the role of Hsp27 in neurite growth by observing growth patterning after knocking down Hsp27 protein levels and over expressing exogenous Hsp27. To study the impact of Hsp27 protein levels on neurite growth dissociated DRG neurons were electroporated with Hsp27 siRNA or a vector encoding exogenous Hsp27, and plated on polylysine. 24 h after plating, when the neurons had down or upregulated Hsp27 levels, the neurons were stimulated with laminin for a further 24 h (Chapter 3).

Objective 3: To investigate the importance of Hsp27 phosphorylation in neurite growth by depleting endogenous Hsp27 with siRNA and over expressing exogenous Hsp27 phosphorylation mutants. Hsp27 constructs encoding for Hsp27 with various mutations to its phosphorylation sites, and the WDPF domain (AA, EE, AE, EA, Δ5-23) were subcloned into an IRES vector encoding for GFP and the mutant Hsp27. Dissociated DRG neurons were electroporated with siRNA and the Hsp27 mutant constructs and plated on polylysine overnight before being stimulated with soluble laminin for 24 h. Using immunocytochemistry, confocal microscopy and Neurolucidia tracing software, neurite growth and patterning was assessed (Chapter 4).

Objective 4: To identify if there is a link between Hsp27 phosphorylation and actin dynamics. Adult DRG neurons were plated on laminin with a pharmacological p38 MAPK inhibitor to inhibit the upstream pathway that leads to the phosphorylation of Hsp27. Effect of the pharmacological p38 MAPK inhibitor on inhibiting Hsp27 phosphorylation at the S15 and S86 site was assessed by western blotting and F-actin/ G-actin ratio were assessed using a commercial *in vitro* assay kit, as well as by measuring F-actin and G-actin levels though cell labeling and confocal microscopy (Chapter 5).

Co-authorship statement

I, Kristy Williams, am the principle author for all manuscripts that are contained within this thesis (chapters 2-5). However, each of these chapters has been co-authored by my supervisor Dr. K. M. Mearow, and her research assistants Mrs. M. Rahimtula, and Ms. F. Nafar. The specific contributions of each author to each manuscript is described below. Chapters 2 and 3 are published manuscripts, while the manuscript in chapter 4 is in preparation, and the manuscript in chapter 5 represents preliminary data for studies to be continued in the Mearow laboratory.

Chapter 2, "Hsp27 and axonal growth in adult sensory neurons *in vitro*". As the principal author, I wrote the manuscript and participated in the experimental design and performed the majority of the experimental work and data analysis for the completion of this manuscript including: culturing the cells, carrying out neurite growth and confocal analysis as well as the western blotting experiments. Mrs. Rahimtula provided technical assistance including animal dissection and preparation of chemical compounds. Dr. Mearow edited the manuscript and was responsible for the experimental concept, design and overall supervision of the experiments, as well as carrying out some of the confocal analysis.

Chapter 3, "Heat Shock Protein 27 Is involved in Neurite Extension and Branching of Dorsal Root Ganglion Neurons *In vitro*". As the principal author, I participated in the

experimental design, wrote the manuscript and performed all experimental work and data analysis, and writing for the completion of this manuscript. Mrs. Rahimtula, provided technical assistance including animal dissection and preparation of chemical compounds. Dr Mearow provided extensive amounts of help with the experimental design and editing of the final draft of this manuscript.

Chapter 4 "Hsp27 phosphorylation is involved in neurite growth in adult sensory neurons *in vitro*" As the principal author, I participated in the experimental design and performed all experimental work and data analysis, and writing for the completion of this manuscript. Mrs. Rahimtula, and Ms. Nafar provided technical assistance including animal dissection and preparation of chemical compounds. Dr Mearow participated in the experimental design, correction and improvement of this manuscript.

Chapter 5 "Inhibition of p38 MAPK activity attenuates Hsp27 phosphorylation and increases the F-actin / G-actin ratio in DRG neurons" As the principal author, I participated in the experimental design and performed all experimental work and data analysis, and writing for the completion of this manuscript. Mrs. Rahimtula, and Ms. Nafar provided technical assistance including animal dissection and preparation of chemical compounds. Dr Mearow participated in the experimental design, correction and improvement of this manuscript.

Chapter 2

Hsp27 and axonal growth in adult sensory neurons *in vitro*

(Published in BMC Neuroscience 2005, 6:24)

2.1 Abstract

Background: Neurite growth can be elicited by growth factors and interactions with extracellular matrix molecules like laminin. Among the targets of the signalling pathways activated by these stimuli are cytoskeletal elements, such as actin, tubulin and neurofilaments. The cytoskeleton can also be modulated by other proteins, such as the small heat shock protein Hsp27. Hsp27 interacts with actin and tubulin in non-neuronal cells and while it has been suggested to play a role in the response of some neurons to injury, there have been no direct studies of its contribution to axonal regeneration.

Results: I have investigated neurite initiation and process extension using cultures of adult dorsal root ganglion (DRG) sensory neurons and a laminin stimulation paradigm. Employing confocal microscopy and biochemical analyses I have examined localization of Hsp27 at early and later stages of neurite growth. Our results show that Hsp27 is colocalized with actin and tubulin in lamellopodia, filopodia, focal contacts, mature neurites and growth cones. Disruption of the actin cytoskeleton with cytochalasin D results in aberrant neurite initiation and extension, effects which may be attributable to alterations in actin polymerization states. Inhibition of Hsp27 phosphorylation in our cultures results in an atypical growth pattern that may be attributable to an effect of pHsp27 on the stability of the actin cytoskeleton.

Conclusion: I observed colocalization of the phosphorylated and non-phosphorylated forms of Hsp27 with actin and tubulin in both very early and later stages of neurite growth from cultured adult DRG neurons. The colocalization of Hsp27 and pHsp27 with actin in lamellopodia and focal contacts at early stages of neurite growth, and in processes, branch points and growth cones at later stages, suggests that Hsp27 may play a role in neuritogenesis and subsequent neurite extension, and potentially in the patterning of this growth. Hsp27 has been reported to play a key role in modulating actin cytoskeletal dynamics as an actin-capping protein in non-neuronal cells. Our results suggest that this may also be the case in neurons and support a role for Hsp27 in neurite outgrowth via its phosphorylation state-dependent interactions with actin.

2.2 Background

I know that various factors can influence and promote regeneration of peripheral axons. In addition to soluble factors (neurotrophins, cytokines and other growth factors), the extracellular environment in which growth occurs is critically important. Axonal regeneration does not occur to any great extent in the CNS, and while this is due to a number of factors, the most prominent is a non-permissive growth environment as well as an unavailability of appropriate growth-promoting factors. In the PNS, on the other hand, peripheral axons (both motor and sensory) generally regenerate quite well.

Growth factors and extracellular matrix (ECM) molecules like laminin act through cell surface receptors that activate often convergent signalling pathways to elicit neurite growth in sensory neurons (Tucker et al., 2005). Among the targets of these pathways are

the cytoskeletal elements responsible for initiating and maintaining the structure of growing processes. Actin, tubulin and intermediate filaments all play a part in growth processes (da Silva and Dotti, 2002; Dehmelt and Halpain, 2004; Dehmelt et al., 2003). There are also a variety of other molecules that interact with these components to modulate or protect the cytoskeleton from deleterious stresses.

One class of molecules known to act as chaperones include the small heat shock protein family, of which heat shock protein 27 is a member. Hsp27, in addition to its roles in regulating apoptosis and protein folding, interacts with different cytoskeletal elements (Charette et al., 2000; Guay et al., 1997; Huot et al., 1996; Lavoie et al., 1995). Much of this work has been carried out using non-neural cells, particularly fibroblast and epithelial derived cells. Part of its protective role in stressed cells has been attributed to its actions as an actin-capping protein (Benndorf et al., 1994; Miron et al., 1991). Hsp27 has been reported to be a component of focal contacts, play an important role in smooth muscle contraction and be important for cellular migration in endothelial cells (Reviewed in Gerthoffer and Gunst, 2001). Rodent Hsp27 can be phosphorylated on 2 sites, Ser15 and Ser 86, although human Hsp27 has 3 serine phosphorylation sites (S15, S78 and S82) (Landry et al., 1992; Mehlen and Arrigo, 1994). MAPKAP-K2, via its activation by p38 MAPK, is reported to be the Hsp27 kinase, although there are reports that PKC α,δ and cAMP-dependent kinase can also phosphorylate Hsp27 (Bitar et al., 2002; Meier et al., 2001). In terms of its influence on actin, pHsp27 acts to promote actin polymerization and stress fibre formation. It also has a role in protecting or stabilizing the actin cytoskeleton, although this appears to depend upon the nature of the pHsp (Benndorf et

al., 1994; Guay et al., 1997; Lavoie et al., 1995). Monomeric and non phosphorylated Hsp27 inhibit actin polymerization *in vitro*, while phosphorylated monomers and non phosphorylated multimers have no effect on actin polymerization (Benndorf et al., 1994).

Prior reports and our own observations have suggested a role for Hsp27 in axonal growth or regeneration, in addition to its role in promoting neuronal survival. Hsp27 is upregulated after injury in DRG neurons *in vivo* and after dissociation *in vitro* ((Costigan et al., 1998); Dodge and Mearow, unpublished observations). Other injury models have shown increases in Hsp27 in Schwann cells and white matter columns (Murashov et al., 2001a) and it has been speculated that Hsp27 might be important in the neuronal response to injury and regeneration (Benn et al., 2002; Costigan et al., 1998). Of direct relevance to a potential role of Hsp27 in axonal growth are the recent reports indicating that Hsp27 and the related Hsp22 gene deletions are responsible for familial peripheral axonopathies (Evgrafov et al., 2004; Irobi et al., 2004b).

In vitro models have been widely used to study the growth behaviour of neurite initiation and extension in both CNS and peripheral neurons. In many models, neurotrophin stimulation is required for neurite growth, although in most of these models neurotrophins are also required for survival. Another widely used paradigm involves the stimulation of plated neurons with soluble laminin or extracellular matrix preparations (e.g., Matrigel^{tm}), both of which elicit neurite initiation (Slaughter et al., 1997; Tang and Goldberg, 2000; Yu et al., 2001). This approach is particularly useful in mature DRG neurons, where not all cells will respond to a given neurotrophin (for example, NGF). Regardless of how process formation is evoked, there appear to be several general stages

that can be identified including the formation of lamellopodia, filopodia, and the eventual emergence of immature neurites with growth cones (da Silva and Dotti, 2002; Dehmelt and Halpain, 2004). The cellular mechanisms responsible for these behaviours are not fully elucidated.

In our cultures of adult DRG neurons I have observed robust expression and distribution of Hsp27 in dissociated DRG neurons, particularly in neuritic networks and growth cones. These observations, along with the reported role of Hsp27 in modulating the actin cytoskeleton in other cells types, led us to investigate the potential role of Hsp27 in interacting with cytoskeletal elements in different stages of neurite initiation and extension. Our hypothesis was that Hsp27 associates with the cytoskeleton in neurons and plays a key role in regulating or fine-tuning the observed ability of the cells to initiate and extend processes in response to the appropriate stimuli.

2.3 Results

2.3.1 Laminin induces several identifiable stages of neurite initiation and growth

In order to investigate stages of neurite initiation and subsequent growth, I employed a laminin stimulation paradigm. As these neurons are adult, they do not require any added trophic factors for their survival, and therefore neither NGF nor any other neurotrophin was required to initiate growth in these experiments. Similar stimulation experiments using laminin or matrigel have been carried out using sympathetic neurons (Slaughter et al., 1997).

Neurons were dissociated and plated on poly-lysine coated 16-well slides and allowed to adhere overnight (approx 18 h). Subsequently, the plating medium was removed and 50 μl of medium containing soluble laminin (40 μg/ml) was added to the cells. Control wells consisted of mock stimulation (e.g., removal and replacement of laminin-free medium). Cells were fixed at 5, 15, 30 min and 1, 6 and 24 h after stimulation and subsequently processed for detection of actin, tubulin and Hsp27. Various distinctive stages in neuronal membrane expansion and neurite growth were observed and are summarized in Figure 2.1. One of the first steps is the appearance of a membranous expansion either around the whole soma or only from a particular portion of the cell body (A, 5 min). These lamellae are positively stained for actin (using phalloidin). Within 15–30 min, small sprouts extend from the lamellae and there are clear examples of focal contacts forming around the periphery of a lamellopodium (B, C, arrows). At later time points (1–6 h) some of the sprouts have elongated into filopodia and often have small growth cones associated with them (D, 1 h; E, 6 h). Subsequently, neurites form and some are selected for extension by a process that is not well characterized (F, 24 h).

2.3.2 Hsp27 colocalizes with actin and tubulin in the early stages of process initiation

Based on our hypothesis that Hsp27 may play a role in process initiation or neurite growth, I examined the localization of Hsp27 in neurons in various stages of process formation using immunocytochemistry and confocal microscopy. Here, examples

Figure 2.1: Laminin stimulation elicits lamellopodia and process formation in adult sensory neurons. DRG neurons plated on polylysine were stimulated with laminin in solution for 5 min, 15 min, 30 min, 1 h, 6 h, 24 h. After fixation, neurons were stained with rhodamine-phalloidin to detect actin and images obtained using confocal microscopy. Panels A-F provide representative examples of the various stages of lamellopodia formation and eventual process protrusion, and show various distinctive stages in neuronal membrane expansion and neurite growth. At the earliest stages, lamellopodia are formed (A- 5 min, B- 15 min, C- 30 min) with evidence of focal contacts (arrows) at the leading edge of the lamellopodia (B, C). In D (1 h) and E (6 h) filopodia begin to protrude from the lamellopodium around the circumference of the neuron. Eventually, these processes appear to coalesce into one or more neurites that continue to extend (F- 24 h, arrow). Scale bar – 20 μm.

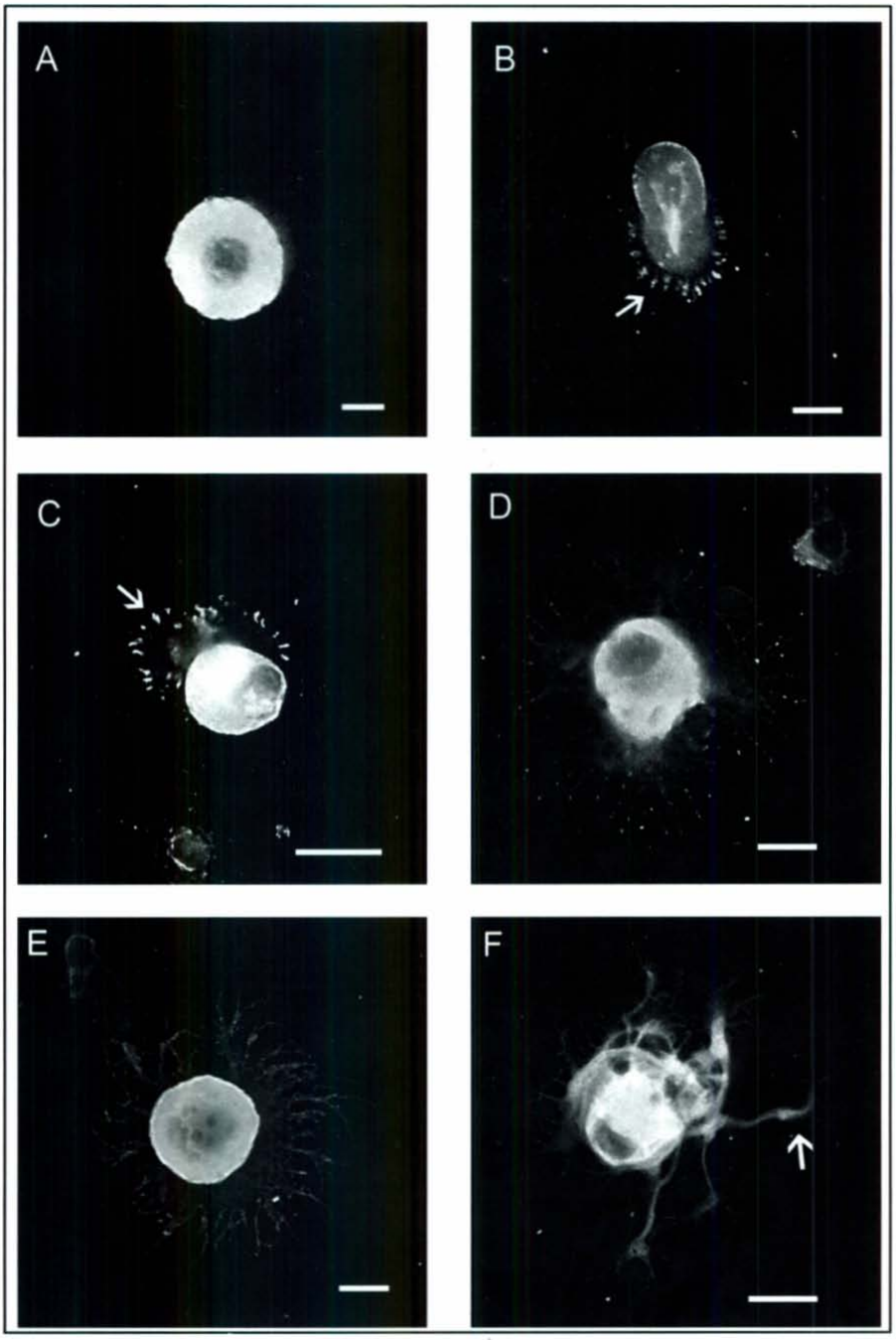
A
B
C
D
E
F

of the different stages as defined in the previous section (e.g., lamellopodia, focal contacts, neurite emergence) were selected from cells stimulated with laminin for 1 h or 6 h. In addition, because of the association of Hsp27 with actin and tubulin in non-neuronal cells (Aquino et al., 1996; Kindas-Mugge et al., 2002; Liang and MacRae, 1997; Mounier and Arrigo, 2002; Panasenko et al., 2003; Pichon et al., 2004; Tessier et al., 2003; Tomasovic et al., 1989), I also examined whether Hsp27 would colocalize with actin and/or tubulin in neurons. Representative results are presented in Figure 2.2. Figures 2.2A and D show actin (red) in contact points (arrows) located at the periphery of a lamellopodium at one end of the neuron in A and around the circumference of the lamellum of the neuron in D. Figures 2.2B and 2.2E show the corresponding images for Hsp27 (green). The merged images (Fig. 2.2C, F) show that Hsp27 and actin appear to be colocalized in focal contacts.

In Figures G-L, the cells were costained with antibodies for Hsp27 (green) and total tubulin (red). The neuron in Figure 2.2G and 2.2I is beginning to show progress from the lamellar stage toward the formation of small filopodia (G-I, arrow). Tubulin staining shows some concentration in the cortical area (G, large arrowhead). There is colocalization with Hsp27 in the cortical area (I, large arrowhead) and filopodia (I, arrow), although there are areas where there is little or no overlap with Hsp27 staining (G-I, small arrowhead). The neuron shown in Figure 2.2J and 2.2L displays a pattern that was seen consistently in several different experiments, with colocalization of tubulin and Hsp27 at the cortical area (arrow) and the emergence of a more discrete process (J-L, arrowhead).

Figure 2.2: Hsp27 co-localizes with actin and tubulin at early stages of neurite growth. Neurons were plated on polylysine and stimulated with laminin for 1–6 h. Following fixation, neurons were labelled with rhodamine-phalloidin (red-A, D) or immunostained with antibodies directed against total tubulin (red – G, J) or Hsp27 (green -B, E, H, K). Images were obtained with confocal microscopy and panels C, F, I, L represent the merged images of the single channel images. Note colocalization of Hsp27 and actin in the lamellopodium (A-C, arrow) and in focal contacts observed in D-F (arrow). In panels G-I, there is some colocalization of the staining for tubulin and Hsp27 in the cortical region (large arrowhead) and in small processes emerging from the soma (arrow). In panels J-L, there is a more distinct colocalization of tubulin and Hsp27 in the cortical area (arrow, J-L) as well as in an obvious process that seems to be wrapping around the cell and finally extending (arrowhead, J-L). Scale bar – 20 μm.

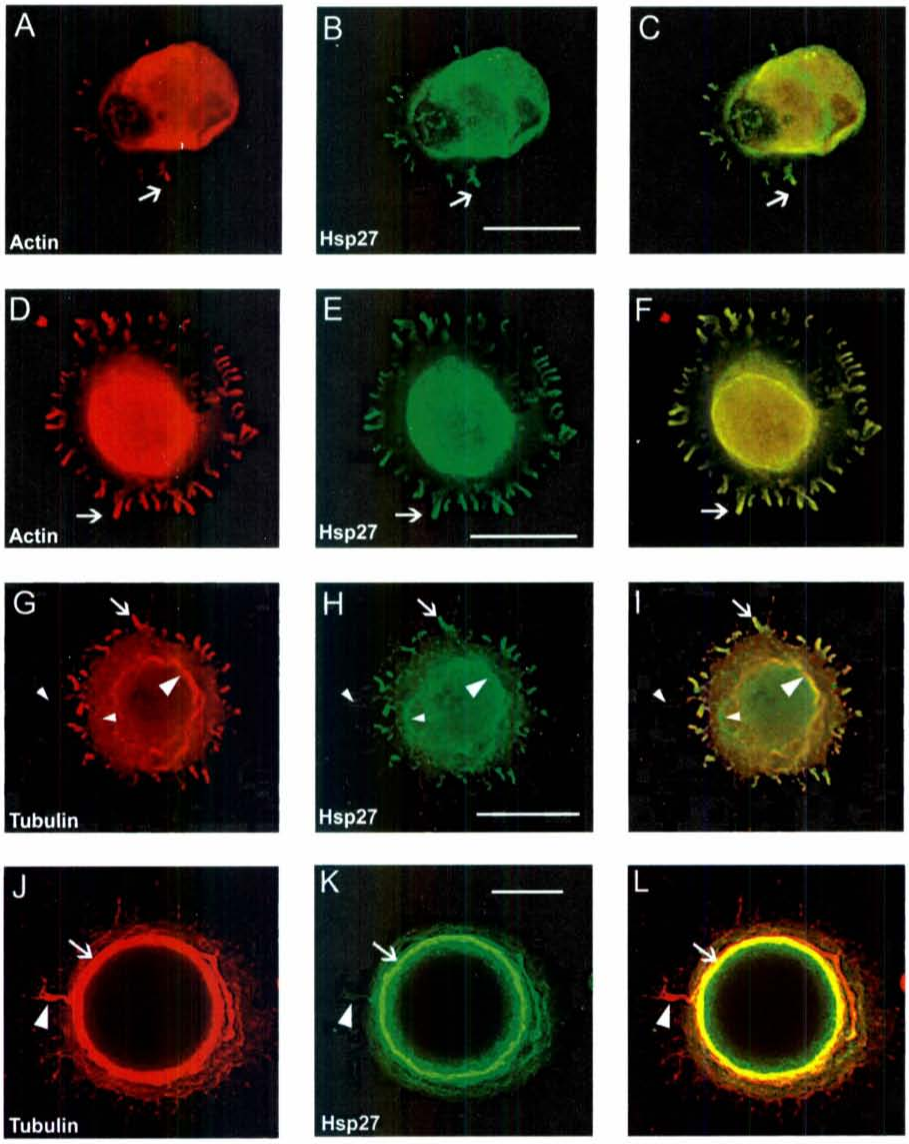
A
Actin
B
Hsp27
C
D
Actin
E
Hsp27
F
G
Tubulin
H
Hsp27
I
J
Tubulin
K
Hsp27
L

2.3.3 Phosphorylated Hsp27 is also localized with actin and tubulin at the early stages of process formation

Hsp27 can be phosphorylated on 2 sites of rat Hsp27 (ser15 and ser 86), and this phosphorylation is reported to be important in the role of Hsp27 in its interactions with actin (Mounier and Arrigo, 2002). Using an antibody that recognizes Hsp27 phosphorylated on the ser15 site (pHsp27 ^{S15}, ABR), I costained neurons at early stages (as defined above) of process formation for pHsp27 and actin (Fig 2.3A and 2.3F) and pHsp27 and tubulin (Fig 2.3G and 2.3L). Actin (A, D) and pHsp27 (B, E) show overlap in the lamellopodium (arrow) and in focal contacts (arrow, D-F). However, this is not complete, as noted by the exclusion of the pHsp27 from the leading edge of the lamellopodium (arrow, B, C). Tubulin (Fig 2.3G,J) and pHsp27 (Fig 2.3H,K) also colocalize in focal contacts (arrow, G-I), emerging filopodia (arrow, J-L) and in the cortical area (small arrowhead, J-L).

2.3.4 Colocalization of Hsp27 and cytoskeletal elements in neurites and growth cones at later stages of neurite growth and extension

Our initial observations indicated that the majority of adult DRG neurons in culture display robust expression of Hsp27, not only in the cell bodies but throughout the neurites when present. Hsp27 expression in sensory neuron cell bodies as well as dendritic and axonal networks has been previously reported for *in vivo* expression (Benn et al., 2002; Costigan et al., 1998; Plumier et al., 1997). In the present study, I further examined this distribution, particularly in terms of co-expression with actin and tubulin.

Figure 2.3: pHsp27 also co-localizes with actin and tubulin at early stages of neurite growth. Neurons plated on polylysine and stimulated with laminin for 1–6 h were also immunostained with antibodies directed against phosphorylated Hsp27 ($pHsp27^{Ser15}$) to examine colocalization with actin or tubulin. A, D – rhodamine-phalloidin (red); B, E, H, K – pHsp27 (green); G, J – tubulin (red). The respective merged images are presented in panels C, F, I, L. Actin and pHsp27 appear to be colocalized in the body of the lamellopodium in A-C, but actin seems to be excluded from the leading edge (arrows). There is also localization of pHsp27 and actin in focal contacts (D-F, arrows). pHsp27 also colocalizes with tubulin in focal contacts (G-I, arrow), in a cortical ring (arrowhead) and in processes emerging from the cell body (J-L, arrow). Scale bar – 20 μm.

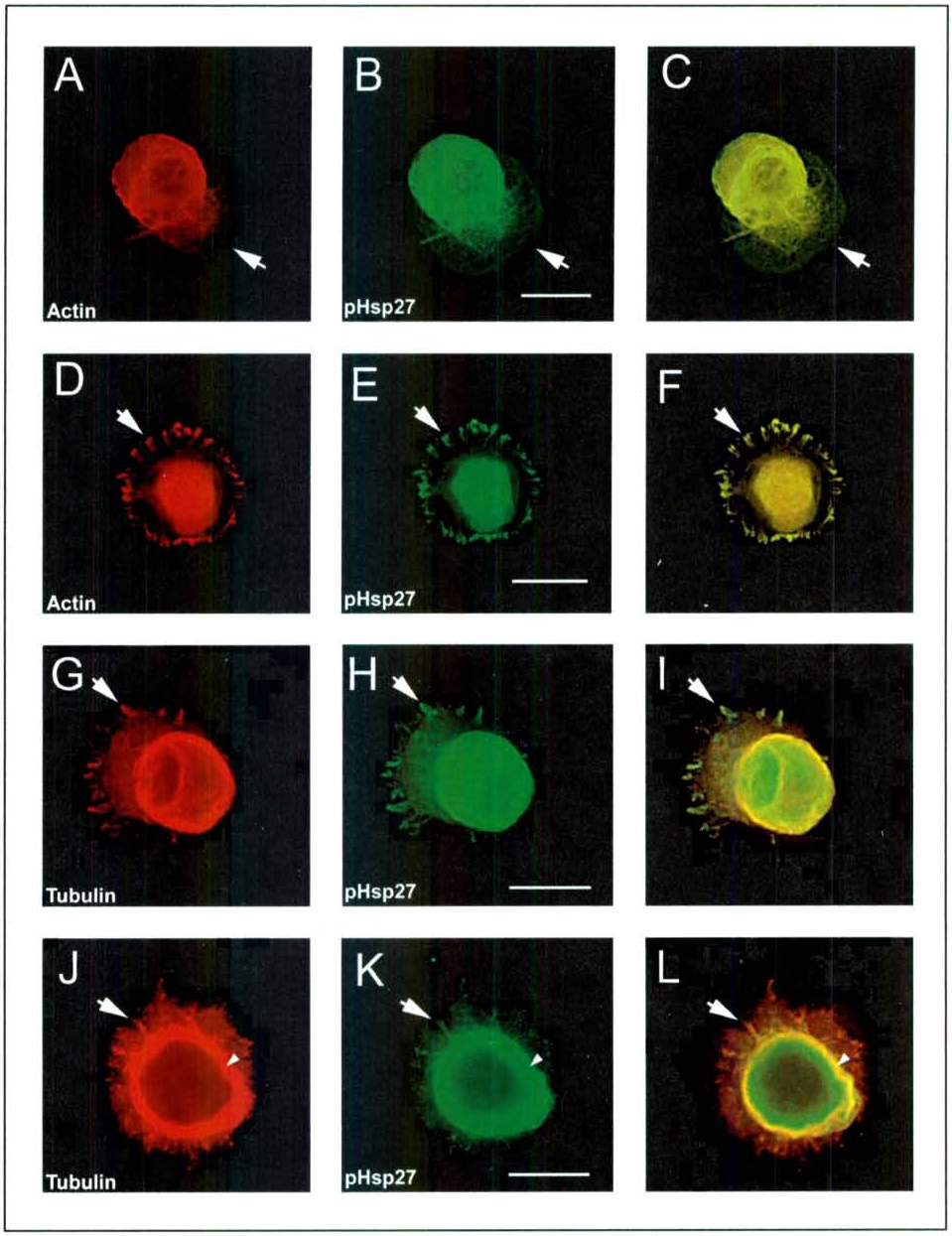
A
Actin
B
pHsp27
C
D
Actin
E
pHsp27
F
G
Tubulin
H
pHsp27
I
J
Tubulin
K
pHsp27
L

Rather than using the soluble laminin stimulation paradigm employed in the experiments examining early events, in these experiments I plated the neurons directly onto laminin-coated slides and then fixed the cultures 24 h after plating. I have previously reported that when adult DRG neurons are cultured on surfaces coated with diluted growth factor-free Matrigel, or laminin, a relatively high percentage of the neurons display significant amount of neurite outgrowth by 24 h after plating (Jones et al., 2003).

Figure 2.4A,F show representative neurons stained for actin (A, D) and pHsp27 (B) or Hsp27 (E) with the merged images displaying colocalization (C, F). The bottom panels show staining for total tubulin (G, J), pHsp27 (H) and Hsp27 (K) and the corresponding merged images in (I, L). As can be seen from the figures, Hsp27 is expressed throughout the neurons and associated neurites. As with the early stages of growth, tubulin strongly stains the cortical aspect of the cell soma as well as being present throughout the processes. One interesting feature of the Hsp27 localization is the presence or local accumulation of Hsp27 and pHsp27 along with actin (but apparently not with tubulin) in branch or nodal points (arrowheads), suggesting a potential role in the pattern of neurite growth and branching. A previous publication reports beading of Hsp27 staining in dendrites of motor neurons and sensory neurons in sectioned material, although there was little discussion of the significance of this staining, other than to indicate that it was not associated with degenerating fibres (Plumier et al., 1997).

I also noted that the Hsp27 and pHsp27 were strongly colocalized in growth cones, further supporting an important role for Hsp27 not only in neurite initiation but also continued neurite extension. Figure 2.5 presents typical growth cones seen in the

Figure 2.4: Hsp27 continues to be expressed and localized with cytoskeletal elements in neurons and neuritic networks. In these experiments, neurons were plated on laminin (no added neurotrophins) and fixed 24 h after plating. As shown in the images, many neurons exhibit extensive neuritic growth under these conditions. A-F: Neurons were labelled with rhodamine-phalloidin (A, D, red), and immunostained for pHsp27 (B, green) and Hsp27 (E, green); C, F – merged images. G-L: Neurons were immunostained for tubulin (G, green; J, red), pHsp27 (H, red), Hsp27 (K, green); I, L – merged images. Hsp27 and pHsp27 are expressed throughout the neuritic network, and there is colocalization of these with actin (C, F) and less so with tubulin (I, L). Note the accumulation of pHsp27 and Hsp27 at point of branching of neurites (arrowheads- B, C, E, F, H, I, K, L). The cortical colocalization of tubulin with pHsp27 and Hsp27 is still evident at this stage of neurite growth (arrows – I, L). Scale bar – 50 μm.

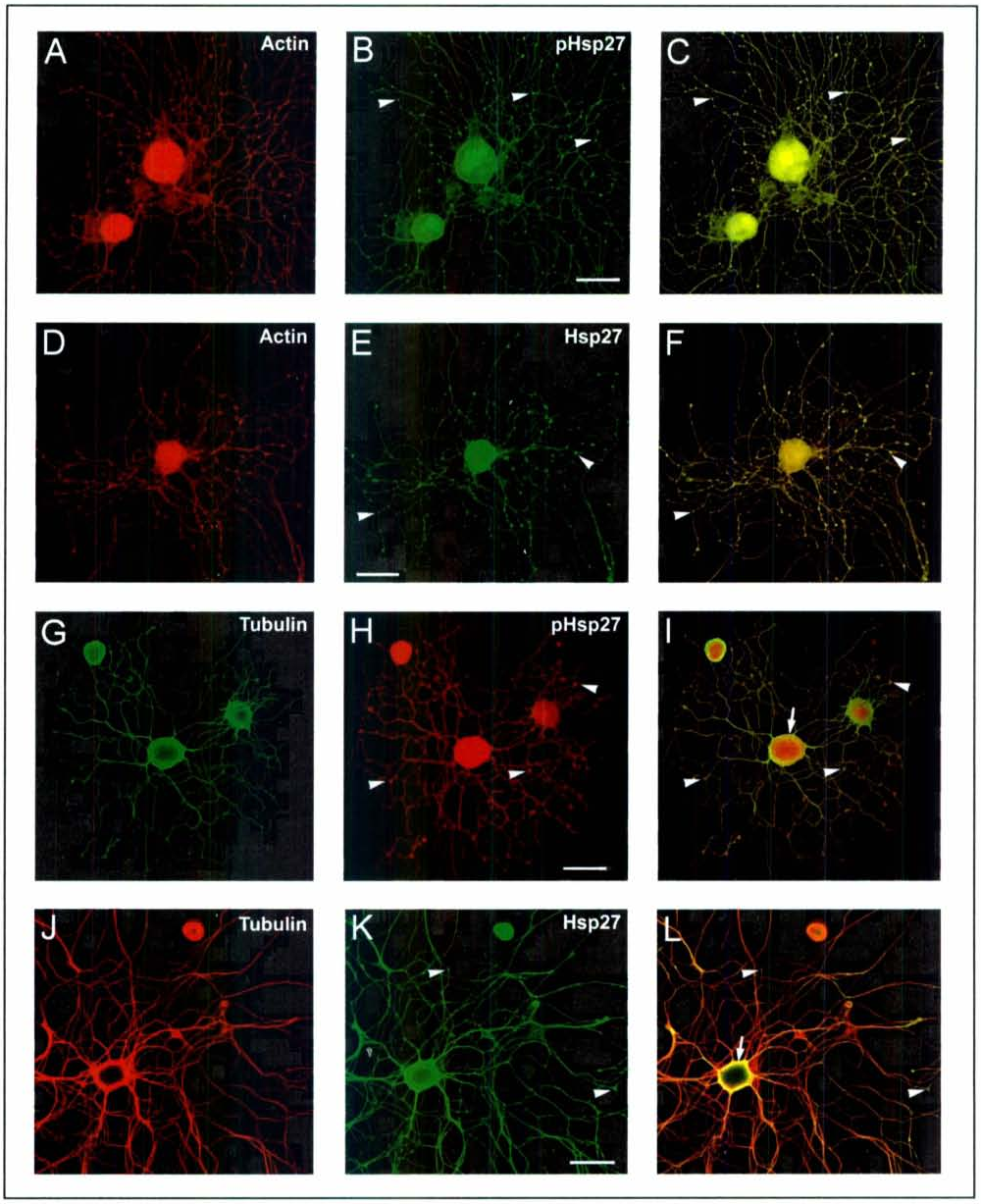
A
Actin
B
pHsp27
C
D
Actin
E
Hsp27
F
G
Tubulin
H
pHsp27
I
J
Tubulin
K
Hsp27
L

Figure 2.5: Co-localization of Hsp27 and tubulin in growth cones of growing neurites. Growth cones from neurons plated on laminin as outlined for Figure 2.4 were observed to express both pHsp27 and Hsp27. pHsp27 (A) and Hsp27 (C, E, red), shown together with tubulin (green-yellow) in the merged images (B, D, F), are present in growth cones and filopodia extending from the growth cones (arrows). There is also an accumulation in the core of growth cones and at points of neurite branching (arrowheads-A-F). Note that the tubulin staining does not completely overlap with pHsp27 or Hsp27, particularly in some of the extending filopodia (B, arrow) and the core of the growth cones in D, F (arrowheads). Scale bar = 10 μm.

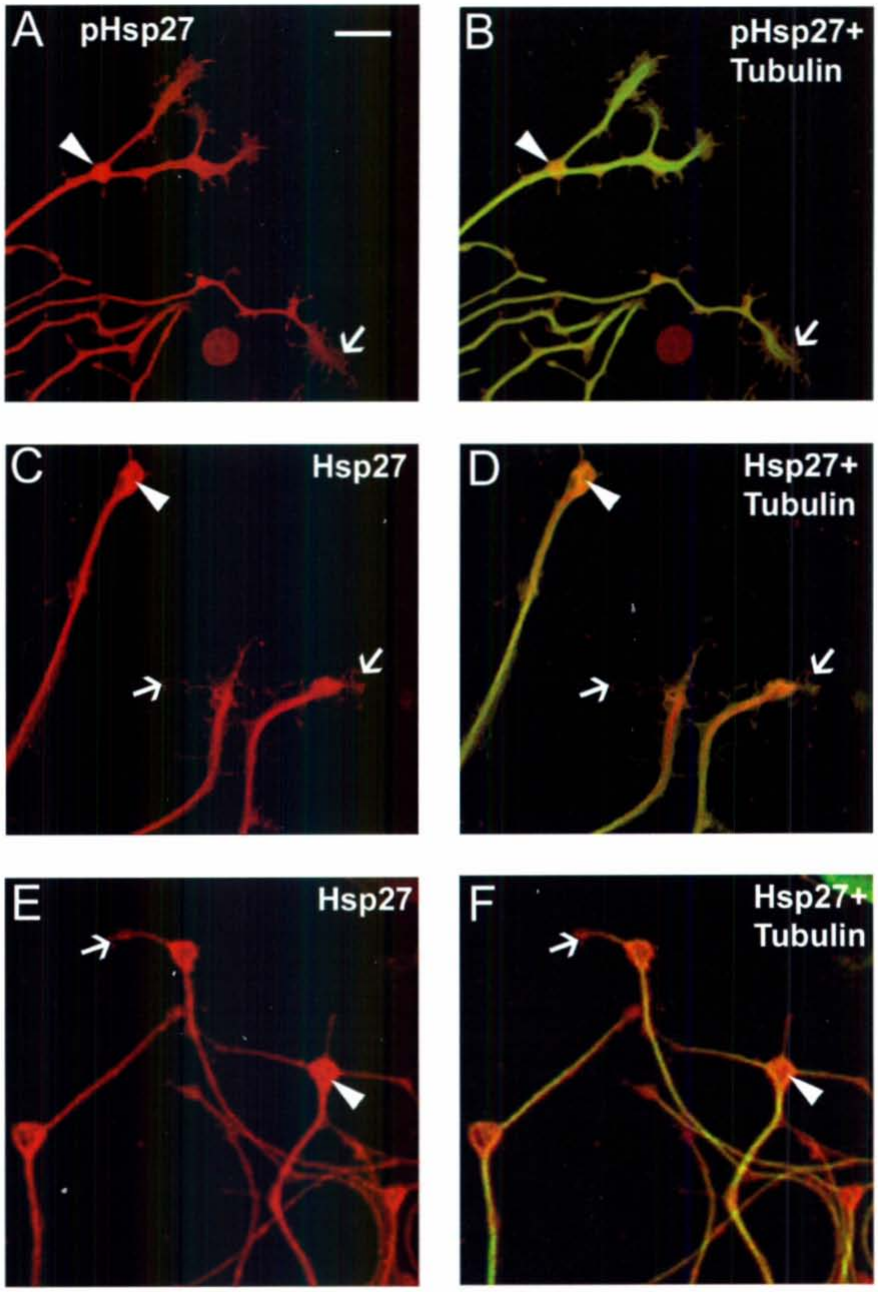
A
pHsp27
B
pHsp27+
Tubulin
C
Hsp27
D
Hsp27+
Tubulin
E
Hsp27
F
Hsp27+
Tubulin

cultures described above. Different types of growth cones were observed with pHsp27 (A, B) and Hsp27 (C-F) being present in the core (arrowheads) of more expanded growth cones as well as in the filopodia (arrows). The growth cones in Figure 2.5C, F resemble the branch points noted in Figure 2.4, with an accumulation of an Hsp27 core and filopodia showing both Hsp27 and tubulin (merged images in D and F; tubulin, green and Hsp27, red). While the significance of this localization is not entirely clear, it is possible that one role of Hsp27 is to stabilize the cytoskeleton at these points where branching may occur (see below).

2.3.5 Disruption of actin cytoskeleton with cytochalasin D results in aberrant neurite growth

Hsp27 has been suggested to play a key role in modulating actin cytoskeletal dynamics by acting as an actin-capping protein. In order to understand the role of Hsp27 in neuritic growth I decided to examine the effects of disrupting the actin cytoskeleton integrity using cytochalasin D (CytD). Neurons were plated on laminin-coated slides and CytD was added to the medium 3 h post-plating (2 μM final concentration). Cultures were fixed 24 h later and examined for changes in neurite growth patterns and expression of Hsp27 and actin or tubulin.

Representative examples of the effects of CytD on neurons are presented in Figure 2.6. There was no discernible distinction between different sizes of neurons in their response to CytD; small, medium and large sized neurons displayed atypical process formation. Compared to the usual patterns of neuritic growth (Fig 2.4), neurons treated

Figure 2.6: Disruption of the actin cytoskeleton results in aberrant neurite growth. Neurons plated on LN were treated with cytochalasin D (2 mM, added 3 h after plating), fixed 24 h later and stained for pHsp27 (B, H), Hsp27 (E, K), actin (A, D) or tubulin (G, J). The respective merged images are presented in panels C, F, I and L. The cytochalasin D treatment resulted in various atypical patterns of growth. One phenotype was the elaboration of numerous processes or microspikes as seen in panels A-C, with obvious accumulation of actin and pHsp27 especially at the tips of the microspikes (arrowheads); pHsp27, but not actin, accumulates in the nucleus (B, C, arrow). Abnormal process extension was also observed. In the neuron shown in D-F, some extension was observed although there was now less colocalization of actin with the Hsp27 (arrowheads). Panels G-L show tubulin staining along with either pHsp27 or Hsp27; the fibillar nature of the cytoskeletal network is clearer in these examples (arrows). Arrowheads point to atypical neurite growth, e.g., lacking the usual radial branching pattern as seen in Fig 4. Scale bar = 20 μm.

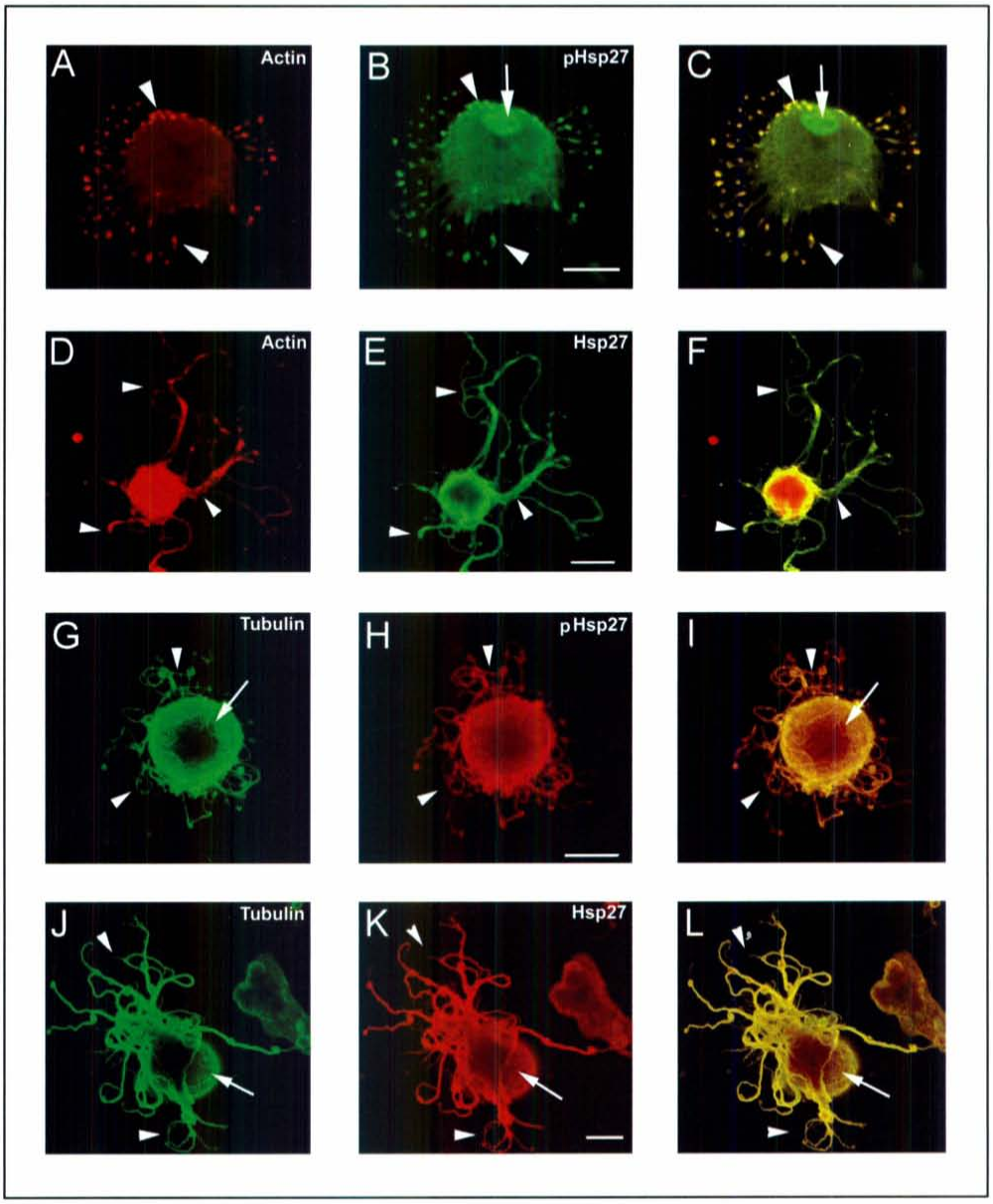
A
Actin
B
pHsp27
C
D
Actin
E
Hsp27
F
G
Tubulin
H
pHsp27
I
J
Tubulin
K
Hsp27
L

with CytD showed aberrant growth (Fig 2.6) including multiple processes emerging from the cell body (A-C), as well as stunted and disorganized neurites (D-L). In the cell displayed in Figure 2.6A,C, the processes show accumulation of actin (red) and pHsp27 (green) in their tips (arrowheads). Another example (D-F) shows several neurites that appear to have a disorganized internal structure resulting in the lack of the normal radial neurite extension and branching (arrowheads). In these examples, I used an antibody against actin, rather than phalloidin, in order to see total actin. In the bottom panels of Figure 2.6, two more examples are presented showing tubulin (green, G and J), pHsp27 (red, H) and Hsp27 (red, K) and the corresponding merged images (I, L). The cytoskeleton is more apparent in these latter examples, where the tubulin (and Hsp27) staining is clearly fibrillar in nature (arrows). Again, the disorganized and looping growth of neurites is apparent (arrowheads). In panels A-F, the actin antibody recognizes total actin, so even though CytD should disrupt the F-actin network, the antibody still detects G-actin.

2.3.6 Inhibition of Hsp27 phosphorylation also results in aberrant neurite growth

Because of the reported role of Hsp27 phosphorylation in modulating the actin cytoskeleton, I wished to determine the effects of inhibiting p38 MAPK. p38 MAPK activity leads to the phosphorylation and activation of MAPKAP-K2, which acts as an Hsp27 kinase (Huot et al., 1995; Larsen et al., 1997). Inhibition of p38MAPK activity has been used to block phosphorylation of Hsp27 in the absence of direct inhibitors of MAPKAP-K2. I have thus used a combination of 2 commercially available p38 MAPK

inhibitors (SB, SB203580 and SB202190, 10 μM each) to investigate the potential contribution of phosphorylated Hsp27 to neurite growth.

I initially determined whether the inhibitors were effective in preventing Hsp27 phosphorylation. Using larger scale cultures, neurons were plated on LN-coated 12-well plates and after 3 h the inhibitors were added; 24 h after SB addition, cell lysates were prepared as described in the Methods. For these experiments, I used a commercially available protocol to fractionate the cells into cytosolic, membrane, nuclear and cytoskeleton fractions. Following electrophoresis, the resulting blots were probed with pHsp27 ^{S15} and total Hsp27 antibodies. The results of a representative experiment presented in Figure 7 show that inhibitors do indeed attenuate the phosphorylation of Hsp27. The blots also show that Hsp27 is found in the cytosolic, membrane and cytoskeletal fractions, while the pHsp27 is associated primarily with the soluble fraction.

Having determined that the inhibitors had the expected effects on pHsp27, I then plated the neurons on laminin-coated slides as for the previous experiments, and treated the cultures with SB 3 h after plating, fixed the cells 24 h later and carried out immunostaining for pHsp27, Hsp27, actin and tubulin as before.

Neurons treated with SB displayed clearly atypical neurite growth. The examples presented are representative of the various patterns of neurite growth observed. As with the CytD treatment, there was no discernible distinction between different sizes of neurons in their response to SB; small, medium and large sized neurons displayed aberrant process formation. In the neuron shown in Figure 2.8 A,C, the neurites emerged from the cell body but wrapped around the soma (arrowheads) and appeared unable to

Figure 2.7: p38 MAPK inhibition blocks phosphorylation of Hsp27. Neurons plated on laminin were exposed to p38 MAPK inhibitors, SB203580 and SB202190 (10 mM each). Cells were sampled at 24 h post SB addition, using cellular subfractionation (as described in the Methods). The resulting protein from cytosol, membrane, nucleus and cytoskeleton fractions was electrophoresed and the blot subsequently probed for pHsp27 and Hsp27. Inhibition of p38 MAPK activity (laminin+SB) results in attenuation of the Hsp27 phosphorylation.

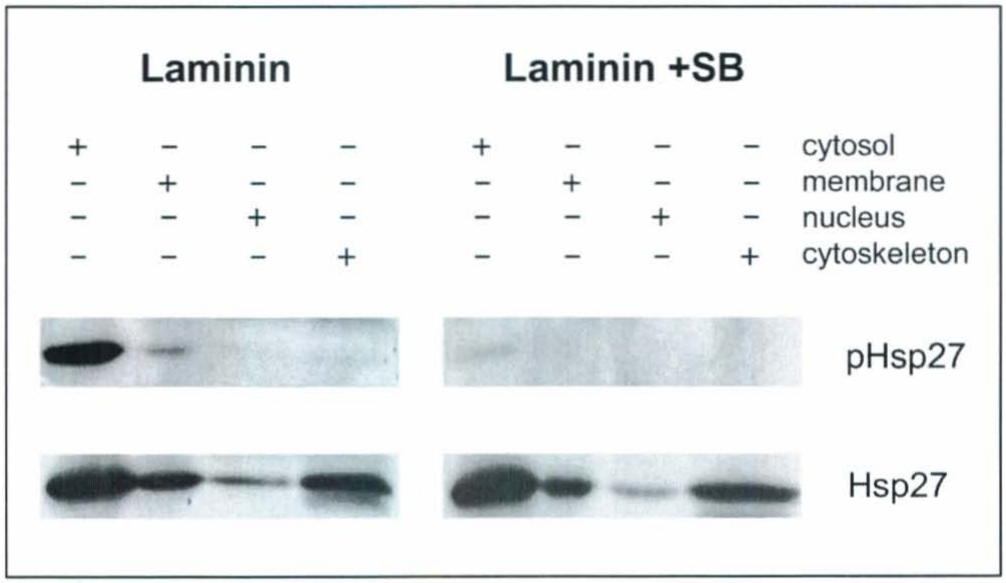
Laminin
Laminin +SB
+ − − − + − − − cytosol
− + − − − + − − membrane
− − + − − − + − nucleus
− − − + − − − + cytoskeleton
pHsp27
Hsp27

undergo appropriate extension. Another common observation was the appearance of relatively short but flattened and expanded processes and growth cones. The example in Figure 2.8D,F is stained for tubulin (D, green) and Hsp27 (E, red), with the merged image (F) showing the disorganized nature of the cytoskeletal elements (arrows). In this example, note that tubulin does not have complete overlap with Hsp27 staining, particularly at the tips of the growth cones (F, arrowheads).

In addition, some neurons displayed extensive neurite growth, although this was again generally characterized by flattened and expanded processes and growth cones. Figure 2.9 presents such an example. This neuron has at least 7–8 processes extending from the cell body, all of which show process expansion. In panels A-C, Hsp27 (red) can clearly be observed colocalized with tubulin (green) in the processes emerging from the cell body (arrows). Areas of the fibrillar nature and overlap of Hsp27 and tubulin are also noted (arrowheads). In Figure 2.9D,F, larger magnification of the area generally noted by the arrowheads in A-C is shown. Here the splaying of the growth cones (arrows) and loss of cytoskeletal bundling is more apparent (arrowheads; compare processes observed in Figure 2.4 or 2.5 with those in Figure 2.9).

These results suggest that attenuation of the phosphorylation of Hsp27 can have adverse effects on the neuritic cytoskeleton, similar to those observed with Cyt D. Although our assumption (based on previous reports in the literature) is that the SB compounds block p38 MAPK activity, its downstream effects on MAPKAP-K2 and the subsequent inhibition of Hsp27 phosphorylation, it is possible that these compounds may have other inhibitory influences, or that they may be influencing the cytoskeletal

Figure 2.8: Aberrant neurite growth following inhibition of Hsp27 phosphorylation. Neurons plated on laminin were treated with p38 MAPK inhibitors (SB203580 and SB202190, 10 μM each, added 3 h after plating) and fixed 24 h later. Representative results are presented. Some neurons showed abortive extension, with neurites wrapping around the cell body, such as the example in panels A-C (arrowheads, A, tubulin, B, Hsp27, C, merged image). In another example, numerous processes were observed, but these terminated in large, flattened and splayed growth cones, as shown in panel D-F (D, tubulin, E, Hsp27, F, merged image). The fibrillar nature of the Hsp27 (E, arrows) and tubulin (D, arrows) is evident and the sites of colocalization with tubulin are also apparent (F, arrows). Also note that there is not a complete overlap of Hsp27 and tubulin at the tips of the growth cones (F, arrowheads). Scale bar – 20 μm.

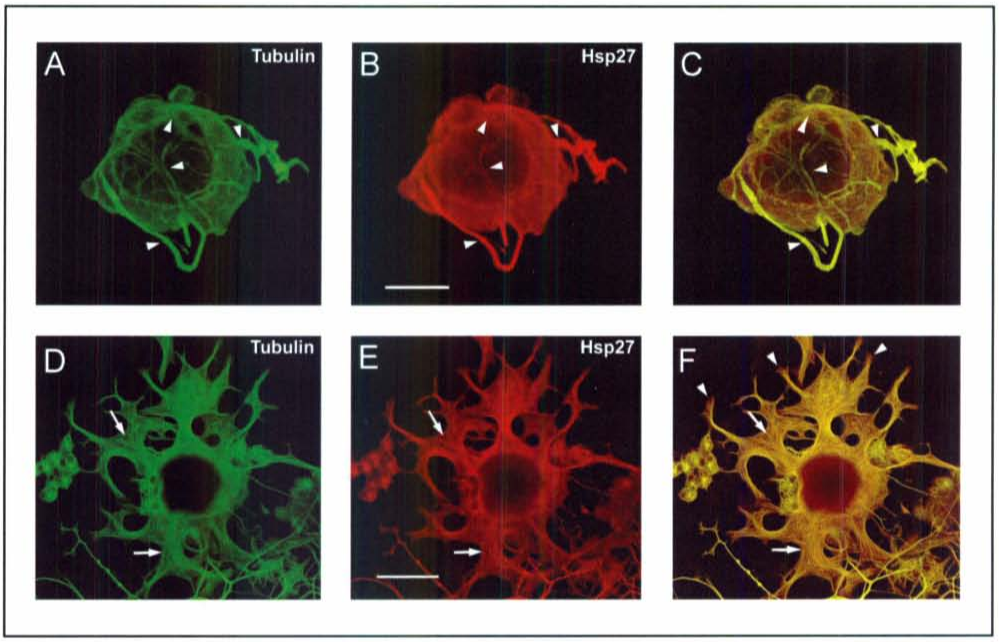
A
Tubulin
B
Hsp27
C
D
Tubulin
E
Hsp27
F

Figure 2.9: Flattened growth cones and processes show co-localization of tubulin and Hsp27. This figure shows another example of a neuron treated with the p38 MAPK inhibitors as outlined in Figure 8. Colocalization of Hsp27 (B, red) with tubulin (A, green) is apparent in the emerging processes (C, arrows), and in the flattened and splayed growth cones (A-C, arrowheads); scale bar =50 μm. At a higher magnification (D-F), loss of microtubule bundling is observed (arrowheads) along with the fibrillar nature of Hsp27 and colocalization with tubulin (arrows); scale bar – 20 μm.

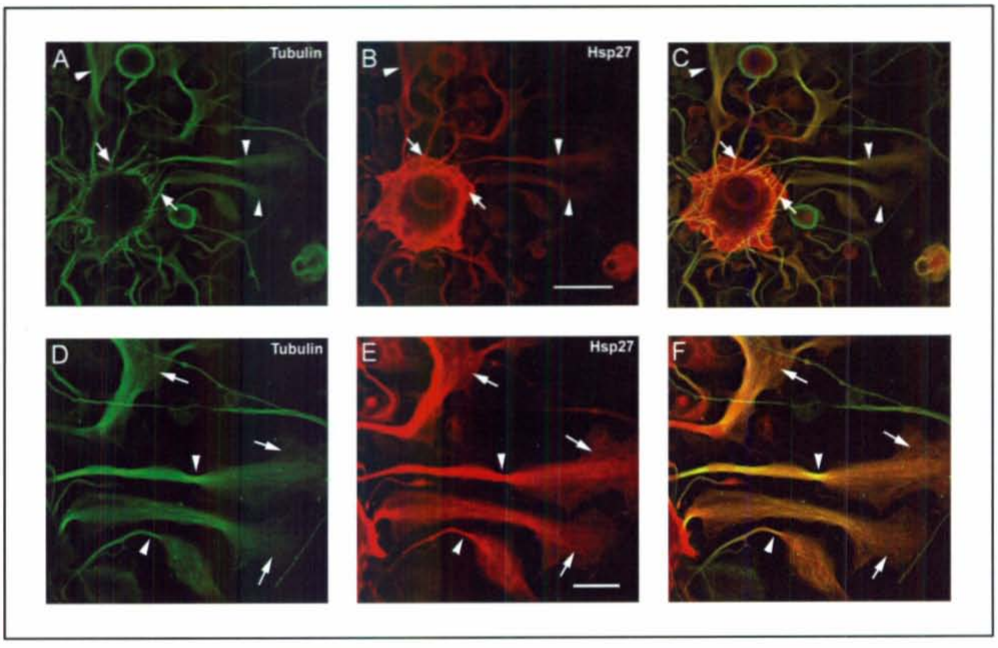
A
Tubulin
B
Hsp27
C
D
Tubulin
E
Hsp27
F

elements through actions not involving Hsp27. While our data show that the SB compounds do inhibit phosphorylation of Hsp27, I cannot completely rule out effects on other signalling components, although at the concentrations I have used, the effects are reported to be specific for p38 MAPK inhibition, rather than any other additional kinases.

2.4 Discussion

I describe early events in adult DRG neuron process formation in response to stimulation with the extracellular matrix protein laminin. Our data show that Hsp27 appears to associate with actin and tubulin in structures found at all stages of neurite initiation. Lamellopodia, filopodia, microspikes and focal contacts all displayed a colocalization of Hsp27 and actin or tubulin. The filamentous nature of the Hsp27 was quite clear in neurites and growth cones supporting the hypothesis that Hsp27 is associating with cytoskeletal elements.

Our results are similar to those described previously for neurite growth initiation and process extension in embryonic cultured CNS neurons. Culture studies of early neuritogenesis events in hippocampal neurons have provided information that demonstrates that events after initial cellular attachment to the substrate are quite similar among different cell types and indeed events in neurons are very similar to those in migratory fibroblasts (Bradke and Dotti, 1999; da Silva and Dotti, 2002; Dehmelt et al., 2003). The cells attach and are surrounded by a thin lamellopodium from which small extensions sprout. These extensions often have growth cones and display dynamic back and forth movements. At some point, one or more of these processes elongates, while the

others remain stationary or retract. All the stages described by DaSilva and Dotti (2002) and Dehmelt and Halpain (2005) could be identified in our cultures of adult DRG neurons, suggesting that this process is intrinsic to all neurons.

Neurite protrusion requires the actin cytoskeleton, with lamellopodia being filled with an actin meshwork necessary for the appropriate adhesion and filopodia having actin bundles with the rapidly growing ends oriented towards the tips. Studies have shown that actin polymerizes at the leading edge of the lamellopodia, and then disassembles and recedes from the peripheral area (Dehmelt and Halpain, 2004; Gallo and Letourneau, 2004). This phenomenon influences growth cone advance and could likely play a role in neurite initiation as well. Microtubules may play a mechanical role in this since they invade the actin cytoskeleton in lamellopodia of various cell types (da Silva and Dotti, 2002; Dehmelt and Halpain, 2004; Gallo and Letourneau, 2004).

In cell-free assay systems, Hsp27 can act as an actin-capping protein which prevents the polymerization of actin and the assembly of F-actin (Benndorf et al., 1994; Miron et al., 1991). Phosphorylation of Hsp27 leads to the loss of its ability to inhibit actin polymerization, and thus increases the rate and extent of actin polymerization and the formation of F-actin (Benndorf et al., 1994; Landry and Huot, 1995, 1999; Lavoie et al., 1995; Miron et al., 1991). In addition to modulating the actin cytoskeleton, Hsp27 interacts with both neurofilaments and microtubules in a phosphorylation-dependent manner (Der Perng and Quinlan, 2004; Perng et al., 1999a). Hsp27 has been inferred to stabilize not only actin, but also neurofilament and microtubules (Mounier and Arrigo, 2002).

Phosphorylation of Hsp27 promotes the polymerization of actin and stress fibre formation (Benndorf et al., 1994; Guay et al., 1997; Huot et al., 1998). Hsp27 is phosphorylated on 3 serines in the human Hsp27 (S15, S78, S82) and 2 in the rodent Hsp27 (S15 and S86 in mouse or S90 in hamster Hsp27). Hsp27 in unstressed cells exists as large oligomers, while upon phosphorylation Hsp27 dissociates in smaller species, including dimers and monomers (Lambert et al., 1999; Rouse et al., 1994). In cell free assays, the unphosphorylated monomers of Hsp27 blocked actin polymerization, while the unphosphorylated oligomers and the phosphorylated monomeric form were ineffective. While the evidence based primarily on structural studies supports a role for phosphorylation of Hsp27 in stabilization of the actin cytoskeleton, a recent study has provided direct functional evidence that this is indeed the case (An et al., 2004).

Hsp27 phosphorylation is regulated by activity of the p38MAPK pathway, whereby p38 MAPK activation of MAP-kinase-activated protein-kinase 2/3 (MAPKAP-K2) leads to the phosphorylation of Hsp27 (Larsen et al., 1997; Rouse et al., 1994). However, PKCδ and cGMP-dependent kinase have also been reported to phosphorylate Hsp27 in smooth muscle (Butt et al., 2001; Maizels et al., 1998). While the classical stress-activated signalling pathway activation of p38 MAPK regulates Hsp27 after heat-shock and other stresses, it is more likely that activation of p38 MAPK is downstream of the Cdc-42 and Rac activation of Pak1 with respect to neurite initiation and growth. For example, laminin can lead to p38 MAPK activation and Hsp27 phosphorylation, as previously reported for Schwann cells (Fragoso et al., 2003), and this is likely via Cdc-42 and Rac activation downstream of integrin-dependent signalling cascades (Mounier and

Arrigo, 2002). Given the role of Rac and Rho in regulating actin dynamics in growth cones and the observations that inhibition of Rho promotes axonal growth on inhibitory substrates (Ellezam et al., 2002; Lehmann et al., 1999), the interactions of Hsp27 with Rho observed in smooth muscle cells (Patil et al., 2004a; Patil et al., 2004b; Wang and Bitar, 1998) suggests an intriguing interplay among these components. Whether a similar interaction occurs in neurons or axons is not known.

Treatment of neurons with agents that disrupt the actin cytoskeleton result in aberrant neurite initiation and growth. Neurons treated with Cyt D, which caps existing actin filaments at barbed ends, consistently show rapid emergence of numerous neurites that elongate in a disorganized fashion (Bradke and Dotti, 1999; da Silva and Dotti, 2002; Dehmelt and Halpain, 2004). Treatment of DRG neurons in our cultures resulted in similar aberrant growth, particularly at the early stages examined where numerous projections emerged from the neurons as early as 1 h after laminin stimulation (data not shown); neurons examined at 24 h showed disoriented growth of processes (e.g., Fig 2.6).

Since Cyt D acts to cap barbed actin filaments and non-phophorylated Hsp27 has been suggested to do the same, I reasoned that if pHsp27 was important for normal neurite initiation and extension, if I inhibited the phosphorylation of Hsp27 I might observe similar effects on neurite initiation. As shown in our results, attenuation of Hsp27 phosphorylation using the p38MAPK inhibitors, does indeed result in atypical growth patterns. At the early stages, results were similar to what I had observed with Cyt D (data not shown), and at later stages, neurite growth was again quite clearly aberrant (Fig 2.8, 2.9). Some neurons showed neurites that tended to wrap around the cell soma or

extend in a disoriented fashion. Another consistent characteristic of the relatively short processes that did extend was the flattened and splayed nature of the neurites and growth cones. There appeared to be a lack of the appropriate actin and microtubular bundling that would result in normal neurite extension and growth cone dynamics (e.g., compare Fig 2.4, 2.5 with Fig 2.6 and 2.8) (Dehmelt and Halpain, 2004; Gallo and Letourneau, 2004). I have inferred that effects of p38 MAPK inhibition on neurite growth were due to the inhibition of Hsp27 phosphorylation. A similar inhibition of neurite initiation by SB has been reported in PC12 cells (Kano et al., 2004); interestingly, in this study induction of Hsp27 by heat shock promoted neuritogenesis. However, there may be effects on other cytoskeletal elements. Ackerley et al (2004) have reported that p38 MAPK also phosphorylates neurofilaments in transfected COS cells, although they did not find any effect of p38 MAPK inhibition on neurofilament phosphorylation in cortical neurons.

There are relatively few reports of the interaction of Hsp27 with cytoskeletal elements other than actin. Hsp27 associates with microtubules in HeLa cells (Hino et al., 2000) and in CHO cells (Hargis et al., 2004). In the latter report, overexpression of Hsp27 protects microtubules from heat shock and pH-induced collapse, although the contribution of pHsp27 to this effect was not reported (Hargis et al., 2004).

pHsp27 also appears to be required for the migration of several cell types (Hedges et al., 1999; Pichon et al., 2004; Piotrowicz et al., 1998; Rousseau et al., 1997). A recent study concluded that p38MAPK activation and Hsp27 phosphorylation played a key role in the regulation of actin polymerization, possibly by regulating the spatial organization of the lamellopodia by promoting branch formation at the leading edge and stability at the

base (Pichon et al., 2004). They suggest that at the dynamic leading edge of lamellopodia, Hsp27 might promote branching by its actin-capping activity, while at the base p38MAPK remains active and Hsp27 is phosphorylated and might stabilize actin filaments.

Mutations of the small Hsp (Hsp22 and Hsp25/27) genes have been linked to axonal Charcot-Marie-Tooth disease and distal hereditary motor neuropathy (dHMN) (Evgrafov et al., 2004; Irobi et al., 2004b). This appears to be related to the disruption of the neurofilament networks by the aggregation of neurofilament proteins and collapse of neurofilament networks (Evgrafov et al., 2004). This study and recent commentaries (Der Perng and Quinlan, 2004; Lee and Leavitt, 2004) point to the importance of the small heat shock proteins like Hsp27 in regulating or modulating the function of cytoskeletal elements other than actin. However, the mechanisms underlying the function of Hsp27 and its regulation remain essentially unknown in neuronal cells.

Our results suggest that Hsp27 is necessary for the initiation of neurite outgrowth in DRG neurons. The data also suggest that phosphorylation of Hsp27 plays a key role in modulating the dynamic interactions of Hsp27 with cytoskeletal elements such as actin and tubulin to regulate the response of DRG neurons to environmental cues that mediate growth.

2.5 Conclusion

Using immunocytochemistry, I observed colocalization of the phosphorylated and non-phosphorylated forms of Hsp27 with actin and tubulin in both very early and later

stages of neurite growth from cultured adult DRG neurons. The colocalization of Hsp27 and pHsp27 with actin in lamellopodia and focal contacts at early neurite initiation stages, and in processes, branch points and growth cones in later stages suggests that Hsp27 may play a role in neurite initiation and extension and potentially in the patterning of this growth. While the mechanisms of action require further investigation, it is possible that one role of Hsp27 is to stabilize the cytoskeleton at potential sites of branching or sprouting. Hsp27 has been reported to play a key role in modulating actin cytoskeletal dynamics as an actin-capping protein in non-neuronal cells and our results suggest that this may also be the case in neurons. Neurons treated with cytochalasin D showed aberrant neurite growth patterns. Neurons treated with p38 MAPK inhibitors, which inhibit the downstream phosphorylation of Hsp27, also displayed either lack of neurite growth or failure of appropriate neurite extension. The similar results from the CytD and inhibition of Hsp27 phosphorylation support a role for Hsp27 in neurite outgrowth via its phosphorylation state-dependent interactions with actin.

2.6 Methods

2.6.1 Neuronal cultures

Dorsal root ganglia (DRG) from young adult (5–6 wk) Sprague-Dawley rats (Memorial University of Newfoundland Vivarium and Charles River Canada, Montreal, QC) were dissected and dissociated using modifications to techniques described previously (Jones et al., 2003; Mearow et al., 2002). Briefly, ganglia from all spinal levels were removed and the roots trimmed, and subsequently incubated in 0.25% collagenase for 45 min, followed by 0.25% trypsin for 20 min (Invitrogen/ Gibco BRL, Burlington, Ont). Dissociated neurons were suspended in serum-free Neurobasal medium (NB, Invitrogen) supplemented with 100 U penicillin/streptomycin, B27 supplement (Invitrogen), and 20 μM cytosine arabinoside (modified NB). This suspension was then layered on top of a 28% Percoll solution (Amersham Bioscience, Baie d'Urfe, QC) in 15 ml conical tubes, centrifuged at 400 g for 20 min at room temperature. Pellets were then carefully extracted with a sterile pasture pipette, placed in a fresh tube, washed with the previous suspension media and centrifuged to remove any remaining Percoll. Neurons were plated in Lab-Tek 16-well chamber slides (Nunc International, Naperville, NC) for neurite growth assessment or 12-well plates for Western blotting and incubated at 37°C, 95% O_2 and 5% CO_2. Slides and culture plates were coated with poly-lysine (PL, 1 μg/ml, BD Bioscience, Bedford, MA) or laminin, (LN, 20–40 μg/ml, Invitrogen) where appropriate. The neurons were cultured in modified serum-free NB alone with no added growth factors.

2.6.2 Immunocytochemistry

Neurons were fixed in 4% paraformaldehyde (pH 7–7.4) in PBS for 20 minutes, permeabilized with 0.1% Triton-X-100 and blocked with 5% normal goat serum in PBS. Antibodies used were as follows: Hsp27 (SPA-801, Stressgen Corp, Victoria, BC) and phospho-Hsp27^{S15} (PAI-018, Affinity BioReagents, Golden, CO), total tubulin (Sigma-Aldrich, St. Louis, MO), actin (Sigma-Aldrich). It should be noted that the Hsp27 antibody recognizes both the non-phosphorylated and phosphorylated Hsp27, while the pHsp27 antibody only recognizes the phosphorylated form. I have also tested two other pHsp27 antibodies [UBI and Santa Cruz, see (Mearow et al., 2002)], but have found the Affinity Bioreagents Antibody to be better for immunostaining.

Cells were incubated with the primary antibodies at 4°C for 16–20 h, followed by Cy2 or Cy5-tagged secondary antibodies (Jackson Immunoresearch Labs, West Grove, PA). In some experiments, cells were also labelled with rhodamine-phalloidin after antibody incubation (Sigma-Aldrich). The cells were coverslipped with glycerol and imaged with confocal laser scanning microscopy using z-stage scanning and image stacking. Stacked digital images were imported into Adobe Photoshop for compilation into the final composite figures.

2.6.3 Laminin stimulation and neurite growth initiation

Neurite initiation was assessed in two ways. The first series of experiments employed neurons plated on laminin-coated slides, with the cells being fixed and analyzed for outgrowth parameters (lamellopodia, filopodia and neurite initiation and

extension) at 24 h after plating. In a second series of experiments, the neurons were first plated on polylysine coated slides and allowed to stabilize overnight prior to being stimulated with soluble laminin (20 μg/ml in basal medium). Following the addition of the laminin solution, cells were then fixed at 5, 15, 30 min, 1 h, 6 h, and 24 h. After fixation, cells were immunostained and analyzed as described above.

2.6.4 Inhibitor experiments

SB 203580 and SB 202190 (10 μM, Calbiochem/EMD Biosciences, San Diego, CA) were used to inhibit p38 MAPK activity, in order to assess the contribution of phosphorylated Hsp27. Inhibitors were added 1 h prior to laminin stimulation. For the 24 h cultures, the inhibitors were added 2–3 h after plating the cells on laminin-coated slides and retained in the medium for the extent of the experiment (usually 24 h). Cytochalasin D (2 μM, Sigma) was also used in longer term experiments, and was added 3 h after plating and maintained in the medium for the extent of the experiment (24 h).

2.6.5 Immunoblotting

For Western analyses, neurons were plated in 12-well plates that had been coated with polylysine alone or with laminin, depending on which experimental paradigm was used (see above). Neurons were subsequently processed according to our established procedures (Jones et al., 2003; Mearow et al., 2002). Cellular fractionation was carried out using a subcellular protein extraction kit (ProteoExtract, Calbiochem/EMD Biosciences, San Diego, CA) to isolate cytoplasmic, membrane, nuclear and cytoskeletal

fractions. This protocol involves sequential isolation of these fractions using specific buffer systems (proprietary, as supplied by the manufacturer) to lyse cells in situ in the tissue culture plates. Subsequently, protein concentrations were determined for the fractions using the BCA protein assay (Pierce Chemicals, Rockford, IL.). Equivalent amounts of protein (40 μg protein) were loaded in each lane. Following transfer to nitrocellulose, the blots were first stained with Ponceau Red to assess protein loading, and subsequently probed with the following antibodies: phospho-Hsp27^{S15} (PAI-016, Affinity Bioreagents) and Hsp27 (SPA-801, Stressgen),. Blots were cut and reprobed sequentially, and visualized with ECL reagents (NEN, Boston, MA) and exposure to X-ray film (Cronex MRF Clear base, Agfa Corp, Greenville, SC). Developed films were subsequently digitized and densitometrically analyzed with a cyclone ChemiImager and AlphaEase software. Digital images of the blots were used to make composite figures with Adobe Photoshop graphics software (Adobe Corp, MountainView CA).

2.7 Acknowledgements

Funding for this work was through an NSERC Discovery grant (KMM). The authors thank Dr. Daniel MacPhee, Elaine Dodge, Sherri Rankin and Budd Tucker for their invaluable assistance and discussion.

Chapter 3

Heat Shock Protein 27 Is Involved in Neurite Extension and Branching of Dorsal Root Ganglion Neurons *In vitro*

(Published in Journal of Neuroscience Research 2006, 84:716-723)

3.1 Abstract:

Alteration of the cytoskeleton in response to growth factors and extracellular matrix proteins is necessary for neurite growth. The cytoskeletal components such as actin and tubulin can be modified through interaction with other cellular proteins including the small heat shock protein, Hsp27. Our previous work suggested that Hsp27 influences neurite growth, potentially via its phosphorylation state interactions with actin. To investigate the role of Hsp27 in neurite outgrowth of adult DRG neurons I have both downregulated endogenous Hsp27 and over expressed exogenous Hsp27. Downregulation of Hsp27 with Hsp27 siRNA resulted in a decrease of neuritic tree length and complexity. In contrast, expression of exogenous Hsp27 in these neurons resulted in an increase in neuritic tree length and branching. Collectively these results demonstrate that Hsp27 may play a role in neuritic growth via modulation of the actin cytoskeleton.

3.2 Introduction

Neurite growth can be elicited through growth factors and extracellular matrix molecules acting via cell surface receptors to activate convergent signaling pathways that result in modulation of cytoskeletal elements (Giancotti and Tarone, 2003; Tonge et al., 1997; Tucker et al., 2005). Regulation of the microtubule and microfilament cytoskeleton is involved in neurite initiation and growth, with stability regulated via control of binding and capping proteins that affect polymerization and depolymerization rates, as well as filament bundling (Dehmelt and Halpain, 2004, 2005; Lebrand et al., 2004). By altering the polymerization and bundling of microtubules and microfilaments, these proteins can play key roles in neurite initiation, extension, and branching.

Heat Shock Protein 27 (Hsp27) is a member of the small heat shock protein family (sHsp), and plays a role in protecting cells from environmental stresses by regulating apoptosis and protein folding. Hsp27 interacts with different cytoskeletal elements (Charette et al., 2000; Guay et al., 1997; Huot et al., 1996; Lavoie et al., 1993a; Lavoie et al., 1995) and its protective role in stressed cells has been attributed to its actions as an actin capping protein (Benndorf et al., 1994; Miron et al., 1991), although its exact role in this process has not been elucidated. The role of Hsp27 in modulating the actin cytoskeleton has been extensively studied in non-neuronal cells, where monomeric and non-phosphorylated Hsp27 can act as an actin-capping protein, preventing the polymerization of actin filaments. Phosphorylated oligomeric and dimeric Hsp27 appear to protect and stabilize actin filaments, although whether this is via direct binding is unclear (Guay et al., 1997; Huot et al., 1998; Mounier and Arrigo, 2002; Sun and

MacRae, 2005). Hsp27 can also interact with tubulin, tau and several species of intermediate filaments including glial fibrillary acidic protein (GFAP), vimentin, and notably neurofilament light chain (NF-L) (Benndorf and Welsh, 2004; Perng et al., 1999a). Furthermore, missense mutations in sHsps including Hsp27 (*HSPB1*) and Hsp22 *(HSPB8)* are associated with peripheral neuropathies, in particular the axonal form of Charcot-Marie-Tooth disease and distal hereditary motor neuropathy (Evgrafov et al., 2004; Irobi et al., 2004a). Interestingly, mutations in both the neurofilament light chain gene (*NEFL*) and Hsp27 result in similar phenotypes. Expression of the mutant NEFL causes a disrupted neurofilament network with subsequent alteration in axonal transport (Perez-Olle et al., 2004; Perez-Olle et al., 2005), while expression of two of the missense Hsp27 mutations results in the formation of insoluble aggregates, destabilization and disruption of neurofilaments, and disturbances in axonal transport (Ackerley et al., 2006; Evgrafov et al., 2004). Thus, Hsp27 has been inferred to stabilize not only actin, but also neurofilament and microtubules.

Prior reports and our own observations have suggested a role for Hsp27 in axonal growth or regeneration, in addition to its role in promoting neuronal survival (Benn et al., 2002; Costigan et al., 1998; Murashov et al., 2001b). Specifically I have suggested a role for Hsp27 in neurite outgrowth via its interaction with actin (Williams et al., 2005), with the balance between actin stability and depolymerization being important for neurite growth. This may occur by a mechanism similar to the role that Hsp27 plays in regulating the actin polymerization, and therefore microfilament extension, necessary for endothelial cell migration (Piotrowicz et al., 1998). Our previous study showed that

Hsp27 was present and colocalized with actin and tubulin at the earliest stages of neurite initiation in lamellipodium, filopodia and focal contacts as well as in mature neurites suggesting that Hsp27 plays a role in neurite growth. Our objective for the present study was to investigate how the knockdown of Hsp27 protein itself by RNA interference (RNAi), and conversely the expression of exogenous Hsp27, would quantitatively influence neurite regeneration.

3.3 Materials and Methods

3.3.1 Neuronal Cultures

Young adult Sprague-Dawley rats (5-6 weeks of age) dorsal root ganglia (DRG) were dissected, dissociated as previously described and the neurons were plated in serum free Neurobasal (NB) supplemented with AraC and B27 (Tucker et al., 2005). After being dissociated the neurons were transfected and then plated on polylysine (PL, 1 μg/ml, BD Bioscience, Bedford, MA) coated Lab-Tek 16-well chamber slides (Nunc International, Naperville NC) for neurite growth assessment or laminin coated (LN 25 μg/ml) 12-well plates for Western blotting and incubated at 37°C, and 5% CO_2. The neurons were cultured in serum-free NB with no added growth factors. For transfection experiments, neurons were transfected using the AMAXA nucleoporation protocol and then plated as noted above.

3.3.2 DNA constructs, siRNA constructs and transfection

The plasmid pSVHa27 codes for hamster wild type Hsp27 (Ha27), and was obtained from Dr. J. Landry (l'Universite Laval). The plasmid pIRES2-EGFP-Ha27 was made by first subcloning HaHsp27 from pSVHa27 as a HindIII (Invitrogen) fragment into pEGFPC2 (Clontech), and further subcloning Hsp27 into pIRES2-EGFP (Clontech) as an EcoR1 (Invitrogen) fragment. The presence of Hsp27 and its orientation in the construct was verified by DNA sequencing. The Hsp27 siRNAs were synthesized commercially (Dharmacon, Colorado, USA) and used at 2 μM. The target sequences for silencing Hsp27 gene expression were: 5'UCA CUG GCA AGC ACG AAG A 3' and 5' GAG UGG UCU CAG UGG UUC A 3'. Cells (1×10^6) were transfected with plasmid DNA (3 μg) or siRNA constructs using the Amaxa electroporation system according to the manufacturers protocol (Rat Neuron Nucleofector kit, program G-13). After transfection, the cells were washed with NB and centrifuged to remove any remaining transfection reagent. The efficiency of transfection of siRNA was more than 60% as assessed by transfection of 2 μM Alexa Fluor labeled negative control siRNA (Qiagen).

3.3.3 Laminin Stimulation

Transfected neurons were first plated on PL coated slides and allowed to stabilize for 12 h or 36 h before being stimulated with soluble LN (40 μg/ml in NB medium) (Williams et al., 2005). Following the addition of the soluble LN, cells were returned to the incubator and fixed at 6, 12, and 24 h after stimulation for immunocytochemistry and growth analyses.

3.3.4 Immunocytochemistry

Neurons were fixed in 4% formaldehyde (pH 7-7.4) in PBS for 20 minutes, permeabilized with 0.1% Triton-X-100, and blocked with 10% goat serum in PBS. Antibodies used were as follows: Hsp27 (SPA-801, Stressgen Corp, Victoria, BC), total tubulin (T9026, Sigma-Aldrich), and actin (A2066, Sigma-Aldrich). Cells were incubated with the primary antibody at 4°C for 16-24 h, followed by Cy2 or Cy5-tagged secondary antibodies (Jackson Immunoresearch Labs, West Grove, PA). In the case of staining with two polyclonal rabbit antibodies, cells were incubated with the first antibody for 16-24 h, followed by Cy3- tagged secondary antibodies, then blocked again with 10% goat serum in PBS followed by incubation with the second antibody for 16-24 h followed by a Cy2 or Cy5 tagged antibody. Controls used included those in which only the secondary antibodies were used without the addition of primary antibodies and those where secondary antibodies directed against species other than that of the primary antibody were employed. The cells were coverslipped with glycerol and imaged with confocal laser scanning microscopy using z-stage scanning and image stacking. Stacked digital images were incorporated into Adobe Photoshop for compilation into the final composite figures.

3.3.5 Measurements of neurite growth

Note that all the measurements of growth were obtained using images of tubulin-stained neurons. Hsp27 staining was carried out on some parallel culture wells to follow the effectiveness of the knockdown compared to controls. Individual tracings of neurons

fluorescently stained for tubulin were carried out using the Neurolucida (MicroBrightField, VT) tracing program as previously described (Jones et al., 2003; Tucker et al., 2005).

Only neurons for which I was able to unambiguously identify the associated neurites or neuritic networks were chosen for tracing analysis. Approximately 15% cells were excluded from tracing because their neurites could not be distinguished from the processes of nearby neurons and nonneuronal cells. Data analyses were carried out with the Neuroexplorer software package; here data of total neurite length, branch point and Sholl analysis of intersection points were collected. Sholl analysis measures the number of intersection points of axons crossing 20 μm concentric circles radiating from the cell body to give a measure of both elaboration and extension of the neurites. Total neurite length is a measure of the cumulative length of neurites produced, branch point data are a measure of the number of branch points that the neurites of a cell possesses, and the measure of total neurite length per branch point provides a measure as to how frequently branching occurs. Data were imported into a graphing and statistical analysis software program (Prism 4, GraphPad Corp) for further analyses. Significance ($P < 0.05$) was determined using an unpaired T-test. For each condition examined, 45-85 neurons were completely traced, with cells being pooled from five different plating experiments.

3.3.6 Immunoblotting

Neurons were plated in 12-well LN-coated plates, and subsequently processed according to our established procedures (Jones et al., 2003). After cell lysis and

centrifugation (10,000 rpm, 5 min), the supernatants were used to determine protein concentration using the BCA protein assay (Pierce Chemicals, Rockford, IL). Equivalent amounts of protein (35 μg) were subjected to SDS-polyacrylamide gel electrophoresis (10% acrylamide). Fractionated proteins were subsequently transferred to nitrocellulose membranes and stained with Ponceau red as an indicator of protein loading. Immunodetection of the protein of interest was performed by blocking the membrane in 3% powdered milk in TBS-T for 1 h and then incubated overnight with primary antibodies directed toward Hsp27 (SPA-801, Stressgen), mitogen-activated protein kinase (MAPK, Santa Cruz Biotech Victoria BC), actin (A2066, Sigma-Aldrich), total tubulin (T9026, Sigma-Aldrich) or neurofilament light chain (NF-L, N5139 Sigma-Aldrich). The nitrocellulose membranes were then probed with HRP-conjugated secondary antibodies (AP307P, AP308P; Chemicon, Temecula, CA) for 1 h at room temperature, followed by visualization using an ECL method. Each experiment was repeated three times, subjected to densitometry and normalized to (MAPK) to ensure equal protein for comparison. Statistical analysis was performed using GraphPad Prism 4 with significance ($P < 0.05$) being determined using one-way ANOVA testing.

3.4 Results

3.4.1 Hsp27 siRNA results in a decrease in Hsp27 protein expression in DRG neurons.

I previously showed that Hsp27 was present colocalized with actin and tubulin at the earliest stages of neurite growth in lamellipodium, filopodia, focal contacts as well as

in mature neurites, suggesting that it plays a role in neurite growth. To assess the functions of Hsp27 in neurite growth and branching I silenced its expression by RNAi. I found that short interfering siRNA directed against two regions of Hsp27 efficiently depressed protein levels of Hsp27 24 h after transfection relative to control. Levels of an unrelated protein, MAPK, as well as actin, tubulin and NF-L, were unaffected. A time course experiment was conducted to determine the optimal time of Hsp27 depression after siRNA treatment. Hsp27 levels were found to be significantly ($P < 0.05$) decreased 12 h after transfection with Hsp27 siRNA and remained decreased over the 72 h time course. Hsp27 levels in cells transfected with control scrambled siRNA increased over the time course. The increase in Hsp27 under control conditions over the 72 h time course is presumably in response to the cells being in culture (Fig. 3.1), and it is possible that Hsp27 protein levels initially rise as an injury response and subsequently further increase as growth increases. The Hsp27 siRNA is able to repress the induction of Hsp27 that occurs after plating and continues to suppress this for up to 72 h. In cell types that I have examined, increasing Hsp27 often results in the detection of 2 bands, with the bottom band potentially representing a small amount of non-phosphorylated Hsp27 or non-posttranslationally modified form of Hsp27. I chose to commence neurite growth experiments 12 h after the siRNA treatment in order to ensure that Hsp27 expression had been decreased prior to LN stimulation. Of interest is the observation that actin, tubulin and NF-L are also upregulated by 24 h (Fig. 3.1), a time I know corresponds to significant neurite outgrowth, suggesting that Hsp27 induction is not simply due to an

Figure 3.1: RNAi efficiently silences Hsp27 protein expression. Dissociated DRG neurons were transfected with siRNA targeting two different sequences in Hsp27 or control scrambled siRNA. A. Protein from the cells was harvested at 12, 24, 36, 48, 60 and 72 h after plating, and immunoblotted for Hsp27, MAPK(loading control), actin, tubulin, and NF-L. B. Densitometric quantitation of western blot data. Values expressed represent the mean Hsp27 protein, relative to MAPK of 3 experiments +/- S.E.M. ★$p<0.05$, ★★$p<0.001$. Note that lanes 3 and 9 had an increased amount of total protein relative to the other lanes, as detected by ponceau red staining. Densitometric quantitation of western blot data for actin, tubulin, and NF-L relative to MAPK showed no significant (($P \geq 0.05$) differences in the levels of these proteins between Hsp27 siRNA and control siRNA conditions (supplementary data).

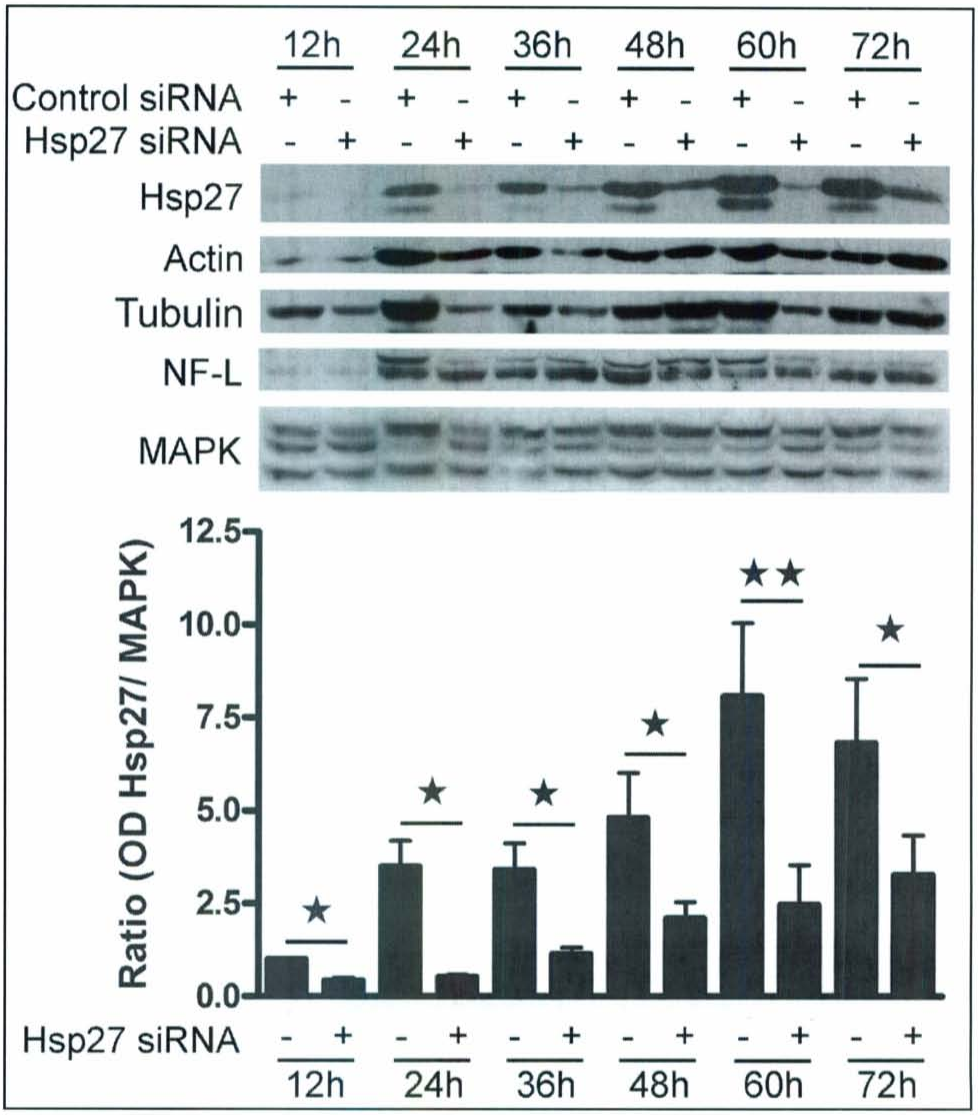
12h
24h
36h
48h
60h
72h
Control siRNA
Hsp27 siRNA
Hsp27
Actin
Tubulin
NF-L
MAPK
Ratio (OD Hsp27/ MAPK)
12.5
10.0
7.5
5.0
2.5
0.0
Hsp27 siRNA

injury response. Also note that the Hsp27 siRNA has no significant effect on actin, tubulin or NF-L levels.

3.4.2 Silencing of Hsp27 expression via RNAi results in decreased neurite growth, and branching.

Knowing that the Hsp27 siRNA suppressed Hsp27 expression 12 h after transfection, I sought to determine whether this decrease in expression would influence neurite growth and branching. Transfected neurons were plated on PL-coated slides, and 12 h later stimulated with soluble LN. The cells were fixed at either 6 or 24 h following stimulation and subsequently immunostained for Hsp27 and/or tubulin prior to analysis of neurite growth. Neurite growth and branching were assessed as outlined in the methods; briefly tubulin stained neurons were individually traced using the Neurolucida tracing program. The Neuroexplorer software package was used for data analyses to collect data for total neurite length, branching points and Sholl analysis of intersection points. Neurons treated with Hsp27 siRNA displayed decreased neurite growth as observed in the representative images in Figure 3.2, where control and treated cells immunostained for tubulin are shown. The control scrambled siRNA-treated cells shown in Figure 3.2 (A, C) display a greater amount of growth following LN stimulation for 6 and 24 h than the Hsp27 siRNA-treated cells at the same time points (Fig. 3.2B, D). Quantitative analysis of neurite length and branching (Fig. 3.3) demonstrate that both are affected by Hsp27 siRNA. Although there is only a minor difference 6 h after LN stimulation, the Hsp27 siRNA treatment results in significantly ($P < 0.05$) decreased total

Figure 3.2: Decreases in Hsp27 expression result in decreased neurite growth. Neurites were transfected with either control siRNA (A, C) or Hsp27 siRNA (B, D) and subsequently fixed and immunostained for tubulin expression at 6 h (A, B) or 24 h (C, D) after transfection. Control transfected wells display relatively higher levels of neurite growth compared to the Hsp27 siRNA treated cells. Scale bar = 50 μm.

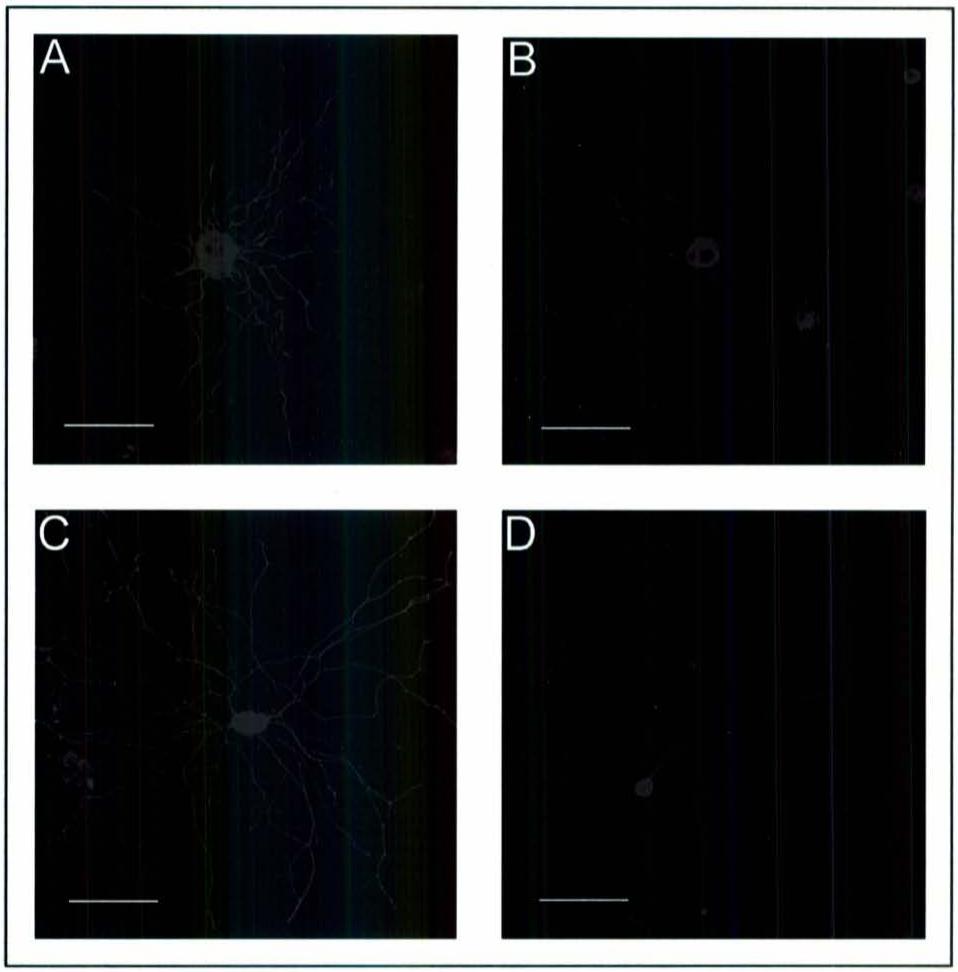
A
B
C
D

Figure 3.3: Silencing Hsp27 protein expression by siRNA results in a decrease in neurite growth and branching. Neurons were transfected with either control or Hsp27 siRNA and fixed at 6 and 24 h after LN stimulation. Neurite growth parameters were analyzed by tracing cells immunostained with tubulin as outlined in methods section. A: 24 h after LN stimulation, Hsp27 siRNA-treated cells had significantly lower total neurite length than control conditions. B: The average length of neurite per branching point is significantly greater for Hsp27 siRNA-treated cells relative to control at 6 and 24 h after LN stimulation. Neurite growth data is presented as the mean of 5 different plating experiments +/- SEM *$P<0.05$, **$P<0.001$, ***$P<0.0001$. C,D: the number of intersections indicating neurite branching and complexity. Cells transfected with Hsp27 siRNA have fewer intersections with Sholl radii indicating less branched structure relative to control. Data are presented as the mean of the number of intersection points in 20 μm radial increments from the cell body.

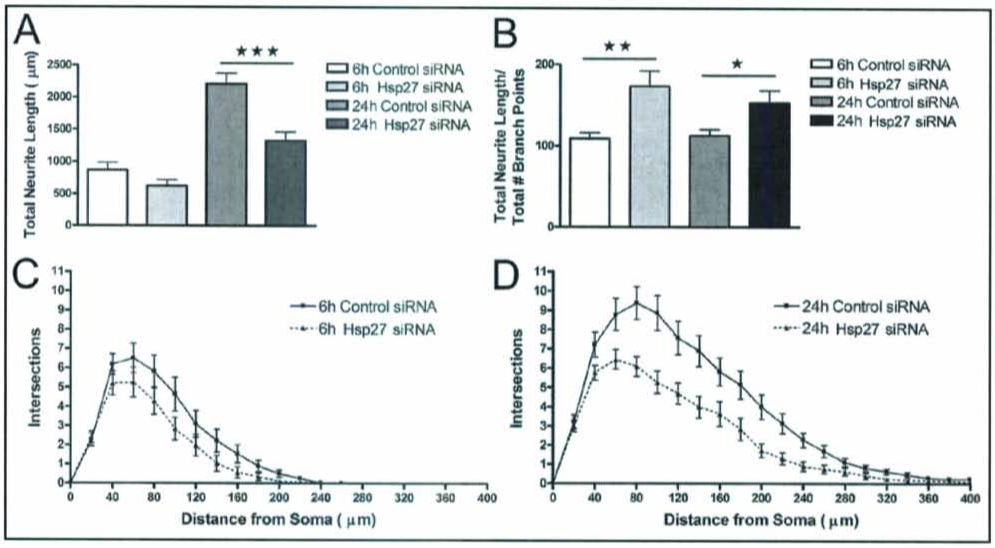
A
Total Neurite Length (μm)
2500
2000
1500
1000
500
0
★★★
6h Control siRNA
6h Hsp27 siRNA
24h Control siRNA
24h Hsp27 siRNA
B
Total Neurite Length/
Total # Branch Points
200
100
0
★★
★
6h Control siRNA
6h Hsp27 siRNA
24h Control siRNA
24h Hsp27 siRNA
C
Intersections
6h Control siRNA
6h Hsp27 siRNA
Distance from Soma (μm)
D
Intersections
24h Control siRNA
24h Hsp27 siRNA
Distance from Soma (μm)

neurite length at 24 h compared to control (Fig. 3.3A). Because of previous data which suggested a potential role for Hsp27 in neurite branching (Williams et al., 2005) I analyzed the relationship between total neurite length and the number of branch points. As shown in Figure 3.3, analysis of the ratio of total neurite length to the total number of branching points demonstrated that Hsp27 siRNA transfected cells have significantly greater length between branching points (Fig. 3.3B). This indicates that the neurites of the Hsp27 siRNA treated cells are less branched relative to control cells (Fig. 3.3B) and that branching rather than total length is more significantly ($P< 0.05$) affected at the early time point than total neurite length. These results are further supported by the Sholl analyses, which show that Hsp27 siRNA treatment resulted in decreased complexity of neurite growth patterns (Fig. 3.3 C, D).

3.4.3 Hsp27 siRNA affects the colocalization of Hsp27 and actin in neurite shafts and growth cones.

Our previous study (Williams et al., 2005) demonstrated that Hsp27 appeared to colocalize with actin and tubulin in axon shafts, branching points and growth cones at all stages of neurite growth. Consequently, I investigated the effects of siRNA induced knock-down of Hsp27 on cytoskeletal structure. As before, transfected neurons were plated on PL-coated slides, and stimulated with soluble LN 12 h later. The cells were fixed 24 h following LN stimulation and immunostained for Hsp27, actin and tubulin. Figure 3.4 shows representative examples of both control (Fig. 3.4 A-F) and Hsp27 siRNA (Fig 3.4 G-L) treated cells displaying Hsp27 (Fig. 3.4 A, D, G, J) or actin

Figure 3.4: Hsp27 siRNA affects colocalization of Hsp27 and actin in neurite shafts and growth cones 24 h after LN stimulation. (A-F) show representative control scramble siRNA-transfected neurons and (G-L) show Hsp27 siRNA-transfected neurons, which have been stained for Hsp27 (A, D, G, J), actin (B, E, H, K) and merged images (C, F, I, L). Images (D, E, F and J, K, L) are enlargements of the areas boxed in (A, B, C and G, H, I) respectively. Under Hsp27 siRNA conditions, Hsp27 staining is punctate, and these puncta are often colocalized with actin (arrows Fig. 4 K-L). (A-C and G-I scale bar = 25 μm, D-F and J-L scale bar =10 μm)

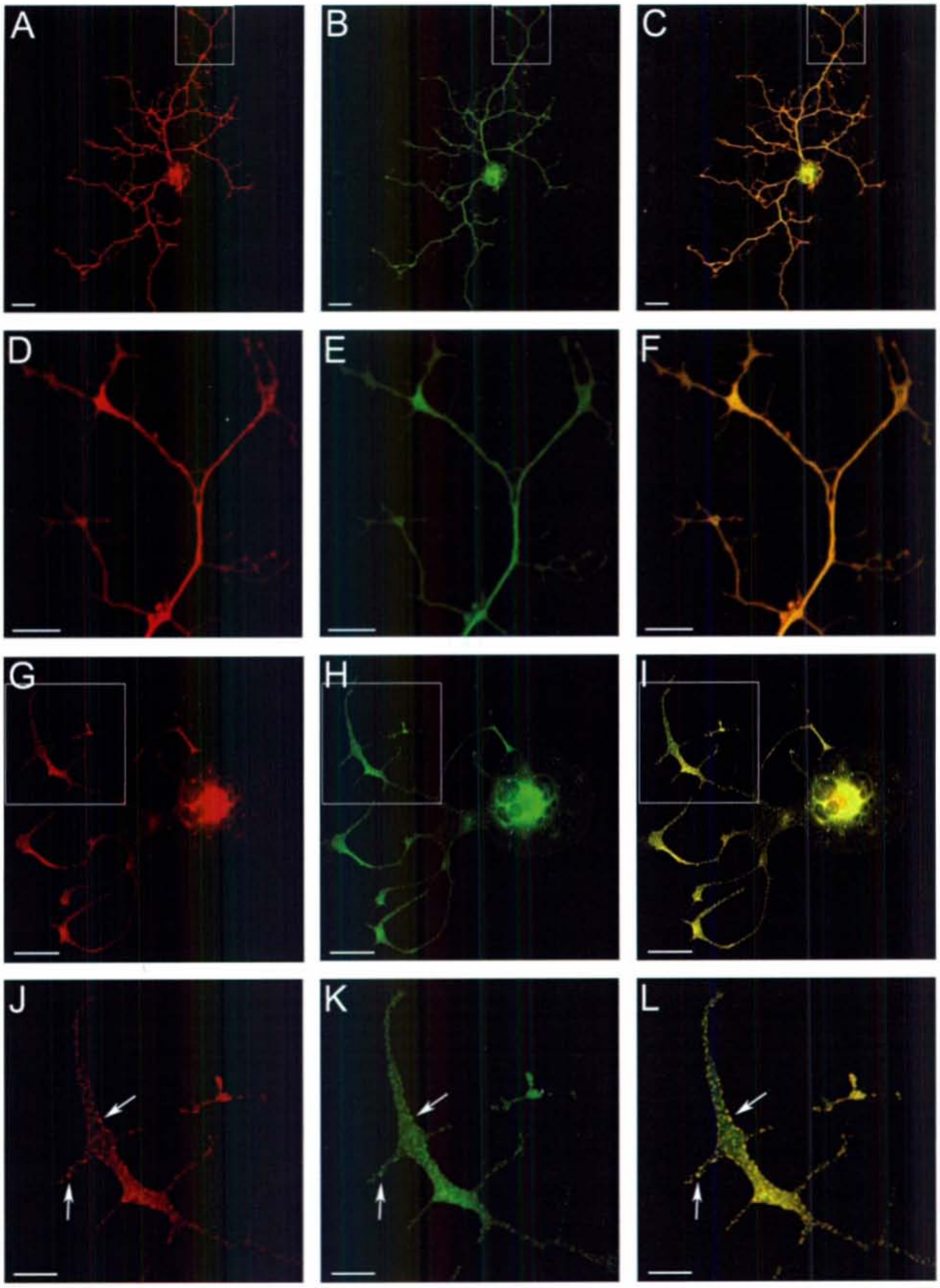
A
B
C
D
E
F
G
H
I
J
K
L

(Fig. 3.4 B, E, H, K) along with the merged images. Figure 3.5 provides similar examples of control (Fig. 3.5 A-F) and Hsp27 siRNA (Fig. 3.5 G-L) stained for Hsp27 (Fig. 3.5 A, D, G, J) and total tubulin expression (Fig. 3.5 B, E, H, K) as well as the merged images. Hsp27 staining in control scrambled siRNA transfected cells colocalizes with actin (Fig 3.4 C, F) and tubulin (Fig 3.5 C, F) in the neurite shaft and growth cones. In contrast Hsp27 staining in Hsp27-siRNA treated cells (Fig 3.4 I, L and Fig 3.5 I, L) exhibit decreased colocalization with actin and tubulin. Interestingly, Hsp27 siRNA-treated cells show punctate Hsp27 staining in the axon shaft and growth cones colocalizing with punctate actin staining (Figure 3.4 I-L arrows indicate examples of such puncta. The anti-actin antibody that has been used for these experiments recognizes both F and G actin preventing the determination of which form of actin is present in the puncta. Hsp27 siRNA treated cells also display decreased levels of colocalization between Hsp27 and tubulin (Fig. 3.5 I, L). Unlike actin, tubulin staining is not punctate nor does it colocalize with the Hsp27 puncta indicated by arrowheads (Fig. 3.5 K-L).

3.4.4 Overexpression of Hsp27 protein levels by transfection with pIRES2-EGFP-Ha27 results in increased neurite growth and branching.

Having determined that the decrease of Hsp27 protein levels negatively affected neurite growth and branching, I then wished to determine if expression of exogenous Hsp27 might result in increased growth. Therefore I expressed exogenous Hsp27 in DRG neurons by transfection with pIRES2-EGFP-Ha27 in order to look at the effect of increased Hsp27 on these growth parameters. The plasmid pIRES2-EGFP-Ha27 permits

Figure 3.5: Hsp27 siRNA treatment influences Hsp27 and tubulin colocalization in neurites and results in punctate Hsp27 (arrowheads Fig5 K-L), which does not colocalize with tubulin. Representative control scrambled siRNA-transfected neurons (A-F) and Hsp27 siRNA transfected neurons (G-L) all have been stained and imaged for Hsp27 (A, D, G, J) and tubulin (B,E,H,K). Merged images are shown in (C,F,I,L). Images (D, E, F and J, K, L) are enlargements of the areas boxed in (A, B, C and G, H, I) respectively. (A-C and G-I scale bar-25 μm, D-F and J-L scale bar =10 μm)

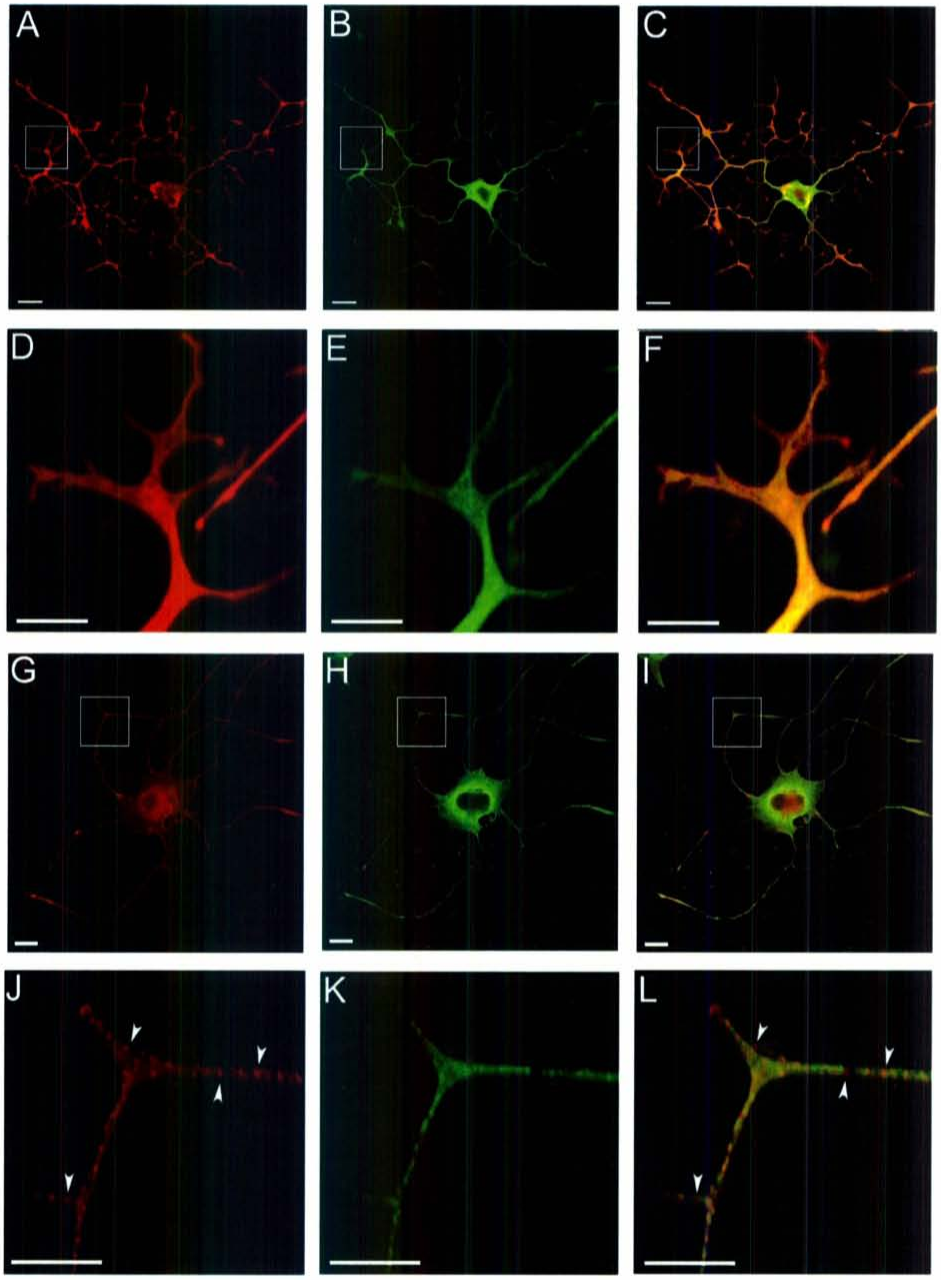
A
B
C
D
E
F
G
H
I
J
K
L

both Hsp27 and enhanced green fluorescent protein (EGFP) to be translated from a single bicistronic mRNA and thereby allows visual detection of plasmid expression while circumventing any problems that could potentially arise from the production of a tagged Hsp27 fusion protein. The cells were plated for 36 h after transfection, to allow significant time for Hsp27 levels to increase before being stimulated with soluble LN for 12 h. Figure 3.6 illustrates that neurons transfected with pIRES2-EGFP-Ha27 display increased Hsp27 expression (Fig. 3.6A) and robust EGFP expression (Fig. 3.6 B arrows). Transfected cells (indicated by arrows) also exhibit increased neurite growth and process initiation relative to non-transfected cells (Fig. 3.6 arrowheads). In these representative images five out of six EGFP expressing cells show significant ($P< 0.05$) neurite growth or stages of neurite initiation, such as lamellipodium and filopodia, while only one of the five non-transfected cells (Fig. 3.6 arrowheads) display any growth or initiation. The observed increase in growth from Hsp27 overexpression in Figure 3.6 was confirmed by quantitative tracing analyses of cells stained with tubulin and expressing EGFP (note cells were not stained with Hsp27 for tracing). Cells transfected with pIRES2-EGFP-Ha27, and stimulated with LN for 12 h showed a significant ($P< 0.05$) increase in total neurite length as well as a decrease in the ratio of neurite length per branch point relative to cells transfected with control vector pIRES2-EGFP (Fig. 3.7 A, B). These data indicate that the overexpression of Hsp27 resulted in increased neurite growth as well as a more branched neuritic tree. The results of the Sholl analyses further supported these findings indicating that expression of exogenous Hsp27 results in an increased complexity of neurite growth patterns (Fig. 3.7 C).

Figure 3.6: Expression of exogenous Hsp27 enhances neurite growth in pIRES2-EGFP-Ha27 transfected neurons, 12 h after transfection. A. Hsp27 staining, B. EGFP fluorescence C. merged images. Cells indicated by white arrows display increased Hsp27 levels (A) and robust EGFP labeling (B). Cells with low or no EGFP expression are indicated by arrowheads, and show correspondingly lower levels of Hsp27 expression. (Scale bar = 50 μm)

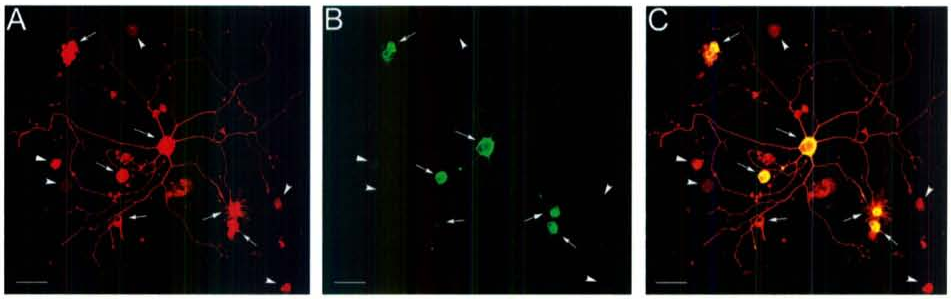
A
B
C

Figure 3.7: Expression of exogenous Hsp27 in DRG neurons significantly affects growth. A. Neurons were fixed and immunostained for tubulin at 12 h following LN stimulation. Tubulin stained cells that were also positive for EGFP were analyzed in both the control (pIRES2-EGFP vector only) and pIRES2-EGFP-Ha27 transfected conditions. pIRES2-EGFP-Ha27 transfected neurons had a significant increase in total neurite length relative to control, B. The average length of neurite per branching point is significantly decreased for pIRES2-EGFP-Ha27 transfected neurons relative to control at 12 h after LN stimulation, ★$p<0.05$. C. Cells expressing exogenous Hsp27 have increased intersections with Sholl radii indicating more branching and growth relative to control.

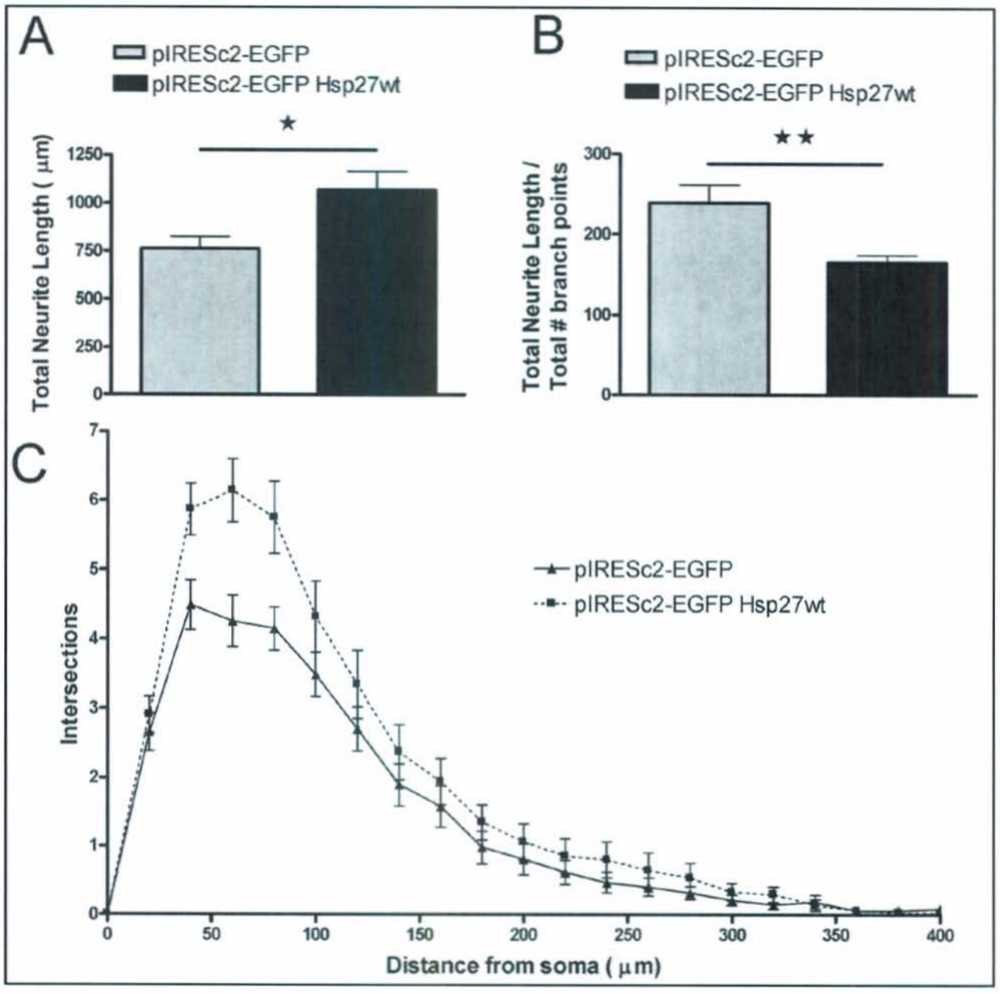
A
pIRESc2-EGFP
pIRESc2-EGFP Hsp27wt
Total Neurite Length (μm)
1250
1000
750
500
250
0
B
pIRESc2-EGFP
pIRESc2-EGFP Hsp27wt
Total Neurite Length / Total # branch points
300
200
100
0
C
pIRESc2-EGFP
pIRESc2-EGFP Hsp27wt
Intersections
Distance from soma (μm)
0
50
100
150
200
250
300
350
400

3.5 Discussion

This study highlights the importance of Hsp27 protein in the regulation of growth patterning of the neuritic tree, likely via influence over polymerization of cytoskeletal elements, rather than controlling expression of these elements. I found that Hsp27 siRNA decreases endogenous Hsp27 levels, as well as the induction that is normally seen after neurons are plated in culture. While most studies of the interaction of small heat shock proteins and cytoskeletal elements have been carried out using non-neuronal cells, recent studies provide new evidence that points to similar interactions of Hsp27 and other small heat shock proteins with cytoskeletal elements in neuronal cells (Evgrafov et al., 2004; Tang et al., 2005).

Our previous data showed that Hsp27 was present at all stages of neurite initiation and growth and colocalized during these stages of growth with actin and tubulin in lamellipodium, filopodia and mature neurites (Williams et al., 2005). These results led us to investigate the role of Hsp27 in neurite extension and branching by manipulating the protein expression levels of Hsp27, and examining resultant alterations of growth patterning of the neuritic trees. Western blotting results illustrated that the Hsp27 siRNA treatment effectively decreased endogenous Hsp27 expression compared to scrambled siRNA treated cells. These data demonstrated that a decrease of Hsp27 protein level did not significantly alter the levels of actin, total tubulin or NF-L protein expression. While our results suggest that Hsp27 is likely not involved in the regulation of actin, total tubulin or NF-L protein expression per se, it does not rule out the possibility that Hsp27 could be involved in the extension of microtubules and microfilaments necessary for

neurite growth and branching in DRG neurons in a manner similar to that reported for other cell types (Benndorf et al., 1994; Evgrafov et al., 2004). In cell-free systems, Hsp27 can act as an actin-capping protein that prevents the polymerization of actin and the assembly of F-actin (Benndorf et al., 1994; Miron et al., 1991). Phosphorylation of Hsp27 leads to the loss of its ability to inhibit actin polymerization, and thus increases the rate and extent of actin polymerization and the formation of F-actin (Benndorf et al., 1994; Guay et al., 1997; Landry and Huot, 1999; Lavoie et al., 1995; Miron et al., 1991). A peptide sequence in Hsp27 (I92-N106) was identified as a region critical to the interaction with actin and a site that is responsible for the inhibition of actin polymerization; when added to solutions of G-actin in the presence of an actin nucleating factor, this peptide prevented the polymerization into F-actin (Wieske et al., 2001). Interestingly these authors also noted that this peptide was more effective than the F-actin binding and depolymerizing factor cofilin. The unphosphorylated peptide inhibited polymerization, whereas the phosphopeptide had reduced activity similar to the behavior of wild type Hsp27 (Wieske et al., 2001). Protein phosphatases inhibitors and heat preconditioning have also prevents Hsp27 dephosphorylation and F-actin disruption (Loktionova and Kabakov, 1998), and the amount of membrane associated F-actin and cellular migration depends on the presence of phosphorylatable Hsp27 (Piotrowicz et al., 1998). Thus it appears that both the presence and phosphorylation of Hsp27 are prerequisites for rapid modulation of the actin cytoskeleton.

The role that the amount of Hsp27 present plays in neurite growth via control of the polymerization of cytoskeletal elements is supported further by the expression of

exogenous Hsp27 in DRG neurons. Analysis of the neurite growth of cells transfected with pIRES2-EGFP-Ha27 showed increased neurite growth and branching, indicating that not only is Hsp27 protein expression required for neurite growth, but also suggests that there exists a temporal relationship between the amount of Hsp27 present and the resulting amount of neurite growth.

Immunocytochemistry of Hsp27 siRNA treated cells showed an altered localization of Hsp27 and actin, with no apparent effect on tubulin. This specific alteration of actin localization further supports the involvement of an interaction of Hsp27 with actin in the alteration of neurite extension and branch patterning. The punctate, colocalized staining of Hsp27 and actin in Hsp27-siRNA treated cells may, in part, be related to recent *in vitro* studies implying that part of the protective effect of Hsp27 is to prevent the aggregation of denatured actin (Pivovarova et al., 2005). Another possibility is that these puncta may play a role in chaperoning activities of Hsp27 and may be present in the neuron under normal conditions, where they remain unseen due to the normally high endogenous levels of Hsp27 in the cell. Non-filamentous actin has been shown to stain as puncta within the cell (Grenklo et al., 2004), leading to the possibility that the decrease in Hsp27 protein levels effects polymerization of actin resulting in an increase in non-filamentous actin. Further biochemical studies of the interacting partners of Hsp27 under control and Hsp27 siRNA conditions are underway to elucidate the components of these puncta.

In conclusion, our results support our hypothesis that Hsp27 plays a role in neurite extension and branching. The exact mechanism underlying this role remains to be

elucidated though it is likely that modulation of the actin cytoskeleton dynamics is important for these processes.

3.6 Acknowledgements:

The authors would like to thank Dr. J. Landry (l'Universite Laval) for providing the plasmid pSVHa27, and Elaine Dodge, Sherri Rankin, and Budd Tucker for their invaluble assistance and discussion. Funding for this work was through an Natural Sciences and Engineering Research Council (NSERC) Discovery Grant (152940, KMM).

Chapter 4

Hsp27 Phosphorylation is involved in neurite growth in adult sensory neurons *in vitro*

4.1 Introduction

Neurite initiation and growth during development, as well as regeneration after injury, is controlled by specific factors and extracellular matrix proteins (da Silva and Dotti, 2002; Teng and Tang, 2006; Tonge et al., 1997; Tucker et al., 2008). Active regions of the cell body and neurite use cell surface receptors to recognize extracellular cues and transduce them, via intracellular signaling cascades, into physical rearrangement of cytoskeletal elements responsible for initiating and maintaining the structure of the growing neurite (Giancotti, 2003; Huber et al., 2003; Lilienbaum et al., 1995). Actin, tubulin and intermediate filaments all play a role in the growth process (da Silva and Dotti, 2002; Dehmelt and Halpain, 2004; Dehmelt et al., 2003). The morphology and dynamics of the microtubule and actin filament cytoskeletons are regulated via control of actin binding proteins and microtubule associated proteins that affect filament initiation, polymerization, depolymerization, stability, as well as association with other filaments and structures within the cell (Bear et al., 2002; Belmont et al., 1996; Bennett and Baines, 2001; Chen et al., 1992; Cooper and Sept, 2008; Dedova et al., 2006; Huang et al., 2006; Jawhari et al., 2003; Komarova et al., 2002; Lansbergen and Akhmanova, 2006; Manna et al., 2006; Ono, 2007; Ono and Ono, 2002; Pantaloni et al., 2001; Tseng et al., 2004; Volkmann et al., 2001). Cytoskeletal binding proteins play key roles in neurite initiation,

extension and branching, and a change in structure of the neurite may result from effecting the operation or presence of a single binding protein (Dehmelt and Halpain, 2005; Ikegami et al., 2007; Korobova and Svitkina, 2008; Lebrand et al., 2004; Song and Poo, 1999).

Heat shock protein 27 (Hsp27) is a member of the class of small heat shock proteins (sHSPs) and has been shown to interact with different cytoskeletal elements as well as to promote survival in the face of environmental stress through numerous mechanisms, including by stabilizing the actin filament cytoskeleton (Huot et al., 1997; Preville et al., 1998; Vigilanza et al., 2008). Hsp27 interacts with actin, tubulin, tau and several species of intermediate filaments, including gilal fibrillary acidic protein (GFAP), vimentin, nestin and NF-L (Benndorf and Welsh, 2004; Jia et al., 2009; Perng et al., 1999a). Mutations in Hsp27 are associated with peripheral neuropathies (Evgrafov et al., 2004; Irobi et al., 2004b). Furthermore Hsp27 may play a key role in GDNF induced neurite outgrowth (Hong et al., 2009).

The interactions between Hsp27 and actin have been extensively studied; Hsp27 plays a role in regulating the actin filament cytoskeleton, in non-neuronal cells, though direct interactions with actin, as well as by modulating the activities of actin binding proteins though signaling pathways (Brophy et al., 1998; Jog et al., 2007; Lee et al., 2007; Lee et al., 2008; Piotrowicz et al., 1998; Schneider et al., 1998). Monomeric non-phosphorylated Hsp27 may directly interact with actin preventing the polymerization of actin filaments.

The activity of Hsp27 depends upon its phosphorylation state as well as its oligomerization, which is affected by interactions between its domains. Hsp27 is phosphorylated on two serines in the rodent Hsp27 (Ser15, and Ser86 in rat, Ser90 in hamster, Ser82 in mouse) through the p38MAPK, MAPKAP kinase-2 (MKK2) pathway (Huot et al., 1995; Landry et al., 1992; Mehlen and Arrigo, 1994). Additionally, Hsp27 contains three domains: a WD/EPF motif in the N-terminal region, a common C-terminal α-crystallin domain, and a non conserved flexible C-terminal tail (Arrigo, 2007; Chavez Zobel et al., 2005; Haslbeck et al., 2005; Theriault et al., 2004).

Hsp27 is present *in vitro* as monomers, dimers and large oligomers consisting of approximately 24 monomers (Lambert et al., 1999). Deletion studies and mutation of phosphorylation sites have shown that the WDPF domain, as well as the phosphorylation state of the protein, are involved in the stability of the oligomeric structure (Kim et al., 1998; Lambert et al., 1999; Rogalla et al., 1999; van Montfort et al., 2001b). Interactions between the WDPF domain and the α-crystallin domain are required in order for the protein to form oligomers larger than dimers (Lambert et al., 1999; Theriault et al., 2004). Phosphorylation of the serine 86 site disrupts this interaction resulting in the oligomer dissociating into dimers. Phosphorylation of the serine 15 site disrupts the interactions between the dimers resulting in their dissociation into monomers.

Non-phosphorylated Hsp27 monomers have been demonstrated to be the only form of Hsp27 that is able to bind actin. Reports differ on the method of action of Hsp27 binding to actin. Hsp27 was originally characterized as a barbed end capping protein, although more recent reports suggest that Hsp27 impairs actin filament assembly by

sequestering actin monomers, rather than by capping (During et al., 2007; Miron et al., 1991; Pichon et al., 2004). Both of these models for Hsp27-based inhibition of actin filament assembly support the finding that only monomeric nonphosphorylated Hsp27 is able to inhibit actin filament polymerization (Benndorf et al., 1994; During et al., 2007).

Prior reports and observations in the Mearow lab have suggested a role for Hsp27 in axon growth or regeneration in addition to its role in promoting neuronal survival. Specifically I have suggested a role for Hsp27 in neurite outgrowth via its interaction with actin with its role in regulating actin dynamics being important for neurite growth. My previous studies showed that Hsp27 was present and colocalized with actin and tubulin in lamellipodium, filopodia and focal contacts at the earliest stages of neurite growth as well as in mature neurites and growth cones (Williams et al., 2005). Knock down of endogenous Hsp27 protein by small interfering RNA (siRNA) resulted in decreased neurite growth, while overexpression of exogenous Hsp27 protein resulted in increased growth. Use of upstream pharmacological inhibitors that inhibit the activity of p38 MAPK resulted in decreased Hsp27 phosphorylation and aberrant neurite growth. These studies support a role for Hsp27 in neurite growth with the protein level and phosphorylation state playing a role. Our objective in the present study was to investigate how the phosphorylation and oligomerization state of Hsp27 quantitatively affected neurite growth by knocking down the endogenous rat Hsp27 in the cell and at the same time overexpressing hamster Hsp27 with mutations to its phosphorylation sites and WDPF domain.

4.2 Materials and methods

4.2.1 Neuronal Cultures

Dorsal root ganglia (DRG) from young adult (5-6 weeks of age) Sprague-Dawley rats (Memorial University of Newfoundland Vivarium) were dissected and dissociated using modifications to techniques described previously (Tucker et al., 2005). Briefly, in accordance with University Animal Care guidelines, animals were decapitated, ganglia were extracted from all spinal cord levels and incubated in 0.25% collagenase type II (Invitrogen, Burlington, Canada) for 45 min at 37°C and then incubated with 0.25% trypsin (Invitrogen) for 20 min at 37°C, and then incubated with 0.2% soybean trypsin inhibitor (Sigma Chemicals) for 5 min at 37°C. The ganglia were dissociated by a series of manual titrations using polished Pasteur pipettes. The cell suspension was washed with serum free Neurobasal medium (NB, Invitrogen) and centrifuged at 500 g, before being layered on top of a 30% Percoll solution (GE healthcare, Baie d'Urfe, QC) in 15 mL conical tubes and centrifuged at 400 g for 20 min at room temperature. Pellets were then carefully extracted with a sterile pasture pipette, placed in a fresh tube and transfected using the AMAXA nucleoporation protocol (Lonza, Cologne Germany). Transfected cells were suspended in serum free modified NB, supplemented with 100 U penicillin/streptomycin, B27 supplement (Invitrogen), and 20 uM cytosine arabinoside (Sigma, St. Louis MO, USA) and plated on polylysine (PL; 1 ug/mL; BD Bioscience, Bedford MA) – coated Lab-Tek 16-well chamber slides (Nunc International, Naperville, IL) for neurite growth assessment or PL coated 12-well plates for Western blotting and

incubated at 37 °C with 5% CO_2. The neurons were cultured in serum-free NB with no added growth factors.

4.2.2 DNA Constructs, siRNA Constructs and Cotransfection

The plasmids pSVHa27, pSVHa27-AA, pSVHa27-EE, pSVHa27-AE, pSVHa27-EA, pSVHa27-Δ(5-23) coding for wild type and mutant hamster Hsp27 were obtained from Dr. J. Landry (l'Universtite Laval). The plasmid pIRES2-EGFP-haHsp27 coding for wild type hamster Hsp27 was subcloned from pSVHa27 as previously outlined (Williams et al., 2006). The plasmid pIRES2-EGFP-Hsp27-EE coding for Hsp27, with serine to glutamic acid mutations at serine amino acid sites 15 and 90, was made by subcloning Hsp27-EE as a Hind III (Invitrogen, La Jolla, CA) fragment into pIRES2-EGFP (Clontech, Palo Alto, CA). The construct orientation was verified by Kpn I (Invitrogen) digestion and DNA sequencing. The plasmids pIRES2-EGFP-Hsp27-AA, pIRES-EGFP-Hsp27-AE, pIRES-EGFP-Hsp27-EA, pIRES-EGFP-Hsp27-Δ(5-23) coding for mutant Hsp27 were made by subcloning the mutant Hsp27 from the pSV vector as a Hind III fragment into pEGFPC2 (Clontech), and further directionally subcloning the mutant Hsp27 into pIRES2-EGFP as an Xho I (Invitrogen), Bam HI (Invitrogen) fragment. The constructs orientation and the sequence of Hsp27 were verified by DNA sequencing.

The Hsp27 siRNA was synthesized commercially (Dharmacon) and used at 2uM. The target sequence for silencing rat Hsp27 protein expression was 5' GAG UGG UCU CAG UGG UUC A-3'.

All cells (1 x 10^6) were cotransfected with plasmid DNA (3 ug) and Hsp27-siRNA, using the AMAXA nucleoporation system according to the manufacturers protocol (Rat Neuron Nucleofector Kit; program G-13), and will be identified in this chapter by the name of the plasmid that was transfected. After transfection the cells were washed with NB and centrifuged to remove any remaining transfection agent.

4.2.3 Laminin Stimulation

Transfected neurons were first plated on PL-coated slides or plates and allowed to stabilize overnight (16 h) before being stimulated with soluble LN [40 ug/mL in NB (Williams et al., 2005)]. After the addition of the soluble LN, cells were returned to the incubator and 24 h after stimulation, the cells werecollected for western blotting or the cells were fixed for immunocytochemistry and growth analysis.

4.2.4 Immunocytochemistry and imaging

Neurons were fixed in 4% paraformaldehyde (pH 7-7.4) in PBS for 15 min, permeabilized with 0.1% Triton-X-100 and blocked with 10% normal goat serum in PBS. Antibodies used were as follows: total tubulin (1:1000; T9026; Sigma), Hsp27 (1:500; SPA-801; Stressgen Corp, Victoria, British Columbia). Cells were incubated with the primary antibody at 4°C for 16-24 h, followed by Cy2 or Cy5-tagged secondary antibodies (Jackson Immunoresearch, West Grove, PA). Phalloidin coupled to Alexa 568 (Molecular Probes/ Invitrogen, Carlshad, CA)) was used to label actin filaments, and was incubated along with the secondary antibody. Controls used included those in which only

the secondary antibodies were used without the addition of primary antibodies, and those in which secondary antibodies directed against species other than that of the primary antibody were employed. The cells were cover slipped with glycerol and imaged with confocal laser scanning microscopy using z-stage scanning and image stacking. Stacked digital images were incorporated into Adobe Photoshop for compilation into the final composite figures.

4.2.5 Measurement of Neurite Growth

Note that all growth measurements were obtained using images of tubulin stained GFP-positive neurons. Individual tracings of neurons fluorescently stained and imaged for tubulin and GFP by confocal microscopy were carried out using Image J (version 1.38x; National Institute of Health, USA), the NeuronJ plug-in (version 1.2.0; E. Meijering (Meijering et al., 2004)), and the Sholl Analysis plug-in (version 1.0, Gosh Lab; University of California, San Diego, CA). Only neurons for which we were able to identify unambiguously the associated neurites or neuritic networks were chosen for tracing analysis. Approximately 20% of cells were excluded from tracing because their neurites could not be distinguished from the processes of nearby neurons and non-neuronal cells. 100-150 cells were traced for each replica of each condition. Confocal images were converted to grayscale TIFF images, capable of being loaded into ImageJ, using Adobe Photoshop. Neurites were traced using NeuronJ, to obtain total neurite length, a measure of the cumulative length of neurites produced, and an image of the tracing was obtained for Sholl analysis using the "make snapshot button". The Sholl

Analysis plug-in was used to measure the mean number of intersection points of neurites crossing 2 μm thick concentric circles radiating from the cell body every 10 μm to give a measure of both elaboration and extension of the neurites. Data was imported into a graphing and statistical analysis program (Prism 4; GraphPad Corp.) for further analysis. Significance ($P< 0.05$) was for total neurite length was determined using one way ANOVA with a Dunnet post test, and significance ($P< 0.05$) was determined at intersection points of the Sholl analysis using a two-tailed T-test. For each condition 100-250 neurons were completely traced with cells being pooled from 3 different plating experiments.

4.2.6 Immunoblotting

Transfected neurons were plated in 12-well plates and subsequently processed according to our established protocols (Jones et al., 2003). After cell lysis and centrifugation (10,000 rpm, 5 min), the supernatants were used to determine protein concentration by using the BCA protein assay (Pierce Chemicals, Rockford, IL). Equivalent amounts of protein (50 ug) were subjected to sodium dodecyl sulfate (SDS)-poly-acrylamide gel electrophoresis (10% acrylamide). Fractionated proteins were subsequently transferred to nitrocellulose membranes and stained with ponceau red as an indicator of protein loading. Immunodetection of the protein of interest was performed by blocking the membrane in 3% powdered milk in TBS-T for 1 h and then incubated overnight with primary antibodies directed towards Hsp27 (SPA-801, Stressgen), mitogen-activated protein kinase (MAPK; Santa Cruz Biotechnology, CA), actin (A2066;

Sigma), phospho-Hsp27^{S15} (PAI-016; Affinity Bioreagents), and phospho-Hsp27^{S82} (E118, Abcam). phospho-Hsp27^{S82} reacts with phosphorylated S82 in human, S90 in hamster, and S86 in rat. The nitrocellulose membranes were then probed with horseradish peroxidase (HRP) conjugated secondary antibodies (AP307P; AP308P; Chemicon, Temecula, CA) for 1 h at room temperature, followed by visualization via the ECL method.

4.3 Results

In order to investigate the role of Hsp27 phosphorylation and oligomerization in neurite growth we employed a cotransfection model where adult rat DRG neurons were transfected with rat specific Hsp27-siRNA to silence endogenous Hsp27, as well as pIRES2-EGFP containing either wild type and mutated hamster Hsp27 (haHsp27) resulting in overexpression of the haHsp27 (Williams et al., 2006). The plasmid pIRES2-EGFP permits both Hsp27 and enhanced green fluorescent protein (EGFP) to be translated from a single bicistronic mRNA and thereby allows visual detection of plasmid expression while circumventing any problems that could potentially arise from the production of a tagged Hsp27 fusion protein. In this model siRNA directed against rat Hsp27 (Hsp27-siRNA) is cotransfected into the neuron with a vector coding for the expression of wild type or mutated hamster Hsp27. Due to the two nucleotide differences between the hamster and rat sequences in the 21 nucleotide region that the siRNA is directed against, the Hsp27-siRNA depresses the endogenous rat Hsp27 protein levels

while having no effect on the exogenous haHsp27. This permitted expression of exogenous haHsp27 while removing the effects of the endogenous rat Hsp27.

I found that siRNA directed against one region of rat Hsp27 effectively depressed rat Hsp27 protein levels in PC12 cells and DRGs relative to control while not affecting haHsp27 expression in Chinese hamster ovary (CHO) cells (data not shown). When the rat specific Hsp27-siRNA was cotransfected with constructs coding for mutant and wild type haHsp27 the endogenous rat Hsp27 protein levels were supressed while the exogenous haHsp27 was expressed (Fig. 4.1). This is most evident in the western blot of cells expressing exogenous deletion mutant Hsp27-Δ(5-23) where the band for the exogenously expressed Hsp27 was observed below that of wild type Hsp27; endogenous Hsp27 in this sample was markedly reduced compared to control. The antibodies specific for phosphorylated Hsp27 (either S15 or S82) do not recognize mutated Hsp27 where glutamic acid (E) or aspartic acid (A) has replaced the phosphorylatable serine (EE, EA, or AE) (Fig. 4.1). We also observed that Hsp27 mutants do not have equal transfection efficiencies; in particular, the EE mutant did not appear to be expressed as well as any of the other single or deletion mutants.

Transfected neurons were plated on polylysine coated 16-well slides and allowed to adhere overnight (approx 18 h). Subsequently the plating medium was removed and medium containing soluble laminin (40 ug/mL) was added to the cells for 24 h, after which slides were fixed and processed for detection of Hsp27, F-actin, and beta-tubulin. Neurite initiation and growth were assessed as outlined in Materials and Methods.

Figure 4.1: Cotransfection of rat Hsp27 siRNA and exogenous hamster Hsp27, depletes endogenous rat Hsp27 while expressing hamster Hsp27.

siRNA specific to rat Hsp27 silences endogenous Hsp27 protein expression while not affecting the over expression of wild type and mutant hamster Hsp27. Protein from the neurons was collected and immunoblotted for Hsp27, Hsp27 ^{S15}, and Hsp27 ^{S82} (recognizes S86 in rat and S90 in hamster), and Actin (loading control).

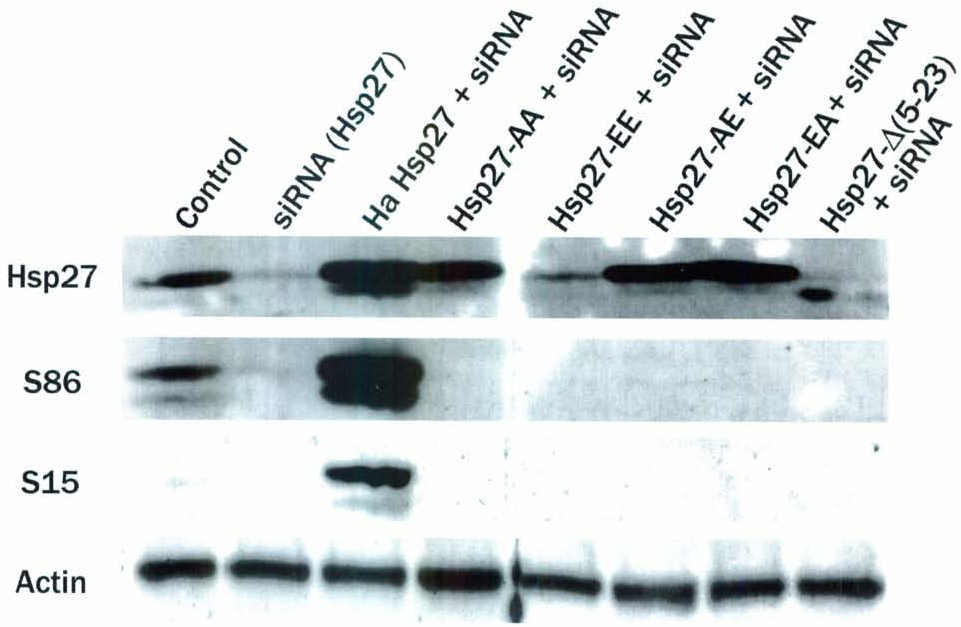
Control
siRNA (Hsp27)
Ha Hsp27 + siRNA
Hsp27-AA + siRNA
Hsp27-EE + siRNA
Hsp27-AE + siRNA
Hsp27-EA + siRNA
Hsp27-Δ(5-23) + siRNA
Hsp27
S86
S15
Actin

4.3.1 The phosphorylation state of Hsp27 affects neurite growth

We have previously shown that the amount of neurite growth varies with the level of Hsp27 present in the cell. When endogenous Hsp27 was depleted by siRNA, cells displayed decreased neurite growth relative to control conditions, and conversely when exogenous Hsp27 was over expressed cells displayed increased neurite growth relative to control (Williams et al., 2006). We sought to determine what affect the mutation of Hsp27 phosphorylation sites and deletion of the WDPF domain would have on neurite growth. Using the co-transfection system described above, all conditions have the endogenous Hsp27 decreased by siRNA permitting us to look at the effects of the haHsp27 mutations on neurite growth. Representative examples of cells transfected with each of the constructs are presented in Figure 4.2. Consistent with our previous observations, neurons treated with siRNA alone displayed decreased neurite growth compared to cells cotransfected with haHsp27. Cells transfected with phosphorylation mutants Hsp27-EE, and Hsp27-EA displayed less growth than wild type Hsp27, but growth similar to the siRNA alone condition (Fig. 4.2A, E, F). Cells transfected with Hsp27-AA and Hsp27-Δ(5-23) displayed growth more similar to the wild type haHsp27 than to siRNA (Fig 4.2 A, B, C,G), and cells transfected with Hsp27-AE displayed growth somewhere in between that of the haHsp27 and siRNA conditions (Fig 4.2 E).

Quantitative analysis of neurite length is presented in Figure 4.3. When total neurite length was enumerated, the results showed that cells expressing haHsp27, Hsp27-AA, Hsp27 AE and Hsp27-Δ(5-23) had neurite growth significantly ($P < 0.05$) greater than that of cells with siRNA alone (Fig. 4.3A). Additionally cells expressing Hsp27-EE,

Figure 4.2: The phosphorylation state of Hsp27 plays a role in neurite growth, while the WDPF domain is not required for rescue of Hsp27-siRNA induced decreased growth.

Neurons were cotransfected with siRNA complementary to Hsp27 and vectors coding for GFP alone (**A**), or GFP and haHsp27 (**B**), Hsp27-AA(**C**), Hsp27-AE (**D**), Hsp27-EE (**E**), Hsp27-EA (**F**), Hsp27-Δ(5-23) (**G**). The neurons were subsequently stimulated with soluble laminin for 24 h and then fixed and immunostained and imaged for tubulin and GFP expression. The cells shown are representative for the average amount of growth within the condition, and additionally are all shown at the same magnification. (Scale bars = 50 μm)

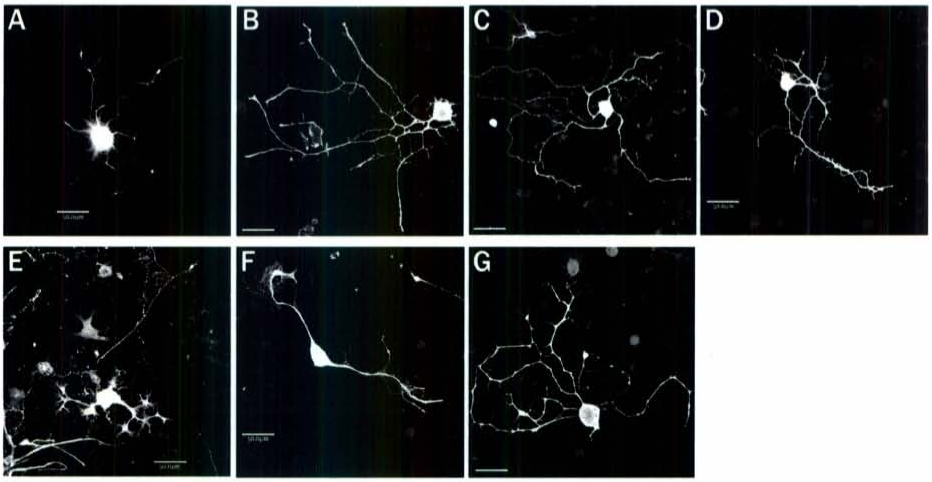
A
B
C
D
E
F
G

Figure 4.3: The phosphorylation state of Hsp27 affects neurite growth.

Neurons were cotransfected with Hsp27-siRNA and constructs containing wild type haHsp27 or mutated Hsp27. Neurite growth parameters were analyzed by tracing cells immunostained with tubulin as outlined in the Materials and Methods.

A. Compared to cells transfected with siRNA alone, cells cotransfected with haHsp27, Hsp27-AA, Hsp27-AE, or Hsp27-Δ(5-23) display significantly greater amounts of growth (one way ANOVA, Dunnet post test with siRNA as control; *P<.05, ** P<.01).

B-F: Number of intersections indicating neurite branching and complexity. Data are presented as the mean of the number of intersection points in 10 μm radial increments from the cell body. **B**. Cells expressing Hsp27-AA display significantly less intersections points, indicating less branching or extension, relative to haHsp27 at radial increments from 30 μm -70 μm from the cell body, and significantly increased intersection points relative to haHsp27 at radial increments 360 μm and 410-440 μm from the cell body, indicating that cells expressing Hsp27-AA have a less branched neurite structure close to the soma, and a more highly branched or extensions farther away from the soma relative to cells expressing haHsp27. **C**. Cells expressing Hsp27-AE display significantly less intersections points, indicating less branching or extension relative to haHsp27 at radial increments from 160-170 μm from the cell body. **D**. Cells expressing Hsp27-EE display significantly less intersections points, indicating less branching or extension relative to haHsp27 at radial increments from 100-120 μm, and 150-160 μm from the cell body. **E.** Cells expressing Hsp27-EA display significantly less intersections points, indicating less branching or extension relative to haHsp27 at radial increments from 30-250 μm from the cell body. **F**. Cells expressing Hsp27-Δ(5-23) do not have Sholl intersection values that are significantly different from haHsp27. (Significance was determined at intersection points of the Sholl analysis using a two-tailed T-test, *P<0.05). Neurite growth and intersection data presented are the mean of 3 different plating experiments ±SEM.

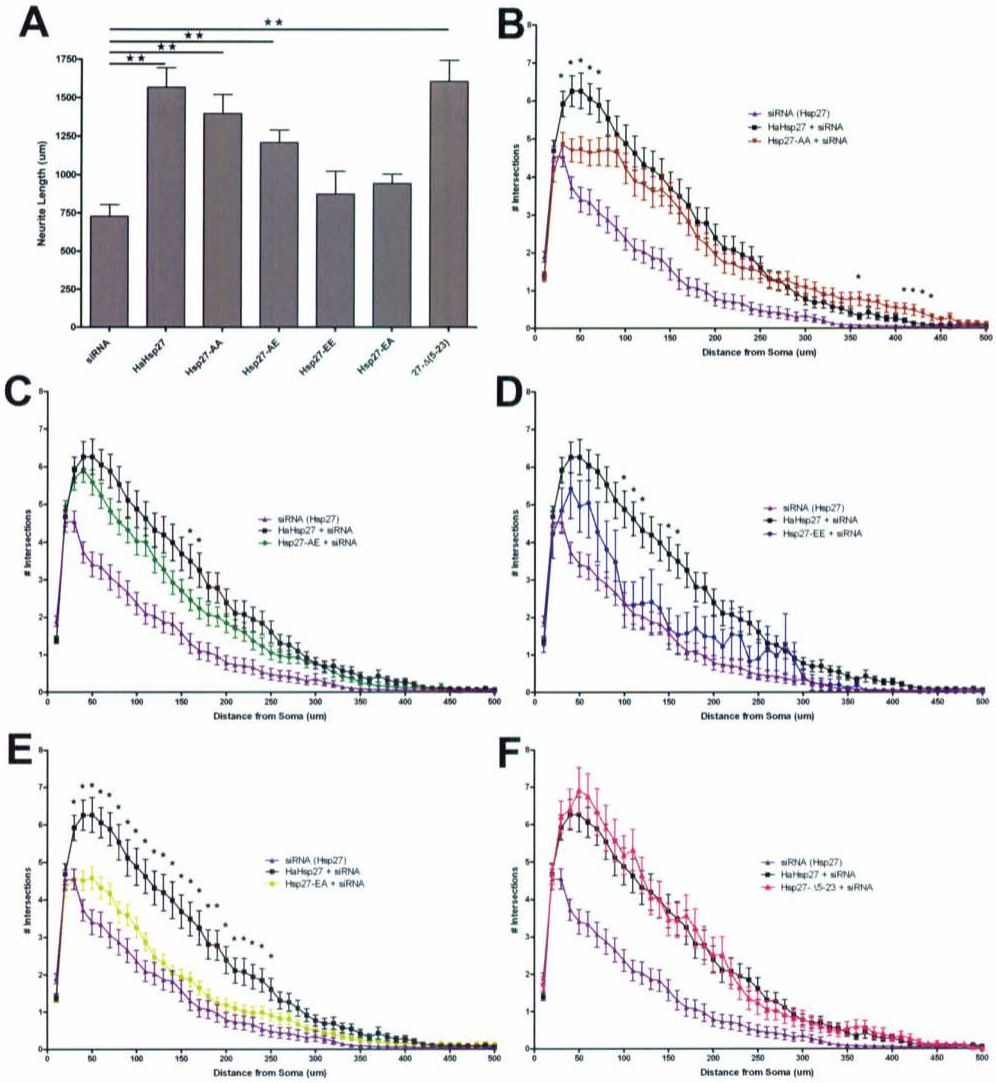
A
Neurite Length (um)
siRNA
HaHsp27
Hsp27-AA
Hsp27-AE
Hsp27-EE
Hsp27-EA
27-Δ(5-23)
B
siRNA (Hsp27)
HaHsp27 + siRNA
Hsp27-AA + siRNA
Intersections
Distance from Soma (um)
C
siRNA (Hsp27)
HaHsp27 + siRNA
Hsp27-AE + siRNA
D
siRNA (Hsp27)
HaHsp27 + siRNA
Hsp27-EE + siRNA
E
siRNA (Hsp27)
HaHsp27 + siRNA
Hsp27-EA + siRNA
F
siRNA (Hsp27)
HaHsp27 + siRNA
Hsp27-Δ5-23 + siRNA

Hsp27-EA and Hsp27-AE had neurite growth significantly ($P < 0.05$) less than cells expressing haHsp27. The effect of Hsp27 mutations on neurite growth patterning was examined further through Sholl analysis, which measures the branching / complexity of neurite growth. Although the total neurite length of cells transfected with Hsp27-AA and haHsp27 were similar, Sholl analysis showed that their growth patterns differ. Relative to haHsp27, cells expressing Hsp27-AA had significantly ($P < 0.05$) less intersections with Sholl radii close to the soma, and significantly($P < 0.05$) more intersections with Sholl radii farther from the soma, indicating that neurites from cells expressing Hsp27-AA, extend farther from the cell and are less branched near the cell than neurites from cells expressing haHsp27 (Fig 4.3B). Hsp27-AE expressing cells had fewer intersections and therefore a less branched structure than haHp27 transfected cells (Fig 4.3C). Cells expressing either Hsp27-EE or Hsp27-EA, showed growth patterning and branching that was significantly ($P < 0.05$) decreased relative to haHsp27 (Fig 4.3 D, E). Cells expressing Hsp27-Δ(5-23) showed growth patterning not significantly ($P < 0.05$) different than that of cells expressing haHsp27 (Fig 4.3F). These results suggest that the expression and phosphorylation state of Hsp27 plays a role in neurite extension and growth patterning. The following section investigates this further.

4.3.2 The phosphorylation state of Hsp27 alters F-actin in structures of the growing neurite.

We previously reported a potential role for Hsp27 in actin localization (Williams et al., 2006) and were interested in what role the phosphorylation state or presence of the

WDPF domain in Hsp27 plays in this process. In order to elucidate the effect of the Hsp27 mutants on actin localization we examined actin location in the neurites under control conditions and compared this localization to cells transfected with mutant and wild type haHsp27.

4.3.2.1 Endogenous Hsp27 and F-actin

In order to observe the localization of F-actin with the presence of endogenous Hsp27 (control condition) DRG neurons were dissociated, and plated on polylysine coated 16 well slides overnight (~16 h). The next day the cells were stimulated with soluble laminin and fixed 24 h later, labeled with Alexa Fluor 555-Phalloidin, and images of F-actin at various stages of neurite growth were obtained using confocal microscopy. Due to the fact that neurite growth is not synchronous we were able to select and examine cells at a variety of stages of neurite growth from one cell plating. F-actin staining in DRG neurons at various stages of neurite growth is presented in Figure 4.4. F-actin was present in various structures of the DRG neuron including nascent processes, mature neurites, growth cones, and the cell body. Condensed regions of F-actin were present in the cell body, and possibly represent sites of focal adhesions (indicated by small yellow arrow (Fig 4.4 A-C, E,F). F-actin was also observed in filopodia (indicated by small green arrowheads (Fig 4.4 A-E)), and at the leading edge of lamellipodium (large orange arrow, Fig 4.4F).

Figure 4.4: F-actin is present in structures of the growing neurite

DRG neurons were plated on polylysine, allowed to attach overnight and were then stimulated with soluble laminin for 24 h. Following fixation, neurons were labeled with Alexa Fluor 555-Phalloidin, and images were obtained with confocal microscopy. The cells shown represent various early stages of neurite growth and are all shown at the same magnification. (Scale bars = 20 μm). F-actin is present in the condensed in the cell body, indicated by a small yellow arrow, at possible sites focal adhesions. F-actin is also present in the filopodia (green arrowhead) and at the edge of lamellipodium (large orange arrow) in growing processes.

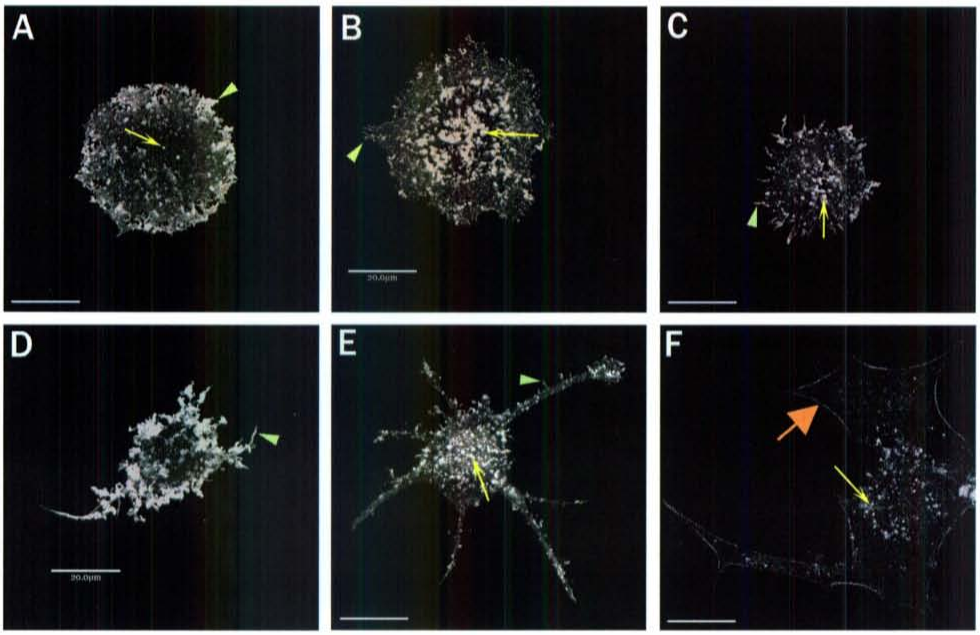
A
B
C
D
E
F
30.0µm
30.0µm

4.3.2.2 Overexpression of haHsp27

Having determined the location of F-actin in the various stages of neurite growth we used the cotransfection model described above and Hsp27 mutant constructs to determine whether the phosphorylation state of Hsp27 or the presence of the WDPF domain had an effect on F-actin localization and its colocalization with Hsp27. We chose to examine cells that were both in the early stages of neurite growth (Fig 4.5) as well as in cells with developed mature neurites (Fig 4.6). Additionally, the different transfections were performed in the same experiment, and cells from each transfection were plated in different wells on the same slide where they were stained and processed together.

Expression of haHsp27 appeared to colocalize with F-actin in the early stages of neurite growth (Fig 4.5 A-C) as well as in mature neurites (Fig 4.6 A-C). In the growth cone, haHsp27 and F-actin colocalized in the distal tips of filopodia and nascent processes, as well as in the cortex region of the nascent shaft. In contrast, in the central region of the growth cone, haHsp27 was present at high levels and F-actin was detectable at low levels (Fig 4.7 A-C).

4.3.2.3 Overexpression of Hsp27-AA

The nonphosphorylatable Hsp27-AA was present at high levels and strongly overlaped with F-actin in the filopodia and focal contacts in selected cells that were in the early stages of neurite growth (Fig 4.5. D-F) as evidenced by strong yellow regions in the merged confocal image demonstrating regions of co-localization. Additionally there was

Figure 4.5: The effect of Hsp27 phosphorylation and the WDPF domain on Hsp27 and F-actin colocalization during early stages of growth

Cotransfected DRG neurons were plated on polylysine, allowed to attach overnight and were then stimulated with soluble laminin for 24 h. Following fixation, neurons were labeled with Alexa Fluor 555-Phalloidin (green- B, E, H, K, N, Q), and immunostained with antibodies directed against Hsp27 (red – A, D, G, J, M, P). Images were obtained with confocal microscopy and panels C, F, I, L, O, R represent the merged images of single channel images. (Scale bars = 20 μm).

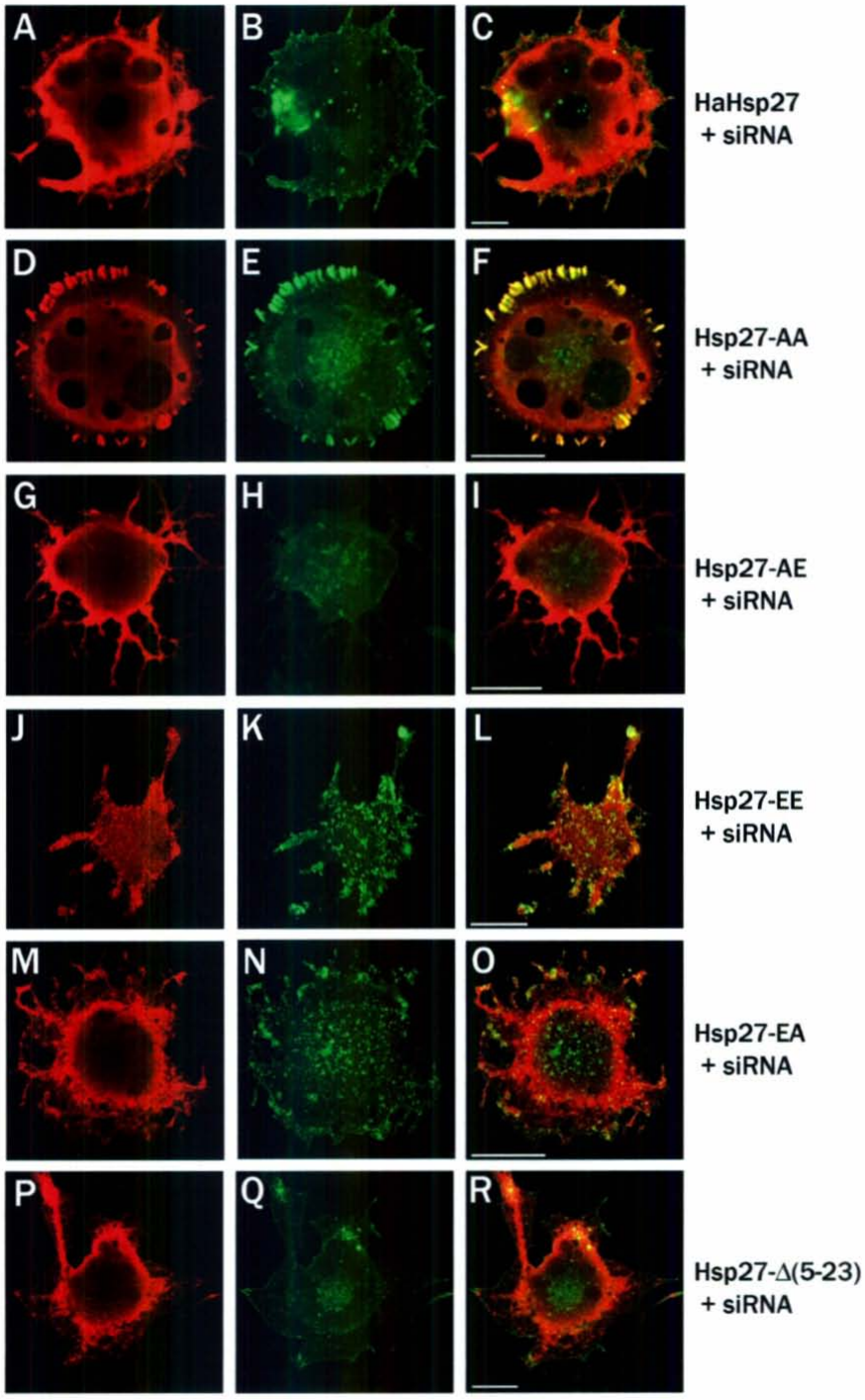
A
B
C
HaHsp27
+ siRNA
D
E
F
Hsp27-AA
+ siRNA
G
H
I
Hsp27-AE
+ siRNA
J
K
L
Hsp27-EE
+ siRNA
M
N
O
Hsp27-EA
+ siRNA
P
Q
R
Hsp27-Δ(5-23)
+ siRNA

Figure 4.6: The effect of Hsp27 phosphorylation and the WDPF domain on Hsp27 and F-actin colocalization in mature neurites.

Transfected DRG neurons were plated on polylysine allowed to attach overnight and were then stimulated with soluble laminin for 24 h. Following fixation, neurons were labeled with Alexa Fluor 555-Phalloidin (green- B, E, H, K, N, Q), and immunostained with antibodies directed against Hsp27 (red – A, D, G, J, M, P). Images were obtained with confocal microscopy and panels C, F, I, L, O, R represent the merged images of single channel images. (Scale bars = 20 μm).

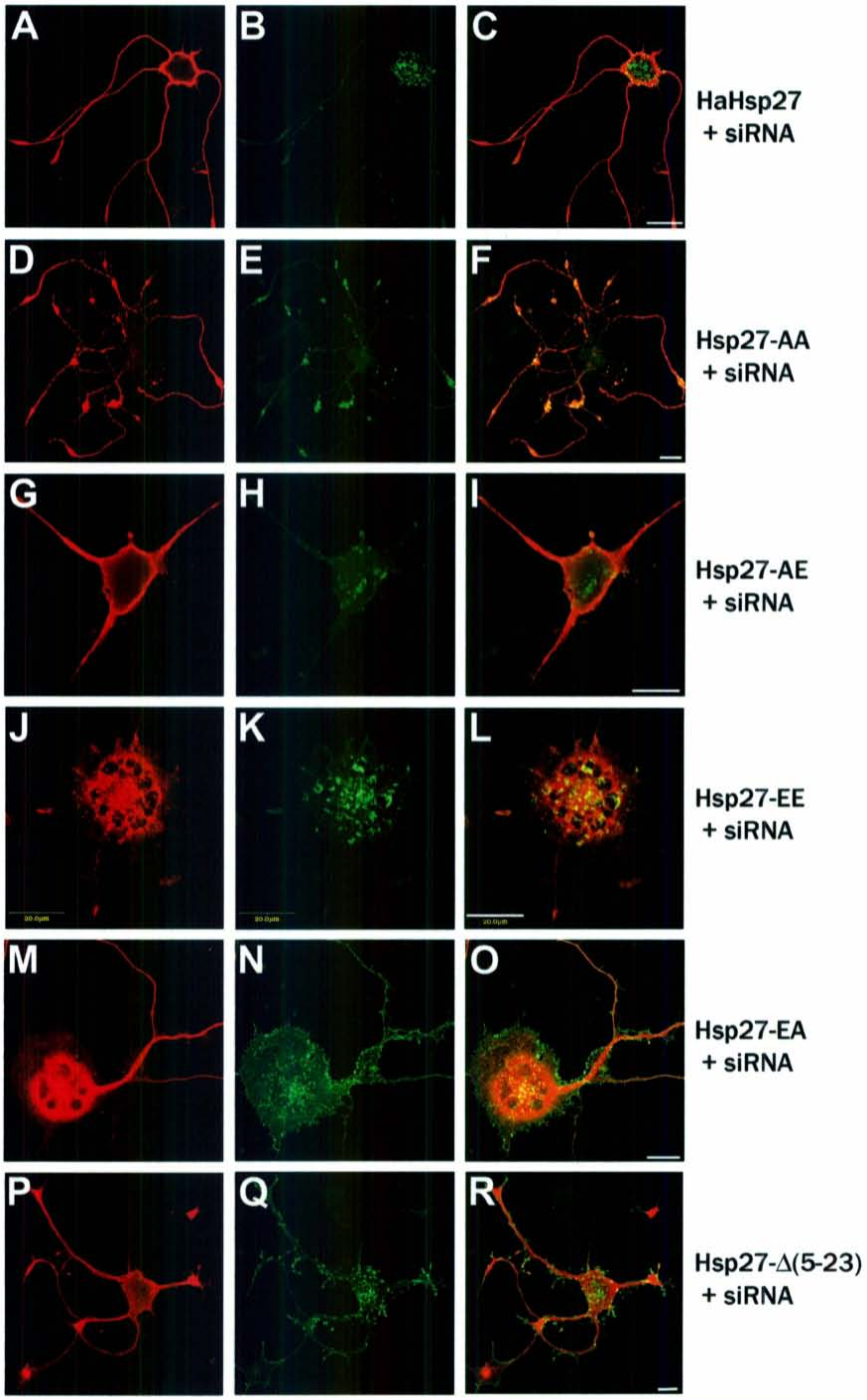
A
B
C
HaHsp27
+ siRNA
D
E
F
Hsp27-AA
+ siRNA
G
H
I
Hsp27-AE
+ siRNA
J
K
L
Hsp27-EE
+ siRNA
M
N
O
Hsp27-EA
+ siRNA
P
Q
R
Hsp27-Δ(5-23)
+ siRNA

Figure 4.7: The phosphorylation state of Hsp27 alters the location of F-actin in the growth cone.

Neurons were plated on polylysine, allowed to attach overnight and were then stimulated with soluble laminin for 24 h. Following fixation, neurons were labeled with Alexa Fluor 555-Phalloidin (green- B, E, H, K, N, Q) and immunostained with antibodies directed against Hsp27 (red – A, D, G, J, M, P). Images of growth cones were obtained with higher magnification than the neurite images via confocal microscopy. Panels C, F, I, L, O, R represent the merged images of single channel images. Scale bars = 10 μm.

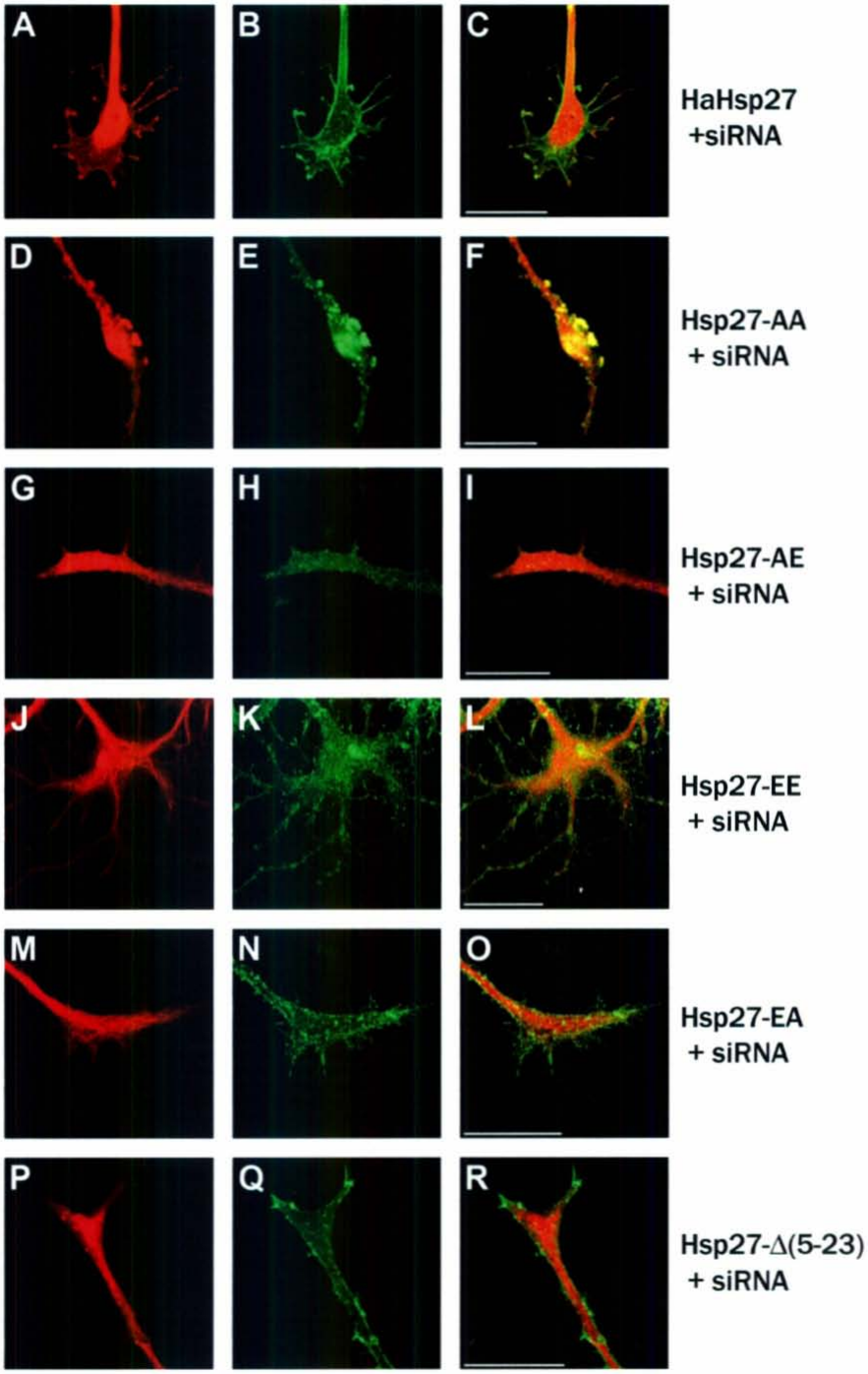
A
B
C
HaHsp27
+siRNA
D
E
F
Hsp27-AA
+ siRNA
G
H
I
Hsp27-AE
+ siRNA
J
K
L
Hsp27-EE
+ siRNA
M
N
O
Hsp27-EA
+ siRNA
P
Q
R
Hsp27-Δ(5-23)
+ siRNA

colocalization in growth cones of mature neurites (Fig 4.6 D-F, and Fig 4.7 D-F). Although densitometry was not performed on these confocal images, all images within one figure were visualized at the same PMTs and magnification. Cells expressing Hsp27-AA displayed large regions of yellow indicating colocalization of F-actin and Hsp27 within the growth cones, and early growth processes that was not seen under other conditions (Fig 4.5 (D-F), Fig 4.6 (D-F), Fig 4.7 (D-F)). This is consistent with nonphosphorylated Hsp27 having a direct interaction with actin possibly to stabilize the actin cytoskeleton (Pichon et al., 2004).

4.3.2.4 Overexpression of Hsp27-AE

DRG neurons expressing Hsp27-AE displayed robust Hsp27 staining in the early stages of neurite initiation as well as into the mature neurites and growth cones (Fig 4.5 G, Fig 4.6 G, Fig 4.7 G). Although, as noted above, densitometry of these images was not performed, from observing the images taken at the same PMT levels, it appeared that the level of F-actin staining was lower for cells expressing Hsp27-AE than for cells under all other conditions (Fig 4.5 H, Fig 4.6 H, Fig 4.7 H). This suggests that the decrease in F-actin may be responsible for the altered growth pattern (less branching) seen in cells expressing Hsp27-AE.

4.3.2.5 Overexpression of Hsp27-EE or Hsp27-EA

Cells expressing Hsp27-EE or Hsp27-EA displayed similar morphology in the structure of their processes and their F-actin localization [Fig 4.5 (J-O), Fig 4.6 (J-O), Fig

4.7 (J-O)]. Hsp27-EA or Hsp27-EE cells displayed large numbers of filopodia and nascent processes stained for Hsp27 and contained F-actin in the early stages of neurite growth (Fig 4.5 J-O) and also displayed large numbers of filopodia and small processes in growth structures and neurite shafts of mature neurites [Fig 4.6 (J-O), Fig 4.7 (J-O)]. Throughout the stages of neurite growth and extension, cells expressing either Hsp27-EE or Hsp27-EA present at higher levels of protrusion (filopodia and nascent processes) relative to all other conditions. The presence of large amounts of protrusions, and decreased neurite extension, suggests that there is increased uncoordinated filament growth and may explain why Hsp27-EE and Hsp27-EA expressing cells have lower neurite extension than cells expressing haHsp27.

4.3.2.6 Overexpression of Hsp27-Δ(5-23)

Cells expressing Hsp27-Δ(5-23) displayed Hsp27 and F-actin colocalized in filopodia and the leading edge of lamellipodium in the early stages of neurite growth as well as in the mature neurites (Fig 4.5 (P-R), Fig 4.6 (P-R)). The localization of Hsp27 and F-actin in cells expressing Hsp27-Δ(5-23) was somewhat similar to that in haHsp27 expressing cells. Under both conditions Hsp27 was present at high levels in the central region of the growth cone, while F-actin was present at high levels in the periphery of the growth cone in the filopodia and lamellipodium as well as in the cortex of the neurite shaft [Fig 4.6 (A-C, P-R), Fig 4.7 (A-C, P-R)]. However one notable difference between the conditions was the presence of high levels of Hsp27 at the distal tips of filopodia and

nascent processes in the growth cone in cells expressing haHsp27 [Fig 4.7(A-C)] that was not present in cells expressing Hsp27-Δ(5-23) [Fig 4.7 (P-R)].

Additionally cells expressing Hsp27 -Δ(5-23) displayed puncta of Hsp27 in approximately 40% of cells (Fig 4.8); these puncta ranged from minute to "ringed" aggregates up to 4 μm in diameter. Neurite length and Sholl analysis on cells with visible aggregates compared to cells without showed no difference in growth and growth patterning between the two populations (Fig 4.8).

4.4 Discussion

This study highlights the importance of Hsp27 phosphorylation in the regulation of neurite extension and growth patterning, likely via influence over polymerization of cytoskeletal elements such as actin.

To investigate the effects of Hsp27 phosphorylation on neurite initiation and growth we used Hsp27 constructs with mutations in the phosphorylation sites, either mimicking constitutively phosphorylated Hsp27 (S→E) or preventing phosphorylation at the site (S→A). Five mutant constructs were employed in this study. Hsp27-Δ(5-23) mutant has the WDPF domain as well as the Ser15 phosphorylation site deleted, allowing me to look at whether the presence of this domain and phosphorylation site are involved in neurite growth. Hsp27-AA is unable to be phosphorylated at amino acids 15 or 90, permitting investigation of what effect preventing phosphorylation Hsp27 phosphorylation has on neurite growth. Hsp27-EE contains negatively charged glutamic acid residues in place of its phosphorylatable serines (Ser15 and Ser90) mimicking

Figure 4.8: When expressed in DRG neurons Hsp27-Δ(5-23) forms aggregates in 40% of cells

Neurons were co-transfected with siRNA complementary to Hsp27 and vectors coding for GFP and Hsp27- Δ(5-23) and were plated on polylysine, allowed to attach overnight and were then stimulated for 24 h. Following fixation neurons were labeled with Alexa Fluor 555-Phalloidin (red- E, F) and immunostained with antibodies directed against Hsp27 (A-C; green – D, F). Panel F represents the merged images of single channel images D and E. Hsp27 is present in ring-like aggregates in the cell body, neurites and growth cones (yellow arrow). (Scale bars = 20 μm).

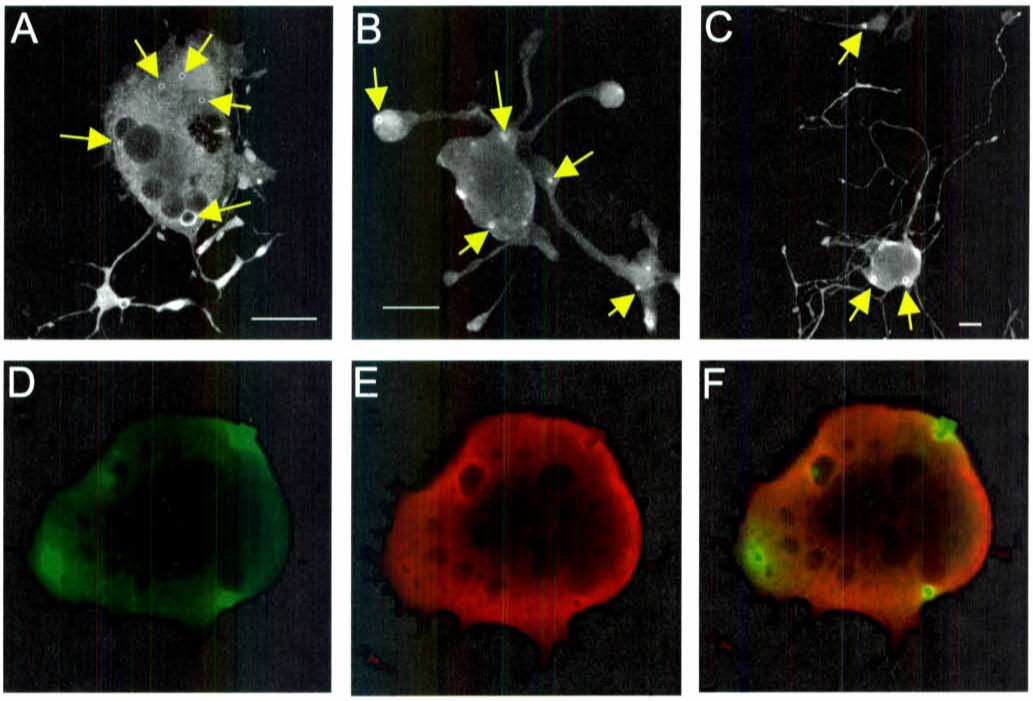
A
B
C
D
E
F

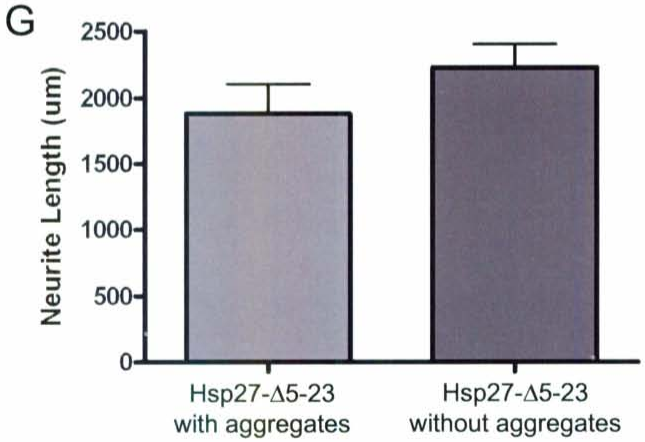
G
Neurite Length (um)
2500
2000
1500
1000
500
0
Hsp27-Δ5-23
with aggregates
Hsp27-Δ5-23
without aggregates

constitutive phosphorylation, permitting investigation of what role constitutive phosphorylation plays in neurite growth. Hsp27-AE, and Hsp27-EA have one of their serine phosphorylation sites mutated to alanine (A) such that it cannot be phosphorylated, and the other serine phosphorylation site mutated to glutamic acid (E) mimicking constitutive phosphorylation. The Hsp27-EA and Hsp27-AE constructs allow us to look at the role that the individual phosphorylation sites are playing in neurite growth by comparing cells expressing these constructs to those expressing haHsp27, Hsp27-AA, and Hsp27-EE.

The phosphorylation state of Hsp27 affects the oligomerization state of the protein in the cell. Biochemical studies analyzing the mutant proteins have suggested that the phosphorylation mutants have an effect on Hsp27 oligomerization (Theriault et al., 2004). It has been reported that Hsp27-EE and Hsp27-EA are present solely as monomers and are unable to form dimers and larger oligomers, while Hsp27-AE is present as monomers and dimers and is unable to form large oligomers (Theriault et al., 2004). Hsp27-Δ(5-23) is unable to form oligomers larger than dimers, and Hsp27-AA is found in all the oligomeric states, although it preferentially forms large oligomeric structures (Theriault et al., 2004).

Expression of the different Hsp27 mutants have distinct effects on their ability to rescue Hsp27-siRNA decreased neurite growth. Cells expressing Hsp27-AA, where phosphorylation at the amino acids 15 and 90 is prevented and Hsp27 is able to form large oligomers, show similar neurite extension to that of haHsp27 that presumably can be phosphorylated. However, the neurite arborization patterns of haHsp27 and Hsp27-

AA are different, possibly indicating aberrant growth patterning due to the mutation. A difference in the growth patterning of cells expressing Hsp27-AA is not surprising given previous results showing that aberrant neurite growth results from the use of a pharmacological upstream inhibitor of Hsp27 phosphorylation (Williams et al., 2005). Cells expressing Hsp27-AA also showed an altered localization of Hsp27 and F-actin compared to cells expressing haHsp27. Unlike haHsp27 expressing cells, those expressing Hsp27-AA displayed high levels of colocalization between Hsp27 and F-actin in nascent processes and filopodia in early stages of growth and also in the central region of growth cones. This possibly represents high levels of Hsp27-AA, some of which would be found in monomeric form and able to bind to F-actin which is consistent with monomeric nonphosphorylated Hsp27 binding actin (Pichon et al., 2004).

Cells expressing Hsp27-Δ(5-23), where the WDPF domain and the S15 phosphorylation site of Hsp27 have been deleted, display neurite extension and growth patenting similar to haHsp27. Studies have shown that Hsp27-Δ(5-23) is unable to form oligomers large than dimers (Theriault et al., 2004), indicating that the formation of large oligomers is not required for the involvement of Hsp27 in neurite initiation and growth. This result in conjunction with those of cells expressing Hsp27-AA suggests that not only is phosphorylation of the S15 site not required for neurite growth, but that the presence of the S15 site is not required for neurite growth, although it is possible that phosphorylation of the S15 site plays an inhibitory role in neurite growth (see below).

Cells expressing Hsp27-EE or Hsp27-EA, where the Hsp27 S15 site has been mutated to mimic constitutive phosphorylation, resulted in significantly ($P < 0.05$) less

growth than cells expressing haHsp27, and similar growth to cells with Hsp27-siRNA alone. Additionally, Sholl analysis of Hsp27-EE or Hsp27-EA expressing cells also displayed decreased neuritic arborization patterns similar to Hsp27-siRNA. Cells transfected with Hsp27-EE or Hsp27-EA, displayed high levels of protrusion (filopodia and nascent processes) at early stages of neurite initiation and growth, and also in growth cones and axon shafts of mature neurites. The mechanism for this excess of protrusion is unknown and it is possible that phosphorylation at the S15 site of Hsp27 may play a role in stabilization of filopodia, or that its dephosphorylation is required for retraction of protrusions. As the only two conditions that failed to result in growth greater than Hsp27-siRNA alone, it is of interest that these mutants are also the only two of the five constructs used that are unable to form dimers or oligomers, and are thus expected to be completely in a monomeric state.

Cells expressing Hsp27-AE fell in between the wild type conditions (haHsp27) and siRNA alone, as they had significantly ($P < 0.05$) less neurite growth and arborization than haHsp27, but significantly ($P < 0.05$) more growth and arborization than Hsp27-siRNA alone. Cells transfected with Hsp27-AE also appear to have lower levels of F-actin than cells expressing haHsp27 and other Hsp27 mutations.

These results suggest that the role that Hsp27 plays in neurite growth can be affected by phosphorylation, oligomerization, or a combination of both (Table 1). The Hsp27 mutants that are able to dimerize and/or form large oligomers [Hsp27-AA, Hsp27-AE, Hsp27-Δ(5-23)] all displayed neurite growth that was significantly greater than that of Hsp27-siRNA alone, while Hsp27 mutants that were unable to form dimers or

Table 4.1: The effect of Hsp27 phosphorylation mutants on neurite growth

	Oligomeric Size	Amount of Neurite Growth	Description of Neurite Growth
HaHsp27	Monomers, dimers and oligomers (Lambert et al., 1999)	+++++	Neurite growth significantly increased relative to siRNA
Hsp27-AA	large oligomers (Lambert et al., 1999)	+++++	Neurite growth similar to haHsp27
Hsp27-AE	Dimers and monomers (Theriault et al., 2004)	+++	Signifigantly less neurite growth than cells transfected with haHsp27, similar growth to siRNA
Hsp27-EE	Monomers (Theriault et al., 2004)	+	Significantly less neurite growth than cells transfected with haHsp27, similar growth to siRNA
Hsp27-EA	Monomers (Theriault et al., 2004)	+	Neurite growth significantly less than haHsp27 and significantly greater than siRNA
Hsp27-Δ(5-23)	Dimers and monomers (Theriault et al., 2004)	+++++	Neurite growth similar to haHsp27

Table 4.2: The effect of Hsp27 phosphorylation mutants on the localization of Hsp27 and F-actin

Mutant	Oligomeric Size	Observations	Possible Explanations
HaHsp27	Monomers, dimers and oligomers	Hsp27 present in the central region of the growth cone, and at filopdia tips, F-actin present in periphery	
Hsp27-AA	large oligomers	Strong colocalization of F-actin and Hsp27 in filopodia	Consistent with non phosphorylated Hsp27 having a direct interaction with actin
Hsp27-AE	Dimers and monomers	Appears to have low F-actin levels	Suggests a decrease in F-actin may be responsible for the altered growth pattern
Hsp27-EE	Monomers	High levels of filopodia and nascent processes with F-actin	- S15 phosphorylation may stabilize filopodia, or - Dephosphorylation is required for retraction?
Hsp27-EA	Monomers	High levels of filopodia and nascent processes with F-actin	
Hsp27-Δ(5-23)	Dimers and monomers	Hsp27 present in the central region of the growth cone, F-actin present in periphery	Suggests WDPF domain does not affect actin localization (Hsp27 not at distal tips)

oligomers (Hsp27-EE and Hsp27-EA) displayed growth similar to Hsp27-siRNA alone. Additionally the differences in growth between the dimer-forming mutants may be accounted for due to the difference in their phosphorylation states.

Phosphorylation of the S15 and S90 sites appears not to be required for Hsp27 mediated neurite outgrowth as seen in the Hsp27-AA and Hsp27-Δ(5-23) conditions. However, constitutive pseudo-phosphorylation of the S15 and S90 sites have a negative effect on the involvement of Hsp27 in neurite growth, with phosphorylation of the S15 site (as evidenced through cells expressing Hsp27-EE and Hsp27-EA) appearing to have a stronger inhibitory effect than phosphorylation of the S90 site (Hsp27-AE). One possible explanation for this effect is that phosphorylation at S15 may be involved in stabilizing the actin cytoskeleton, possibly through promoting actin filament growth and preventing plus end degradation [this would account for an increase in protrusions with Hsp27-EE and Hsp27-EA (Table 4.2)], while phosphorylation at the S90 site may be involved in destabilizing the cytoskeleton (accounting for the seemingly lower F-actin levels with Hsp27-AE). A shift in the dynamic balance between polymerization and depolymerization in the cell in either direction will affect the control of neurite extension and growth patterning that may account for the differences in growth seen in this study with use of the Hsp27 phosphorylation mutants.

These results are the first to show that differences between the phosphorylation sites have an influence on neurite growth parameters. Although many studies (in non-neuronal cells) support phosphorylation-dependant direct and indirect mechanisms for Hsp27 regulation of the F-actin cytoskeleton, the specific phosphorylation site involved

in each of these mechanisms has not been elucidated. With respect to the finding that constitutive phosphorylation has a negative impact on growth, under normal conditions Hsp27 is also present in its unphosphorylated state and is rapidly phosphorylated and dephosphorylated through cell signaling pathways in response to stimuli and changing environments. So while these results support the involvement of Hsp27 in neurite growth and suggest differential involvement of the phosphorylation sites in this process, it is also possible that the effect of Hsp27 phosphorylation depends on its localized activation and deactivation. Through being dynamically regulated itself, Hsp27 is able to play a role in modulating the dynamics of actin.

Chapter 5

Inhibition of p38 MAPK activity attenuates Hsp27 phosphorylation and increases the F-actin/G-actin ratio in DRG neurons

5.1 Introduction:

Actin is a component of the neuronal cytoskeleton and is responsible for many of the structures that determine the shape of the neuron. Due to the ability of actin to form dynamic structures it imparts flexibility to the cell allowing it to change shape to respond to varying conditions. Within the cell, actin exists in two states: actin monomers, also known as globular actin (G-actin) and actin filaments, also known as filamentous actin (F-actin) (Choo and Bray, 1978). Actin binding proteins can regulate actin filament dynamics via regulation of polymerization, depolymerization, stabilization, and attachment of actin to other structures (Dent and Gertler, 2003; Mattila and Lappalainen, 2008).

Heat shock protein 27 (Hsp27) is a member of the class of small heat shock proteins and has been shown to interact with different cytoskeletal elements, as well as to promote survival in the face of environmental stress through numerous mechanisms, including by stabilizing the actin filament cytoskeleton (Huot et al., 1997; Preville et al., 1998; Vigilanza et al., 2008). The interactions between Hsp27 and actin have been extensively studied. Hsp27 plays a role in regulating the actin filament cytoskeleton though direct interactions with actin as well as by modulating the activities of actin

binding proteins though signaling pathways. The interactions of Hsp27 and actin are important for many cell functions, including smooth muscle contraction, neutrophil chemotaxis and exocytosis, cell division, cell survival, cell migration, and cell attachment via focal adhesions, and recently in GDNF induced neurite growth (Brophy et al., 1998; Hong et al., 2009; Jog et al., 2007; Lee et al., 2007; Lee et al., 2008; Piotrowicz et al., 1998; Schneider et al., 1998). Additionally, Hsp27 colocalizes with actin filaments in cardiac (Lutsch et al., 1997), skeletal (Benndorf et al., 1994), and smooth muscle (Bitar et al., 1991; Ibitayo et al., 1999).

The role that Hsp27 plays in regulating the actin cytoskeleton through both direct and indirect mechanisms depends upon the phosphorylation state of Hsp27. Hsp27 is phosphorylated on two serines in the rodent Hsp27 (Ser15, and Ser86 in rat, Ser90 in hamster, Ser82 in mouse) by MAPKAP kinase-2 (MKK2) at both sites in many cell types; MKK2 is generally thought to be activated by p38 MAPK (Huot et al., 1995; Landry et al., 1992; Mehlen and Arrigo, 1994). In smooth muscle and other cell types, other kinases such as MK3 (McLaughlin et al., 1996), MK5 (New et al., 1998), PKCδ (Maizels et al., 1998), and PKD (Doppler et al., 2005), have been implicated in the phosphorylation of Hsp27, although the specific sites phosphorylated have not been determined.

Previous studies have suggested a role for Hsp27 in neurite growth via regulation of the actin cytoskeleton (Williams et al., 2009; Williams et al., 2005, 2006). I have shown that Hsp27 was present and colocalized with actin in lamellipodium, filopodia and focal contacts at the earliest stages of neurite growth as well as in mature neurites and

growth cones (Williams et al., 2005). Knock down of endogenous Hsp27 protein by small interfering RNAs (siRNA) resulted in decreased neurite growth as well as an altered localization of Hsp27 and actin (Williams et al., 2006). Additionally we observed that the phosphorylation state of Hsp27 was important for neurite growth (see Ch 4). Use of upstream pharmacological inhibitors that inhibit the activity of p38 MAPK resulted in decreased Hsp27 phosphorylation and aberrant neurite growth similar to cells treated with cytochalasin D (Williams et al., 2005). Transfection of neurons with mutant Hsp27 constructs containing Hsp27-EE which mimics constitutively phosphorylated Hsp27, resulted in decreased growth relative to control conditions, as well as high levels of protrusions (filopodia and nascent processes) at early stages of neurite initiation and growth as well as in growth cones and axon shafts of mature neurites (Williams, 2009). These studies support a role for Hsp27 in regulating actin dynamics, with the phosphorylation state of Hsp27 being important. Our objective in the present study was to investigate whether upstream pharmacological inhibition of Hsp27 phosphorylation affected actin dynamics in the cell.

5.2 Materials and Methods

5.2.1 Neuronal Cultures

Dorsal root ganglia (DRG) from young adult (5-6 weeks of age) Sprague-Dawley rats (Memorial University of Newfoundland Vivarium) were dissected and dissociated using the procedure described in previous chapters sections 2.6.1, 3.3, and 4.2. Briefly, in accordance with University Animal Care guidelines, animals were decapitated, ganglia

were extracted from all spinal cord levels and incubated in 0.25% collagenase type II (Invitrogen, Burlington, Canada) for 45 min at 37°C and then incubated with 0.25% trypsin (Invitrogen) for 20 min at 37°C, and then incubated with 0.2% soybean trypsin inhibitor for 5 min at 37°C. The ganglia were dissociated by a series of manual titrations using polished Pasteur pipettes. The cell suspension was washed with serum free Neurobasal medium (NB, Invitrogen) and centrifuged at 5 G, before being layered on top of a 30% Percoll solution (GE healthcare, Baie d'Urfe, QC) in 15 mL conical tubes and centrifuged at 400 g for 20 min at room temperature. Pellets were then carefully extracted with a sterile pasture pipette, placed in a fresh tube and transfected using the AMAXA nucleoporation protocol (AMAXA/LONZA, Cologne, Germany). Transfected cells were suspended in serum free modified NB, containing supplemented 100 U penicillin/ streptomycin, B27 supplement (Invitrogen), and 20 uM cytosine arabinoside (Sigma, St. Louis MO, USA) and plated on laminin (LN; 40 ug/mL) – coated Lab-Tek 16-well chamber slides (Nunc International, Naperville, IL) for neurite growth assessment or PL coated 12-well plates for Western blotting and G-actin/F-actin *in vivo* assay kit, and incubated at 37 °C with 5% CO_2. The neurons were cultured in serum-free NB with no added growth factors.

5.2.2 Inhibitor Experiments

SB 203580 and SB 202190 (10 uM Calbiochem/ EMD Biosciences, San Diego, CA) were used to inhibit p38 MAPK activity, in order to assess the contribution of

phosphorylated Hsp27. Inhibitors were added 2 h after the cells were plated on LN coated slides and retained in the medium for the extent of the experiment.

5.2.3 Immunoblotting

Transfected neurons were plated in 12-well plates and subsequently processed according to our established protocols (Jones et al., 2003), and as previously described. After cell lysis and centrifugation (10,000 rpm, 5 min), the supernatants were used to determine protein concentration by using the BCA protein assay (Pierce Chemicals, Rockford, IL). Equivalent amounts of protein (50 ug) were subjected to sodium dodecyl sulfate (SDS)-poly-acrylamide gel electrophoresis (10% acrylamide). Fractionated proteins were subsequently transferred to nitrocellulose membranes and stained with ponceau red as an indicator of protein loading. Immunodetection of the protein of interest was performed by blocking the membrane in 3% powdered milk in TBS-T for 1 h and incubated overnight with primary antibodies directed towards Hsp27 (SPA-801, Stressgen), mitogen-activated protein kinase (MAPK; Santa Cruz Biotechnology, CA), actin (A2066; Sigma) and phospho-Hsp27^{S15} (PAI-016; Affinity Bioreagents), and phospho-Hsp27^{S82} (E118, Abcam). phospho-Hsp27^{S82} reacts with phosphorylated S82 in human and S86 in rat. The nitrocellulose membranes were then probed with horseradish peroxidase (HRP) conjugated secondary antibodies (AP307P; AP308P; Chemicon, Temecula, CA) for 1 h at room temperature, followed by visualization via the ECL method.

5.2.4 G-actin / F-actin In vivo Assay Kit

The F-actin / G-actin ratio with the cells was determined using the G-actin/ F-actin *in vivo* assay kit (Cytoskeleton, Denver CO). The F and G-actin populations are isolated from cell lysates by differential centrifugation to separate the insoluble F-actin from soluble G-actin. The cellular F-actin to G-actin ratio is maintained by performing cell collections and centrifugations at 37°C. The separated F-actin and G-actin levels are analyzed by immunoblotting as detailed above.

5.2.5 Cell labeling and imaging

Neurons were fixed in 4% paraformaldehyde (pH 7-7.4) in PBS for 15 min, permeabilized with 0.1% Triton-X-100 and blocked with 10% normal goat serum in PBS. Cells were incubated for 2 h with Alexa 568-Phalloidin (Molecular Probes/ Invitrogen) to label actin filaments (F-actin), and Deoxy Ribonuclease1 Alexa Fluor 488 (D12371, Molecular Probes/ Invitrogen) to label G-actin. The cells were cover slipped with glycerol and imaged with confocal laser scanning microscopy using z-stage scanning and image stacking. Stacked digital images were incorporated into Adobe Photoshop for compilation into the final composite figures. 20 cells were imaged for each of 3 replicas of each condition.

5.2.6 Mean Grey Values of Labeled Cells

Confocal images of F-actin and G-actin stained cells were converted to inverted grayscale tiff's using Adobe Photoshop, and imported into Image J (version 1.38x; NIH, USA). The ImageJ measurement function was used to determine the mean grey values for the

image. Mean grey values for F-actin stained cells were divided by mean grey values for G-actin stained cells, and these values were expressed as the mean density of F-actin/ G-actin.

5.3 Results

Due to numerous reports suggesting a role for Hsp27 phosphorylation in modulating the actin cytoskeleton (Benndorf et al., 1994; Butt et al., 2001; Guay et al., 1997; Lavoie et al., 1993a; Schafer et al., 1999; Vigilanza et al., 2008) we wished to determine the effects of inhibiting p38 MAPK, and thus inhibiting Hsp27 phosphorylation, on the actin cytoskeleton. p38 MAPK activation leads to the phosphorylation and activation of MKK2, that acts as an Hsp27 kinase (Huot et al., 1995). I have previously shown that inhibition of p38MAPK activity, using a combination of p38 MAPK inhibitors (SB 203580 and SB202190), blocks the phosphorylation of Hsp27 at the Ser15 site, and results in aberrant growth (Williams et al., 2005).

I initially determined whether the inhibitors were effective in preventing Hsp27 phosphorylation at both the S15 and S86 sites. DRG neurons were plated on LN-coated 12 well pates and after 2 h the SB inhibitors were added; 24 h after SB addition, cell lysates were immunoblotted as described in the Methods. The immunoblots were probed with pHsp27^{S15}, pHsp27^{S82} (recognizes rat S86), and total Hsp27 antibodies. The results presented in Figure 5.1 show that treatment with SB resulted in decreased phosphorylation at both the S15 and S86 sites.

Figure 5.1: p38 MAPK inhibition blocks phosphorylation of Hsp27 at the S15 and S86 sites. Adult DRG neurons were plated on laminin coated plates, allowed to attach for 2 h and were treated with p38 MAPK inhibitors, SB203580 and SB 202190 (10 μm each). Cells were sampled at 24 h post SB addition, and protein was analyzed by western blotting **(A)**. Inhibition of p38 MAPK activity results in significantly decreased levels of both S15 **(B)** and S86 **(C)** phosphorylation relative to control. Graphs represent the mean ± SEM of relative densitometric data of 4 blots from 2 experiments; data are expressed as percentages with the control value for each experiment taken as 1. Significance was tested using T-test, * $p < 0.05$.

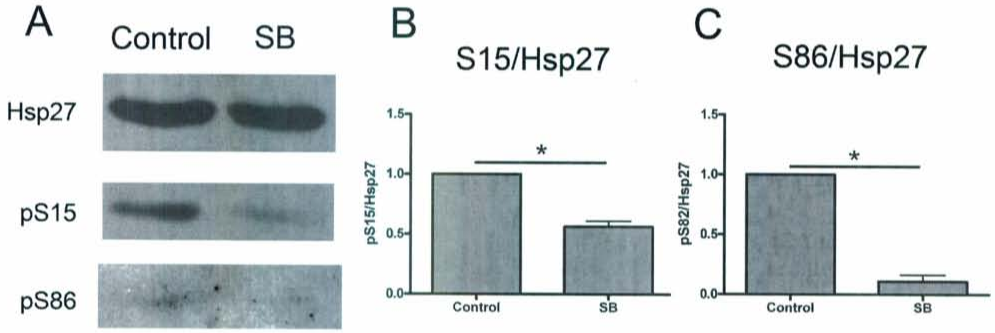
A
Control
SB
Hsp27
pS15
pS86
B
S15/Hsp27
pS15/Hsp27
1.5
1.0
0.5
0.0
*
Control
SB
C
S86/Hsp27
pS82/Hsp27
1.5
1.0
0.5
0.0
*
Control
SB

Having determined that the inhibitors had the expected effects on the phosphorylation of Hsp27, we sought to determine their effect on actin filament polymerization. For these experiments, we used a commercially available protocol to isolate the F-actin and G-actin populations within the cells. Neurons were plated on LN-coated 12 well plates as for the previous experiment, and were treated with SB 2 h after plating, and cell lysates were collected 24 h later and prepared as described in the Methods for the G-actin/ F-actin *in vivo* assay kit. Following electrophoresis, the resulting blots were probed with actin and loading control MAPK antibodies. The blots display increased F-actin levels in conditions treated with SB relative to control (Fig 5.2A). Densitometric analysis of the western blots shows that the F-actin/ G-actin ratio in cells treated with SB is significantly greater than that in control cells (Fig 5.2 B).

Having determined that inhibition of p38 MAPK results in an alteration of the F-actin / G-actin ratio in the neuron, we sought to confirm these results with cell staining. Neurons were plated on LN coated 16 well slides, and were treated with SB 2 h after plating, and were fixed 24 h later and labeled for F-actin and G-actin as outlined in the Methods. The neurons were imaged using confocal microscopy for visualization of F-actin and G-actin (Fig 5.2 C). All images were obtained at the same magnification, and all with a particular label (ex. F-actin) were obtained at the same PMTs to permit comparison of the images. These images were converted into inverted grayscale images using Adobe Photoshop and imported into ImageJ to determine the mean grey values / densities of the images. Mean densities of the images were expressed as a ratio of the F-actin to the G-actin. The results supported the result from the *in vivo* G-actin / F-actin

Figure 5.2: p38 MAPK inhibition alters the F-actin to G-actin ratio within the DRG neuron, resulting in increased F-actin and decreased G-actin. Adult DRG neurons were plated on laminin coated plates or slides, allowed to attach for 2 h and were treated with p38 MAPK inhibitors, SB203580 and SB 202190 (10 μm each). 24 h after SB addition cells were either collected for analysis of their G-actin/ F-actin using an *in vivo* assay kit (See Methods) (**A, B**), or fixed, permeabilized and treated with Alexa 568-Phalloidin to label F-actin, and DeoxyRiboNuclease1 (DNAse I) coupled to Alexa Fluor 488 to label G-actin (**C**). **A:** Treatment with SB resulted in an increase in F-actin levels. **B.** Densitometric analysis of the F-actin/G-actin blots showed that treatment with SB resulted in a significantly increased F-actin/ G-actin ratio relative to loading control MAPK (where individual F-actin and G-actin levels were normalized to MAPK levels) . Graphs represent the mean ± SEM of relative densitometric data of 5 blots from 5 experiments; data are expressed as percentages with the control value for each experiment taken as 1. **C.** Confocal images of cells with and without SB treatment, and treated with Phalloidin-Alexa 568 and DNAse-Alexa Fluor 488 for visualization of F-actin and G-actin, were obtained at the same PMTs and magnification. **D.** Confocal images of F-actin and G-actin stained cells were converted to inverted grayscale using Adobe Photoshop, and imported into ImageJ. The ImageJ measurement function was used to determine the mean grey values for the image. Mean grey values for F-actin stained cells were divided by mean grey values for G-actin stained cells, and these values were expressed as the mean density of F-actin/ G-actin. Cells treated with SB had a significantly increased F-actin/ G-actin ratio than control cells. Inhibition of p38 MAPK activity results in significantly increased F-actin/ G-actin within DRG neurons. Graphs represent the mean ± SEM of mean grey values (F-actin/ G-actin) of 12 cells from 2 plating experiments. Significance was tested using T-test, * $p<0.05$.

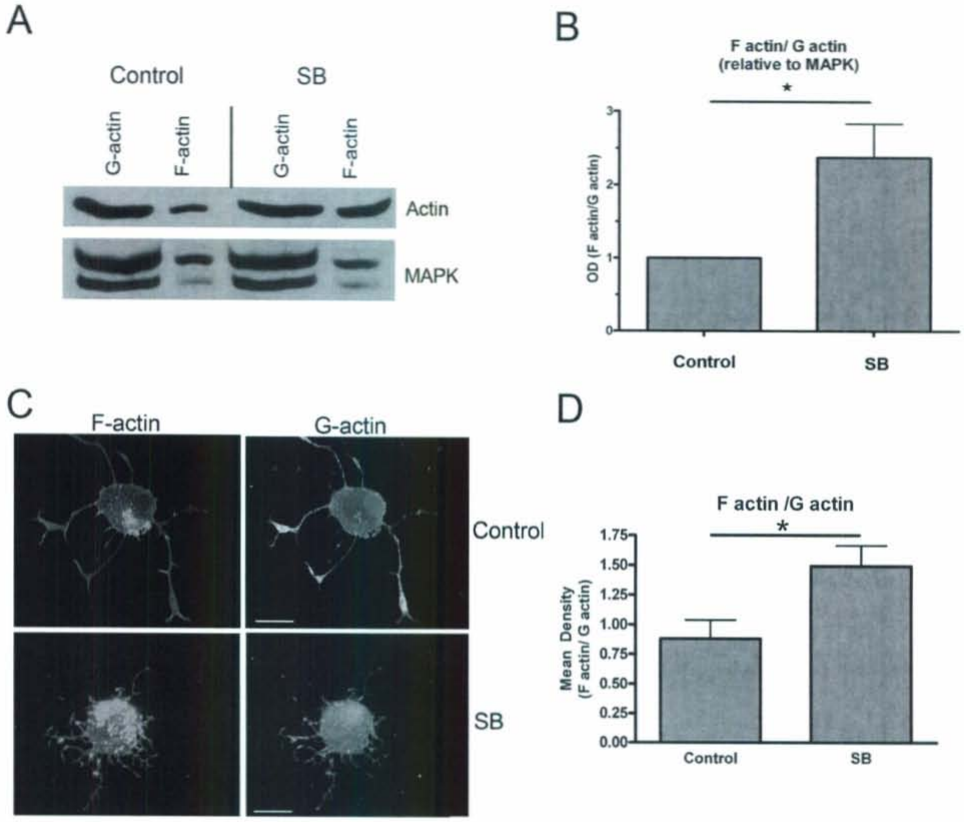
A
Control
SB
G-actin
F-actin
G-actin
F-actin
Actin
MAPK
B
F actin/ G actin
(relative to MAPK)
*
OD (F actin/G actin)
3
2
1
0
Control
SB
C
F-actin
G-actin
Control
SB
D
F actin /G actin
*
Mean Density
(F actin/ G actin)
1.75
1.50
1.25
1.00
0.75
0.50
0.25
0.00
Control
SB

assay kit, as cells treated with SB had a significantly increased F-actin/ G-actin ratio of mean grey values relative to control cells.

5.4 Discussion

This study highlights the importance of p38 MAPK activity, possibly via its upstream regulation of Hsp27 phosphorylation, in regulating the neuronal actin cytoskeleton. Results suggest that inhibition of Hsp27 phosphorylation alters the balance of F-actin / G-actin in the neuron. This is based on the assumption that the effects on the actin cytoskeleton are due to the SB compounds acting as an upstream inhibitor of Hsp27 phosphorylation, via inhibition of p38 MAPK. Although the concentration of the inhibitor was chosen empirically and is within the range of specific/selective effects on p38 MAPK, it is possible that it may have other inhibitory influences, or that it may be influencing the actin cytoskeleton though actions not involving Hsp27.

p38 MAPK control of the actin cytoskeleton via the regulation of Hsp27 phosphorylation is supported by numerous studies demonstrating that Hsp27 plays a role in regulating the actin filament cytoskeleton through direct interaction with actin, as well as by modulating the activities of actin binding proteins through cell signaling pathways (During et al., 2007; Gehler et al., 2004; Loudon et al., 2006; Miron et al., 1991; Pichon et al., 2004). My previous studies have suggested a role for Hsp27 and Hsp27 phosphorylation in neurite growth via regulation of the actin cytoskeleton (Williams, 2009; Williams et al., 2009; 2006).

Two mechanisms for direct Hsp27-based inhibition of actin filament assembly have been proposed. Hsp27 was originally characterized as a barbed end capping protein, although recent reports suggest that Hsp27 impairs actin filament assembly by sequestering actin monomers rather than by capping (During et al., 2007; Miron et al., 1991; Pichon et al., 2004). Both of these mechanisms support a phosphorylation dependant interaction for Hsp27 with actin, suggesting that only nonphosphorylated Hsp27 monomers are able to bind to actin to inhibit actin filament polymerization (Benndorf et al., 1994; During et al., 2007; Guay et al., 1997; Landry and Huot, 1999; Lavoie et al., 1995; Miron et al., 1991).

These results suggest that Hsp27 regulates the actin cytoskeleton in a mechanism that is dependent on its phosphorylation state, however unlike models for direct interactions of Hsp27 and actin, that show decreased F-actin (Miron et al., 1991), our results show that the p38 MAPK inhibitor SB203580 treatment led to decreased Hsp27 phosphorylation, along with increased F-actin. These results could be explained by the role Hsp27 plays in regulating the actin filament cytoskeleton independent of its ability to directly bind to actin via regulating actin binding proteins through its involvement in cell signaling pathways. Hsp27 has been suggested to interact with 14-3-3 protein and RhoA, both of which are involved in regulation of the actin cytoskeleton dynamics (Gehler et al., 2004; Loudon et al., 2006).

Phosphorylated Hsp27 binds 14-3-3 protein in fibroblasts, and inhibition of Hsp27 phosphorylation with the p38 MAPK inhibitor SB203580 blocks this interaction (Vertii et al., 2006). It has been hypothesized that the interaction of pHsp27 and 14-3-3

protein prevents the binding of 14-3-3 and pCofilin; binding of pHsp27 to 14-3-3 results in the dephosphorylation and activation of cofilin, and thereby promotes actin filament depolymerization (Gaestel, 2006). This possible indirect role for Hsp27 affecting actin polymerization supports our findings that SB treatment results in stabilization of the cytoskeleton and increased F-actin levels.

An indirect role for Hsp27 in regulating actin filament dynamics is further supported by the finding that the Hsp27 phosphorylation mutant, Hsp27EE, inhibits actin polymerization in HeLa cells but not in brain extracts (During et al., 2007). The different effects of Hsp27 on actin polymerization depending on the cell type suggests the presence of cell type specific actin binding proteins and signaling intermediates that could influence actin filament polymerization.

These results show that upstream pharmacological inhibition of Hsp27 phosphorylation alters the actin dynamic in the cells resulting in an increase in F-actin.

Chapter 6

Discussion and Summary

6.1 Research outcomes

The main goal of my research was to determine what role Hsp27 played in neurite growth of the sensory DRG neurons. This investigation stemmed from previous work in the Mearow lab looking at the role of Hsp27 in survival of DRG neurons. It is clear that Hsp27 can play a protective role in neurons and that its effects may be unique from those of Hsp70 and other HSPs (Reviewed in Franklin et al., 2005; Latchman, 2005; Stetler et al., 2008). The protective effects of Hsp27 have been attributed to its actions as a chaperone, its ability to inhibit apoptosis, and its ability to stabilize the actin cytoskeleton (Huot et al., 1997; Mounier and Arrigo, 2002; Perng et al., 1999a; Sun and MacRae, 2005; Theriault et al., 2004). The role of Hsp27 in modulating the actin cytoskeleton has been extensively studied in non-neuronal cells and interactions of Hsp27 and actin have been determined to be important for many cell functions, including smooth muscle contraction, neutrophil chemotaxis and exocytosis, cell division, cell survival, cell migration, and cell attachment via focal adhesions (Brophy et al., 1998; Jog et al., 2007; Lee et al., 2007; Lee et al., 2008; Piotrowicz et al., 1998; Schneider et al., 1998). In cultures of dissociated adult DRG neurons I observed robust expression of Hsp27 in the neurites and growth cones. The combination of the location of Hsp27 in neurites and growth cones along with the reported role of Hsp27 in modulating the cytoskeleton, led

me to examine whether Hsp27 was involved in neurite growth via regulation of the actin cytoskeleton.

Besides its interactions with actin, it is also clear that Hsp27 can interact with tubulin, tau and several species of intermediate filaments including GFAP, vimentin, nestin and neurofilaments (NF) (Benndorf and Welsh, 2004; Jia et al., 2009; Perng et al., 1999a; Shimura et al., 2004). Furthermore, recent studies have shown that missense mutations in sHSPs including Hsp27, Hsp22, and Hsp8 are associated with peripheral neuropathies in particular the axonal form of Charcot-Marie-Tooth disease and distal hereditary motor neuropathy (Evgrafov et al., 2004; Irobi et al., 2004b; Zhai et al., 2007). Interestingly, mutations in both NF-L and Hsp27 result in similar phenotypes. Expression of the mutant NF-L causes a disrupted neurofilament network with subsequent alteration in axonal transport (Perez-Olle et al., 2004; Perez-Olle et al., 2005) while expression of two of the missense Hsp27 mutations results in the formation of insoluble aggregates and destabilization and disruption of NFs and disturbances in axonal transport (Ackerley et al., 2006; Evgrafov et al., 2004; Zhai et al., 2007). Thus Hsp27 has been inferred to stabilize not only actin but also neurofilament and microtubules, which we hypothesize indicate possible mechanisms for the involvement of Hsp27 in neurite growth. As obvious from previous chapters, a variety of different experiments were performed in order to test these hypotheses. To summarize my results I have placed my findings in 3 separate categories: (1) The effects of the presence or absence of Hsp27 in neurite initiation and growth; (2) The role that phosphorylation of Hsp27 plays in neurite growth, (3) The effect of Hsp27 on the cytoskeleton.

6.1.1 The Effects of the presence or absence of Hsp27 in neurite initiation and growth.

Exposure of DRG neurons to LN, either through plating on LN or stimulation with soluble LN enhances process formation and neurite outgrowth, compared to neurons plated on a non-permissive substrate alone (Tucker et al., 2006). By stimulating cells with LN for short time periods we were able to observe various distinctive stages in neuronal membrane expansion and neurite growth. Initially a membranous expansion, referred to as a lamellipodium, appears either around the whole soma or a portion thereof. The lamellipodium is filled with an actin meshwork and its formation is driven by actin polymerization; I observed the lamellipodium to stain positive for actin. Small sprouts are then seen to extend from the lamellae as filopodia or nascent processes. These processes appear to either elongate into neurites with the lamellipodium and filopodia remaining as leading growth cones, or retract. Based on the hypothesis that Hsp27 may play a role in process initiation or neurite growth we examined the localization of Hsp27 in various stages of process formation using immunocytochemistry and confocal microscopy. My data shows that Hsp27 and pHsp27^{S15} appear to colocalize with actin and tubulin in structures found at all stages of neurite initiation including lamellipodium, filopodia, focal contacts, neurite shafts, branch points and growth cones (Note that I will be discussing the possible role for phosphorylation of Hsp27 in more detail in section 6.1.2 below). The filamentous nature of Hsp27 was clear in the neurites and growth cones supporting the hypothesis that Hsp27 is associating with cytoskeletal elements. Given the vast literature suggesting a role for Hsp27 in stabilizing the non-neuronal

cytoskeleton, it is possible that one role of Hsp27 is to stabilize the neuronal cytoskeleton at potential sites of branching or sprouting.

These results showed that Hsp27 colocalized with actin and tubulin during various stages of neurite growth, and suggested that Hsp27 was present in a location where it could be playing a role in neurite growth via regulating or interacting with the neuronal cytoskeleton (Williams et al., 2005). To assess further the role of Hsp27 in this process we decreased its expression using siRNA. siRNA directed against a region of Hsp27 effectively depressed Hsp27 protein levels while the levels of actin, tubulin, and NF-L were unaffected. Depletion of Hsp27 protein levels by siRNA resulted in the neurons having less neurite growth and branching relative to cells transfected with control siRNA, indicating that the presence of Hsp27 plays a positive role in neurite growth and extension (Williams et al., 2006). After we published these results, we were posed with the question of how the siRNA affected neurite initiation. We went back and counted the number of cells with and without growth under each condition and were able to show that, not only did the siRNA-induced decrease in Hsp27 protein levels results in decreased neurite growth, but that it also resulted in fewer cells initiating neurites (Figure 6.1).

Having determined that the decrease of Hsp27 protein levels negatively affected neurite growth and branching we transfected the neurons with a construct to express exogenous Hsp27 to look at the effect of increased Hsp27 on these growth parameters. Data from these experiments indicated that the overexpression of Hsp27 resulted in increased neurite growth as well as a more branched neuritic tree. Together these studies

Figure 6.1: Silencing Hsp27 expression by siRNA results in a decrease in neurite initiation. Neurons were transfected with either control or Hsp27 siRNA, plated in 16 well slides coated with PL, allowed to fix overnight and stimulated with LN. 24 h after LN stimulation cells were fixed and immunostained with Hsp27 and tubulin. The percentage of cells with growth was analyzed by counting the number of cells immunostained with tubulin, with and without neurites. Cells treated with siRNA had less cells with neurite growth than control conditions (1000 cells analyzed from each condition).

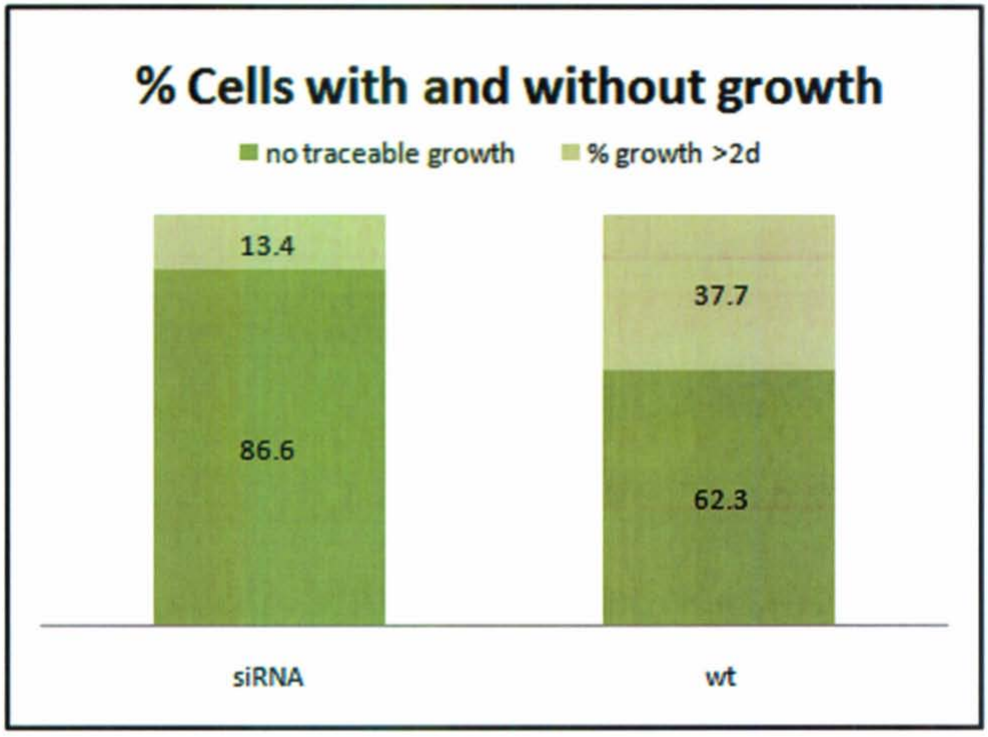
% Cells with and without growth
no traceable growth
% growth >2d
13.4
86.6
37.7
62.3
siRNA
wt

indicate that Hsp27 plays a role in neurite initiation, extension and branching in a manner that is dependent on the level of Hsp27 present in the neuron.

As described earlier the DRG is made up of a heterogeneous population of cells, which can be crudely classified based on cell body diameter, and on their ability to bind the IB4 lectin. Recent studies from the Mearow lab (Tucker et al., 2008) have shown that the different populations of neurons respond to LN on different timescales to initiate neurite growth, with small diameter peptidergic neurons taking longer to put out extensive neuritic networks than large and medium diameter neurons. In order to address the question of whether population diversity was having an impact on my experiments I first looked at whether Hsp27 levels differed between cell populations. Using slices of DRG's I observed that although Hsp27 levels vary from neuron to neuron, there is no specific correlation with neurons from a particular population having higher or lower Hsp27 than the others (Figure 6.2). I next used Image J to determine the size of cell soma used in neurite growth analysis, and determined that the percentage of small cells in each condition was approximately 20%, and that when neurite length was analyzed by size, the small cells (diameter less than 21 μm) displayed less growth than larger cells in the same condition (Figure 6.3). These results correspond to previous data, given that cells were stimulated for 24 h with LN and at that time period there is a difference in growth between small and large cells in the absence of added neurotrophins (e.g., Tucker et al, 2005, 2006, 2008; Tucker and Mearow, 2008). This data suggests that Hsp27 is not having a cell population-specific effect.

Figure 6.2: Expression of Hsp27 in adult DRG cryosections. DRGs were extracted from adult rats, frozen in liquid nitrogen and sectioned into 10 μm thick sections. DRG neurons can be categorized on the basis of their size and the proteins they express/ bind to. Large neurons stain positive for NF200 (A,D), while small cells bind the IB4 lectin (B). Hsp27 expression is not uniform throughout all cells of the DRG (E-F), however the level of expression is not dependant on the size of the cell, and therefore the category which the cell falls into, both large and smaller cells have high and low levels of Hsp27 (D-F). Scale = 50 nm.

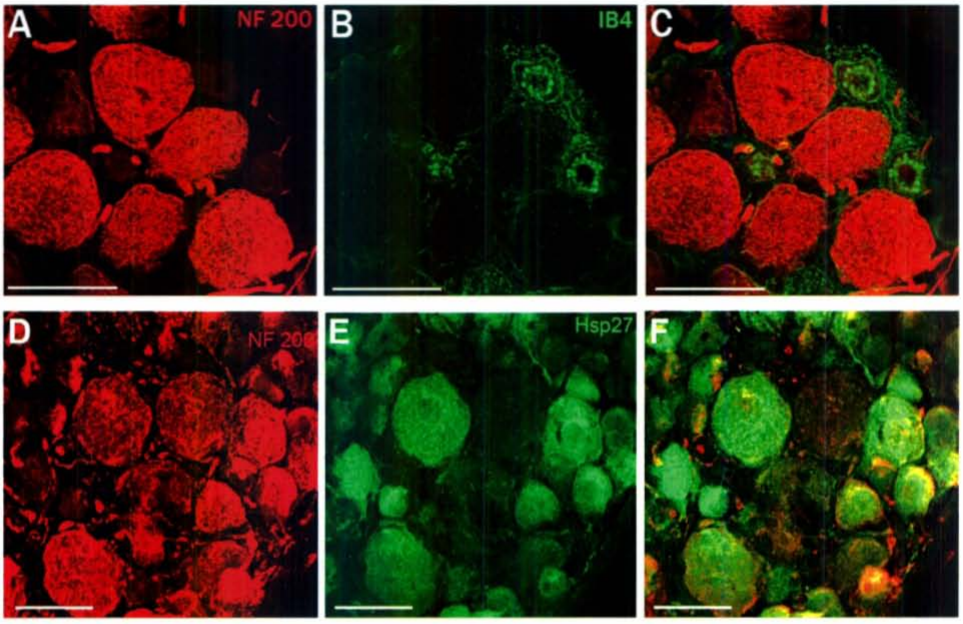
A
NF 200
B
IB4
C
D
E
Hsp27
F

Figure 6.3: Neurite growth is affected by different populations of DRG neurons

The DRG is made up a hetereogeneous population of cells that can be classified on the basis of cell body diameter and the ability of the cell to bind the lectin IB4. Non-peptadergic neurons bind the lectin IB4 and have cell bodies with a small diameter and unmyelinated axons (Averill et al., 1995; Ishikawa et al., 2005; Priestley et al., 2002). In order to classify cells that were stained with Hsp27 and Tubulin as small IB4 positive cells the cell bodies of DRG neurons were stained with IB4 and NF200 were traced. It was found that IB4 positive cells all had a smaller diameter than 21μm, and so the traced cells were separated into two populations: cells with a diameter under 21μm and cells with a diameter greater than 21 μm. DRG neurons were transfected with Hsp27-siRNA or a control scramble-siRNA, plated on polylysine, allowed to attach overnight then stimulated with soluble laminin for 24 h. Following fixation, neurons were immunostained with antibodies directed against Hsp27 and Tubulin and imaged using confocal microscopy. Neurite initiation and growth were assessed by the tubulin stained cells being individually traced using Image J to obtain cell body size and the length of neurites. Under both control and siRNA conditions the small cells have decreased neurite length compared to that of the large transfected cells. Additionally the large siRNA cells have less growth than large control cells, and the small siRNA cells have less growth than the control small cells. Signifigance was tested using T-test $*p<0.05$.

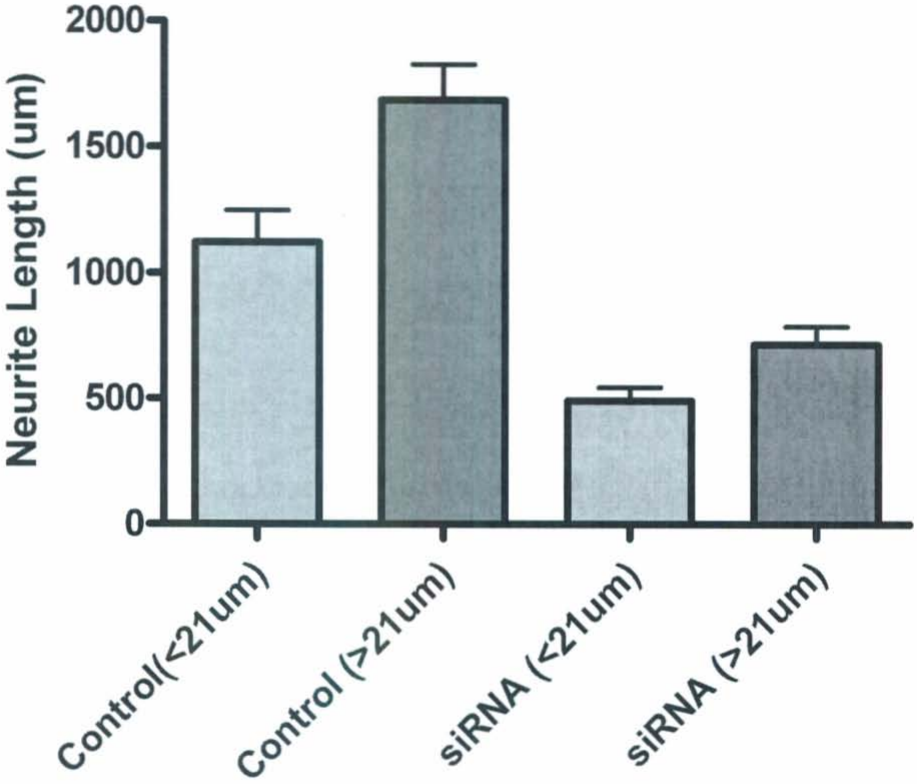
Neurite Length (um)
2000
1500
1000
500
0
Control(<21um)
Control (>21um)
siRNA (<21um)
siRNA (>21um)

Figure 6.4: ClustalW alignment of rat and hamster Hsp27

ClustalW alignment of rat Hsp27 (accession number NM_031970.3) and hamster Hsp27 (accession number X51747). The Hsp27 siRNA construct has been individually aligned against the hamster and rat Hsp27 sequences and an astrix indicates the nucleotides that are not complementary between the siRNA constructs and the hamster sequence. Hsp27 domains and phosphorylation sites have been identified within the sequences, the WDPF domain is outlined in orange, the alpha-crystallin in blue and the phosphorylatable serines indicated in green.

6.1.2 The role that phosphorylation of Hsp27 plays in neurite growth

I employed two distinct methods to elucidate the role that Hsp27 phosphorylation plays in neurite growth. Initially through pharmacological inhibition of upstream p38 MAPK I was able to attenuate the phosphorylation of Hsp27 at the S15 and S86 sites. This was based on the rationale that p38 MAPK activity leads to the phosphorylation and activation of MKK2, which acts as an Hsp27 kinase (Huot et al., 1995; Larsen et al., 1997). In addition to the attenuation of Hsp27 phosphorylation, use of p38 MAPK inhibitors resulted in aberrant neurite growth similar to cells treated with cytochalasin D, supporting a role for Hsp27 in neurite growth through regulation of the actin cytoskeleton.

To elucidate further the role of Hsp27 phosphorylation in neurite growth, specifically the role of individual phosphorylation sites in Hsp27, I used mutant Hsp27 constructs and a co-transfection model where adult rat DRG neurons were transfected with rat specific Hsp27-siRNA to decrease endogenous Hsp27 protein levels, as well as a plasmid containing either wild type or mutated Hamster Hsp27 resulting in overexpression of the hamster Hsp27 (Figure 6.4). In order to investigate the role of specific phosphorylation sites I used hamster Hsp27 constructs that had the S15 and S90 (corresponds to the S86 site in rat) phosphorylation sites mutated to either Alanine (A) or Glutamic Acid (E) to mimic a constitutively unphosphorylated or constitutively phosphorylated site respectively (Figure 6.5). In addition to the phosphorylation mutants I also used a mutant with a deletion in amino acids 5-23 (Hsp27-Δ5-23) that results in the removal of the WDPF domain, as well as the S15 phosphorylation site. This domain, as

```
ratHsp27        ATGACCGAGCGCCGCGTGCCCTTCTCGCTACTGCGGAGCCCCAGCTGGGAGCCGTTCCGG 60
HamsterHsp27    ATGACCGAGCGCCGCGTGCCCTTCTCGCTGCTGCGGAGCCCCAGCTGGGAACCATTCCGG 60

ratHsp27        GACTGGTACCCTGCCCACAGCCGCCTCTTCGATCAAGCTTTCGGGGTGCCTCGGTTTCCC 120
HamsterHsp27    GACTGGTACCCGGCCCACAGCCGCCTCTTCGACCAAGCCTTCGGGGTGCCCCGCTTGCCG 120

ratHsp27        GATGAGTGGTCTCAGTGGTTCAGCTCCGCTGGTTGGCCCGGCTATGTGCGCCCTCTGCCC 180
HamsterHsp27    GATGAGTGGTCGCAGTGGTTCAGCGCCGCTGGTTGGCCCGGCTACGTGCGCCCACTGCCC 180
siRNA              GAGUGGUCUCAGUGGUUCA
                          *
ratHsp27        GCCGCGACCGCCGAGGGCCCCGCAGCAGTGACCCTGGCC-------CGGCCG-------- 225
HamsterHsp27    GCCGCGACCGCCGAGGGACCCGCGGCGGTGGCCCTGGCCGCGCCCCTGGCCGCGCCCGCC 240

ratHsp27        TTCAGCCGGGCGCTCAACCGGCAACTCAGCAGCGGTGTGTCAGAGATCCGACAGACGGCC 285
HamsterHsp27    TTCCACCGTGCGCTCAACCGGCAGCTGAGCAGCGGAGTCTCGGAGATCCGGCAGACGGCC 300

ratHsp27        GATCGCTGGCGCGTGTCCCTGGACGTCAACCACTTCGCTCCTGAGGAGCTCACAGTGAAG 345
HamsterHsp27    GATCGCTGGCGCGTGTCCCTGGACGTCAACCACTTCGCTCCGGAGGAGCTCACGGTCAAG 360

ratHsp27        ACCAAGGAAGGCGTGGTGGAGATCACTGGCAAGCACGAAGAAAGGCAGGATGAACATGGC 405
HamsterHsp27    ACCAAGGAAGGCGTGGTGGAGATCACCGGCAAGCACGAAGAAAGGCAGGACGAACATGGC 420

ratHsp27        TACATCTCTCGGTGCTTCACCCGGAAATACACGCTCCCTCCAGGTGTGGACCCCACCTTG 465
HamsterHsp27    TACATCTCCCGGTGCTTTACCCGGAAATACACGCTGCCTCCCGGTGTGGACCCCACCCTG 480

ratHsp27        GTGTCCTCTTCCCTGTCCCCTGAGGGCACACTCACGGTGGAGGCTCCGCTGCCCAAAGCA 525
HamsterHsp27    GTGTCCTCTTCCCTGTCCCCTGAGGGCACACTTACCGTGGAGGCTCCGCTGCCCAAAACA 540

ratHsp27        GTCACACAATCAGCGGAGATCACCATTCCGGTCACTTTCGAGGCCCGTGCCCAAATTGGA 585
HamsterHsp27    GCCACACAATCCGCGGAGATCACCATTCCGGTCACTTTCGAGGCCCGCGCCCAAATTGGG 600

ratHsp27        GGCCCAGA----------GTCGGAACAGTCTGGAGCCAAGTAG 618
HamsterHsp27    GGCCAGGAAGCTGGGAAGTCGGAACAGTCTGGAGCCAAGTAG 642
```

Figure 6.5: Diagram of wild type, phosphorylation mutants, and deletion mutant hamster Hsp27. The WDPF domain is outlined in orange, the alpha crystallin in blue and the phosphorylatable serines indicated in green. For the Hsp27 phosphorylation mutants, where the serine site has been mutated to a nonphosphorylatable alanine, the site is shown in brown, and where the serine site has been mutated to a glutamic acid mimicking constitutive phosphorylation the site is shown in blue.

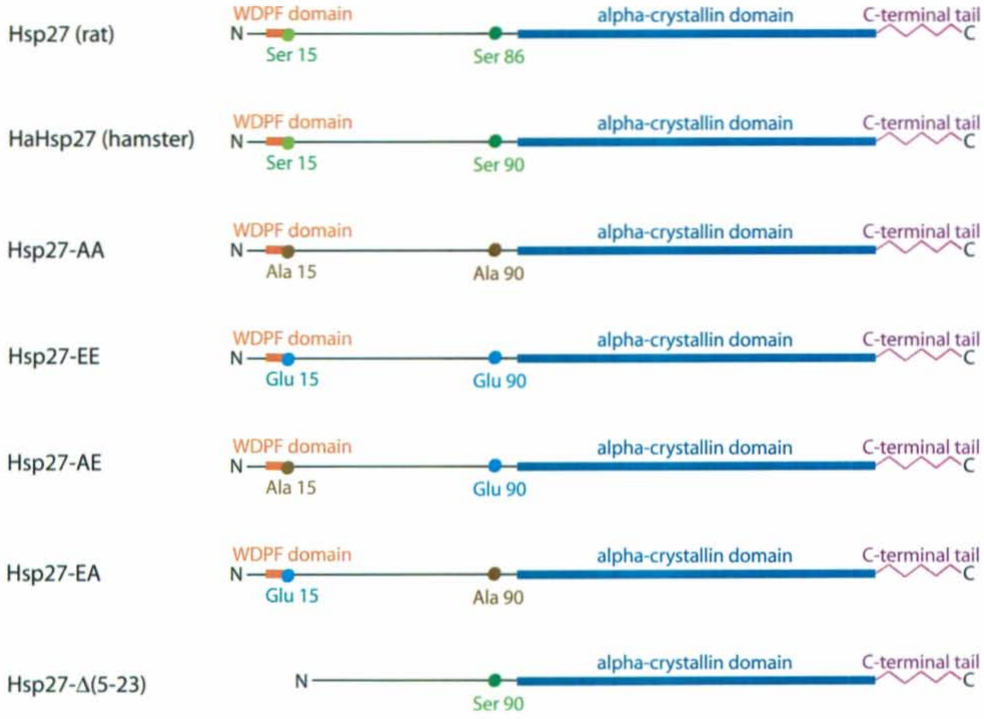
Hsp27 (rat)
WDPF domain
alpha-crystallin domain
C-terminal tail
N
C
Ser 15
Ser 86
HaHsp27 (hamster)
WDPF domain
alpha-crystallin domain
C-terminal tail
N
C
Ser 15
Ser 90
Hsp27-AA
WDPF domain
alpha-crystallin domain
C-terminal tail
N
C
Ala 15
Ala 90
Hsp27-EE
WDPF domain
alpha-crystallin domain
C-terminal tail
N
C
Glu 15
Glu 90
Hsp27-AE
WDPF domain
alpha-crystallin domain
C-terminal tail
N
C
Ala 15
Glu 90
Hsp27-EA
WDPF domain
alpha-crystallin domain
C-terminal tail
N
C
Glu 15
Ala 90
Hsp27-Δ(5-23)
alpha-crystallin domain
C-terminal tail
N
C
Ser 90

as well as the phosphorylation state of the protein, have been shown to be involved in the stability of the oligomeric structure. As previously described and illustrated in Figure 6.6, the phosphorylation status of the Hsp27 mutant constructs have been reported to influence the oligomeric structure such that non-phosphorylated Hsp27 exists preferentially as oligomers, but also as dimers and monomers, phosphorylation on the S90 site results in the dissociation of oligomers into dimers, and phosphorylation on the S15 site, results in the dissociation of oligomers and dimers into monomers (Figure 6.6).

I hypothesized that expression of the constitutively unphosphorylated Hsp27 (Hsp27-AA) would result in aberrant growth similar to treatment with SB203580. Hsp27-AA did result in an altered growth patterning relative to control conditions, although this patterning was not as drastically aberrant as we had previously observed with SB203580 treatment, and was able to rescue neurite extension to the level of wild type Hsp27. The difference in growth patterning between cells treated with SB 203580 and those expressing Hsp27-AA may be accounted for by considering low levels of endogenous wild type Hsp27 being present in cells expressing Hsp27-AA or alternatively the SB is affecting other proteins (e.g., NFs) phosphorylated by p38. Expression of Hsp27-Δ5-23 was able to rescue total neurite extension and growth patterning to the extent of wild type Hsp27, indicating that not only is phosphorylation of the S15 site not required for neurite growth, but that the physical presence of the phosphorylation site and WDPF doman is also not required. This also suggests that the ability of Hsp27 subunits to form large oligomers is not required for neurite growth, but does suggest that the ability of Hsp27 to form dimers is required for its positive effect on neurite growth.

Figure 6.6: Hsp27 phosphorylation mutants affect oligomerizaton. A. Hsp27 is phosphorylated through the classical stress activated P38MAPK, MAPKap Kinase 2 (MKK2) pathway. In its unphosphorylated state Hsp27 is found as monomers, dimers and additionally is able to form large oligomers. Hsp27 oligomers dissociate into dimers upon phosphorylation of the serine 86 site(serine 90 in hamster) and into monomers upon phosphorylation of the serine 15 site. **B.** The Hsp27-AA mutant, cannot be phosphorylated, and therefore is preferentially found as large oligomers, and is unable to dissociate into dimers and monomers via phosphorylation in response to MKK2 signaling. **C.** The Hsp27-EE mutant, contains glutamic acid amino acids in place of its phosphorylatable serines. Glutamic acid has a large negative charge and mimics phosphorylation resulting in Hsp27-EE being preferentially found as monomers. **D.** Hsp27-AE – mimics Hsp27 that is phsophoylated only on its serine 90 site and forms dimers. **E.** Hsp27-EA mimics Hsp27 that is phosphorylated at its serine 15 site and is preferentially found as monomers. **F.** Hsp27-Δ(5-23) is missing the entire WDPF domain including the serine 15 site. Interactions between the WDPF domain and the α-crystallin domain are required for the association of Hsp27 dimers into oligomers, and therefore the deletion mutant will be found as dimers and monomers.

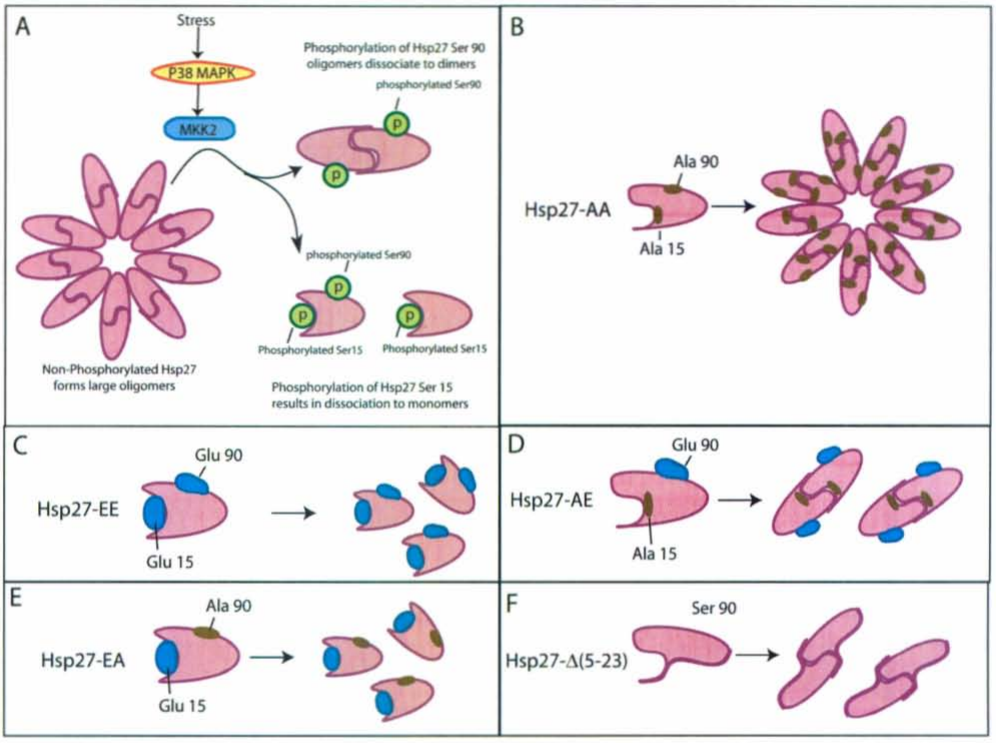
A
Stress
P38 MAPK
MKK2
Phosphorylation of Hsp27 Ser 90 oligomers dissociate to dimers
phosphorylated Ser90
P
phosphorylated Ser90
Phosphorylated Ser15
Phosphorylated Ser15
Non-Phosphorylated Hsp27 forms large oligomers
Phosphorylation of Hsp27 Ser 15 results in dissociation to monomers
B
Hsp27-AA
Ala 90
Ala 15
C
Hsp27-EE
Glu 90
Glu 15
D
Hsp27-AE
Glu 90
Ala 15
E
Hsp27-EA
Ala 90
Glu 15
F
Hsp27-Δ(5-23)
Ser 90

Constitutive phosphorylation at the S15 site (Hsp27-EE or Hsp27-EA) prevented rescue of the siRNA decreased growth. Additionally expression of Hsp27 with constitutive phosphorylation at the S90 site (Hsp27-AE) was able to rescue growth that was significantly greater than that of siRNA alone, but significantly less that wild type Hsp27. These studies indicate that phosphorylation of either the S15 or S90 site is inhibitory to neurite extension, with the S15 site having a stronger inhibitory effect.

6.1.3 The effect of Hsp27 on the cytoskeleton.

As was outlined earlier Hsp27 has been found to interact with different cytoskeletal elements (Benndorf and Welsh, 2004; Charette et al., 2000; Evgrafov et al., 2004; Guay et al., 1997; Huot et al., 1996; Lavoie et al., 1993a; Lavoie et al., 1995; Perng et al., 1999a). I was primarily interested in its interactions with actin, tubulin and neurofilament due to their potential role in neurite growth.

Hsp27 has been shown to play a role in regulating the actin cytoskeleton of non-neuronal cells though both direct binding to actin and indirect signaling cascades leading to actin binding proteins (During et al., 2007; Gehler et al., 2004; Jia et al., 2009; Loudon et al., 2006; Miron et al., 1991; Pichon et al., 2004; Vertii et al., 2006). Our results suggest a role for both of these mechanisms being involved in Hsp27 regulating or interacting with the actin cytoskeleton of neuronal cells.

Knowing that phosphorylation of Hsp27 had an effect on neurite growth I investigated what affect this had on the actin cytoskeleton. I initially observed that attenuation of Hsp27 phosphorylation via upstream pharmacological inhibition of p38

MAPK resulted in aberrant growth similar to growth seen with cytochalasin D treatment. Using a commercially available kit and protocol, I isolated F-actin and G-actin fractions from the cells, and showed that the F-actin/G-actin ratio was increased in cells treated with SB, suggesting that inhibition of Hsp27 phosphorylation alters the balance of F-actin/G-actin in the neuron. Given that an increase in F-actin with attenuation of Hsp27 phosphorylation is contrary to direct binding results seen in non-neuronal cells, I hypothesized that Hsp27 may be affecting the actin cytoskeleton through an indirect signaling pathway, possibly through cofilin or Rho, although no effect on cofillin phosphorylation was observed using western blotting (data not shown).

I next sought to determine the effect of the Hsp27 phosphorylation mutants on the actin cytoskeleton. However due to the low transfection efficiency of the mutant constructs it was not practical to carry out the biochemical studies in order to observe any effects on protein signaling or changes in the F-actin/ G-actin ratio. I was, however, able to observe the colocalization of F-actin and Hsp27 in the cells through immunocytochemistry and cell labeling. In these experiments I observed that nonphosphorylatable Hsp27 (Hsp27-AA) displayed a strong colocalization with F-actin in filopodia and focal contacts in early stages of neurite initiation and growth cones of mature neurites: these results potentially support a direct binding mechanism for actin and Hsp27 in neurons where non-phosphorylated Hsp27 binds to actin to cap it (Lavoie et al., 1993b; Pichon et al., 2004). Additionally Hsp27 with a constitutively phosphorylated S15 site (Hsp27-EE or Hsp27-EA) displayed large amounts of membrane protrusion, including high levels of filopodia and nascent processes in growth structures and neurite

shafts of mature neurites. Although the amount of protrusion was not quantified, its presence may explain why Hsp27-EE and Hsp27-EA expressing cells have lower neurite extension than cells expressing HaHsp27. Cells transfected with Hsp27-AE display lower amounts of F-actin than cells expressing Hsp27 wild type and or the other mutants. One possible explanation is that phosphorylation of S15 may be involved in stabilizing the actin cytoskeleton (possibly by increasing filament levels and preventing their degradation), while phosphorylation at the S90 site may be involved in destabilizing the actin cytoskeleton, and that the involvement of the S15 site overpowers that of the S90 site, such that where there is phosphorylation of both sites (Hsp27-EE) the stabilizing function overpowers the destabilizing function. Stabilization of the F-actin cytoskeleton results in an increase in F-actin and membrane protrusion, that is necessary for neurite initiation and growth. It is possible that the different phosphorylation sites act through different mechanisms, and that this has not yet been observed because the availability of phosphorylation specific antibodies has been poor until recently. However, overall, these results support my hypothesis that Hsp27 is involved in neurite growth via regulation of the actin cytoskeleton.

Although a direct interaction between Hsp27 and actin has been reported I was unable to observe any direct interaction though biochemical techniques. I employed the following techniques without any success: immunoprecipitation of both Hsp27 and actin, GST- pull down using a GST::Hsp27 construct, or treatment of cells with gluteraldehyde (for protein crosslinking) and subsequent immunoprecipitation (data not shown). These

results might indicate that if there is a direct interaction between Hsp27 and actin in neurons that it is transient and/or not very strong.

I was also interested in whether Hsp27 interacted with tubulin in the neuron, and although initial colocalization studies suggested that Hsp27 colocalized with tubulin in neuronal processes throughout the stages of neurite initiation and growth, I was unable to find any further support for the interactions between Hsp27 and tubulin using the methods noted above. When Hsp27 location was altered by Hsp27 siRNA induced Hsp27 protein depletion or expression of Hsp27 phosphorylation mutants, the total tubulin localization within the cell appeared to remain unchanged. Additionally depletion of Hsp27 protein levels did not affect the level of post-translational modifications of tubulin (acetylation and tyrosination) as detected by immunoblotting, and immunoprecipitation of Hsp27 was unable to pull down tubulin (data not shown).

Studies have shown interactions between Hsp27 and NF-L, with recent developments suggesting a role for Hsp27 in NF-L stabilization (Ackerley et al., 2006; Evgrafov et al., 2004; Zhai et al., 2007). My results showed that depletion of Hsp27 protein by siRNA did not significantly alter NF-L protein expression within the DRG neuron, and additionally did not alter the ability of NF-L to bind to itself or NF-200 (Figure 6.7). These results suggest that Hsp27 is not required for formation of the neurofilament structures in neurite initiation and growth in DRG neurons.

Figure 6.7: Immunoprecipitation of Hsp27, NF-L and NF-200.

Neurons were transfected with either control or Hsp27 siRNA, plated in 12 well plates coated with PL, allowed to fix overnight and stimulated with soluble LN. 24 h after LN stimulation protein was collected and protein levels were quantified by BCA protein assay, and subjected to Immunoprecipitation. Briefly, 100 ug of protein were pre-cleared by being incubated with 30 μL of agarose A and G beads. The supernatant was washed with pre-lysis buffer and incubated with 5 uL of antibody for 6 h. Three antibodies were used Hsp27, NF-L, and NF-200. After 6 h, 30 μL of agarose A/G beads was added and the mix was rotated at 4°C overnight (~16 h). The supernatant was removed and discarded and the pellets were washed with lysis buffer. The remaining pellet was boiled with loading buffer and subjected to SDS PAGE, and immunoblotting along with a samples of the protein used for the immunoprecipitation. The control protein showed that Hsp27 protein levels were decreased under the Hsp27-siRNA condition, and that NF-L and NF-200 protein levels were unaffected by the Hsp27-siRNA. Immunoprecipitation with the Hsp27 antibody was unable to pull down any visible amount of Hsp27 under siRNA conditions, but was able to pull down Hsp27 in control conditions. The Hsp27 antibody was unable to co-immunoprecipitate NF-L or NF-200. Under both the siRNA and control conditions the NF-L antibody, pulled down NF-L and NF-200 protein. Conversely the NF-200 antibody pulled down the NF-200 and NF-L protein under both siRNA and control conditions as well. This indicates that Hsp27 does not have strong interactions with NF-L or NF-200. Additionally depletion of Hsp27 protein by siRNA does not affect the ability of NF-L and NF-200 to interact.

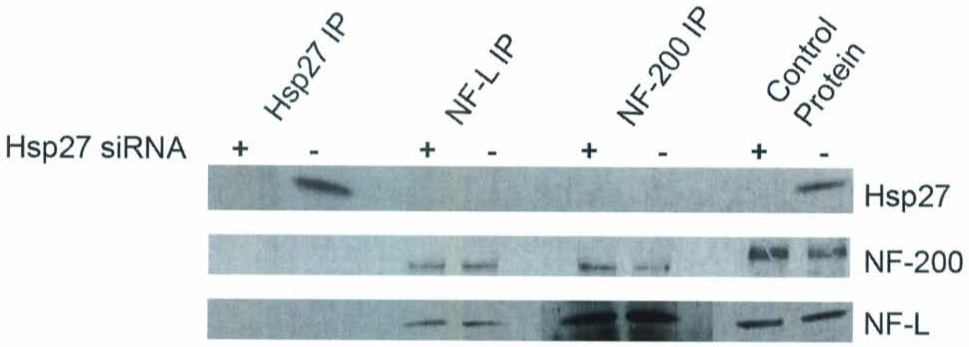
Hsp27 IP
NF-L IP
NF-200 IP
Control Protein
Hsp27 siRNA
+ - + - + - + -
Hsp27
NF-200
NF-L

6.2 Future Directions

Although I have demonstrated that Hsp27 plays a role in neurite initiation and growth, and that this is dependent on the level of Hsp27 and its phosphorylation state, many questions still remain on the mechanisms behind these effects. I will briefly discuss five lines of work that I see as being important to advance this area.

(1) I have shown that Hsp27 plays a role in neurite initiation and growth that appears to be via regulation of the actin cytoskeleton. I have suggested that some of these interactions may be through indirect signaling pathways, as well as though the ability of Hsp27 to bind directly to actin. My data from upstream pharmacological inhibition of Hsp27 phosphorylation suggests that Hsp27 phosphorylation affects actin dynamics through an indirect signaling pathway. In order to understand fully the mechanisms behind the effect of Hsp27 on neurite growth, the signaling pathways that are involved in this process must be elucidated. These pathways may be studied by western blotting of cells transfected with Hsp27 phosphorylation mutants, although in order for this technique to be effective transfection efficiencies of the mutant constructs must be improved. Transfection of the plasmid (pIRES2-EGFP) containing the Hsp27 phosphorylation mutants into DRG neurons using the AMAXA nucleoporation system gives a range of transfection efficiencies, with the majority of the mutants having a transfection efficiency of less than 20%. A recent modification of the AMAXA system which allows for small cell numbers to be transfected, as well as a more robust EGFP-IRES construct appears to result in higher efficiencies. In addition, a more efficient

transfection mechanism, such as use of a lentivirus, would permit the effect of Hsp27 phosphorylation on signaling intermediates to be studied. Additionally better transfection efficiencies would permit the use of a commercial kit to identify an impact on F-actin / G actin ratios.

(2) The studies in chapter 4 demonstrate the importance of phosphorylation of particular Hsp27 phosphorylation sites in neurite growth. Further analysis of the role that individual sites are playing in this process could be identified with the use of single phosphorylation site mutations (SA, AS, SE, ES). Such studies would also benefit from the knowledge of whether different signaling pathways are responsible for the phosphorylation of Hsp27 at different sites.

(3) Studies using the Hsp27 phosphorylation mutants in chapter 4, suggest that Hsp27 phosphorylation alters neurite growth via regulation of the actin cytoskeleton. If this interaction is due to Hsp27 having an effect on the stabilization or destabilization of the actin cytoskeleton, an interesting study would be whether treatment of the cells with compounds to promote or inhibit actin polymerization, such as jasplakinolide - a cell membrane permeable promoter of actin filament polymerization (Bubb et al., 1994), latrunculin A – binds actin monomers – preventing their addition to the actin filament (Morton et al., 2000), or cytochalasin D – binds the barbed end of actin filaments promoting the depolymerization of actin filaments (Cooper, 1987), would reverse the growth effects of the Hsp27 phosphorylation mutants.

(4) Hsp27 is known to interact directly with actin filaments in non-neuronal cells, although I was unsuccessful using biochemical pull-down techniques to see an interaction between Hsp27 and actin, it is possible that an *in vivo* technique such as FRET could be used to see interactions between Hsp27, actin and possibly other cytoskeletal elements. Such a technique would allow for the location of such interactions to be studied and would assist in elucidating the role of Hsp27 in neurite growth.

(5) Mutations in Hsp27 have been identified in CMT and dHMN, one of which is involved in stabilization of the NFL network (Zhai et al., 2007). Additionally co-expression of wild-type Hsp27 and mutant (CMT) NFL diminishes the aggregation of the mutant NFL. These studies further explain the role for Hsp27 with cytoskeletal proteins other than actin in neurite growth processes. The present study clearly demonstrates the importance of Hsp27 protein levels and phosphorylation state in neurite growth processes. It seems as if the study of Hsp27 in this process has only just begun and it is hoped that experiments presented in this thesis can provide a basis for further understanding the nteractions of Hsp27 with actin, as well as the process of neurite initiation and growth.

References

Ackerley, S., Grierson, A.J., Banner, S., Perkinton, M.S., Brownlees, J., Byers, H.L., Ward, M., Thornhill, P., Hussain, K., Waby, J.S., *et al.* (2004). p38alpha stress-activated protein kinase phosphorylates neurofilaments and is associated with neurofilament pathology in amyotrophic lateral sclerosis. Mol Cell Neurosci *26*, 354-364.

Ackerley, S., James, P.A., Kalli, A., French, S., Davies, K.E., and Talbot, K. (2006). A mutation in the small heat-shock protein HSPB1 leading to distal hereditary motor neuronopathy disrupts neurofilament assembly and the axonal transport of specific cellular cargoes. Hum Mol Genet *15*, 347-354.

Ackerley, S., Thornhill, P., Grierson, A.J., Brownlees, J., Anderton, B.H., Leigh, P.N., Shaw, C.E., and Miller, C.C. (2003). Neurofilament heavy chain side arm phosphorylation regulates axonal transport of neurofilaments. J Cell Biol *161*, 489-495.

Aletta, J.M., Angeletti, R., Liem, R.K., Purcell, C., Shelanski, M.L., and Greene, L.A. (1988). Relationship between the nerve growth factor-regulated clone 73 gene product and the 58-kilodalton neuronal intermediate filament protein (peripherin). J Neurochem *51*, 1317-1320.

Aletta, J.M., and Greene, L.A. (1988). Growth cone configuration and advance: a time-lapse study using video-enhanced differential interference contrast microscopy. J Neurosci *8*, 1425-1435.

Aletta, J.M., Shelanski, M.L., and Greene, L.A. (1989). Phosphorylation of the peripherin 58-kDa neuronal intermediate filament protein. Regulation by nerve growth factor and other agents. J Biol Chem *264*, 4619-4627.

Amano, M., Chihara, K., Kimura, K., Fukata, Y., Nakamura, N., Matsuura, Y., and Kaibuchi, K. (1997). Formation of actin stress fibers and focal adhesions enhanced by Rho-kinase. Science *275*, 1308-1311.

Amaratunga, A., Morin, P.J., Kosik, K.S., and Fine, R.E. (1993). Inhibition of kinesin synthesis and rapid anterograde axonal transport in vivo by an antisense oligonucleotide. J Biol Chem *268*, 17427-17430.

Amos, L.A. (2000). Focusing-in on microtubules. Curr Opin Struct Biol *10*, 236-241.

An, S.S., Fabry, B., Mellema, M., Bursac, P., Gerthoffer, W.T., Kayyali, U.S., Gaestel, M., Shore, S.A., and Fredberg, J.J. (2004). Role of heat shock protein 27 in cytoskeletal remodeling of the airway smooth muscle cell. J Appl Physiol *96*, 1701-1713.

Aquino, D.A., Padin, C., Perez, J.M., Peng, D., Lyman, W.D., and Chiu, F.C. (1996). Analysis of glial fibrillary acidic protein, neurofilament protein, actin and heat shock proteins in human fetal brain during the second trimester. Brain Res Dev Brain Res *91*, 1-10.

Arrigo, A.P. (2007). The cellular "networking" of mammalian Hsp27 and its functions in the control of protein folding, redox state and apoptosis. Adv Exp Med Biol *594*, 14-26.

Arrigo, A.P., Firdaus, W.J., Mellier, G., Moulin, M., Paul, C., Diaz-Latoud, C., and Kretz-Remy, C. (2005). Cytotoxic effects induced by oxidative stress in cultured mammalian cells and protection provided by Hsp27 expression. Methods *35*, 126-138.

Averill, S., McMahon, S.B., Clary, D.O., Reichardt, L.F., and Priestley, J.V. (1995). Immunocytochemical localization of trkA receptors in chemically identified subgroups of adult rat sensory neurons. Eur J Neurosci *7*, 1484-1494.

Bamburg, J.R., McGough, A., and Ono, S. (1999). Putting a new twist on actin: ADF/cofilins modulate actin dynamics. Trends Cell Biol *9*, 364-370.

Bard, L., Boscher, C., Lambert, M., Mege, R.M., Choquet, D., and Thoumine, O. (2008). A molecular clutch between the actin flow and N-cadherin adhesions drives growth cone migration. J Neurosci *28*, 5879-5890.

Baum, P.D., and Garriga, G. (1997). Neuronal migrations and axon fasciculation are disrupted in ina-1 integrin mutants. Neuron *19*, 51-62.

Bausero, M.A., Bharti, A., Page, D.T., Perez, K.D., Eng, J.W., Ordonez, S.L., Asea, E.E., Jantschitsch, C., Kindas-Muegge, I., Ciocca, D., and Asea, A. (2006). Silencing the hsp25 gene eliminates migration capability of the highly metastatic murine 4T1 breast adenocarcinoma cell. Tumour Biol *27*, 17-26.

Bear, J.E., Svitkina, T.M., Krause, M., Schafer, D.A., Loureiro, J.J., Strasser, G.A., Maly, I.V., Chaga, O.Y., Cooper, J.A., Borisy, G.G., and Gertler, F.B. (2002). Antagonism between Ena/VASP proteins and actin filament capping regulates fibroblast motility. Cell *109*, 509-521.

Belmont, L., Mitchison, T., and Deacon, H.W. (1996). Catastrophic revelations about Op18/stathmin. Trends Biochem Sci *21*, 197-198.

Benn, S.C., Perrelet, D., Kato, A.C., Scholz, J., Decosterd, I., Mannion, R.J., Bakowska, J.C., and Woolf, C.J. (2002). Hsp27 upregulation and phosphorylation is required for injured sensory and motor neuron survival. Neuron *36*, 45-56.

Benndorf, R., Hayess, K., Ryazantsev, S., Wieske, M., Behlke, J., and Lutsch, G. (1994). Phosphorylation and supramolecular organization of murine small heat shock protein HSP25 abolish its actin polymerization-inhibiting activity. J Biol Chem *269*, 20780-20784.

Benndorf, R., and Welsh, M.J. (2004). Shocking degeneration. Nat Genet *36*, 547-548.

Bennett, D.L., Michael, G.J., Ramachandran, N., Munson, J.B., Averill, S., Yan, Q., McMahon, S.B., and Priestley, J.V. (1998). A distinct subgroup of small DRG cells express GDNF receptor

components and GDNF is protective for these neurons after nerve injury. J Neurosci *18*, 3059-3072.

Bennett, V., and Baines, A.J. (2001). Spectrin and ankyrin-based pathways: metazoan inventions for integrating cells into tissues. Physiol Rev *81*, 1353-1392.

Bitar, K.N., Ibitayo, A., and Patil, S.B. (2002). HSP27 modulates agonist-induced association of translocated RhoA and PKC-alpha in muscle cells of the colon. J Appl Physiol *92*, 41-49.

Bitar, K.N., Kaminski, M.S., Hailat, N., Cease, K.B., and Strahler, J.R. (1991). Hsp27 is a mediator of sustained smooth muscle contraction in response to bombesin. Biochem Biophys Res Commun *181*, 1192-1200.

Bohil, A.B., Robertson, B.W., and Cheney, R.E. (2006). Myosin-X is a molecular motor that functions in filopodia formation. Proc Natl Acad Sci U S A *103*, 12411-12416.

Bova, M.P., McHaourab, H.S., Han, Y., and Fung, B.K. (2000). Subunit exchange of small heat shock proteins. Analysis of oligomer formation of alphaA-crystallin and Hsp27 by fluorescence resonance energy transfer and site-directed truncations. J Biol Chem *275*, 1035-1042.

Bova, M.P., Yaron, O., Huang, Q., Ding, L., Haley, D.A., Stewart, P.L., and Horwitz, J. (1999). Mutation R120G in alphaB-crystallin, which is linked to a desmin-related myopathy, results in an irregular structure and defective chaperone-like function. Proc Natl Acad Sci U S A *96*, 6137-6142.

Bradke, F., and Dotti, C.G. (1999). The role of local actin instability in axon formation. Science *283*, 1931-1934.

Bray, D., and Chapman, K. (1985). Analysis of microspike movements on the neuronal growth cone. J Neurosci *5*, 3204-3213.

Brophy, C.M., Woodrum, D., Dickinson, M., and Beall, A. (1998). Thrombin activates MAPKAP2 kinase in vascular smooth muscle. J Vasc Surg *27*, 963-969.

Brose, K., and Tessier-Lavigne, M. (2000). Slit proteins: key regulators of axon guidance, axonal branching, and cell migration. Curr Opin Neurobiol *10*, 95-102.

Brown, A., Li, Y., Slaughter, T., and Black, M.M. (1993). Composite microtubules of the axon: quantitative analysis of tyrosinated and acetylated tubulin along individual axonal microtubules. J Cell Sci *104 (Pt 2)*, 339-352.

Bruey, J.M., Ducasse, C., Bonniaud, P., Ravagnan, L., Susin, S.A., Diaz-Latoud, C., Gurbuxani, S., Arrigo, A.P., Kroemer, G., Solary, E., and Garrido, C. (2000a). Hsp27 negatively regulates cell death by interacting with cytochrome c. Nat Cell Biol *2*, 645-652.

Bruey, J.M., Paul, C., Fromentin, A., Hilpert, S., Arrigo, A.P., Solary, E., and Garrido, C. (2000b). Differential regulation of HSP27 oligomerization in tumor cells grown in vitro and in vivo. Oncogene *19*, 4855-4863.

Bubb, M.R., Senderowicz, A.M., Sausville, E.A., Duncan, K.L., and Korn, E.D. (1994). Jasplakinolide, a cytotoxic natural product, induces actin polymerization and competitively inhibits the binding of phalloidin to F-actin. J Biol Chem *269*, 14869-14871.

Bulinski, J.C. (2007). Microtubule modification: acetylation speeds anterograde traffic flow. Curr Biol *17*, R18-20.

Butt, E., Immler, D., Meyer, H.E., Kotlyarov, A., Laass, K., and Gaestel, M. (2001). Heat shock protein 27 is a substrate of cGMP-dependent protein kinase in intact human platelets: phosphorylation-induced actin polymerization caused by HSP27 mutants. J Biol Chem *276*, 7108-7113.

Cafferty, W.B., Yang, S.H., Duffy, P.J., Li, S., and Strittmatter, S.M. (2007). Functional axonal regeneration through astrocytic scar genetically modified to digest chondroitin sulfate proteoglycans. J Neurosci *27*, 2176-2185.

Cai, D., Qiu, J., Cao, Z., McAtee, M., Bregman, B.S., and Filbin, M.T. (2001). Neuronal cyclic AMP controls the developmental loss in ability of axons to regenerate. J Neurosci *21*, 4731-4739.

Cajal, S.R.y. (1890). A quelle epoque apparaissent les expansions des cellulas nerveuses de la moelle epiniere du poulet? Anatomomischer Anzeiger *21-22*, 609-639.

Cajal, S.R.y. (1928). Degeneration and regeneration of the nervous system. Hafner, New York.

Calderwood, S.K., and Ciocca, D.R. (2008). Heat shock proteins: stress proteins with Janus-like properties in cancer. Int J Hyperthermia *24*, 31-39.

Cao, Z., Gao, Y., Bryson, J.B., Hou, J., Chaudhry, N., Siddiq, M., Martinez, J., Spencer, T., Carmel, J., Hart, R.B., and Filbin, M.T. (2006). The cytokine interleukin-6 is sufficient but not necessary to mimic the peripheral conditioning lesion effect on axonal growth. J Neurosci *26*, 5565-5573.

Carper, S.W., Rocheleau, T.A., Cimino, D., and Storm, F.K. (1997). Heat shock protein 27 stimulates recovery of RNA and protein synthesis following a heat shock. J Cell Biochem *66*, 153-164.

Charette, S.J., Lavoie, J.N., Lambert, H., and Landry, J. (2000). Inhibition of Daxx-mediated apoptosis by heat shock protein 27. Mol Cell Biol *20*, 7602-7612.

Chavez Zobel, A.T., Lambert, H., Theriault, J.R., and Landry, J. (2005). Structural instability caused by a mutation at a conserved arginine in the alpha-crystallin domain of Chinese hamster heat shock protein 27. Cell Stress Chaperones *10*, 157-166.

Chavez Zobel, A.T., Loranger, A., Marceau, N., Theriault, J.R., Lambert, H., and Landry, J. (2003). Distinct chaperone mechanisms can delay the formation of aggresomes by the myopathy-causing R120G alphaB-crystallin mutant. Hum Mol Genet *12*, 1609-1620.

Chen, J., Kanai, Y., Cowan, N.J., and Hirokawa, N. (1992). Projection domains of MAP2 and tau determine spacings between microtubules in dendrites and axons. Nature *360*, 674-677.

Chen, M.S., Huber, A.B., van der Haar, M.E., Frank, M., Schnell, L., Spillmann, A.A., Christ, F., and Schwab, M.E. (2000). Nogo-A is a myelin-associated neurite outgrowth inhibitor and an antigen for monoclonal antibody IN-1. Nature *403*, 434-439.

Choo, Q.L., and Bray, D. (1978). Two forms of neuronal actin. J Neurochem *31*, 217-224.

Clark, E.A., and Brugge, J.S. (1995). Integrins and signal transduction pathways: the road taken. Science *268*, 233-239.

Cochard, P., and Paulin, D. (1984). Initial expression of neurofilaments and vimentin in the central and peripheral nervous system of the mouse embryo in vivo. J Neurosci *4*, 2080-2094.

Cohan, C.S., Welnhofer, E.A., Zhao, L., Matsumura, F., and Yamashiro, S. (2001). Role of the actin bundling protein fascin in growth cone morphogenesis: localization in filopodia and lamellipodia. Cell Motil Cytoskeleton *48*, 109-120.

Concannon, C.G., Gorman, A.M., and Samali, A. (2003). On the role of Hsp27 in regulating apoptosis. Apoptosis *8*, 61-70.

Cooper, J.A. (1987). Effects of cytochalasin and phalloidin on actin. J Cell Biol *105*, 1473-1478.

Cooper, J.A., Buhle, E.L., Jr., Walker, S.B., Tsong, T.Y., and Pollard, T.D. (1983). Kinetic evidence for a monomer activation step in actin polymerization. Biochemistry *22*, 2193-2202.

Cooper, J.A., and Sept, D. (2008). New insights into mechanism and regulation of actin capping protein. Int Rev Cell Mol Biol *267*, 183-206.

Costigan, M., Mannion, R.J., Kendall, G., Lewis, S.E., Campagna, J.A., Coggeshall, R.E., Meridith-Middleton, J., Tate, S., and Woolf, C.J. (1998). Heat shock protein 27: developmental regulation and expression after peripheral nerve injury. J Neurosci *18*, 5891-5900.

Couillard-Despres, S., Zhu, Q., Wong, P.C., Price, D.L., Cleveland, D.W., and Julien, J.P. (1998). Protective effect of neurofilament heavy gene overexpression in motor neuron disease induced by mutant superoxide dismutase. Proc Natl Acad Sci U S A *95*, 9626-9630.

Cuesta, R., Laroia, G., and Schneider, R.J. (2000). Chaperone hsp27 inhibits translation during heat shock by binding eIF4G and facilitating dissociation of cap-initiation complexes. Genes Dev *14*, 1460-1470.

Cunningham, C.C., Stossel, T.P., and Kwiatkowski, D.J. (1991). Enhanced motility in NIH 3T3 fibroblasts that overexpress gelsolin. Science *251*, 1233-1236.

da Silva, J.S., and Dotti, C.G. (2002). Breaking the neuronal sphere: regulation of the actin cytoskeleton in neuritogenesis. Nat Rev Neurosci *3*, 694-704.

Dai, C., Whitesell, L., Rogers, A.B., and Lindquist, S. (2007). Heat shock factor 1 is a powerful multifaceted modifier of carcinogenesis. Cell *130*, 1005-1018.

Dancker, P., Low, I., Hasselbach, W., and Wieland, T. (1975). Interaction of actin with phalloidin: polymerization and stabilization of F-actin. Biochim Biophys Acta *400*, 407-414.

de Graauw, M., Tijdens, I., Cramer, R., Corless, S., Timms, J.F., and van de Water, B. (2005). Heat shock protein 27 is the major differentially phosphorylated protein involved in renal epithelial cellular stress response and controls focal adhesion organization and apoptosis. J Biol Chem *280*, 29885-29898.

de Waegh, S.M., Lee, V.M., and Brady, S.T. (1992). Local modulation of neurofilament phosphorylation, axonal caliber, and slow axonal transport by myelinating Schwann cells. Cell *68*, 451-463.

Dedova, I.V., Nikolaeva, O.P., Safer, D., De La Cruz, E.M., and dos Remedios, C.G. (2006). Thymosin beta4 induces a conformational change in actin monomers. Biophys J *90*, 985-992.

Dehmelt, L., and Halpain, S. (2004). Actin and microtubules in neurite initiation: are MAPs the missing link? J Neurobiol *58*, 18-33.

Dehmelt, L., and Halpain, S. (2005). The MAP2/Tau family of microtubule-associated proteins. Genome Biol *6*, 204.

Dehmelt, L., Smart, F.M., Ozer, R.S., and Halpain, S. (2003). The role of microtubule-associated protein 2c in the reorganization of microtubules and lamellipodia during neurite initiation. J Neurosci *23*, 9479-9490.

Dent, E.W., and Gertler, F.B. (2003). Cytoskeletal dynamics and transport in growth cone motility and axon guidance. Neuron *40*, 209-227.

Dent, E.W., and Kalil, K. (2001). Axon branching requires interactions between dynamic microtubules and actin filaments. J Neurosci *21*, 9757-9769.

Dent, E.W., Kwiatkowski, A.V., Mebane, L.M., Philippar, U., Barzik, M., Rubinson, D.A., Gupton, S., Van Veen, J.E., Furman, C., Zhang, J., *et al.* (2007). Filopodia are required for cortical neurite initiation. Nat Cell Biol *9*, 1347-1359.

Dent, E.W., Tang, F., and Kalil, K. (2003). Axon guidance by growth cones and branches: common cytoskeletal and signaling mechanisms. Neuroscientist *9*, 343-353.

Der Perng, M., and Quinlan, R.A. (2004). Neuronal diseases: small heat shock proteins calm your nerves. Curr Biol *14*, R625-626.

Desai, A., and Mitchison, T.J. (1997). Microtubule polymerization dynamics. Annu Rev Cell Dev Biol *13*, 83-117.

Devor, M. (1999). Unexplained peculiarities of the dorsal root ganglion. Pain *Suppl 6*, S27-35.

Dodge, M.E., Wang, J., Guy, C., Rankin, S., Rahimtula, M., and Mearow, K.M. (2006). Stress-induced heat shock protein 27 expression and its role in dorsal root ganglion neuronal survival. Brain Res *1068*, 34-48.

Dompierre, J.P., Godin, J.D., Charrin, B.C., Cordelieres, F.P., King, S.J., Humbert, S., and Saudou, F. (2007). Histone deacetylase 6 inhibition compensates for the transport deficit in Huntington's disease by increasing tubulin acetylation. J Neurosci *27*, 3571-3583.

Dong, D.L., Xu, Z.S., Chevrier, M.R., Cotter, R.J., Cleveland, D.W., and Hart, G.W. (1993). Glycosylation of mammalian neurofilaments. Localization of multiple O-linked N-acetylglucosamine moieties on neurofilament polypeptides L and M. J Biol Chem *268*, 16679-16687.

Doppler, H., Storz, P., Li, J., Comb, M.J., and Toker, A. (2005). A phosphorylation state-specific antibody recognizes Hsp27, a novel substrate of protein kinase D. J Biol Chem *280*, 15013-15019.

Doshi, B.M., Hightower, L.E., and Lee, J. (2009). The role of Hsp27 and actin in the regulation of movement in human cancer cells responding to heat shock. Cell Stress Chaperones *14*, 445-457.

During, R.L., Gibson, B.G., Li, W., Bishai, E.A., Sidhu, G.S., Landry, J., and Southwick, F.S. (2007). Anthrax lethal toxin paralyzes actin-based motility by blocking Hsp27 phosphorylation. EMBO J *26*, 2240-2250.

Ehrnsperger, M., Graber, S., Gaestel, M., and Buchner, J. (1997). Binding of non-native protein to Hsp25 during heat shock creates a reservoir of folding intermediates for reactivation. EMBO J *16*, 221-229.

Ellezam, B., Dubreuil, C., Winton, M., Loy, L., Dergham, P., Selles-Navarro, I., and McKerracher, L. (2002). Inactivation of intracellular Rho to stimulate axon growth and regeneration. Prog Brain Res *137*, 371-380.

Ellis, J. (1987). Proteins as molecular chaperones. Nature *328*, 378-379.

Erck, C., Peris, L., Andrieux, A., Meissirel, C., Gruber, A.D., Vernet, M., Schweitzer, A., Saoudi, Y., Pointu, H., Bosc, C., *et al.* (2005). A vital role of tubulin-tyrosine-ligase for neuronal organization. Proc Natl Acad Sci U S A *102*, 7853-7858.

Erturk, A., Hellal, F., Enes, J., and Bradke, F. (2007). Disorganized microtubules underlie the formation of retraction bulbs and the failure of axonal regeneration. J Neurosci *27*, 9169-9180.

Etienne-Manneville, S., and Hall, A. (2002). Rho GTPases in cell biology. Nature *420*, 629-635.

Etienne-Manneville, S., Manneville, J.B., Nicholls, S., Ferenczi, M.A., and Hall, A. (2005). Cdc42 and Par6-PKCzeta regulate the spatially localized association of Dlg1 and APC to control cell polarization. J Cell Biol *170*, 895-901.

Evgrafov, O.V., Mersiyanova, I., Irobi, J., Van Den Bosch, L., Dierick, I., Leung, C.L., Schagina, O., Verpoorten, N., Van Impe, K., Fedotov, V., *et al.* (2004). Mutant small heat-shock protein 27 causes axonal Charcot-Marie-Tooth disease and distal hereditary motor neuropathy. Nat Genet *36*, 602-606.

Fenrich, K., and Gordon, T. (2004). Canadian Association of Neuroscience review: axonal regeneration in the peripheral and central nervous systems--current issues and advances. Can J Neurol Sci *31*, 142-156.

Firdaus, W.J., Wyttenbach, A., Diaz-Latoud, C., Currie, R.W., and Arrigo, A.P. (2006). Analysis of oxidative events induced by expanded polyglutamine huntingtin exon 1 that are differentially restored by expression of heat shock proteins or treatment with an antioxidant. FEBS J *273*, 3076-3093.

Fiumelli, H., Riederer, I.M., Martin, J.L., and Riederer, B.M. (2008). Phosphorylation of neurofilament subunit NF-M is regulated by activation of NMDA receptors and modulates cytoskeleton stability and neuronal shape. Cell Motil Cytoskeleton *65*, 495-504.

Fragoso, G., Robertson, J., Athlan, E., Tam, E., Almazan, G., and Mushynski, W.E. (2003). Inhibition of p38 mitogen-activated protein kinase interferes with cell shape changes and gene expression associated with Schwann cell myelination. Exp Neurol *183*, 34-46.

Franklin, T.B., Krueger-Naug, A.M., Clarke, D.B., Arrigo, A.P., and Currie, R.W. (2005). The role of heat shock proteins Hsp70 and Hsp27 in cellular protection of the central nervous system. Int J Hyperthermia *21*, 379-392.

Frieden, C. (1983). Polymerization of actin: mechanism of the Mg2+-induced process at pH 8 and 20 degrees C. Proc Natl Acad Sci U S A *80*, 6513-6517.

Fu, S.Y., and Gordon, T. (1997). The cellular and molecular basis of peripheral nerve regeneration. Mol Neurobiol *14*, 67-116.

Gaestel, M. (2006). MAPKAP kinases - MKs - two's company, three's a crowd. Nat Rev Mol Cell Biol *7*, 120-130.

Galbraith, C.G., Yamada, K.M., and Galbraith, J.A. (2007). Polymerizing actin fibers position integrins primed to probe for adhesion sites. Science *315*, 992-995.

Galjart, N. (2005). CLIPs and CLASPs and cellular dynamics. Nat Rev Mol Cell Biol *6*, 487-498.

Gallo, G., and Letourneau, P.C. (2004). Regulation of growth cone actin filaments by guidance cues. J Neurobiol *58*, 92-102.

Gallo, G., Yee, H.F., Jr., and Letourneau, P.C. (2002). Actin turnover is required to prevent axon retraction driven by endogenous actomyosin contractility. J Cell Biol *158*, 1219-1228.

Galtrey, C.M., and Fawcett, J.W. (2007). The role of chondroitin sulfate proteoglycans in regeneration and plasticity in the central nervous system. Brain Res Rev *54*, 1-18.

Garcia, M.L., Lobsiger, C.S., Shah, S.B., Deerinck, T.J., Crum, J., Young, D., Ward, C.M., Crawford, T.O., Gotow, T., Uchiyama, Y., *et al.* (2003). NF-M is an essential target for the myelin-directed "outside-in" signaling cascade that mediates radial axonal growth. J Cell Biol *163*, 1011-1020.

Garrido, C., Bruey, J.M., Fromentin, A., Hammann, A., Arrigo, A.P., and Solary, E. (1999). HSP27 inhibits cytochrome c-dependent activation of procaspase-9. FASEB J *13*, 2061-2070.

Gavazzi, I., Kumar, R.D., McMahon, S.B., and Cohen, J. (1999). Growth responses of different subpopulations of adult sensory neurons to neurotrophic factors in vitro. Eur J Neurosci *11*, 3405-3414.

Gehler, S., Shaw, A.E., Sarmiere, P.D., Bamburg, J.R., and Letourneau, P.C. (2004). Brain-derived neurotrophic factor regulation of retinal growth cone filopodial dynamics is mediated through actin depolymerizing factor/cofilin. J Neurosci *24*, 10741-10749.

Gerthoffer, W.T., and Gunst, S.J. (2001). Invited review: focal adhesion and small heat shock proteins in the regulation of actin remodeling and contractility in smooth muscle. J Appl Physiol *91*, 963-972.

Giancotti, F.G. (2003). A structural view of integrin activation and signaling. Dev Cell *4*, 149-151.

Giancotti, F.G., and Ruoslahti, E. (1999). Integrin signaling. Science *285*, 1028-1032.

Giancotti, F.G., and Tarone, G. (2003). Positional control of cell fate through joint integrin/receptor protein kinase signaling. Annu Rev Cell Dev Biol *19*, 173-206.

Glass, J.R., DeWitt, R.G., and Cress, A.E. (1985). Rapid loss of stress fibers in Chinese hamster ovary cells after hyperthermia. Cancer Res *45*, 258-262.

Godsel, L.M., Hobbs, R.P., and Green, K.J. (2008). Intermediate filament assembly: dynamics to disease. Trends Cell Biol *18*, 28-37.

Goldberg, D.J., and Burmeister, D.W. (1986). Stages in axon formation: observations of growth of Aplysia axons in culture using video-enhanced contrast-differential interference contrast microscopy. J Cell Biol *103*, 1921-1931.

Goode, B.L., and Eck, M.J. (2007). Mechanism and function of formins in the control of actin assembly. Annu Rev Biochem *76*, 593-627.

Goold, R.G., and Gordon-Weeks, P.R. (2005). The MAP kinase pathway is upstream of the activation of GSK3beta that enables it to phosphorylate MAP1B and contributes to the stimulation of axon growth. Mol Cell Neurosci *28*, 524-534.

Gordon-Weeks, P.R. (2004). Actin dynamics: re-drawing the map. Nat Cell Biol *6*, 390-391.

GrandPre, T., Nakamura, F., Vartanian, T., and Strittmatter, S.M. (2000). Identification of the Nogo inhibitor of axon regeneration as a Reticulon protein. Nature *403*, 439-444.

Grenklo, S., Johansson, T., Bertilson, L., and Karlsson, R. (2004). Anti-actin antibodies generated against profilin:actin distinguish between non-filamentous and filamentous actin, and label cultured cells in a dotted pattern. Eur J Cell Biol *83*, 413-423.

Grimpe, B., and Silver, J. (2002). The extracellular matrix in axon regeneration. Prog Brain Res *137*, 333-349.

Guay, J., Lambert, H., Gingras-Breton, G., Lavoie, J.N., Huot, J., and Landry, J. (1997). Regulation of actin filament dynamics by p38 map kinase-mediated phosphorylation of heat shock protein 27. J Cell Sci *110 (Pt 3)*, 357-368.

Guo, W., and Giancotti, F.G. (2004). Integrin signalling during tumour progression. Nat Rev Mol Cell Biol *5*, 816-826.

Guzik, B.W., and Goldstein, L.S. (2004). Microtubule-dependent transport in neurons: steps towards an understanding of regulation, function and dysfunction. Curr Opin Cell Biol *16*, 443-450.

Hall, A. (1998). Rho GTPases and the actin cytoskeleton. Science *279*, 509-514.

Hammond, J.W., Cai, D., and Verhey, K.J. (2008). Tubulin modifications and their cellular functions. Curr Opin Cell Biol *20*, 71-76.

Hargis, M.T., Storck, C.W., Wickstrom, E., Yakubov, L.A., Leeper, D.B., and Coss, R.A. (2004). Hsp27 anti-sense oligonucleotides sensitize the microtubular cytoskeleton of Chinese hamster ovary cells grown at low pH to 42 degrees C-induced reorganization. Int J Hyperthermia *20*, 491-502.

Haslbeck, M., Franzmann, T., Weinfurtner, D., and Buchner, J. (2005). Some like it hot: the structure and function of small heat-shock proteins. Nat Struct Mol Biol *12*, 842-846.

Hedges, J.C., Dechert, M.A., Yamboliev, I.A., Martin, J.L., Hickey, E., Weber, L.A., and Gerthoffer, W.T. (1999). A role for p38(MAPK)/HSP27 pathway in smooth muscle cell migration. J Biol Chem *274*, 24211-24219.

Heins, S., and Aebi, U. (1994). Making heads and tails of intermediate filament assembly, dynamics and networks. Curr Opin Cell Biol *6*, 25-33.

Helfand, B.T., Mendez, M.G., Pugh, J., Delsert, C., and Goldman, R.D. (2003). A role for intermediate filaments in determining and maintaining the shape of nerve cells. Mol Biol Cell *14*, 5069-5081.

Herrmann, H., Strelkov, S.V., Feja, B., Rogers, K.R., Brettel, M., Lustig, A., Haner, M., Parry, D.A., Steinert, P.M., Burkhard, P., and Aebi, U. (2000). The intermediate filament protein consensus motif of helix 2B: its atomic structure and contribution to assembly. J Mol Biol *298*, 817-832.

Hightower, L.E. (1991). Heat shock, stress proteins, chaperones, and proteotoxicity. Cell *66*, 191-197.

Hino, M., Kurogi, K., Okubo, M.A., Murata-Hori, M., and Hosoya, H. (2000). Small heat shock protein 27 (HSP27) associates with tubulin/microtubules in HeLa cells. Biochem Biophys Res Commun *271*, 164-169.

Hirano, S., Shelden, E.A., and Gilmont, R.R. (2004). HSP27 regulates fibroblast adhesion, motility, and matrix contraction. Cell Stress Chaperones *9*, 29-37.

Hirokawa, N., Glicksman, M.A., and Willard, M.B. (1984). Organization of mammalian neurofilament polypeptides within the neuronal cytoskeleton. J Cell Biol *98*, 1523-1536.

Hirokawa, N., and Takemura, R. (2004). Molecular motors in neuronal development, intracellular transport and diseases. Curr Opin Neurobiol *14*, 564-573.

Hisanaga, S., and Hirokawa, N. (1988). Structure of the peripheral domains of neurofilaments revealed by low angle rotary shadowing. J Mol Biol *202*, 297-305.

Hisanaga, S., and Hirokawa, N. (1990). Molecular architecture of the neurofilament. II. Reassembly process of neurofilament L protein in vitro. J Mol Biol *211*, 871-882.

Hong, Z., Zhang, Q.Y., Liu, J., Wang, Z.Q., Zhang, Y., Xiao, Q., Lu, J., Zhou, H.Y., and Chen, S.D. (2009). Phosphoproteome study reveals Hsp27 as a novel signaling molecule involved in GDNF-induced neurite outgrowth. J Proteome Res *8*, 2768-2787.

Huang, T.Y., DerMardirossian, C., and Bokoch, G.M. (2006). Cofilin phosphatases and regulation of actin dynamics. Curr Opin Cell Biol *18*, 26-31.

Huber, A.B., Kolodkin, A.L., Ginty, D.D., and Cloutier, J.F. (2003). Signaling at the growth cone: ligand-receptor complexes and the control of axon growth and guidance. Annu Rev Neurosci *26*, 509-563.

Huot, J., Houle, F., Marceau, F., and Landry, J. (1997). Oxidative stress-induced actin reorganization mediated by the p38 mitogen-activated protein kinase/heat shock protein 27 pathway in vascular endothelial cells. Circ Res *80*, 383-392.

Huot, J., Houle, F., Rousseau, S., Deschesnes, R.G., Shah, G.M., and Landry, J. (1998). SAPK2/p38-dependent F-actin reorganization regulates early membrane blebbing during stress-induced apoptosis. J Cell Biol *143*, 1361-1373.

Huot, J., Houle, F., Spitz, D.R., and Landry, J. (1996). HSP27 phosphorylation-mediated resistance against actin fragmentation and cell death induced by oxidative stress. Cancer Res *56*, 273-279.

Huot, J., Lambert, H., Lavoie, J.N., Guimond, A., Houle, F., and Landry, J. (1995). Characterization of 45-kDa/54-kDa HSP27 kinase, a stress-sensitive kinase which may activate the phosphorylation-dependent protective function of mammalian 27-kDa heat-shock protein HSP27. Eur J Biochem *227*, 416-427.

Ibitayo, A.I., Sladick, J., Tuteja, S., Louis-Jacques, O., Yamada, H., Groblewski, G., Welsh, M., and Bitar, K.N. (1999). HSP27 in signal transduction and association with contractile proteins in smooth muscle cells. Am J Physiol *277*, G445-454.

Iida, K., Iida, H., and Yahara, I. (1986). Heat shock induction of intranuclear actin rods in cultured mammalian cells. Exp Cell Res *165*, 207-215.

Ikegami, K., Heier, R.L., Taruishi, M., Takagi, H., Mukai, M., Shimma, S., Taira, S., Hatanaka, K., Morone, N., Yao, I., *et al.* (2007). Loss of alpha-tubulin polyglutamylation in ROSA22 mice is associated with abnormal targeting of KIF1A and modulated synaptic function. Proc Natl Acad Sci U S A *104*, 3213-3218.

Ingolia, T.D., and Craig, E.A. (1982). Four small Drosophila heat shock proteins are related to each other and to mammalian alpha-crystallin. Proc Natl Acad Sci U S A *79*, 2360-2364.

Irobi, J., Van Impe, K., Seeman, P., Jordanova, A., Dierick, I., Verpoorten, N., Michalik, A., De Vriendt, E., Jacobs, A., Van Gerwen, V., *et al.* (2004a). Hot-spot residue in small heat-shock protein 22 causes distal motor neuropathy. Nat Genet *36*, 597-601.

Irobi, J., Van Impe, K., Seeman, P., Jordanova, A., Dierick, I., Verpoorten, N., Michalik, A., De Vriendt, E., Jacobs, A., Van Gerwen, V., *et al.* (2004b). Hot-spot residue in small heat-shock protein 22 causes distal motor neuropathy. Nat Genet *36*, 597-601.

Ishikawa, T., Miyagi, M., Ohtori, S., Aoki, Y., Ozawa, T., Doya, H., Saito, T., Moriya, H., and Takahashi, K. (2005). Characteristics of sensory DRG neurons innervating the lumbar facet joints in rats. Eur Spine J *14*, 559-564.

Jakob, U., Gaestel, M., Engel, K., and Buchner, J. (1993). Small heat shock proteins are molecular chaperones. J Biol Chem *268*, 1517-1520.

Jawhari, A.U., Buda, A., Jenkins, M., Shehzad, K., Sarraf, C., Noda, M., Farthing, M.J., Pignatelli, M., and Adams, J.C. (2003). Fascin, an actin-bundling protein, modulates colonic epithelial cell invasiveness and differentiation in vitro. Am J Pathol *162*, 69-80.

Jia, Y., Wu, S.L., Isenberg, J.S., Dai, S., Sipes, J.M., Field, L., Zeng, B., Bandle, R.W., Ridnour, L.A., Wink, D.A., *et al.* (2009). Thiolutin inhibits endothelial cell adhesion by perturbing Hsp27 interactions with components of the actin and intermediate filament cytoskeleton. Cell Stress Chaperones.

Joester, A., and Faissner, A. (2001). The structure and function of tenascins in the nervous system. Matrix Biol *20*, 13-22.

Jog, N.R., Jala, V.R., Ward, R.A., Rane, M.J., Haribabu, B., and McLeish, K.R. (2007). Heat shock protein 27 regulates neutrophil chemotaxis and exocytosis through two independent mechanisms. J Immunol *178*, 2421-2428.

Jones, D.M., Tucker, B.A., Rahimtula, M., and Mearow, K.M. (2003). The synergistic effects of NGF and IGF-1 on neurite growth in adult sensory neurons: convergence on the PI 3-kinase signaling pathway. J Neurochem *86*, 1116-1128.

Jourdain, L., Curmi, P., Sobel, A., Pantaloni, D., and Carlier, M.F. (1997). Stathmin: a tubulin-sequestering protein which forms a ternary T2S complex with two tubulin molecules. Biochemistry *36*, 10817-10821.

Jung, C., Lee, S., Ortiz, D., Zhu, Q., Julien, J.P., and Shea, T.B. (2005). The high and middle molecular weight neurofilament subunits regulate the association of neurofilaments with kinesin: inhibition by phosphorylation of the high molecular weight subunit. Brain Res Mol Brain Res *141*, 151-155.

Kalil, K. (1996). Growth cone behaviors during axon guidance in the developing cerebral cortex. Prog Brain Res *108*, 31-40.

Kalil, K., and Dent, E.W. (2005). Touch and go: guidance cues signal to the growth cone cytoskeleton. Curr Opin Neurobiol *15*, 521-526.

Kamada, M., So, A., Muramaki, M., Rocchi, P., Beraldi, E., and Gleave, M. (2007). Hsp27 knockdown using nucleotide-based therapies inhibit tumor growth and enhance chemotherapy in human bladder cancer cells. Mol Cancer Ther *6*, 299-308.

Kampinga, H.H., Hageman, J., Vos, M.J., Kubota, H., Tanguay, R.M., Bruford, E.A., Cheetham, M.E., Chen, B., and Hightower, L.E. (2009). Guidelines for the nomenclature of the human heat shock proteins. Cell Stress Chaperones *14*, 105-111.

Kano, Y., Nakagiri, S., Nohno, T., Hiragami, F., Kawamura, K., Kadota, M., Numata, K., Koike, Y., and Furuta, T. (2004). Heat shock induces neurite outgrowth in PC12m3 cells via the p38 mitogen-activated protein kinase pathway. Brain Res *1026*, 302-306.

Kashiba, H., Uchida, Y., and Senba, E. (2001). Difference in binding by isolectin B4 to trkA and c-ret mRNA-expressing neurons in rat sensory ganglia. Brain Res Mol Brain Res *95*, 18-26.

Kato, K., Hasegawa, K., Goto, S., and Inaguma, Y. (1994). Dissociation as a result of phosphorylation of an aggregated form of the small stress protein, hsp27. J Biol Chem *269*, 11274-11278.

Khor, T.O., Gul, Y.A., Ithnin, H., and Seow, H.F. (2004). Positive correlation between overexpression of phospho-BAD with phosphorylated Akt at serine 473 but not threonine 308 in colorectal carcinoma. Cancer Lett *210*, 139-150.

Kim, K.K., Kim, R., and Kim, S.H. (1998). Crystal structure of a small heat-shock protein. Nature *394*, 595-599.

Kindas-Mugge, I., Rieder, C., Frohlich, I., Micksche, M., and Trautinger, F. (2002). Characterization of proteins associated with heat shock protein hsp27 in the squamous cell carcinoma cell line A431. Cell Biol Int *26*, 109-116.

Kohno, K., Kawakami, T., and Hiruma, H. (2005). Effects of soluble laminin on organelle transport and neurite growth in cultured mouse dorsal root ganglion neurons: difference between primary neurites and branches. J Cell Physiol *205*, 253-261.

Komarova, Y.A., Akhmanova, A.S., Kojima, S., Galjart, N., and Borisy, G.G. (2002). Cytoplasmic linker proteins promote microtubule rescue in vivo. J Cell Biol *159*, 589-599.

Konishi, H., Matsuzaki, H., Tanaka, M., Takemura, Y., Kuroda, S., Ono, Y., and Kikkawa, U. (1997). Activation of protein kinase B (Akt/RAC-protein kinase) by cellular stress and its association with heat shock protein Hsp27. FEBS Lett *410*, 493-498.

Korn, E.D., Carlier, M.F., and Pantaloni, D. (1987). Actin polymerization and ATP hydrolysis. Science *238*, 638-644.

Kornack, D.R., and Giger, R.J. (2005). Probing microtubule +TIPs: regulation of axon branching. Curr Opin Neurobiol *15*, 58-66.

Korobova, F., and Svitkina, T. (2008). Arp2/3 complex is important for filopodia formation, growth cone motility, and neuritogenesis in neuronal cells. Mol Biol Cell *19*, 1561-1574.

Koteiche, H.A., and McHaourab, H.S. (2002). The determinants of the oligomeric structure in Hsp16.5 are encoded in the alpha-crystallin domain. FEBS Lett *519*, 16-22.

Kubisch, C., Dimagno, M.J., Tietz, A.B., Welsh, M.J., Ernst, S.A., Brandt-Nedelev, B., Diebold, J., Wagner, A.C., Goke, B., Williams, J.A., and Schafer, C. (2004). Overexpression of heat shock protein Hsp27 protects against cerulein-induced pancreatitis. Gastroenterology *127*, 275-286.

Kumar, L.V., Ramakrishna, T., and Rao, C.M. (1999). Structural and functional consequences of the mutation of a conserved arginine residue in alphaA and alphaB crystallins. J Biol Chem *274*, 24137-24141.

Labelle, C., and Leclerc, N. (2000). Exogenous BDNF, NT-3 and NT-4 differentially regulate neurite outgrowth in cultured hippocampal neurons. Brain Res Dev Brain Res *123*, 1-11.

Lambert, H., Charette, S.J., Bernier, A.F., Guimond, A., and Landry, J. (1999). HSP27 multimerization mediated by phosphorylation-sensitive intermolecular interactions at the amino terminus. J Biol Chem *274*, 9378-9385.

Landry, J., and Huot, J. (1995). Modulation of actin dynamics during stress and physiological stimulation by a signaling pathway involving p38 MAP kinase and heat-shock protein 27. Biochem Cell Biol *73*, 703-707.

Landry, J., and Huot, J. (1999). Regulation of actin dynamics by stress-activated protein kinase 2 (SAPK2)-dependent phosphorylation of heat-shock protein of 27 kDa (Hsp27). Biochem Soc Symp *64*, 79-89.

Landry, J., Lambert, H., Zhou, M., Lavoie, J.N., Hickey, E., Weber, L.A., and Anderson, C.W. (1992). Human HSP27 is phosphorylated at serines 78 and 82 by heat shock and mitogen-activated kinases that recognize the same amino acid motif as S6 kinase II. J Biol Chem *267*, 794-803.

Lansbergen, G., and Akhmanova, A. (2006). Microtubule plus end: a hub of cellular activities. Traffic *7*, 499-507.

Larsen, J.K., Yamboliev, I.A., Weber, L.A., and Gerthoffer, W.T. (1997). Phosphorylation of the 27-kDa heat shock protein via p38 MAP kinase and MAPKAP kinase in smooth muscle. Am J Physiol *273*, L930-940.

Latchman, D.S. (2005). HSP27 and cell survival in neurones. Int J Hyperthermia *21*, 393-402.

Lavoie, J.N., Gingras-Breton, G., Tanguay, R.M., and Landry, J. (1993a). Induction of Chinese hamster HSP27 gene expression in mouse cells confers resistance to heat shock. HSP27 stabilization of the microfilament organization. J Biol Chem *268*, 3420-3429.

Lavoie, J.N., Hickey, E., Weber, L.A., and Landry, J. (1993b). Modulation of actin microfilament dynamics and fluid phase pinocytosis by phosphorylation of heat shock protein 27. J Biol Chem *268*, 24210-24214.

Lavoie, J.N., Lambert, H., Hickey, E., Weber, L.A., and Landry, J. (1995). Modulation of cellular thermoresistance and actin filament stability accompanies phosphorylation-induced changes in the oligomeric structure of heat shock protein 27. Mol Cell Biol *15*, 505-516.

Le Clainche, C., and Carlier, M.F. (2008). Regulation of actin assembly associated with protrusion and adhesion in cell migration. Physiol Rev *88*, 489-513.

Lebrand, C., Dent, E.W., Strasser, G.A., Lanier, L.M., Krause, M., Svitkina, T.M., Borisy, G.G., and Gertler, F.B. (2004). Critical role of Ena/VASP proteins for filopodia formation in neurons and in function downstream of netrin-1. Neuron *42*, 37-49.

Lee, J.H., Sun, D., Cho, K.J., Kim, M.S., Hong, M.H., Kim, I.K., and Lee, J.S. (2007). Overexpression of human 27 kDa heat shock protein in laryngeal cancer cells confers chemoresistance associated with cell growth delay. J Cancer Res Clin Oncol *133*, 37-46.

Lee, J.S., Zhang, M.H., Yun, E.K., Geum, D., Kim, K., Kim, T.H., Lim, Y.S., and Seo, J.S. (2005). Heat shock protein 27 interacts with vimentin and prevents insolubilization of vimentin subunits induced by cadmium. Exp Mol Med *37*, 427-435.

Lee, J.W., Kwak, H.J., Lee, J.J., Kim, Y.N., Park, M.J., Jung, S.E., Hong, S.I., Lee, J.H., and Lee, J.S. (2008). HSP27 regulates cell adhesion and invasion via modulation of focal adhesion kinase and MMP-2 expression. Eur J Cell Biol *87*, 377-387.

Lee, S., and Leavitt, B. (2004). Turning up the heat on hereditary neuropathies. Clin. Genetics *66*, 294-296.

Lee, V.M., Otvos, L., Jr., Schmidt, M.L., and Trojanowski, J.Q. (1988). Alzheimer disease tangles share immunological similarities with multiphosphorylation repeats in the two large neurofilament proteins. Proc Natl Acad Sci U S A *85*, 7384-7388.

Lehmann, M., Fournier, A., Selles-Navarro, I., Dergham, P., Sebok, A., Leclerc, N., Tigyi, G., and McKerracher, L. (1999). Inactivation of Rho signaling pathway promotes CNS axon regeneration. J Neurosci *19*, 7537-7547.

Leonard, D.G., Gorham, J.D., Cole, P., Greene, L.A., and Ziff, E.B. (1988). A nerve growth factor-regulated messenger RNA encodes a new intermediate filament protein. J Cell Biol *106*, 181-193.

Letourneau, P.C., Shattuck, T.A., and Ressler, A.H. (1987). "Pull" and "push" in neurite elongation: observations on the effects of different concentrations of cytochalasin B and taxol. Cell Motil Cytoskeleton *8*, 193-209.

Lewis, S.E., Mannion, R.J., White, F.A., Coggeshall, R.E., Beggs, S., Costigan, M., Martin, J.L., Dillmann, W.H., and Woolf, C.J. (1999). A role for HSP27 in sensory neuron survival. J Neurosci *19*, 8945-8953.

Liang, P., and MacRae, T.H. (1997). Molecular chaperones and the cytoskeleton. J Cell Sci *110 (Pt 13)*, 1431-1440.

Lilienbaum, A., Reszka, A.A., Horwitz, A.F., and Holt, C.E. (1995). Chimeric integrins expressed in retinal ganglion cells impair process outgrowth in vivo. Mol Cell Neurosci *6*, 139-152.

Litt, M., Kramer, P., LaMorticella, D.M., Murphey, W., Lovrien, E.W., and Weleber, R.G. (1998). Autosomal dominant congenital cataract associated with a missense mutation in the human alpha crystallin gene CRYAA. Hum Mol Genet *7*, 471-474.

Liu, B.P., Cafferty, W.B., Budel, S.O., and Strittmatter, S.M. (2006). Extracellular regulators of axonal growth in the adult central nervous system. Philos Trans R Soc Lond B Biol Sci *361*, 1593-1610.

Liu, Q., Xie, F., Siedlak, S.L., Nunomura, A., Honda, K., Moreira, P.I., Zhua, X., Smith, M.A., and Perry, G. (2004). Neurofilament proteins in neurodegenerative diseases. Cell Mol Life Sci *61*, 3057-3075.

Loktionova, S.A., and Kabakov, A.E. (1998). Protein phosphatase inhibitors and heat preconditioning prevent Hsp27 dephosphorylation, F-actin disruption and deterioration of morphology in ATP-depleted endothelial cells. FEBS Lett *433*, 294-300.

Loudon, R.P., Silver, L.D., Yee, H.F., Jr., and Gallo, G. (2006). RhoA-kinase and myosin II are required for the maintenance of growth cone polarity and guidance by nerve growth factor. J Neurobiol *66*, 847-867.

Luduena, R.F. (1998). Multiple forms of tubulin: different gene products and covalent modifications. Int Rev Cytol *178*, 207-275.

Luo, L. (2002). Actin cytoskeleton regulation in neuronal morphogenesis and structural plasticity. Annu Rev Cell Dev Biol *18*, 601-635.

Lutsch, G., Vetter, R., Offhauss, U., Wieske, M., Grone, H.J., Klemenz, R., Schimke, I., Stahl, J., and Benndorf, R. (1997). Abundance and location of the small heat shock proteins HSP25 and alphaB-crystallin in rat and human heart. Circulation *96*, 3466-3476.

Mailhos, C., Howard, M.K., and Latchman, D.S. (1993). Heat shock protects neuronal cells from programmed cell death by apoptosis. Neuroscience *55*, 621-627.

Maizels, E.T., Peters, C.A., Kline, M., Cutler, R.E., Jr., Shanmugam, M., and Hunzicker-Dunn, M. (1998). Heat-shock protein-25/27 phosphorylation by the delta isoform of protein kinase C. Biochem J *332 (Pt 3)*, 703-712.

Mallavarapu, A., and Mitchison, T. (1999). Regulated actin cytoskeleton assembly at filopodium tips controls their extension and retraction. J Cell Biol *146*, 1097-1106.

Manna, T., Thrower, D., Miller, H.P., Curmi, P., and Wilson, L. (2006). Stathmin strongly increases the minus end catastrophe frequency and induces rapid treadmilling of bovine brain microtubules at steady state in vitro. J Biol Chem *281*, 2071-2078.

Marin-Vinader, L., Shin, C., Onnekink, C., Manley, J.L., and Lubsen, N.H. (2006). Hsp27 enhances recovery of splicing as well as rephosphorylation of SRp38 after heat shock. Mol Biol Cell *17*, 886-894.

Marsh, L., and Letourneau, P.C. (1984). Growth of neurites without filopodial or lamellipodial activity in the presence of cytochalasin B. J Cell Biol *99*, 2041-2047.

Mattila, P.K., and Lappalainen, P. (2008). Filopodia: molecular architecture and cellular functions. Nat Rev Mol Cell Biol.

McKerracher, L., Chamoux, M., and Arregui, C.O. (1996). Role of laminin and integrin interactions in growth cone guidance. Mol Neurobiol *12*, 95-116.

McKerracher, L., David, S., Jackson, D.L., Kottis, V., Dunn, R.J., and Braun, P.E. (1994). Identification of myelin-associated glycoprotein as a major myelin-derived inhibitor of neurite growth. Neuron *13*, 805-811.

McLaughlin, M.M., Kumar, S., McDonnell, P.C., Van Horn, S., Lee, J.C., Livi, G.P., and Young, P.R. (1996). Identification of mitogen-activated protein (MAP) kinase-activated protein kinase-3, a novel substrate of CSBP p38 MAP kinase. J Biol Chem *271*, 8488-8492.

Mearow, K.M., Dodge, M.E., Rahimtula, M., and Yegappan, C. (2002). Stress-mediated signaling in PC12 cells - the role of the small heat shock protein, Hsp27, and Akt in protecting cells from heat stress and nerve growth factor withdrawal. J Neurochem *83*, 452-462.

Mehlen, P., and Arrigo, A.P. (1994). The serum-induced phosphorylation of mammalian hsp27 correlates with changes in its intracellular localization and levels of oligomerization. Eur J Biochem *221*, 327-334.

Mehlen, P., Kretz-Remy, C., Preville, X., and Arrigo, A.P. (1996a). Human hsp27, Drosophila hsp27 and human alphaB-crystallin expression-mediated increase in glutathione is essential for the protective activity of these proteins against TNFalpha-induced cell death. EMBO J *15*, 2695-2706.

Mehlen, P., Schulze-Osthoff, K., and Arrigo, A.P. (1996b). Small stress proteins as novel regulators of apoptosis. Heat shock protein 27 blocks Fas/APO-1- and staurosporine-induced cell death. J Biol Chem *271*, 16510-16514.

Meier, M., King, G.L., Clermont, A., Perez, A., Hayashi, M., and Feener, E.P. (2001). Angiotensin AT(1) receptor stimulates heat shock protein 27 phosphorylation in vitro and in vivo. Hypertension *38*, 1260-1265.

Meijering, E., Jacob, M., Sarria, J.C., Steiner, P., Hirling, H., and Unser, M. (2004). Design and validation of a tool for neurite tracing and analysis in fluorescence microscopy images. Cytometry A *58*, 167-176.

Mejillano, M.R., Kojima, S., Applewhite, D.A., Gertler, F.B., Svitkina, T.M., and Borisy, G.G. (2004). Lamellipodial versus filopodial mode of the actin nanomachinery: pivotal role of the filament barbed end. Cell *118*, 363-373.

Miron, T., Vancompernolle, K., Vandekerckhove, J., Wilchek, M., and Geiger, B. (1991). A 25-kD inhibitor of actin polymerization is a low molecular mass heat shock protein. J Cell Biol *114*, 255-261.

Molliver, D.C., Wright, D.E., Leitner, M.L., Parsadanian, A.S., Doster, K., Wen, D., Yan, Q., and Snider, W.D. (1997). IB4-binding DRG neurons switch from NGF to GDNF dependence in early postnatal life. Neuron *19*, 849-861.

Moores, C.A., and Milligan, R.A. (2006). Lucky 13-microtubule depolymerisation by kinesin-13 motors. J Cell Sci *119*, 3905-3913.

Morton, W.M., Ayscough, K.R., and McLaughlin, P.J. (2000). Latrunculin alters the actin-monomer subunit interface to prevent polymerization. Nat Cell Biol *2*, 376-378.

Moseley, J.B., Bartolini, F., Okada, K., Wen, Y., Gundersen, G.G., and Goode, B.L. (2007). Regulated binding of adenomatous polyposis coli protein to actin. J Biol Chem *282*, 12661-12668.

Mounier, N., and Arrigo, A.P. (2002). Actin cytoskeleton and small heat shock proteins: how do they interact? Cell Stress Chaperones *7*, 167-176.

Mullins, R.D., Heuser, J.A., and Pollard, T.D. (1998). The interaction of Arp2/3 complex with actin: nucleation, high affinity pointed end capping, and formation of branching networks of filaments. Proc Natl Acad Sci U S A *95*, 6181-6186.

Murashov, A.K., Ul Haq, I., Hill, C., Park, E., Smith, M., Wang, X., Goldberg, D.J., and Wolgemuth, D.J. (2001a). Crosstalk between p38, Hsp25 and Akt in spinal motor neurons after sciatic nerve injury. Brain Res Mol Brain Res *93*, 199-208.

Murashov, A.K., Ul Haq, I., Hill, C., Park, E., Smith, M., Wang, X., Wang, X., Goldberg, D.J., and Wolgemuth, D.J. (2001b). Crosstalk between p38, Hsp25 and Akt in spinal motor neurons after sciatic nerve injury. Brain Res Mol Brain Res *93*, 199-208.

Nakamura, Y., Hashimoto, R., Kashiwagi, Y., Aimoto, S., Fukusho, E., Matsumoto, N., Kudo, T., and Takeda, M. (2000). Major phosphorylation site (Ser55) of neurofilament L by cyclic AMP-dependent protein kinase in rat primary neuronal culture. J Neurochem *74*, 949-959.

New, L., Jiang, Y., Zhao, M., Liu, K., Zhu, W., Flood, L.J., Kato, Y., Parry, G.C., and Han, J. (1998). PRAK, a novel protein kinase regulated by the p38 MAP kinase. EMBO J *17*, 3372-3384.

Nixon, R.A. (1993). The regulation of neurofilament protein dynamics by phosphorylation: clues to neurofibrillary pathobiology. Brain Pathol *3*, 29-38.

Nobes, C.D., and Hall, A. (1995). Rho, rac, and cdc42 GTPases regulate the assembly of multimolecular focal complexes associated with actin stress fibers, lamellipodia, and filopodia. Cell *81*, 53-62.

Nomura, N., Nomura, M., Sugiyama, K., and Hamada, J. (2007). Phorbol 12-myristate 13-acetate (PMA)-induced migration of glioblastoma cells is mediated via p38MAPK/Hsp27 pathway. Biochem Pharmacol *74*, 690-701.

O'Connor, T.P., and Bentley, D. (1993). Accumulation of actin in subsets of pioneer growth cone filopodia in response to neural and epithelial guidance cues in situ. J Cell Biol *123*, 935-948.

Oblinger, M.M., Wong, J., and Parysek, L.M. (1989). Axotomy-induced changes in the expression of a type III neuronal intermediate filament gene. J Neurosci *9*, 3766-3775.

Ono, S. (2007). Mechanism of depolymerization and severing of actin filaments and its significance in cytoskeletal dynamics. Int Rev Cytol *258*, 1-82.

Ono, S., and Ono, K. (2002). Tropomyosin inhibits ADF/cofilin-dependent actin filament dynamics. J Cell Biol *156*, 1065-1076.

Pak, C.W., Flynn, K.C., and Bamburg, J.R. (2008). Actin-binding proteins take the reins in growth cones. Nat Rev Neurosci *9*, 136-147.

Panasenko, O.O., Kim, M.V., Marston, S.B., and Gusev, N.B. (2003). Interaction of the small heat shock protein with molecular mass 25 kDa (hsp25) with actin. Eur J Biochem *270*, 892-901.

Pantaloni, D., Clainche, C.L., and Carlier, M.-F. (2001). Mechanism of Actin-Based Motility. Science *292*, 1502-1506.

Patil, S.B., and Bitar, K.N. (2006). RhoA- and PKC-alpha-mediated phosphorylation of MYPT and its association with HSP27 in colonic smooth muscle cells. Am J Physiol Gastrointest Liver Physiol *290*, G83-95.

Patil, S.B., Pawar, M.D., and Bitar, K.N. (2004a). Phosphorylated HSP27 essential for acetylcholine-induced association of RhoA with PKCalpha. Am J Physiol Gastrointest Liver Physiol *286*, G635-644.

Patil, S.B., Tsunoda, Y., Pawar, M.D., and Bitar, K.N. (2004b). Translocation and association of ROCK-II with RhoA and HSP27 during contraction of rabbit colon smooth muscle cells. Biochem Biophys Res Commun *319*, 95-102.

Paul, C., and Arrigo, A.P. (2000). Comparison of the protective activities generated by two survival proteins: Bcl-2 and Hsp27 in L929 murine fibroblasts exposed to menadione or staurosporine. Exp Gerontol *35*, 757-766.

Paul, C., Manero, F., Gonin, S., Kretz-Remy, C., Virot, S., and Arrigo, A.P. (2002). Hsp27 as a negative regulator of cytochrome C release. Mol Cell Biol *22*, 816-834.

Perez-Olle, R., Jones, S.T., and Liem, R.K. (2004). Phenotypic analysis of neurofilament light gene mutations linked to Charcot-Marie-Tooth disease in cell culture models. Hum Mol Genet *13*, 2207-2220.

Perez-Olle, R., Lopez-Toledano, M.A., Goryunov, D., Cabrera-Poch, N., Stefanis, L., Brown, K., and Liem, R.K. (2005). Mutations in the neurofilament light gene linked to Charcot-Marie-Tooth disease cause defects in transport. J Neurochem *93*, 861-874.

Perng, M.D., Cairns, L., van den, I.P., Prescott, A., Hutcheson, A.M., and Quinlan, R.A. (1999a). Intermediate filament interactions can be altered by HSP27 and alphaB-crystallin. J Cell Sci *112 (Pt 13)*, 2099-2112.

Perng, M.D., Muchowski, P.J., van Den, I.P., Wu, G.J., Hutcheson, A.M., Clark, J.I., and Quinlan, R.A. (1999b). The cardiomyopathy and lens cataract mutation in alphaB-crystallin alters its protein structure, chaperone activity, and interaction with intermediate filaments in vitro. J Biol Chem *274*, 33235-33243.

Petruska, J.C., Napaporn, J., Johnson, R.D., Gu, J.G., and Cooper, B.Y. (2000). Subclassified acutely dissociated cells of rat DRG: histochemistry and patterns of capsaicin-, proton-, and ATP-activated currents. J Neurophysiol *84*, 2365-2379.

Pichon, S., Bryckaert, M., and Berrou, E. (2004). Control of actin dynamics by p38 MAP kinase - Hsp27 distribution in the lamellipodium of smooth muscle cells. J Cell Sci *117*, 2569-2577.

Piotrowicz, R.S., Hickey, E., and Levin, E.G. (1998). Heat shock protein 27 kDa expression and phosphorylation regulates endothelial cell migration. Faseb J *12*, 1481-1490.

Pivovarova, A.V., Mikhailova, V.V., Chernik, I.S., Chebotareva, N.A., Levitsky, D.I., and Gusev, N.B. (2005). Effects of small heat shock proteins on the thermal denaturation and aggregation of F-actin. Biochem Biophys Res Commun *331*, 1548-1553.

Plumier, J.C., Hopkins, D.A., Robertson, H.A., and Currie, R.W. (1997). Constitutive expression of the 27-kDa heat shock protein (Hsp27) in sensory and motor neurons of the rat nervous system. J Comp Neurol *384*, 409-428.

Preville, X., Gaestel, M., and Arrigo, A.P. (1998). Phosphorylation is not essential for protection of L929 cells by Hsp25 against H2O2-mediated disruption actin cytoskeleton, a protection which appears related to the redox change mediated by Hsp25. Cell Stress Chaperones *3*, 177-187.

Preville, X., Salvemini, F., Giraud, S., Chaufour, S., Paul, C., Stepien, G., Ursini, M.V., and Arrigo, A.P. (1999). Mammalian small stress proteins protect against oxidative stress through their ability to increase glucose-6-phosphate dehydrogenase activity and by maintaining optimal cellular detoxifying machinery. Exp Cell Res *247*, 61-78.

Price, L.S., Leng, J., Schwartz, M.A., and Bokoch, G.M. (1998). Activation of Rac and Cdc42 by integrins mediates cell spreading. Mol Biol Cell *9*, 1863-1871.

Priestley, J.V., Michael, G.J., Averill, S., Liu, M., and Willmott, N. (2002). Regulation of nociceptive neurons by nerve growth factor and glial cell line derived neurotrophic factor. Can J Physiol Pharmacol *80*, 495-505.

Quigney, D.J., Gorman, A.M., and Samali, A. (2003). Heat shock protects PC12 cells against MPP+ toxicity. Brain Res *993*, 133-139.

Rane, M.J., Pan, Y., Singh, S., Powell, D.W., Wu, R., Cummins, T., Chen, Q., McLeish, K.R., and Klein, J.B. (2003). Heat shock protein 27 controls apoptosis by regulating Akt activation. J Biol Chem *278*, 27828-27835.

Rauvala, H., and Peng, H.B. (1997). HB-GAM (heparin-binding growth-associated molecule) and heparin-type glycans in the development and plasticity of neuron-target contacts. Prog Neurobiol *52*, 127-144.

Reed, N.A., Cai, D., Blasius, T.L., Jih, G.T., Meyhofer, E., Gaertig, J., and Verhey, K.J. (2006). Microtubule acetylation promotes kinesin-1 binding and transport. Curr Biol *16*, 2166-2172.

Richards, T.A., and Cavalier-Smith, T. (2005). Myosin domain evolution and the primary divergence of eukaryotes. Nature *436*, 1113-1118.

Ritossa, F. (1962). A new puffing pattern induced by a temperature shock and DNP in Drosophilia. . Experientia *18*, 571-573.

Ritossa, F. (1996). Discovery of the heat shock response. Cell Stress Chaperones *1*, 97-98.

Robles, E., and Gomez, T.M. (2006). Focal adhesion kinase signaling at sites of integrin-mediated adhesion controls axon pathfinding. Nat Neurosci *9*, 1274-1283.

Rocchi, P., Jugpal, P., So, A., Sinneman, S., Ettinger, S., Fazli, L., Nelson, C., and Gleave, M. (2006). Small interference RNA targeting heat-shock protein 27 inhibits the growth of prostatic cell lines and induces apoptosis via caspase-3 activation in vitro. BJU Int *98*, 1082-1089.

Rogalla, T., Ehrnsperger, M., Preville, X., Kotlyarov, A., Lutsch, G., Ducasse, C., Paul, C., Wieske, M., Arrigo, A.P., Buchner, J., and Gaestel, M. (1999). Regulation of Hsp27 oligomerization, chaperone function, and protective activity against oxidative stress/tumor necrosis factor alpha by phosphorylation. J Biol Chem *274*, 18947-18956.

Rouse, J., Cohen, P., Trigon, S., Morange, M., Alonso-Llamazares, A., Zamanillo, D., Hunt, T., and Nebreda, A.R. (1994). A novel kinase cascade triggered by stress and heat shock that stimulates MAPKAP kinase-2 and phosphorylation of the small heat shock proteins. Cell *78*, 1027-1037.

Rousseau, S., Houle, F., Landry, J., and Huot, J. (1997). p38 MAP kinase activation by vascular endothelial growth factor mediates actin reorganization and cell migration in human endothelial cells. Oncogene *15*, 2169-2177.

Roy, S., Coffee, P., Smith, G., Liem, R.K., Brady, S.T., and Black, M.M. (2000). Neurofilaments are transported rapidly but intermittently in axons: implications for slow axonal transport. J Neurosci *20*, 6849-6861.

Saibil, H.R. (2008). Chaperone machines in action. Curr Opin Struct Biol *18*, 35-42.

Sanchez, I., Hassinger, L., Paskevich, P.A., Shine, H.D., and Nixon, R.A. (1996). Oligodendroglia regulate the regional expansion of axon caliber and local accumulation of neurofilaments during development independently of myelin formation. J Neurosci *16*, 5095-5105.

Sanchez, I., Hassinger, L., Sihag, R.K., Cleveland, D.W., Mohan, P., and Nixon, R.A. (2000). Local control of neurofilament accumulation during radial growth of myelinating axons in vivo. Selective role of site-specific phosphorylation. J Cell Biol *151*, 1013-1024.

Sarge, K.D., Murphy, S.P., and Morimoto, R.I. (1993). Activation of heat shock gene transcription by heat shock factor 1 involves oligomerization, acquisition of DNA-binding activity, and nuclear localization and can occur in the absence of stress. Mol Cell Biol *13*, 1392-1407.

Schafer, C., Clapp, P., Welsh, M.J., Benndorf, R., and Williams, J.A. (1999). HSP27 expression regulates CCK-induced changes of the actin cytoskeleton in CHO-CCK-A cells. Am J Physiol *277*, C1032-1043.

Schneider, G.B., Hamano, H., and Cooper, L.F. (1998). In vivo evaluation of hsp27 as an inhibitor of actin polymerization: hsp27 limits actin stress fiber and focal adhesion formation after heat shock. J Cell Physiol *177*, 575-584.

Shamovsky, I., and Nudler, E. (2008). New insights into the mechanism of heat shock response activation. Cell Mol Life Sci *65*, 855-861.

Shea, T.B., Jung, C., and Pant, H.C. (2003). Does neurofilament phosphorylation regulate axonal transport? Trends Neurosci *26*, 397-400.

Shi, J., Koteiche, H.A., McHaourab, H.S., and Stewart, P.L. (2006). Cryoelectron microscopy and EPR analysis of engineered symmetric and polydisperse Hsp16.5 assemblies reveals determinants of polydispersity and substrate binding. J Biol Chem *281*, 40420-40428.

Shimura, H., Miura-Shimura, Y., and Kosik, K.S. (2004). Binding of tau to heat shock protein 27 leads to decreased concentration of hyperphosphorylated tau and enhanced cell survival. J Biol Chem *279*, 17957-17962.

Sihag, R.K., and Nixon, R.A. (1991). Identification of Ser-55 as a major protein kinase A phosphorylation site on the 70-kDa subunit of neurofilaments. Early turnover during axonal transport. J Biol Chem *266*, 18861-18867.

Slaughter, T., Wang, J., and Black, M.M. (1997). Microtubule transport from the cell body into the axons of growing neurons. J Neurosci *17*, 5807-5819.

Slep, K.C., and Vale, R.D. (2007). Structural basis of microtubule plus end tracking by XMAP215, CLIP-170, and EB1. Mol Cell *27*, 976-991.

Sobel, A. (1991). Stathmin: a relay phosphoprotein for multiple signal transduction? Trends Biochem Sci *16*, 301-305.

Song, H.J., and Poo, M.M. (1999). Signal transduction underlying growth cone guidance by diffusible factors. Curr Opin Neurobiol *9*, 355-363.

Steffen, A., Rottner, K., Ehinger, J., Innocenti, M., Scita, G., Wehland, J., and Stradal, T.E. (2004). Sra-1 and Nap1 link Rac to actin assembly driving lamellipodia formation. EMBO J *23*, 749-759.

Sternberger, L.A., and Sternberger, N.H. (1983). Monoclonal antibodies distinguish phosphorylated and nonphosphorylated forms of neurofilaments in situ. Proc Natl Acad Sci U S A *80*, 6126-6130.

Stetler, R.A., Cao, G., Gao, Y., Zhang, F., Wang, S., Weng, Z., Vosler, P., Zhang, L., Signore, A., Graham, S.H., and Chen, J. (2008). Hsp27 protects against ischemic brain injury via attenuation of a novel stress-response cascade upstream of mitochondrial cell death signaling. J Neurosci *28*, 13038-13055.

Stoll, G., Jander, S., and Myers, R.R. (2002). Degeneration and regeneration of the peripheral nervous system: from Augustus Waller's observations to neuroinflammation. J Peripher Nerv Syst *7*, 13-27.

Sun, Y., and MacRae, T.H. (2005). The small heat shock proteins and their role in human disease. Febs J *272*, 2613-2627.

Suzuki, A., Sugiyama, Y., Hayashi, Y., Nyu-i, N., Yoshida, M., Nonaka, I., Ishiura, S., Arahata, K., and Ohno, S. (1998). MKBP, a novel member of the small heat shock protein family, binds and activates the myotonic dystrophy protein kinase. J Cell Biol *140*, 1113-1124.

Tang, B.S., Zhao, G.H., Luo, W., Xia, K., Cai, F., Pan, Q., Zhang, R.X., Zhang, F.F., Liu, X.M., Chen, B., *et al.* (2005). Small heat-shock protein 22 mutated in autosomal dominant Charcot-Marie-Tooth disease type 2L. Hum Genet *116*, 222-224.

Tang, D., and Goldberg, D.J. (2000). Bundling of microtubules in the growth cone induced by laminin. Mol Cell Neurosci *15*, 303-313.

Taylor, R.P., and Benjamin, I.J. (2005). Small heat shock proteins: a new classification scheme in mammals. J Mol Cell Cardiol *38*, 433-444.

Teng, F.Y., and Tang, B.L. (2006). Axonal regeneration in adult CNS neurons--signaling molecules and pathways. J Neurochem *96*, 1501-1508.

Tessier, D.J., Komalavilas, P., Panitch, A., Joshi, L., and Brophy, C.M. (2003). The small heat shock protein (HSP) 20 is dynamically associated with the actin cross-linking protein actinin. J Surg Res *111*, 152-157.

Tezel, G.M., Seigel, G.M., and Wax, M.B. (1999). Density-dependent resistance to apoptosis in retinal cells. Curr Eye Res *19*, 377-388.

Theriault, J.R., Lambert, H., Chavez-Zobel, A.T., Charest, G., Lavigne, P., and Landry, J. (2004). Essential role of the NH2-terminal WD/EPF motif in the phosphorylation-activated protective function of mammalian Hsp27. J Biol Chem *279*, 23463-23471.

Theriot, J.A. (1997). Accelerating on a treadmill: ADF/cofilin promotes rapid actin filament turnover in the dynamic cytoskeleton. J Cell Biol *136*, 1165-1168.

Tissieres, A., Mitchell, H.K., and Tracy, U.M. (1974). Protein synthesis in salivary glands of Drosophila melanogaster: Relation to chromosome puffs. J Mol Biol *85*, 389-398.

Tobacman, L.S., and Korn, E.D. (1983). The kinetics of actin nucleation and polymerization. J Biol Chem *258*, 3207-3214.

Toivola, D.M., Tao, G.Z., Habtezion, A., Liao, J., and Omary, M.B. (2005). Cellular integrity plus: organelle-related and protein-targeting functions of intermediate filaments. Trends Cell Biol *15*, 608-617.

Tokuo, H., Mabuchi, K., and Ikebe, M. (2007). The motor activity of myosin-X promotes actin fiber convergence at the cell periphery to initiate filopodia formation. J Cell Biol *179*, 229-238.

Tomasovic, S.P., Simonette, R.A., Wolf, D.A., Kelley, K.L., and Updyke, T.V. (1989). Co-isolation of heat stress and cytoskeletal proteins with plasma membrane proteins. Int J Hyperthermia *5*, 173-190.

Tonge, D.A., Golding, J.P., Edbladh, M., Kroon, M., Ekstrom, P.E., and Edstrom, A. (1997). Effects of extracellular matrix components on axonal outgrowth from peripheral nerves of adult animals in vitro. Exp Neurol *146*, 81-90.

Tonkiss, J., and Calderwood, S.K. (2005). Regulation of heat shock gene transcription in neuronal cells. Int J Hyperthermia *21*, 433-444.

Troy, C.M., Brown, K., Greene, L.A., and Shelanski, M.L. (1990). Ontogeny of the neuronal intermediate filament protein, peripherin, in the mouse embryo. Neuroscience *36*, 217-237.

Tseng, Y., An, K.M., Esue, O., and Wirtz, D. (2004). The bimodal role of filamin in controlling the architecture and mechanics of F-actin networks. J Biol Chem *279*, 1819-1826.

Tsvetkov, A.S., Samsonov, A., Akhmanova, A., Galjart, N., and Popov, S.V. (2007). Microtubule-binding proteins CLASP1 and CLASP2 interact with actin filaments. Cell Motil Cytoskeleton *64*, 519-530.

Tucker, B.A., and Mearow, K.M. (2008). Peripheral Sensory Axon Growth: From Receptor Binding to Cellular Signalling. Canadian Journal of Neurological Sciences.

Tucker, B.A., Rahimtula, M., and Mearow, K.M. (2005). Integrin activation and neurotrophin signaling cooperate to enhance neurite outgrowth in sensory neurons. J Comp Neurol *486*, 267-280.

Tucker, B.A., Rahimtula, M., and Mearow, K.M. (2006). Laminin and growth factor receptor activation stimulates differential growth responses in subpopulations of adult DRG neurons. Eur J Neurosci *24*, 676-690.

Tucker, B.A., Rahimtula, M., and Mearow, K.M. (2008). Src and FAK are key early signalling intermediates required for neurite growth in NGF-responsive adult DRG neurons. Cell Signal *20*, 241-257.

Tucker, K.L., Meyer, M., and Barde, Y.A. (2001). Neurotrophins are required for nerve growth during development. Nat Neurosci *4*, 29-37.

Turney, S.G., and Bridgman, P.C. (2005). Laminin stimulates and guides axonal outgrowth via growth cone myosin II activity. Nat Neurosci *8*, 717-719.

Van Montfort, R., Slingsby, C., and Vierling, E. (2001a). Structure and function of the small heat shock protein/alpha-crystallin family of molecular chaperones. Adv Protein Chem *59*, 105-156.

van Montfort, R.L., Basha, E., Friedrich, K.L., Slingsby, C., and Vierling, E. (2001b). Crystal structure and assembly of a eukaryotic small heat shock protein. Nat Struct Biol *8*, 1025-1030.

Van Why, S.K., Mann, A.S., Ardito, T., Thulin, G., Ferris, S., Macleod, M.A., Kashgarian, M., and Siegel, N.J. (2003). Hsp27 associates with actin and limits injury in energy depleted renal epithelia. J Am Soc Nephrol *14*, 98-106.

Verhey, K.J., and Gaertig, J. (2007). The tubulin code. Cell Cycle *6*, 2152-2160.

Vertii, A., Hakim, C., Kotlyarov, A., and Gaestel, M. (2006). Analysis of properties of small heat shock protein Hsp25 in MAPK-activated protein kinase 2 (MK2)-deficient cells: MK2-dependent insolubilization of Hsp25 oligomers correlates with susceptibility to stress. J Biol Chem *281*, 26966-26975.

Vicart, P., Caron, A., Guicheney, P., Li, Z., Prevost, M.C., Faure, A., Chateau, D., Chapon, F., Tome, F., Dupret, J.M., *et al.* (1998). A missense mutation in the alphaB-crystallin chaperone gene causes a desmin-related myopathy. Nat Genet *20*, 92-95.

Vigilanza, P., Aquilano, K., Rotilio, G., and Ciriolo, M.R. (2008). Transient cytoskeletal alterations after SOD1 depletion in neuroblastoma cells. Cell Mol Life Sci *65*, 991-1004.

Vogelezang, M.G., Liu, Z., Relvas, J.B., Raivich, G., Scherer, S.S., and ffrench-Constant, C. (2001). Alpha4 integrin is expressed during peripheral nerve regeneration and enhances neurite outgrowth. J Neurosci *21*, 6732-6744.

Vogelezang, M.G., Scherer, S.S., Fawcett, J.W., and ffrench-Constant, C. (1999). Regulation of fibronectin alternative splicing during peripheral nerve repair. J Neurosci Res *56*, 323-333.

Volkmann, N., DeRosier, D., Matsudaira, P., and Hanein, D. (2001). An atomic model of actin filaments cross-linked by fimbrin and its implications for bundle assembly and function. J Cell Biol *153*, 947-956.

Wade, R.H. (2007). Microtubules: an overview. Methods Mol Med *137*, 1-16.

Wakatsuki, T., Schwab, B., Thompson, N.C., and Elson, E.L. (2001). Effects of cytochalasin D and latrunculin B on mechanical properties of cells. J Cell Sci *114*, 1025-1036.

Wang, L., and Brown, A. (2001). Rapid intermittent movement of axonal neurofilaments observed by fluorescence photobleaching. Mol Biol Cell *12*, 3257-3267.

Wang, L., Ho, C.L., Sun, D., Liem, R.K., and Brown, A. (2000). Rapid movement of axonal neurofilaments interrupted by prolonged pauses. Nat Cell Biol *2*, 137-141.

Wang, P., and Bitar, K.N. (1998). Rho A regulates sustained smooth muscle contraction through cytoskeletal reorganization of HSP27. Am J Physiol *275*, G1454-1462.

Wegner, A. (1976). Head to tail polymerization of actin. J Mol Biol *108*, 139-150.

Welch, W.J., and Suhan, J.P. (1985). Morphological study of the mammalian stress response: characterization of changes in cytoplasmic organelles, cytoskeleton, and nucleoli, and appearance of intranuclear actin filaments in rat fibroblasts after heat-shock treatment. J Cell Biol *101*, 1198-1211.

Westermann, S., and Weber, K. (2003). Post-translational modifications regulate microtubule function. Nat Rev Mol Cell Biol *4*, 938-947.

Westwood, J.T., and Wu, C. (1993). Activation of Drosophila heat shock factor: conformational change associated with a monomer-to-trimer transition. Mol Cell Biol *13*, 3481-3486.

White, H.E., Orlova, E.V., Chen, S., Wang, L., Ignatiou, A., Gowen, B., Stromer, T., Franzmann, T.M., Haslbeck, M., Buchner, J., and Saibil, H.R. (2006). Multiple distinct assemblies reveal conformational flexibility in the small heat shock protein Hsp26. Structure *14*, 1197-1204.

Wieske, M., Benndorf, R., Behlke, J., Dolling, R., Grelle, G., Bielka, H., and Lutsch, G. (2001). Defined sequence segments of the small heat shock proteins HSP25 and alphaB-crystallin inhibit actin polymerization. Eur J Biochem *268*, 2083-2090.

Williams, K.L., Mearow, K.M (2009). Mutation of Hsp27 Phosphorylation sites has an effect on neurite growth.

Williams, K.L., Rahimtula, M., and Mearow, K.M. (2005). Hsp27 and axonal growth in adult sensory neurons in vitro. BMC Neurosci *6*, 24.

Williams, K.L., Rahimtula, M., and Mearow, K.M. (2006). Heat shock protein 27 is involved in neurite extension and branching of dorsal root ganglion neurons in vitro. J Neurosci Res *84*, 716-723.

Wittmann, T., Bokoch, G.M., and Waterman-Storer, C.M. (2004). Regulation of microtubule destabilizing activity of Op18/stathmin downstream of Rac1. J Biol Chem *279*, 6196-6203.

Wodarz, A., Ramrath, A., Kuchinke, U., and Knust, E. (1999). Bazooka provides an apical cue for Inscuteable localization in Drosophila neuroblasts. Nature *402*, 544-547.

Wong, P.C., and Cleveland, D.W. (1990). Characterization of dominant and recessive assembly-defective mutations in mouse neurofilament NF-M. J Cell Biol *111*, 1987-2003.

Xie, L., and Forer, A. (2008). Jasplakinolide, an actin stabilizing agent, alters anaphase chromosome movements in crane-fly spermatocytes. Cell Motil Cytoskeleton *65*, 876-889.

Yabe, J.T., Jung, C., Chan, W.K., and Shea, T.B. (2000). Phospho-dependent association of neurofilament proteins with kinesin in situ. Cell Motil Cytoskeleton *45*, 249-262.

Yano, H., Lee, F.S., Kong, H., Chuang, J., Arevalo, J., Perez, P., Sung, C., and Chao, M.V. (2001). Association of Trk neurotrophin receptors with components of the cytoplasmic dynein motor. J Neurosci *21*, RC125.

Yu, W., Ling, C., and Baas, P.W. (2001). Microtubule reconfiguration during axogenesis. J Neurocytol *30*, 861-875.

Yu, W., Qiang, L., Solowska, J.M., Karabay, A., Korulu, S., and Baas, P.W. (2008). The Microtubule-severing Proteins Spastin and Katanin Participate Differently in the Formation of Axonal Branches. Mol Biol Cell *19*, 1485-1498.

Yuan, A., Rao, M.V., Kumar, A., Julien, J.P., and Nixon, R.A. (2003). Neurofilament transport in vivo minimally requires hetero-oligomer formation. J Neurosci *23*, 9452-9458.

Zhai, J., Lin, H., Julien, J.P., and Schlaepfer, W.W. (2007). Disruption of neurofilament network with aggregation of light neurofilament protein: a common pathway leading to motor neuron degeneration due to Charcot-Marie-Tooth disease-linked mutations in NFL and HSPB1. Hum Mol Genet *16*, 3103-3116.

Zhao, C., Takita, J., Tanaka, Y., Setou, M., Nakagawa, T., Takeda, S., Yang, H.W., Terada, S., Nakata, T., Takei, Y., *et al.* (2001). Charcot-Marie-Tooth disease type 2A caused by mutation in a microtubule motor KIF1Bbeta. Cell *105*, 587-597.

Zhou, F.Q., Zhou, J., Dedhar, S., Wu, Y.H., and Snider, W.D. (2004). NGF-induced axon growth is mediated by localized inactivation of GSK-3beta and functions of the microtubule plus end binding protein APC. Neuron *42*, 897-912.